Neural Plasticity

Stress Induced Neuroplasticity and Mental Disorders

Lead Guest Editor: Fushun Wang
Guest Editors: Fushun Wang, Fang Pan, Lee Shapiro, and Jason H. Huang

Stress Induced Neuroplasticity and Mental Disorders

Neural Plasticity

Stress Induced Neuroplasticity and Mental Disorders

Lead Guest Editor: Fushun Wang
Guest Editors: Fang Pan, Lee Shapiro, and Jason H. Huang

Editorial Board

Contents

Hindawi
Neural Plasticity
Volume 2017, Article ID 9634501, 3 pages
https://doi.org/10.1155/2017/9634501

Editorial

Stress Induced Neuroplasticity and Mental Disorders

Fushun Wang,[1] Fang Pan,[2] Lee A. Shapiro,[3] and Jason H. Huang[4]

[1]*School of Psychology, Nanjing University of Chinese Medicine, Nanjing 210023, China*
[2]*Department of Medical Psychology, School of Basic Medical Sciences, Shandong University, Jinan 250012, China*
[3]*Department of Surgery, Texas A&M College of Medicine, Temple, TX 76504, USA*
[4]*Department of Neurosurgery, Baylor Scott & White Health, Temple, TX 76508, USA*

Correspondence should be addressed to Fushun Wang; 13814541138@163.com

Received 19 March 2017; Accepted 20 March 2017; Published 13 July 2017

Stress was introduced by Hans Selye as the general adaptation syndrome, which is a process under which the body confronts noxious agents. In the face of stress, the first reaction of the body is an alarm reaction, and the body prepares itself for "fight or flight." And the second stage is adaptation of resistance, for the organism cannot sustain this motivated state too long. Finally, "due to wear and tear," the body enters a third stage of exhaustion. Selye's brilliant ideas about stress helped an entirely new field to be forged and attracted thousands of researchers to work on the biological mechanism of stress. Stress was later extended to the field of psychology and redefined as the presence of acute or persistent physiological or psychological threats to the organism that result in significant strain on the body's compensatory systems, because anticipated thoughts about the stressful events can also induce stressful reactions. In addition, if the biological threat is easily avoidable, the body will not be stressed. Therefore, stressful reactions depend on the uncertain thought about the stressful events.

Lazarus proposed that stress depends on the thoughts and appraisals of the importance of the individual analysis of subjective appraisal of the situation. He distinguished two kinds of appraisals. The first appraisal is automatic, unreflective and unconscious, and fast activating, which is related to harm and threat, and induces fearful emotion to motivate avoidance and withdraw. The second is conscious and concerned with coping. In the face of threat, the organism was scared at first and showed fearful emotions. And then to cope with the threats, the organism collects energy in the body trying to "fight or flight" and shows angry emotions. Therefore, fear and anger usually come in a tandem at stressful events; fear is the scariness at the stressful events, and anger is coping with the threats. Lazarus suggested that fear and anger are hard to be detached and are two sides of the same coin. Similar to Selye's three stages of stress, Lazarus suggested another stage of reappraisal after coping with the situation. An individual employs two kinds of reappraisals: problem-focused and emotion-focused. If the organism can cope successfully with the stressful situation, the organism will get positive emotions and be happy. If the organism failed to cope with the situation, the organism would get negative emotions and be sad. Therefore, stressful event-induced emotions will go through a "fear-anger-joy-sadness" process, like a rainbow after a storm (Figure 1). If the organism cannot overcome the stressful events, like chronic stresses, some mental disorders will appear. The relation of the process with the emotional changes and mental disorders is shown in Figure 1.

The mechanisms whereby external stressors affect brain function have been the subject of extensive study over the past 60 years. Corticotropin-releasing hormone (CRH), which was named the stress hormone, has become the focus of the study. In both animals and humans, CRH can simulate norepinephrine (NE) synthesis and release. The central NE system innervates many brain areas, sympathetic nervous systems. CRH release also activates the hypothalamic-pituitary-adrenal (HPA) axis, which has been widely accepted as one of the central mechanisms involved in stress. The CRH induced release of ACTH (adrenocorticotropic hormone) and can in turn alter the

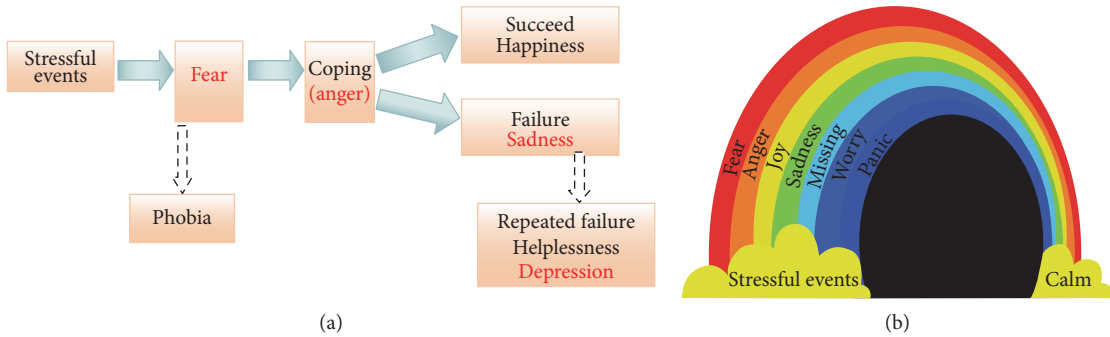

Figure 1: Stress-induced emotion flow and mental disorders. (a) At stressful events or threatening events, an organism will first be scared with the fear emotion. And to cope with the stressful events, the organism collects energy in the body to try to "fight or flight" with angry emotions. Fear is the scariness at the stressful events, and anger is coping with the stressful events. If the organism can cope successfully with the stressful situation, the organism will reappraise the situation and get positive emotions and be happy. If the organism failed to cope with the situation, the organism would get negative emotions and be sad. Stress-fear-response (anger)-consequences (happiness or sadness) constitute the emotion flow in our lives. (b) The emotion flow at stressful events is like a rainbow after a storm.

function of the neural network by altering building blocks in the networks and by altering the integrative properties, and thus the behavioral or emotional changes. This neural plasticity underlying stress undoubtedly affects the brain function and may prompt functional alternations in mental disorders. Indeed, stress-induced neuroplasticity plays a critical role in almost all of the mental disorders, and stress has become a synonym for diverse terms of negative emotions, such as depression and anxiety. In this special issue, we collected papers on stress-induced neural plasticity and some neurological diseases. These reviews and experimental papers present the evidence that stress indeed affects long-term synaptic changes and induces many diseases such as depression and chronic pain.

In the review paper "Safety Needs Mediate Stressful Events Induced Mental Disorders," Z. Zheng et al. reviewed recent papers about stress and proposed a new theory about human needs, which challenged the cornerstone theory of Maslow's famous theory of hierarchy of needs: safety needs come second to physiological needs. In this article, they propose that safety needs are more important and basic than physiological needs. They also probed into the neural basis of the stress system to be LC/NE system, and HPA system, which can be regarded as a "safety circuitry," whose major behavior function is "fight or flight" and "fear and anger" emotions.

In the experimental paper "Shuyu Capsules Relieve Premenstrual Syndrome Depression by Reducing 5-HT_{3A}R and 5-HT_{3B}R Expression in the Rat Brain," F. Li et al. reported a special treatment for the premenstrual depression. In this paper, the author reported that the premenstrual syndrome depression is characterized by changes in the subtypes of 5-HT receptors, especially the 5-HT_3 receptors. In a special kind of rat depression model, they found that a kind of Chinese herb named Shuyu capsule can affect the expression levels of these receptors and can possibly be used to treat depression.

In the experimental paper "ATP Induces Disruption of Tight Junction Proteins via IL-1 Beta-Dependent MMP-9 Activation of Human Blood-Brain Barrier *In Vitro*," F. Yang et al. reported that ATP released after blood-brain barrier impairments under brain traumatic stress affected P_2X_7 receptors and induced neural plasticity in the brain.

In the experimental paper "Activation of Sphingosine 1-Phosphate Receptor 1 Enhances Hippocampus Neurogenesis in a Rat Model of Traumatic Brain Injury: An Involvement of MEK/Erk Signaling Pathway," Y. Ye et al. reported MEK/ERK signaling pathway in the neural plasticity under traumatic events.

In the review paper "The Role of Stress Regulation on Neural Plasticity in Pain Chronification," the authors X. Li and L. Hu reviewed papers about stress and reported two pathways for stress: the faster pathway is the catecholamine, including norepinephrine and dopamine, priming the body into a kind of "fight or flight" state, and the slower process, including HPA changes. The neural plasticity under stress might be the substrate for chronic pain.

In the experimental paper "Profiling Proteins in the Hypothalamus and Hippocampus of a Rat Model of Premenstrual Syndrome Irritability," M. Qiao et al. reported molecular changes in the hypothalamus and hippocampus under premenstrual depression, including Ulip2, tubulin, actin, interleukin, increased Kapp-beta binding motif phosphoprotein, and many other proteins. This paper will help understand the pathogenesis of premenstrual depression.

In the experimental paper "Neuroplastic Correlates in the mPFC Underlying the Impairment of Stress-Coping Ability and Cognitive Flexibility in Adult Rats Exposed to Chronic Mild Stress during Adolescence," Y. Zhang et al. reported very interesting studies about influences of chronic mild stress in adolescence on cognition emotion and behavior and neurochemistry changes in the prefrontal cortex and suggested that the chronic stress-induced epigenetic changes might be the reason for the correlation between the emotional changes and neurochemistry changes.

In the experimental paper "A Combined Water Extract of Frankincense and Myrrh Alleviates Neuropathic Pain in Mice via Modulation of TRPV1," D. Hu et al. reported some changes in TRPV1 channels under chronic pain, and they

introduced a kind of Chinese herb which helps recovery from the chronic pain by modulation of TRPV1 channels.

In the experimental paper "Pathological Role of Peptidyl-Prolyl Isomerase Pin1 in the Disruption of Synaptic Plasticity in Alzheimer's Disease," L. Xu et al. reported stress-induced loss of Pin1 protein activity enhances ubiquitin, which in turn induced synaptic loss and leads to Alzheimer's disease.

Collectively, these studies demonstrate that stress can induce many critical changes in the neural plasticity underlying many neurological diseases. We hope that this special issue will stimulate interests in the field of mechanisms of stress-inducing synaptic disorder and will help achieve a deeper understanding of the molecular mechanism of stress-induced disorders.

Acknowledgments

This work was supported, in part, by NIH R01 NS067435 (Jason H. Huang), Scott & White Plummer Foundation grant (Jason H. Huang), Jiangsu Specially Appointed Professorship Foundation (Fushun Wang), Jiangsu Nature Science Foundation (BK20151565, Fushun Wang), Jiangsu Traditional Chinese Medicine Foundation (ZD201501, Fushun Wang) and Jiangsu Six Talent Peak (2015YY006), National Science Foundation of China (816280007, Jason H. Huang and Fushun Wang), the Priority Academic Program Development (Integrated Chinese and West Medicine) of Jiangsu Higher Education Institute (Fushun Wang), and the National Science Foundation of China (31371036, Fang Pan).

Fushun Wang
Fang Pan
Lee A. Shapiro
Jason H. Huang

Hindawi
Neural Plasticity
Volume 2017, Article ID 3710821, 11 pages
https://doi.org/10.1155/2017/3710821

Research Article

A Combined Water Extract of Frankincense and Myrrh Alleviates Neuropathic Pain in Mice via Modulation of TRPV1

Danyou Hu,[1,2] Changming Wang,[1,2] Fengxian Li,[3] Shulan Su,[4] Niuniu Yang,[1,2] Yan Yang,[1,2] Chan Zhu,[1,2] Hao Shi,[1,2] Lei Yu,[1,2] Xiao Geng,[1,2] Leying Gu,[1,2] Xiaolin Yuan,[1,2] Zhongli Wang,[1,2] Guang Yu,[1,2,4] and Zongxiang Tang[1,2]

[1]*Key Laboratory for Chinese Medicine of Prevention and Treatment in Neurological Diseases, Nanjing University of Chinese Medicine, 138 Xianlin Rd, Nanjing, 210023 Jiangsu, China*
[2]*School of Medicine and Life Sciences, Nanjing University of Chinese Medicine, 138 Xianlin Rd, Nanjing, 210023 Jiangsu, China*
[3]*Department of Anesthesiology, Zhujiang Hospital of Southern Medical University, 253 Gongye Rd, Guangzhou, 510282 Guangdong, China*
[4]*Jiangsu Key Laboratory for High Technology Research of TCM Formulae, Nanjing University of Chinese Medicine, 138 Xianlin Rd, Nanjing, 210023 Jiangsu, China*

Correspondence should be addressed to Guang Yu; yuguang928@126.com and Zongxiang Tang; zongxiangtang1@163.com

Received 28 October 2016; Revised 24 January 2017; Accepted 6 February 2017; Published 27 June 2017

Academic Editor: Fang Pan

Frankincense and myrrh are widely used in clinics as a pair of herbs to obtain a synergistic effect for relieving pain. To illuminate the analgesia mechanism of frankincense and myrrh, we assessed its effect in a neuropathic pain mouse model. Transient receptor potential vanilloid 1 (TRPV1) plays a crucial role in neuropathic pain and influences the plasticity of neuronal connectivity. We hypothesized that the water extraction of frankincense and myrrh (WFM) exerted its analgesia effect by modulating the neuronal function of TRPV1. In our study, WFM was verified by UHPLC-TQ/MS assay. In vivo study showed that nociceptive response in mouse by heat and capsaicin induced were relieved by WFM treatment. Furthermore, thermal hypersensitivity and mechanical allodynia were also alleviated by WFM treatment in a chronic constriction injury (CCI) mouse model. CCI resulted in increased TRPV1 expression at both the mRNA and protein levels in predominantly small-to-medium neurons. However, after WFM treatment, TRPV1 expression was reverted in real-time PCR, Western blot, and immunofluorescence experiments. Calcium response to capsaicin was also decreased in cultured DRG neurons from CCI model mouse after WFM treatment. In conclusion, WFM alleviated CCI-induced mechanical allodynia and thermal hypersensitivity via modulating TRPV1.

1. Introduction

The main characteristics of neuropathic pain are allodynia, hyperalgesia, and persistent pain [1, 2], which changes the quality of life for millions of people worldwide. Massive studies have been designed to disclose the precise mechanisms [3, 4]. However, the randomized clinical trial drugs have shown that the analgesic effect is less than that of patients treated with conventional drugs [5]. This prompts us to find new strategies for the affliction. There is growing interest in herbal remedies. Clinical data have shown promising effects of multiple herbs including frankincense and myrrh in pain relief [6].

Frankincense is the dried gum resin of *Boswellia carterii,* one of 43 species in the genus *Boswellia* of the *family Burseraceae*. It has been commonly used to alleviate pain in different diseases [7, 8]. In vitro studies have shown that boswellic acids, which are isolated from frankincense, have the potential to regulate immune function [9]. Myrrh is an aromatic gum resin, which is the plant stem resinous exudate of *Commiphora myrrha* (Nees) Engl. (*Burseraceae*) and other different species of the *Commiphora* family. Myrrh is widely used

Table 1: The cone voltage and collision energy optimized for each analyte and selected values.

Analytes	Ionization mode	MRM transitions (precursor-product)	Cone voltage (V)	Collision energy (eV)
β-Boswellic acid	ES^-	455.415 → 377.356	44	30
3α-Acetoxy-tirucall-7,24- dien-21-oic acid	ES^+	455.479 → 437.426	14	8
3-Acetyl-11-keto-β-boswellic acid	ES^+	513.479 → 95.06	40	42
3-Keto-tirucall-8,24-dien-21-oic acid	ES^+	455.479 → 133.112	14	36
Abietic acid	ES^+	303.287 → 93.109	16	30

in clinics in India, China, Rome, and Greece to treat painful diseases such as ache and dysmenorrhea [10]. Pharmacological studies have shown that myrrh has multiple activities (effects), including anti-inflammatory and antimicrobial [11, 12]. However, the mechanism is not fully understood for frankincense and myrrh, which are used as a pair of herbs to relieve pain sensation. Although several elements are thought to be the key mechanisms—including reactive oxygen species and inflammatory cytokines for their antinociceptive effect, the precise molecular mechanisms are still obscure [13].

The transient receptor potential vanilloid 1 (TRPV1) is a nonselective cation channel involved in the detection and transduction of nociceptive stimulus [14]. Upregulation of TRPV1 transcription can be induced by inflammation and nerve damage. Modulating of TRPV1 activity is considered an effective strategy in treating inflammatory and neuropathic pain conditions [15, 16]. Hence, TRPV1 has become a promising target for screening analgesics via either blocking the function of the receptor or eliminating the nociceptor by utilizing a high dose of agonists [17–19].

In China, formula is commonly used in pain treatment. The main herb pair is recognized to be the most important part of the formula. Frankincense and myrrh as an herb pair has shown promising effects in pain relief. It is possible that they might have the potential of alleviating neuropathic pain by modulating TRPV1. However, there is almost no literature report on this pair of herb to relieve neuropathic pain by regulating TRPV1. Here, we obtained WFM from frankincense and myrrh in boiled water and verified some effective components by UHPLC-TQ/MS assay. A CCI mouse model was then conducted to elucidate the modulating effect of WFM on TRPV1, which achieved the pain relief effect. Furthermore, we checked the inhibition effect of WFM on the expression, sensitivity of TRPV1.

2. Materials and Methods

2.1. WFM Extraction and UHPLC-TQ/MS Assay. The frankincense and myrrh were purchased from the Jiangsu Traditional Chinese Medical Hospital (Nanjing, China), identified and authenticated by Dr. Shulan Su in the College of Pharmacy, Nanjing University of Chinese Medicine. Chemical standards including β-boswellic acid, 3α-acetoxy-tirucall-7,24-dien-21-oic acid, 3-aectyl-11-keto-β-boswellic acid, 3-keto-tirucall-8,24-dien-21-oic acid, and abietic acid were separated and identified in previous studies. The dry herb of frankincense (100 g) and myrrh (100 g) were extracted from boiling water (1600 ml) twice and filtered through gauze. Filtrates were then evaporated by rotary evaporation under vacuum at 55°C. Finally, a semi dry mass of about 50 g was obtained and used in the experiment.

The UHPLC-TQ/MS method was applied for determining the components of WFM as follows: Chromatographic analysis was performed on a Waters Acquity UHPLC system (Waters, Corp., Milford, MA, USA), consisting of a binary pump solvent management system, an online degasser, and an autosampler. An Acquity™ UPLC BEH C_{18} column (2.1 mm × 50 mm, 1.7 μm) was employed, and the column temperature was maintained at 30°C. The mobile phase was composed of A (acetonitrile) and B (0.1% formic acid) using a gradient elution of 10% A at 0-1 min, 5% A at 1–9 min, and 10% A at 9-10 min with a flow rate set at 0.4 ml·min^{-1}. The sample injection volume was 2 μl. The ESI source was set in both positive and negative ionization mode. The scanning mode was set multiple reaction monitoring (MRM) mode, and the range of selected monitor ion was m/z 100–m/z 1000. The TQ mass spectrometer was operated with a capillary voltage of 3.5 kV, a sampling cone voltage of 35 V, and a capillary temperature of 275°C. The Helium gas flow was at 35 arb, and the auxiliary gas flow rate was at 15 arb. All of the data acquisition and analyses of data were controlled by Waters MassLynx v4.1 software. The cone voltage and collision energy optimized for each analyte and selected values are given in Table 1.

2.2. Animals. All experiments were performed under protocols approved by the Animal Care and Use Committee of the Nanjing University of Chinese Medicine. All mice used in the behavioral tests were 8- to 10-week old males in a C57Bl/6 background (WT mice). Tested animals were housed, and behavior experiments were performed in a controlled environment of 20–24°C, humidity of 45–65%, and with a 12-hour day/night cycle.

2.3. CCI Model and Treatment. Unilateral CCI surgery was performed in mice under chloral hydrate anesthesia (50 mg/kg, i.p.). Briefly, after skin preparation and iodine complex disinfection, the skin was incised and muscles were bluntly separated. The right sciatic nerve was found at the mid-thigh level. Then two ligations with gut were performed loosely on the nerve, each spaced 1 mm apart. Mice in the sham group received the same procedure without sciatic nerve hypodesmus. Seventy two male mice were randomly divided into six groups ($n = 12$ per group) based on the

treatment, naïve + vehicle (distilled water), sham + vehicle, CCI + vehicle, CCI + WFM-L (WFM 1.5 g/kg/day), CCI + WFM-H (WFM 7.5 g/kg/day), and CCI + GBPT (Gabapentin) as a positive control treatment (delivered at 0.2 g/kg/day). All mice received vehicle or drug treatment from 7th day to 16th day (Figure 1(a)). The same volume of drugs or vehicle was administrated blindly by intragastric gavage by the same person. No mice or data points were excluded.

2.4. Behavioural Assay. Animals were acclimated to the testing environment for 10 minutes before the initiation of behavior tests. Animal behavior was analyzed by investigators who were blind to the grouping and treatment. The tail-flick experiments were carried out as previously reported in the 50°C water bath [20]. Mice were gently restrained in a towel and handheld. Approximately 1 cm of the tip of the tail was submerged in a hot water bath maintained at 50°C, and the latency to withdraw the tail was measured. Capsaicin (3 μg/mouse) was injected into the dorsal surface of the right hind paw 3 hours after WFM administration. Licking and biting behavior induced by subcutaneously injected capsaicin were observed for 15 minutes. Mechanical withdrawal threshold (MWT) and thermal withdrawal latency (TWL) were recorded at the 1st, 3rd, 5th, 7th, 10th, 13th, and 16th day. Mice were treated with WFM (once/day) 7 days after unilateral CCI, when all injured mice have developed hindpaw mechanical allodynia and thermal hypersensitivity on the injured side.

2.5. DRG Neuron Culture and Calcium Imaging. DRGs (L4-5 and S1–3) were dissected from different groups of tested mice and collected in DH10 medium on ice (90% DMEM/F-12, 10% FBS, 100 U/ml penicillin, 100 mg/ml streptomycin, Gibco). Dissected DRGs were then digested for 25 minutes at 37°C in a protease solution (5 mg/ml dispase, 1 mg/ml collagenase type I in HBSS without Ca^{2+} and Mg^{2+}, and Gibco) before being triturated to free neurons and pelleted by centrifugation. Pelleted neurons were then resuspended in DH10 medium supplemented with NGF (20 ng/ml) and GDNF (25 ng/ml) and plated onto glass coverslips coated with poly-D-lysine (0.5 mg/ml, Sigma) and laminin (10 mg/ml, Sigma). Neurons were cultured in an incubator (95% O_2 and 5% CO_2) for 24 hours before they were used for calcium imaging [21]. Neurons were loaded with Fura 2-acetomethoxy ester (Molecular Probes) for 30 min at room temperature. After washing and recovery for 5 min, cells were imaged at 340 and 380 nm excitation to detect the intracellular-free calcium. Cells were considered responding if their fluorescence ratio is greater than or equal to 0.5 (fluorescence ratio = $\Delta F/F0$, ΔF means maximal value of fluorescence-baseline value of fluorescence, F0 means baseline value of fluorescence). Calcium imaging assays were performed with an experimenter blind to the grouping [22]. Each test was done three times.

2.6. RNA Extraction and Real-Time PCR. Total RNA from freshly dissected DRGs (L4–5 and S1–3) was isolated and purified using a TRIzol/chloroform (Life Technologies, Carlsbad, California, USA) and an isopropanol precipitation procedure in accordance with the manufacture's protocols. cDNA was compiled using the Transcript First Strand cDNA Synthesis Kit (Roche, Basel, Switzerland). Real-time PCR was performed using LightCycler 480 SYBR Green 1 Master Mix (Roche, Basel, Switzerland) and a LightCycler 480 2 Real-Time PCR instrument (Roche, Basel, Switzerland). Briefly, 1 μl of cDNA from each sample was used for reaction. Primers (forward primer: ATCATCAACGAGGACCCAGG, reverse primer: TGCTATGCCTATCTCGAGTGC) were used to amplify TRPV1 expression. Calibrations and normalizations were done using the $2^{-\triangle\triangle CT}$ method, where $\triangle\triangle CT = (CT\ (\text{target gene}) - CT\ (\text{reference gene})) - (CT\ (\text{calibrator}) - CT\ (\text{reference gene}))$. GAPDH was used as the reference gene for real-time PCR experiments (forward primer: TGGATTTGGACGCATTGGTC, reverse primer: TTTGCACTGGTACGTGTTGAT). After real-time quantification, amplification products were analyzed by electrophoresis on 1.5% agarose gel for band size consistency.

2.7. Protein Extraction and Western Blotting. Total protein from freshly dissected DRGs (L4-5 and S1–3) was isolated and purified using a TRIzol/chloroform (Life Technologies, Carlsbad, California, USA) and an isopropanol precipitation procedure after RNA extraction in accordance with the manufacture's protocols. The protein concentration was determined by BCA assay. β-actin was selected as an internal control. Polyclonal antibody of TRPV1 (Neuromics, USA) was used at 1/500 dilution, and a monoclonal antibody of β-actin (Santa Cruz Biotechnology, Dallas, TX) was used at a 1/1000 dilution. Equal quantities of protein (60 μg per lane) were resolved on 12% SDS-polyacrylamide gels. Western blotting was performed as detailed previously [23]. The intensity of the signals was used to estimate the relative concentration of TRPV1 protein in the DRG extracts.

2.8. Immunohistochemical Staining. Mice were anesthetized with 1% sodium pentobarbital (50 mg/kg, i.p.) and transcardially perfused with 0.1 M phosphate-buffered saline (PBS, pH 7.4, 4°C) followed by 4% paraformaldehyde in PBS (pH 7.4, 4°C). DRGs (L4-5) were dissected from perfusion mice and postfixed in 4% paraformaldehyde in PBS for 30 minutes and cryoprotected in 30% sucrose at 4°C for 24 hours. DRGs were then embedded in an optimum cutting temperature compound (OCT, Leica, Wetalar, Germany) and rapidly frozen at −20°C (CM1950, Leica). Cryoembedded tissues were then cut into 20 μm thick slices using a sliding microtome (CM1950, Leica).

Sectioned DRGs were incubated in blocking solution (10% fetal bovine serum in PBS containing 0.1% Triton X-100) for 30 min at room temperature, followed by anti-TRPV1 (1 : 500; Neuromics, USA) at 4°C overnight. Afterwards, tissue sections were washed with 0.1% PBST and incubated in secondary antibody (1 : 200; Beyotime Biotechnology, China) at room temperature for 2 hours in the dark. Sections were then washed with 0.1% PBS and mounted with glycerol. All imaging was performed with an Olympus fluorescence microscope (BX51, Olympus Japan). Three mice from each group were analyzed.

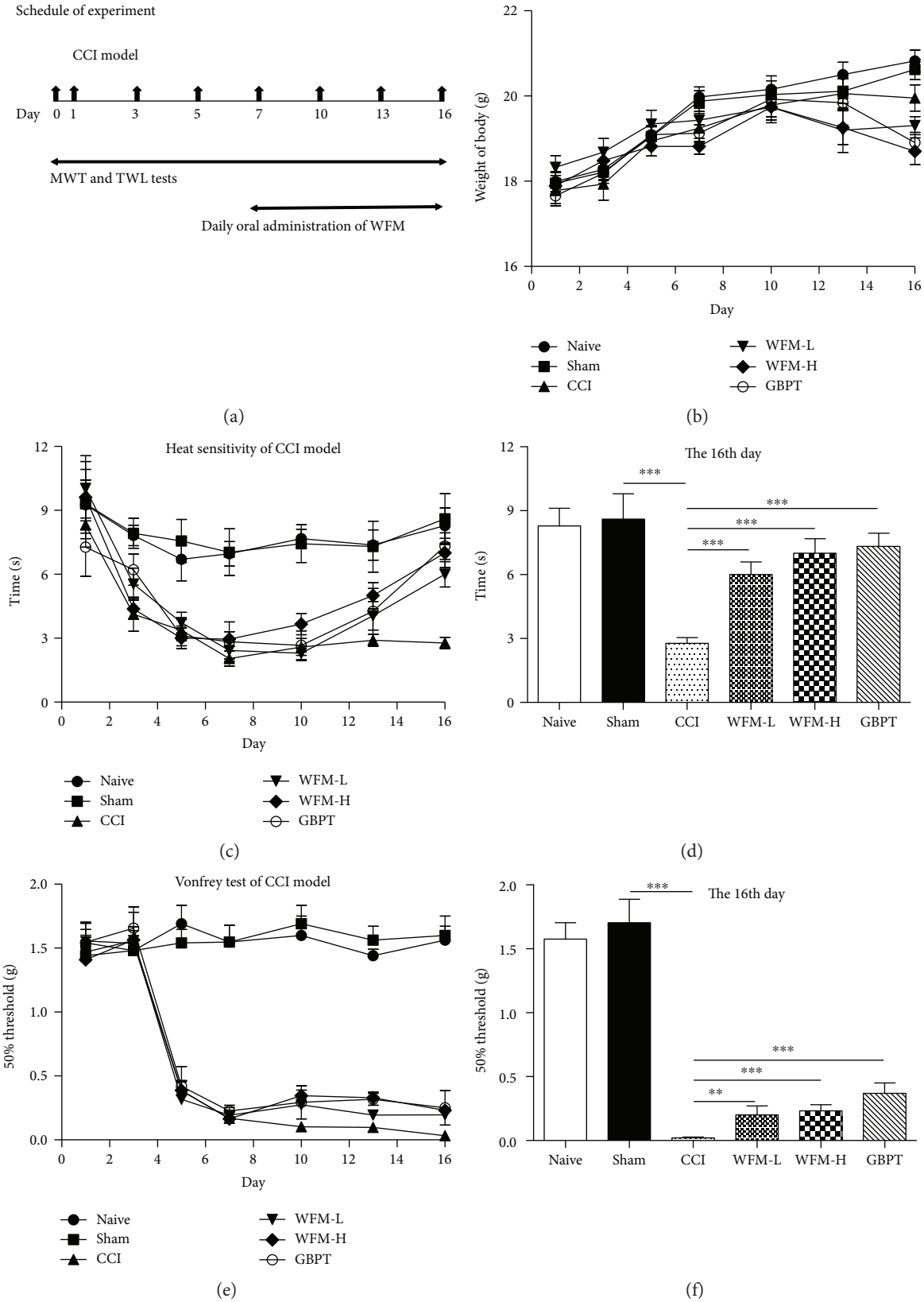

Figure 1: Effects of WFM on chronic constriction injury (CCI) of sciatic nerve treated mouse. (a) Schedule of CCI model and WFM treatment. (b) There was no difference in the body weight after vehicle or drug treatment among six groups. (c, d) Effects of WFM in the thermal withdrawal latency (TWL) was recorded ($n = 12$). (e, f) Effects of WFM in the mechanical withdrawal threshold (MWT) was recorded ($n = 12$). $^{*}p < 0.05$, $^{**}p < 0.01$, $^{***}p < 0.001$.

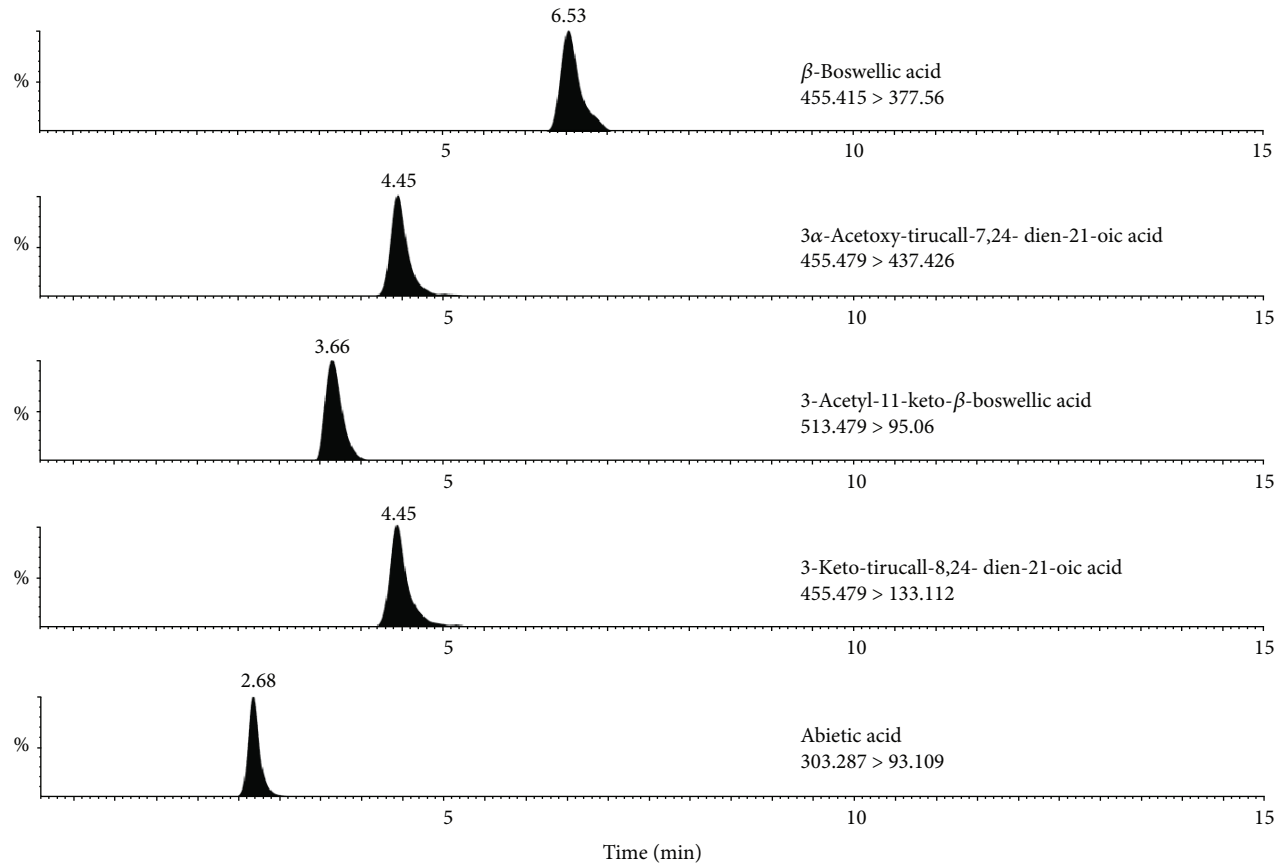

Figure 2: The UHPLC-TQ/MS method was adopted to qualitify the main bioactive components of WFM. By comparing the characterization of tR, λmax, and m/z with standard compounds, β-boswellic acid, 3α-acetoxy-tirucall-7,24-dien-21-oic acid, 3-aectyl-11-keto-β-boswellic acid, 3-keto-tirucall-8,24-dien-21-oic acid, and abietic acid were used as the marker to identify the WFM.

Quantitative analysis of immune response was consistent with previous studies [24].

2.9. Data Analysis. All data are presented as mean ± SEM. Statistical comparisons are performed using 2-tailed Student's *t*-tests. The difference is considered statistically significant at $p < 0.05$.

3. Results

3.1. UHPLC-TQ/MS Identified and Determined WFM. Five main compounds of β-boswellic acid, 3α-acetoxy-tirucall-7,24-dien-21-oic acid, 3-acetyl-11-keto-β-boswellic acid, 3-keto-tirucall-8,24-dien-21-oic acid, and abietic acid in the WFM were identified and determined by the UHPLC-TQ/MS method (Figure 2). They were by comparing the characterization of t_R, λ_{max}, and m/z with standard compounds. The percentage composition of these five compounds in the WFM extraction were 1.07%, 2.02%, 1.65%, 0.92%, and 0.28%, respectively.

3.2. WFM Alleviated Nociceptive Behavior in Mice. Thermal pain is a typical form of pain in daily life. The high temperature water bath of 50°C induced tail-flicking behavior in a short time in mice (1.6 ± 0.21 s) without WFM treatment in our experiment. However, WFM by intragastric gavage (1.5 g/kg) significantly increased the delay tail-flicking behavior in a dose-dependent manner after 3 hours (2.6 ± 0.29 s) and 4 hours (2.5 ± 0.23 s); the data were shown in Figure 3(a) ($P < 0.05$ and $P < 0.01$, respectively). To extend our understanding of its antinociceptive efficacy, we tested WFM in the capsaicin assay. We were surprised to find that WFM significantly alleviated capsaicin-induced licking and biting response by intragastic gavage. The bouts of licking and biting were decreased from 26 ± 2.3 s to 11 ± 2.5 s, while the time spent on licking and biting was also significantly decreased from 45 ± 6.0 s to 17 ± 5.4 s during a 5 min period (Figures 3(b) and 3(c), $P < 0.01$).

3.3. WFM Alleviated Nociceptive Behavior in a CCI Mouse Model. Nerve ligation is commonly used as an animal model of neuropathic pain, which induces mechanical allodynia and thermal hypersensitivity [25]. The mechanical withdrawal threshold (MWT) and thermal withdrawal latency (TWL) of each experimental animal were recorded as baseline before CCI model (day 0). Then MWT and TWL were measured once every two days until the entire experiment was completed (a total of 16 days). From the 7th day after CCI model, mice were treated with WFM once a day. The experimental process of animal behavior was shown in Figure 2. There was no difference in the body weight among six group experiments (Figure 1(b)). Thermal hypersensitivity and

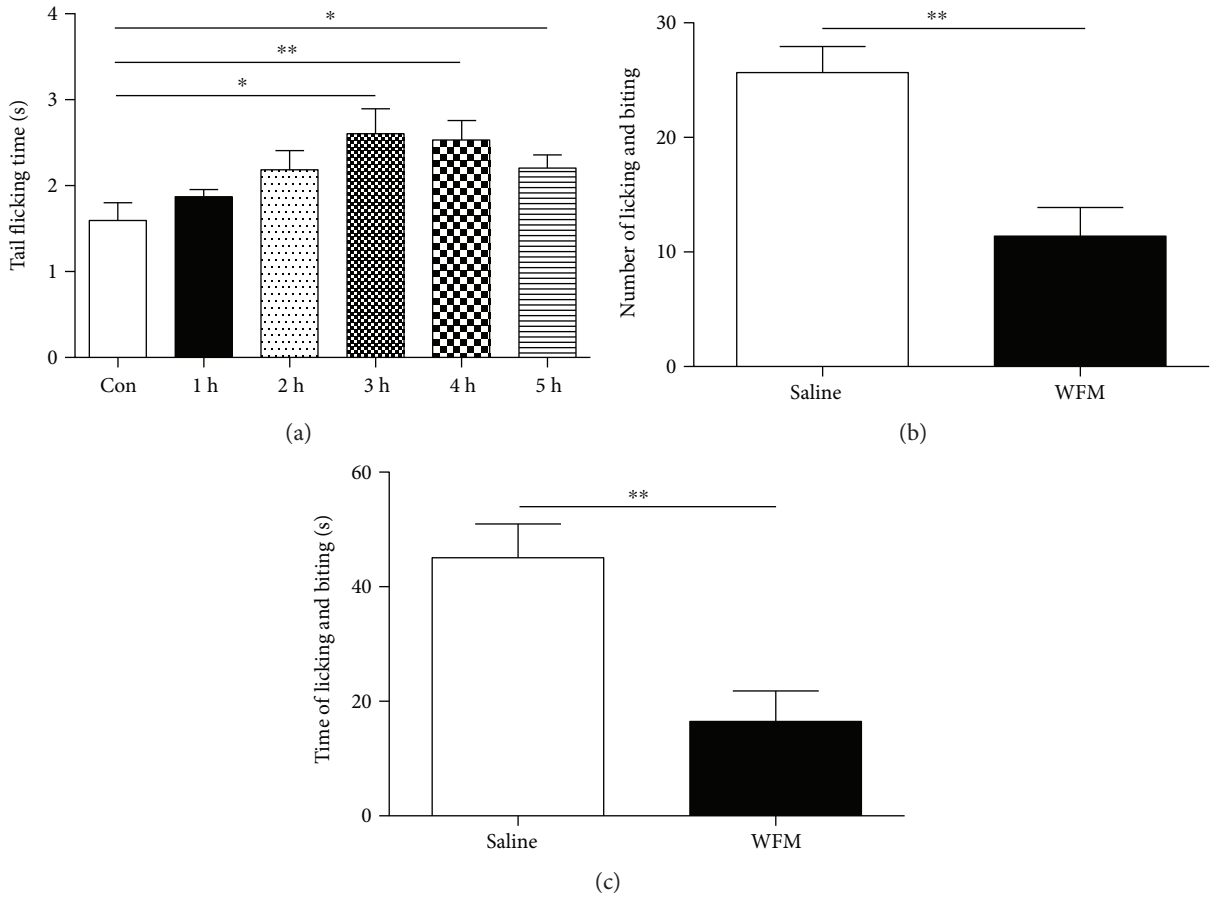

Figure 3: Antinociceptive effects of WFM in the tail-flick and capsaicin injection assay. (a) Antinociceptive effects in the tail-flick assay. WT mice were used in this assay. The time course of the tail-flick latencies was observed after WFM treatment ($n = 8$). (b, c) Effects of WFM in the capsaicin assay. WT mice were used in this assay ($n = 8$). (b) Number of licking and biting. (c) Time of licking and biting. Two-way ANOVA revealed significant drug effect. $^{*}p < 0.05$, $^{**}p < 0.01$, $^{***}p < 0.001$.

mechanical allodynia appeared a significant difference from 3rd day to 5th day in CCI model (Figures 1(c) and 1(e)). However, after treatment with WFM on the 7th day, the temperature and mechanical pain behaviors of mice were improved gradually. The effect of WFM on pain relief has become apparent on the 16th day, and the roles of this relief will remain if WFM continues to be administered. The analgesic of WFM was dose-dependent, and the high concentration of WFM had strong effect. The role of WFM is almost the same as that of gabapentin (GBPT) which is a common clinical analgesic drug (Figures 1(d) and 1(f)). Because there were no difference between naïve and sham group in MWT and TWL tests (Figures 1(c) and 1(e)), we chose the sham group as a control in other experiments including q-PCR, Western blot, immunohistochemical staining, and calcium imaging.

3.4. WFM Attenuated TRPV1 Expression in CCI Model. To reveal the cellular mechanism of WFM relieving nociceptive behavior in CCI model, the TRPV1 expression level was examined in L4-5 and S1–3 DRGs. The percentage of TRPV1 immunoreactive neurons significantly increased from 26.4 ± 1.63% in the sham group to 43.1 ± 1.09% in the CCI group and then attenuated from 43.1 ± 1.09% to 38.3 ± 2.45% in the low-dose group (WFM-L) and 32.1 ± 2.50% in the high-dose group (WFM-H) after WFM treatment ($P < 0.001$). The inhibitory effect of WFM was weaker than that of GBPT (28.5 ± 4.21%) in our experiment (Figure 4). These results combined with other experiments including real-time PCR and Western blot assays confirmed that the expression of TRPV1 in the DRGs was significantly increased in CCI model and was inhibited by WFM. GBPT as a positive control also showed a significant inhibitory effect (Figure 5).

3.5. WFM Attenuated the Response of DRG Neurons to Capsaicin in CCI Model. We further studied the sensitivity of DRG neurons from CCI model mice to capsaicin. The DRG neurons from CCI ipsilateral and contralateral on the same segment were cultured in different culture dishes. Capsaicin was used to activate these DRG neurons. The results indicated that both the ratio of response neurons (from 0.21 ± 0.020 to 0.30 ± 0.022, $P < 0.01$) and the amplitude of response neurons (from 1.8 ± 0.06 to 2.3 ± 0.15, $P < 0.001$) significantly increased. However, before capsaicin stimulus with WFM treatment, both the ratio and the amplitude of response DRG neurons significantly reduced. Low-dose

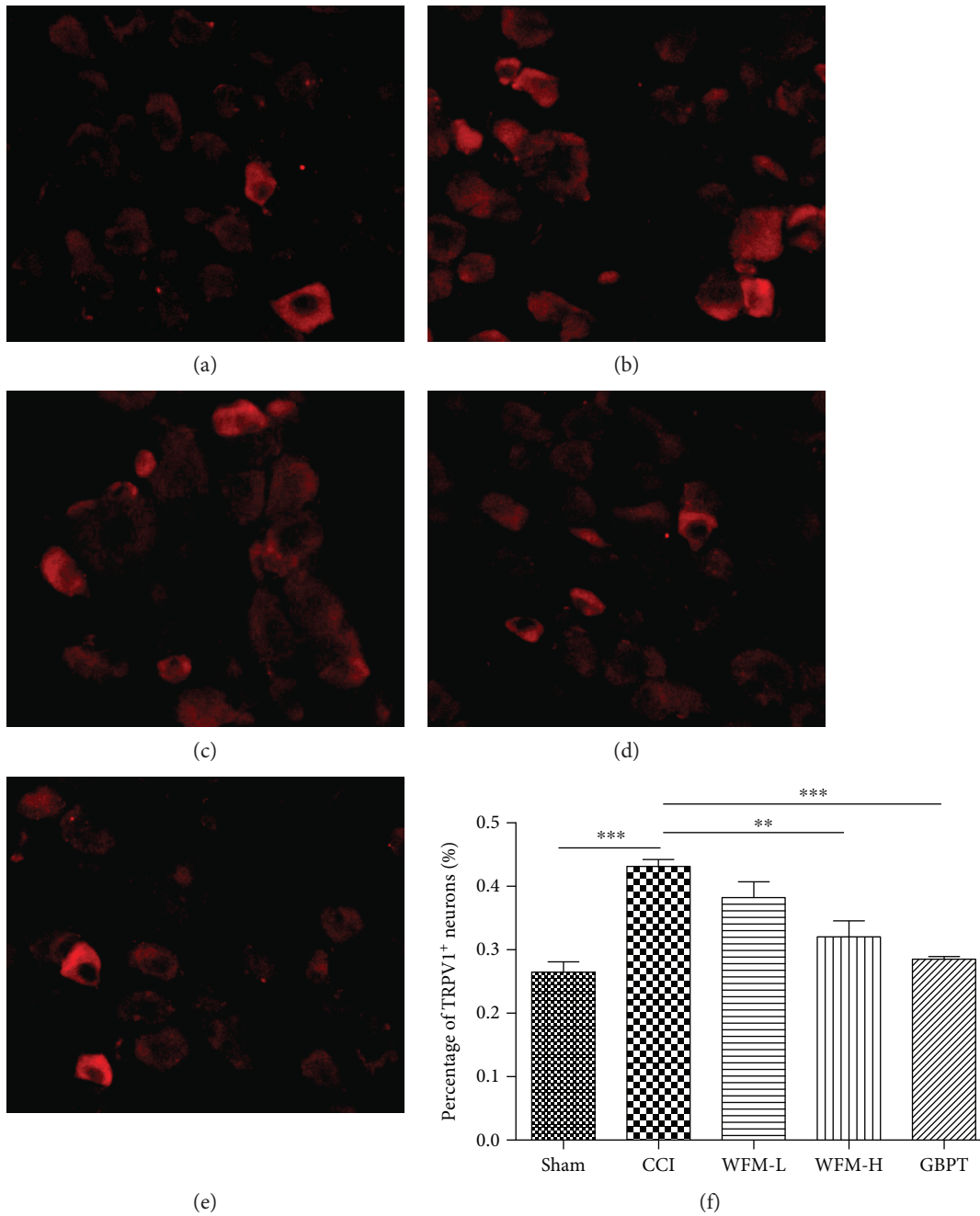

Figure 4: TRPV1$^+$ neuron is increased in CCI model and can be restored by WFM treatment. Histochemistry staining of DRG from CCI model and WFM treatment groups. (a, b) The proportion of TRPV1$^+$ population is increased in CCI model. (c, d) The fraction TRPV1$^+$ neuron in DRG is significantly decreased after WFM treatment. (e) The fraction TRPV1$^+$ neuron in DRG is significantly decreased after GBPT treatment. (f) Data are presented as mean ± SEM, $^*p < 0.05$, $^{**}p < 0.01$, $^{***}p < 0.001$. Scale bar: 50 μm.

WFM attenuated the ratio of DRG neurons to capsaicin response from 0.30 ± 0.022 to $0.22 \pm 0.021 (P < 0.001)$ and the amplitude from 2.3 ± 0.15 to 1.3 ± 0.05 $(P < 0.001)$. High-dose WFM attenuated the ratio of DRG neurons to capsaicin response from 0.30 ± 0.022 to 0.13 ± 0.008 $(P < 0.001)$ and the amplitude of response neurons from 2.3 ± 0.15 to 1.2 ± 0.09 $(P < 0.001)$. The attenuated effect of WFM was almost the same as that of GBPT in our experiment (Figure 6).

4. Discussion

Nociceptors conduct noxious information from sensory nerve endings to the central nervous system; hence, inhibition of the peripheral nociceptor activity can effectively attenuate pain sensation. It is well-known that TRPV1 acts as an integrator of painful stimuli, which has become a promising target for screening analgesics [26]. Either blocking the function of the receptor or utilizing the lasting loss of

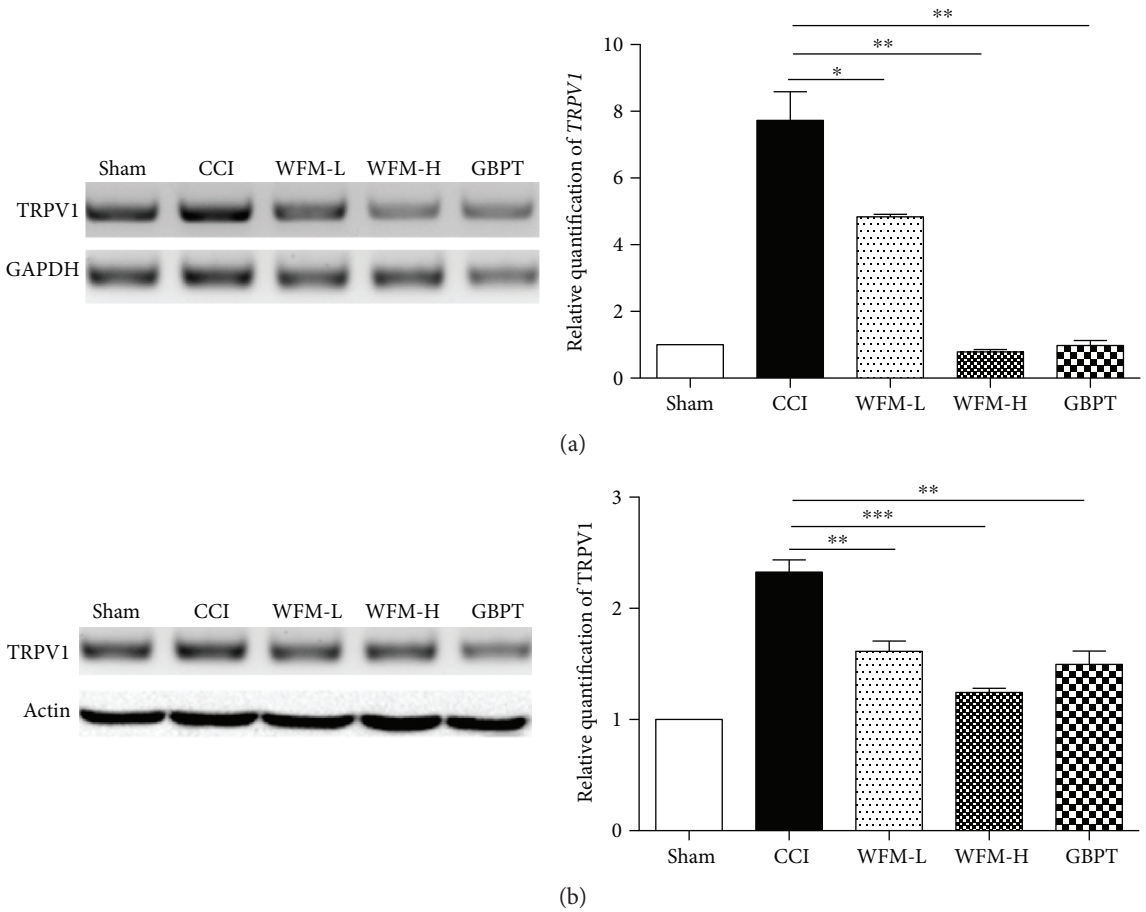

Figure 5: TRPV1 expression is significantly decreased in the DRG after WFM treatment. (a) Real-time PCR results indicate that *TRPV1* expression is decreased after WFM treatment. (b) Western blot results confirm that TRPV1 expression is decreased after WFM treatment. $^{*}p < 0.05$, $^{**}p < 0.01$, $^{***}p < 0.001$.

function of the receptor is believed to be the effective treatment, especially under pathological pain conditions [27]. However, drugs based on pharmacologically synthesis of TRPV1 antagonists and agonists have failed to achieve the ideal therapeutic effects [28]. Hyperthermia and impaired noxious heat sensation were discovered to be the main obstacle in preclinical studies and clinical trials [29].

TRPV1 enhancement is thought to be the critical element during inflammatory and neuropathic pain, so therapeutic strategies have focused on the modulating effects of TRPV1 with antagonists [30]. Studies have indicated that downregulated TRPV1 expression might attenuate neuropathic pain [31, 32]; hence, new strategies have focused on the regulation or modulation of TRPV1 functions to produce better outcomes and fewer side effects. In the history of drug developmental, the discovery of many new drugs comes from the bioactive compounds of herbal medicines, which are natural or long-tested by traditional usage. Among herbal medicines, frankincense and myrrh have been widely used as clinical treatment for various pain diseases because of their effects, so frankincense and myrrh should be a good candidate for relieving neuropathic pain. Our experiment showed that WFM effectively relieved heat and capsaicin-induced pain in normal conditions as well as attenuated heat hypersensitivity and mechanical allodynia in a CCI mouse model. Our study also showed that the analgesic effect of a high dose of WFM was similar to GBPT, which is one of the classical antipain drugs [33]. Furthermore, this antinociceptive effect of WFM is related to the inhibition of TRPV1 expression and activation. In our study, the inhibition effect of WFM on behavior and calcium response was dramatic, which was directly related to the downregulation of TRPV1 expression and sensitivity. Although NGF can enhance the activity of TRPV1, both the ratio and the amplitude of the response to capsaicin were significantly reduced in cultured DRG neurons after WFM treatment in our experiment. This perhaps due to CCI model led to greater effect in the activity of TRPV1 than NGF. Actually, neurons cultured with NGF also showed different activity to 50°C stimulus. Hence, this indicated that WFM is a potential analgesic which is targeted to TRPV1.

Nevertheless, the antinociceptive effect of WFM is from the multiple elements in the extraction; however, whether the monomers within the WFM have the same effect on TRPV1 modulation is still unknown. Further studies should focus on the characteristics of WFM on human antipain effects.

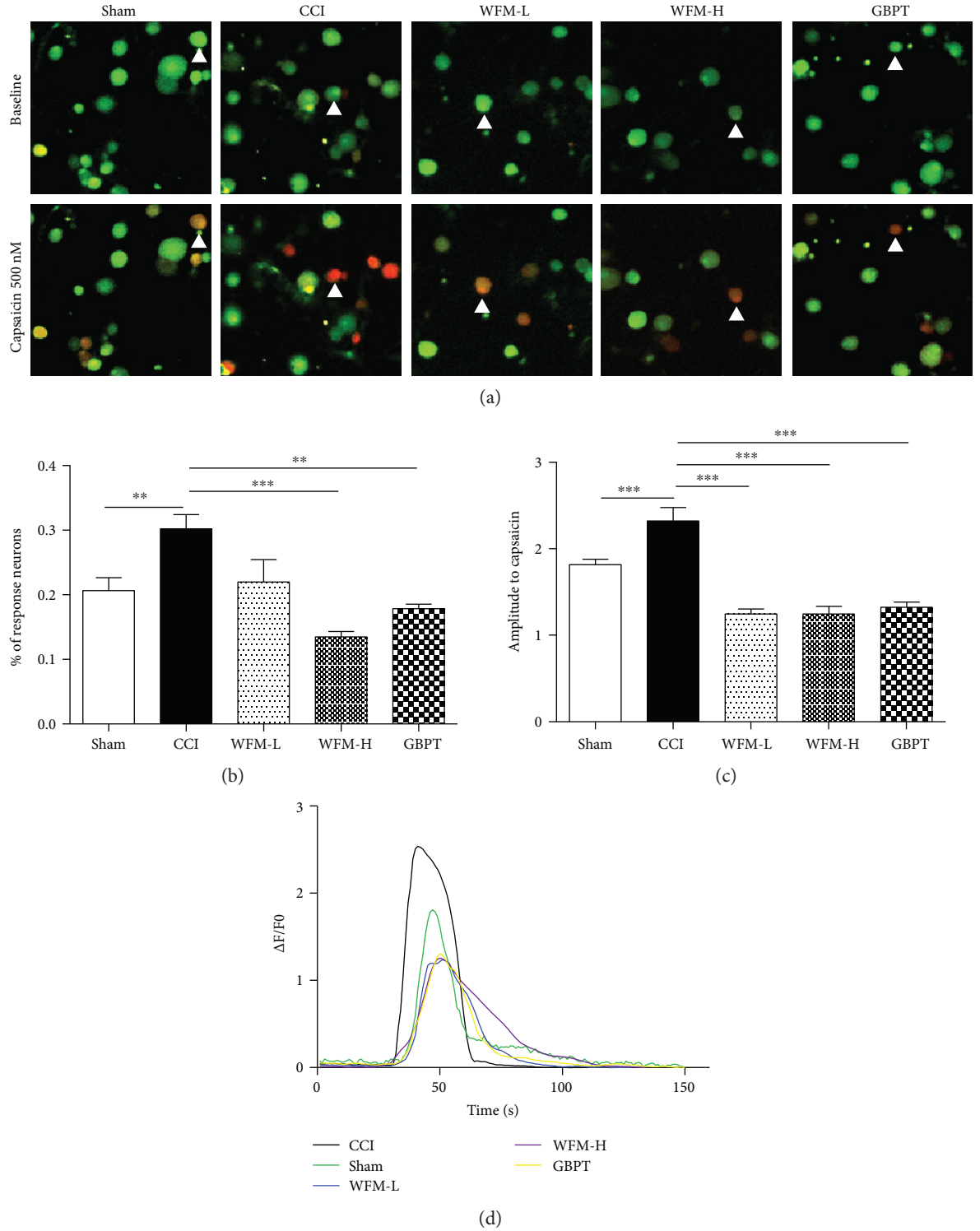

Figure 6: WFM attenuated capsaicin-induced response in CCI-treated sensory neurons. (a) Representative calcium images in cultured DRG neurons from CCI contralateral and ipsilateral. WFM and GBPT could significantly inhibit the responses of DRG neurons from CCI ipsilateral to 500 nM capsaicin. (b) The percentage of reactive neurons to 500 nM capsaicin stimulus. The percentage of DRG neuron response to 500 nM capsaicin stimulus was significantly higher in the ipsilateral (CCI) than in the contralateral (control). WFM and GBPT could significantly reduce the response percentage of DRG neurons to the same concentration of capsaicin stimulus. (c) The amplitude of the response neurons to 500 nM capsaicin stimulus. The amplitude of DRG neurons response to 500 nM capsaicin stimulus was significantly larger in the ipsilateral (CCI) than in the contralateral (control). Both WFM (high dose and low dose) and GBPT could effectively inhibit capsaicin-induced response. (d) Calcium imaging response curves of DRG neurons to different stimulus. White arrows indicate these active neurons. $^{*}p < 0.05$, $^{**}p < 0.01$, $^{***}p < 0.001$.

5. Conclusion

In summary, our results showed the efficacy of WFM in relieving CCI-induced hyperalgesia in a mouse model, which shed light on effective and novel therapies for pain management via downregulating TRPV1. Further observations should be conducted to reveal the antipain characteristics of WFM in further studies.

Abbreviations

CCI: Chronic constriction injury
DRG: Dorsal root ganglia
MWT: Mechanical withdrawal threshold
TRPV1: The transient receptor potential vanilloid 1
TWL: Thermal withdrawal latency
WFM: Water extract of frankincense and myrrh.

Ethical Approval

All experiments were performed in accordance with protocols approved by the Animal Care and Use Committee at the Nanjing University of Chinese Medicine.

Disclosure

Danyou Hu and Changming Wang are co-first authors.

Conflicts of Interest

The authors declare that they have no conflicts of interest.

Authors' Contributions

Danyou Hu, Changming Wang, and Guang Yu carried out the experiments and performed statistical analyses. Guang Yu and Zongxiang Tang conceived, designed and planned the project, reviewed the statistical analyses, and wrote the manuscript. Fengxian Li, Niuniu Yang, Shulan Su, Yan Yang, Chan Zhu, Xiaolin Yuan, Zhongli Wang, Hao Shi, Lei Yu, Xiao Geng, and Leying Gu helped perform experiments. All authors read and approved the final manuscript.

Acknowledgments

This work was supported by the Natural Science Foundation of Jiangsu Province to Guang Yu (BK20151571), the Open Project Program of the Jiangsu Key Laboratory for High Technology Research of TCM Formulae to Shulan Su and Guang Yu (FJGJS-2015-12), the National Natural Science Foundation of China to Fengxian Li (81501082), the National Natural Science Foundation of China to Changming Wang (81600966), the National Natural Science Foundation of China to Zongxiang Tang (31271181, 31328012), the Hunan Cooperative Innovation Center for Molecular Target New Drug Study and Jiangsu Collaborative Innovation Center of Traditional Chinese Medicine (TCM) Prevention and Treatment of Tumor, and a project funded by the Priority Academic Program Development of Jiangsu Higher Education Institutions (Integration of Traditional Chinese and Western Medicine), sponsored by Qing Lan Project in Jiangsu Province.

References

[1] D. Bridges, S. W. Thompson, and A. S. Rice, "Mechanisms of neuropathic pain," *British Journal of Anaesthesia*, vol. 87, no. 1, pp. 12–26, 2001.

[2] K. Iwata, Y. Imamura, K. Honda, and M. Shinoda, "Physiological mechanisms of neuropathic pain: the orofacial region," *International Review of Neurobiology*, vol. 97, pp. 227–250, 2011, (0074-7742 (Print)).

[3] G. R. Tibbs, D. J. Posson, and P. A. Goldstein, "Voltage-gated ion channels in the PNS: novel therapies for neuropathic pain?" *Trends in Pharmacological Sciences*, vol. 37, no. 7, pp. 522–542, 2016.

[4] Y. S. Gwak, H. Y. Kim, B. H. Lee, and C. H. Yang, "Combined approaches for the relief of spinal cord injury-induced neuropathic pain," *Complementary Therapies in Medicine*, vol. 25, pp. 27–33, 2016.

[5] R. H. Dworkin, D. C. Turk, N. P. Katz et al., "Evidence-based clinical trial design for chronic pain pharmacotherapy: a blueprint for ACTION," *Pain*, vol. 152, 3 Supplement, pp. S107–S115, 2011.

[6] S. Su, Y. Hua, Y. Wang et al., "Evaluation of the anti-inflammatory and analgesic properties of individual and combined extracts from Commiphora myrrha, and Boswellia carterii," *Journal of Ethnopharmacology*, vol. 139, no. 2, pp. 649–656, 2012.

[7] H. Safayhi, T. Mack, J. Sabieraj, M. I. Anazodo, L. R. Subramanian, and H. P. Ammon, "Boswellic acids: novel, specific, nonredox inhibitors of 5-lipoxygenase," *The Journal of Pharmacology and Experimental Therapeutics*, vol. 261, no. 3, pp. 1143–1146, 1992.

[8] A. Y. Fan, L. Lao, R. X. Zhang et al., "Effects of an acetone extract of Boswellia carterii Birdw. (Burseraceae) gum resin on adjuvant-induced arthritis in lewis rats," *Journal of Ethnopharmacology*, vol. 101, no. 1–3, pp. 104–109, 2005.

[9] H. P. Ammon, "Modulation of the immune system by *Boswellia serrata* extracts and boswellic acids," *Phytomedicine : International Journal of Phytotherapy and Phytopharmacology*, vol. 17, no. 11, pp. 862–867, 2010.

[10] E. S. El Ashry, N. Rashed, O. M. Salama, and A. Saleh, "Components, therapeutic value and uses of myrrh," *Die Pharmazie*, vol. 58, no. 3, pp. 163–168, 2003.

[11] A. M. Massoud, F. H. El Ebiary, M. M. Abou-Gamra, G. F. Mohamed, and S. M. Shaker, "Evaluation of schistosomicidal activity of myrrh extract: parasitological and histological study," *Journal of the Egyptian Society of Parasitology*, vol. 34, no. 3 Suppl, pp. 1051–1076, 2004.

[12] M. A. Shalaby and A. A. Hammouda, "Analgesic, anti-inflammatory and anti-hyperlipidemic activities of Commiphora molmol extract (myrrh)," *Journal of Intercultural Ethnopharmacology*, vol. 3, no. 2, pp. 56–62, 2014.

[13] N. Kiguchi, Y. Kobayashi, and S. Kishioka, "Chemokines and cytokines in neuroinflammation leading to neuropathic pain," *Current Opinion in Pharmacology*, vol. 12, no. 1, pp. 55–61, 2012.

[14] M. J. Caterina, M. A. Schumacher, M. Tominaga, T. A. Rosen, J. D. Levine, and D. Julius, "The capsaicin receptor: a heat-

activated ion channel in the pain pathway," *Nature*, vol. 389, no. 6653, pp. 816–824, 1997.

[15] D. Spicarova, P. Adamek, N. Kalynovska, P. Mrozkova, and J. Palecek, "TRPV1 receptor inhibition decreases CCL2-induced hyperalgesia," *Neuropharmacology*, vol. 81, pp. 75–84, 2014.

[16] X. Xiao, X. T. Zhao, L. C. Xu et al., "Shp-1 dephosphorylates TRPV1 in dorsal root ganglion neurons and alleviates CFA-induced inflammatory pain in rats," *Pain*, vol. 156, no. 4, pp. 597–608, 2015.

[17] L. S. Premkumar, "Targeting TRPV1 as an alternative approach to narcotic analgesics to treat chronic pain conditions," *The AAPS Journal*, vol. 12, no. 3, pp. 361–370, 2010.

[18] L. Arendt-Nielsen, S. Harris, G. T. Whiteside et al., "A randomized, double-blind, positive-controlled, 3-way cross-over human experimental pain study of a TRPV1 antagonist (V116517) in healthy volunteers and comparison with preclinical profile," *Pain*, vol. 157, no. 9, pp. 2057–2067, 2016.

[19] S. Su, J. Duan, T. Chen et al., "Frankincense and myrrh suppress inflammation via regulation of the metabolic profiling and the MAPK signaling pathway," *Scientific Reports*, vol. 5, article no. 13668, 2015.

[20] K. Hole and A. Tjolsen, "The tail-flick and formalin tests in rodents: changes in skin temperature as a confounding factor," *Pain*, vol. 53, no. 3, pp. 247–254, 1993.

[21] Q. Liu, H. J. Weng, K. N. Patel et al., "The distinct roles of two GPCRs, MrgprC11 and PAR2, in itch and hyperalgesia," *Science Signaling*, vol. 4, no. 181, p. ra45, 2011.

[22] C. Wang, Z. Wang, Y. Yang et al., "Pirt contributes to uterine contraction-induced pain in mice," *Molecular Pain*, vol. 11, p. 57, 2015.

[23] B. T. Kurien and R. H. Scofield, "Western blotting: an introduction," *Methods in Molecular Biology*, vol. 1312, pp. 17–30, 2015.

[24] W. Ma, Y. Zhang, C. Bantel, and J. C. Eisenach, "Medium and large injured dorsal root ganglion cells increase TRPV-1, accompanied by increased alpha2C-adrenoceptor co-expression and functional inhibition by clonidine," *Pain*, vol. 113, no. 3, pp. 386–394, 2005.

[25] E. Gabay and M. Tal, "Pain behavior and nerve electrophysiology in the CCI model of neuropathic pain," *Pain*, vol. 110, no. 1-2, pp. 354–360, 2004.

[26] M. Tominaga, M. J. Caterina, A. B. Malmberg et al., "The cloned capsaicin receptor integrates multiple pain-producing stimuli," *Neuron*, vol. 21, no. 3, pp. 531–543, 1998.

[27] R. Brito, S. Sheth, D. Mukherjea, L. P. Rybak, and V. Ramkumar, "TRPV1: a potential drug target for treating various diseases," *Cell*, vol. 3, no. 2, pp. 517–545, 2014.

[28] A. Szallasi, D. N. Cortright, C. A. Blum, and S. R. Eid, "The vanilloid receptor TRPV1: 10 years from channel cloning to antagonist proof-of-concept," *Nature Reviews Drug Discovery*, vol. 6, no. 5, pp. 357–372, 2007.

[29] T. Trang, R. Al-Hasani, D. Salvemini, M. W. Salter, H. Gutstein, and C. M. Cahill, "Pain and poppies: the good, the bad, and the ugly of opioid analgesics," *The Journal of Neuroscience*, vol. 35, no. 41, pp. 13879–13888, 2015.

[30] J. Szolcsanyi and Z. Sandor, "Multisteric TRPV1 nocisensor: a target for analgesics," *Trends in Pharmacological Sciences*, vol. 33, no. 12, pp. 646–655, 2012.

[31] E. Palazzo, L. Luongo, V. de Novellis, L. Berrino, F. Rossi, and S. Maione, "Moving towards supraspinal TRPV1 receptors for chronic pain relief," *Molecular Pain*, vol. 6, p. 66, 2010.

[32] M. B. Sant'Anna, R. Kusuda, T. A. Bozzo et al., "Medial plantar nerve ligation as a novel model of neuropathic pain in mice: pharmacological and molecular characterization," *Scientific Reports*, vol. 6, article no. 26955, 2016.

[33] R. Baron, A. Binder, N. Attal, R. Casale, A. H. Dickenson, and R. D. Treede, "Neuropathic low back pain in clinical practice," *European Journal of Pain*, vol. 20, no. 6, pp. 861–873, 2016.

Hindawi
Neural Plasticity
Volume 2017, Article ID 3270725, 12 pages
https://doi.org/10.1155/2017/3270725

Research Article

Pathological Role of Peptidyl-Prolyl Isomerase Pin1 in the Disruption of Synaptic Plasticity in Alzheimer's Disease

Lingyan Xu,[1] Zhiyun Ren,[1] Frances E. Chow,[2] Richard Tsai,[2] Tongzheng Liu,[3] Flavio Rizzolio,[4,5] Silvia Boffo,[4,5] Yungen Xu,[6] Shaohui Huang,[7] Carol F. Lippa,[2] and Yuesong Gong[1,2]

[1] *Jiangsu Key Laboratory for Functional Substance of Chinese Medicine, Department of Biopharmaceutics and Food Science, School of Pharmacy, Nanjing University of Chinese Medicine, Nanjing 210023, China*
[2] *Department of Neurology, Drexel University College of Medicine, Philadelphia, PA 19102, USA*
[3] *Department of Oncology, Mayo Clinic, Rochester, MN 55905, USA*
[4] *Sbarro Institute for Cancer Research and Molecular Medicine, Center for Biotechnology, Temple University, Philadelphia, PA 19122, USA*
[5] *Department of Molecular Science and Nanosystems, Ca' Foscari Università di Venezia, Via Torino 155, 30172 Venezia-Mestre, Italy*
[6] *Department of Medicinal Chemistry, China Pharmaceutical University, Nanjing 21009, China*
[7] *Department of Physiology, University of Pennsylvania School of Medicine, Philadelphia, PA 19104, USA*

Correspondence should be addressed to Carol F. Lippa; carol.lippa@drexelmed.edu and Yuesong Gong; ygong@njucm.edu.cn

Received 28 October 2016; Accepted 12 December 2016; Published 26 March 2017

Academic Editor: Jason Huang

Synaptic loss is the structural basis for memory impairment in Alzheimer's disease (AD). While the underlying pathological mechanism remains elusive, it is known that misfolded proteins accumulate as β-amyloid (Aβ) plaques and hyperphosphorylated Tau tangles decades before the onset of clinical disease. The loss of Pin1 facilitates the formation of these misfolded proteins in AD. Pin1 protein controls cell-cycle progression and determines the fate of proteins by the ubiquitin proteasome system. The activity of the ubiquitin proteasome system directly affects the functional and structural plasticity of the synapse. We localized Pin1 to dendritic rafts and postsynaptic density (PSD) and found the pathological loss of Pin1 within the synapses of AD brain cortical tissues. The loss of Pin1 activity may alter the ubiquitin-regulated modification of PSD proteins and decrease levels of Shank protein, resulting in aberrant synaptic structure. The loss of Pin1 activity, induced by oxidative stress, may also render neurons more susceptible to the toxicity of oligomers of Aβ and to excitation, thereby inhibiting NMDA receptor-mediated synaptic plasticity and exacerbating NMDA receptor-mediated synaptic degeneration. These results suggest that loss of Pin1 activity could lead to the loss of synaptic plasticity in the development of AD.

1. Introduction

The hallmark pathological lesions of Alzheimer's disease (AD) are β-amyloid (Aβ) plaques, neurofibrillary tangles, and synaptic loss [1]. Among these, Aβ plaques and tangles can be detected decades before AD symptoms arise [2–4]. Synaptic loss begins in preclinical AD and is the strongest anatomical correlate of the degree of clinical impairment [5]. The molecular pathophysiology of synaptic dysfunction remains elusive, particularly the molecular events that lead up to the loss of synaptic plasticity decades before the onset of clinical disease [6].

Oligomers of Aβ, the early aggregates of Aβ peptides, have been suggested as culprits in dysfunction of synaptic plasticity in early AD patient brains [1]. Pin1 is a unique peptidyl-prolyl isomerase that catalyzes cis-trans isomerization of phosphorylated Ser/Thr-Pro motifs. Increase in oligomers of Aβ and other age-related insults induce oxidative stress [7], which could cause the loss of Pin1 activity [8, 9]. Interestingly, loss of Pin1 facilitates formation of plaques

and tangles [10–12], suppresses neuronal differentiation [13], and induces neurodegeneration [14]. The early aggregates of plaques and tangles associate with detergent-resistant rafts and with the postsynaptic density (PSD) [15, 16] which is crucial in organizing glutamate receptors within dendritic rafts. Activation of an NMDA receptor can induce the phosphorylation of several hundred PSD proteins [17]. This includes hundreds of Ser/Thr-Pro motifs [18], a set of which upon cis-trans isomerization by Pin1 may affect ubiquitin modification of proteins [19, 20]. The activity of the ubiquitin proteasome system (UPS) can directly alter the plasticity of the PSD [21, 22]. PSD proteins are organized by Shank proteins [23, 24]. Mutation of Shank3 leads to modification of ubiquitin in Shank3 protein and results in loss of glutamate receptors within an aberrant PSD structure [25–27]. Shank3 protein is lost and highly modified by ubiquitin in synapses of AD patient brains [28, 29]. Pin1 controls protein synthesis in dendritic spines [30]. These findings indicate that loss of Pin1 activity could directly affect synaptic plasticity in the brains of AD patients.

We localized Pin1 to dendritic rafts and to the PSD and found a pathological loss of Pin1 within the synapses of AD patient brains. Loss of Pin1 activity may increase the modification of ubiquitin in PSD proteins and lead to the loss of Shank protein, resulting in aberrant PSD structure. This renders the synapse more susceptible to the toxic assault of oligomers of Aβ and excitation, thereby inhibiting synaptic plasticity and inducing synaptic degeneration, which may accelerate synaptic loss in preclinical AD. These findings could distinguish Pin1 as a target with the potential to protect synaptic function in preclinical AD.

2. Results

2.1. Pin1, Phosphorylated Tau, Oligomers of Aβ, and Glutamate Receptor Coincidently Exist in Detergent-Resistant Dendritic Rafts and PSD Fractions. To detect Pin1 proteins in detergent-resistant dendritic rafts and PSD, synaptosome fractions were effectively isolated from the frontal cortical tissues of human AD and normal control brains, and the synaptic markers PSD95 and Shank3 were enriched up to 9 and 8 times in synaptosome fractions, respectively (Figure 1(b)). The synaptosomes were further treated to isolate dendritic rafts and PSDs, and dendritic rafts and PSDs were analyzed by Western blot or dot blot.

First, to analyze the dendritic rafts, flotillin and GM1 ganglioside were used as markers. Both raft markers were detected in fraction 4 of the sucrose gradient. Calnexin, an ER marker used as a negative marker, was not detected in fraction 4. Pin1, NR1, and Shank3 coincidently were found in fraction 4 of the sucrose gradient from cortical tissues of human control and AD brains (Figure 1(a)). Meanwhile, phosphorylated Tau and oligomers of Aβ were detected obviously in dendritic rafts isolated from cortical tissues of human AD brains, but much less from cortical tissues of control brains (Figure 1(a)).

Second, to analyze PSD, PSD95 and Shank3 were used as markers of PSD. The PSD1 fraction was comprised of pellets of synaptosomes that were treated once by Triton X-100, and the PSD2 fraction was comprised of pellets of PSD1 treated by Triton X-100 one additional time [31] (Figure 1(b)). We found Pin1 proteins in the synaptosome and in the PSD fractions from cortical tissues of AD and control brains. Pin1 proteins exist in PSD fraction coincidently containing: PSD95, Shank3, and NR1. However, oligomers of Aβ and hyperphosphorylated Tau were observed only in PSD fractions of AD brain cortical tissues and not in PSD of control cortical tissues (Figure 1(b)). Although Pin1 proteins were not enriched in synaptosome and PSD fractions, these results suggest that Pin1 exist in dendritic rafts and in PSD.

Third, to further clarify the location of Pin1 at the synapse, the cultured cortical neurons of C57/BL6 mice at 21 DIV were used to detect the distribution of Pin1, Shank3, and NR1 proteins by immunocytochemical analysis. Shank3 proteins are expressed at the PSD in the dendritic spine of excitatory neurons [23]. We found that Pin1 proteins also partly colocalized with NR1 proteins along with Shank3 proteins at the dendritic spines of excitatory neurons (Figure 2).

2.2. Pin1 Proteins Are Altered at Synapses of Human AD and Tg2576 AD Mice Brains. Pin1 proteins have been identified at detergent-resistant synaptic structures: dendritic rafts and PSD (Figures 1 and 2). The loss of Pin1 is involved in the formation of Aβ plaques and hyperphosphorylated Tau tangles in AD patient brains [10, 11]. To detect whether Pin1 proteins were involved in the pathological changes found in synapses of AD patient brains, the cortical frontal tissues of human AD and age-matched control brains were used to isolate synaptosomes (Figure 1(b)). Synaptosomes were fractioned in 0.5% Triton X-100 by ultracentrifuge into a soluble synaptic fraction, synaptic rafts fraction, and PSD fraction. The Pin1 proteins in these fractions were separated by 16.5% Tris-tricine gel and the levels of these Pin1 proteins were detected by Western blot. We found total synaptic Pin1 protein to be significantly lost by 39% in human AD patient frontal cortical tissues compared with that in control tissues. The soluble synaptic Pin1 proteins were also significantly decreased by 76% in these AD samples, and the detergent-resistant Pin1 was significantly increased in dendritic rafts but significantly decreased in PSD fractions from cortical tissues of AD patient brains (Figure 3(a)). To confirm these pathological changes, the experiment was repeated with cortical tissues isolated from cortical tissues of Tg2576 amyloid-AD model mice brains at 18 months, which are equivalent to 55 years in human [32]. The total synaptic Pin1 protein and soluble synaptic Pin1 protein also showed significant loss, and the levels of Pin1 protein at dendritic rafts showed significant increase in Tg2576 mice brains (Figure 3(b)). These results indicate that the pathological loss of Pin1 proteins at the synapse could be involved in synaptic dysfunction in AD development.

2.3. Blocking of Pin1 Activity Increases the Modification of Ubiquitin in PSD Proteins. The activity of Pin1 protein affects ubiquitin modification of proteins [20], and the activity of the UPS can directly alter the plasticity of the PSD [21, 22]. The loss of Pin1 could alter the modification of ubiquitin in PSD proteins, leading to the alteration of structural and functional

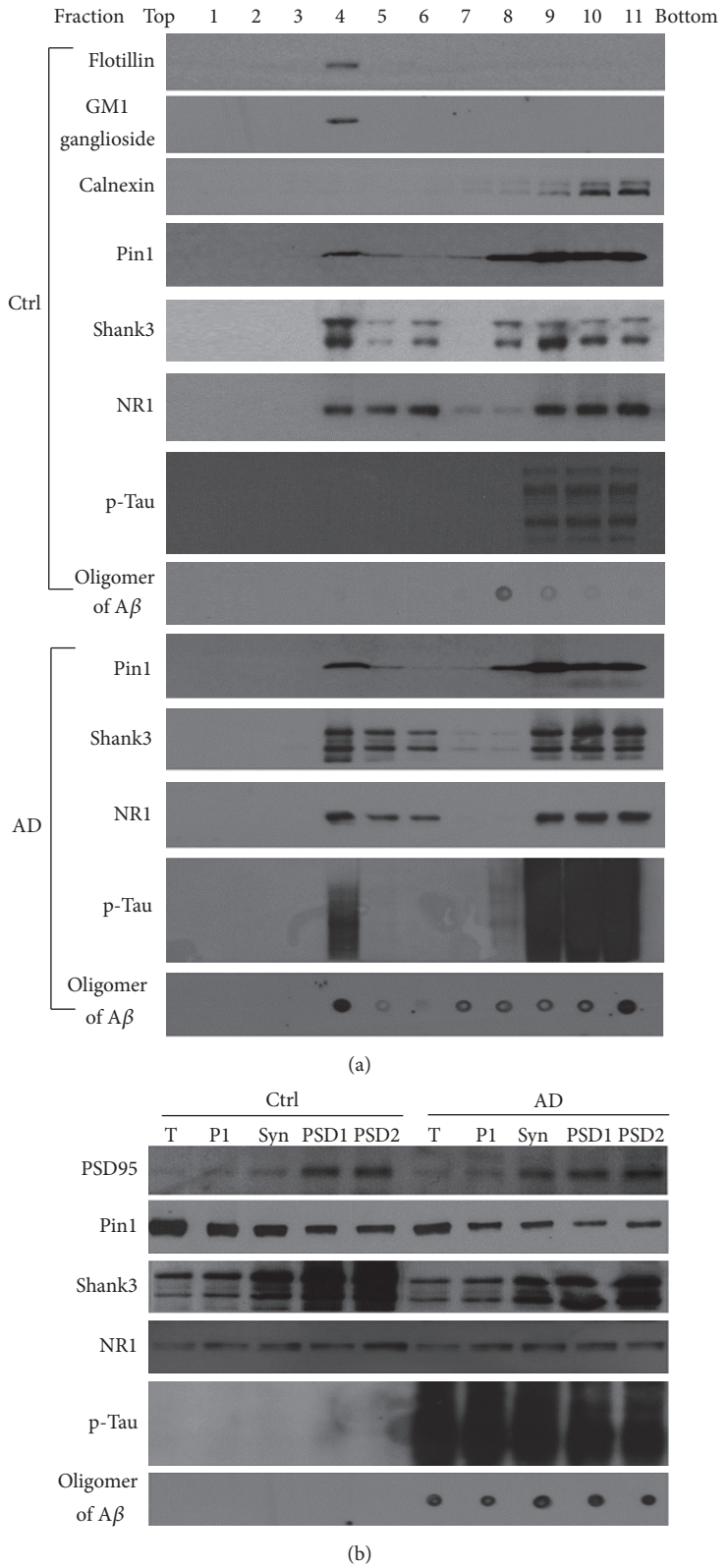

Figure 1: Pin1 proteins exist in detergent-resistant dendritic rafts and PSD fractions coincidently containing phosphorylated Tau, oligomers of Aβ, and glutamate receptor. The detergent-resistant synaptosome suspension was fractionated by sucrose gradient ultracentrifugation to isolate dendritic rafts and PSDs. (a) Analysis of dendritic rafts. Proteins in ultracentrifuged fractions at equal volume were analyzed by Western blot or dot blot. Fraction 4 contained flotillin and GM1 ganglioside, known markers for rafts, along with Pin1, p-Tau, oligomers of Aβ, Shank3, and NR1 proteins. Fraction 4 did not show calnexin, a marker of endoplasmic reticulum (ER). (b) Analysis of the PSD. PSD proteins at equal amounts were analyzed by Western blot or dot blot. PSD95 and Shank3, both known protein markers of the PSD, were enriched in the PSD fraction (PSD2), along with Pin1, NR1, p-Tau, and oligomers of Aβ. Ctrl: human control tissues; AD: human AD tissues; T: total tissue; P1: total membrane; NR1: a subunit of NMDA receptor; Syn: synaptosome; PSD1: pellets from the synaptosome treated once by 0.5% Triton X-100; PSD2: pellets from PSD1 treated once more by 0.5% Triton X-100.

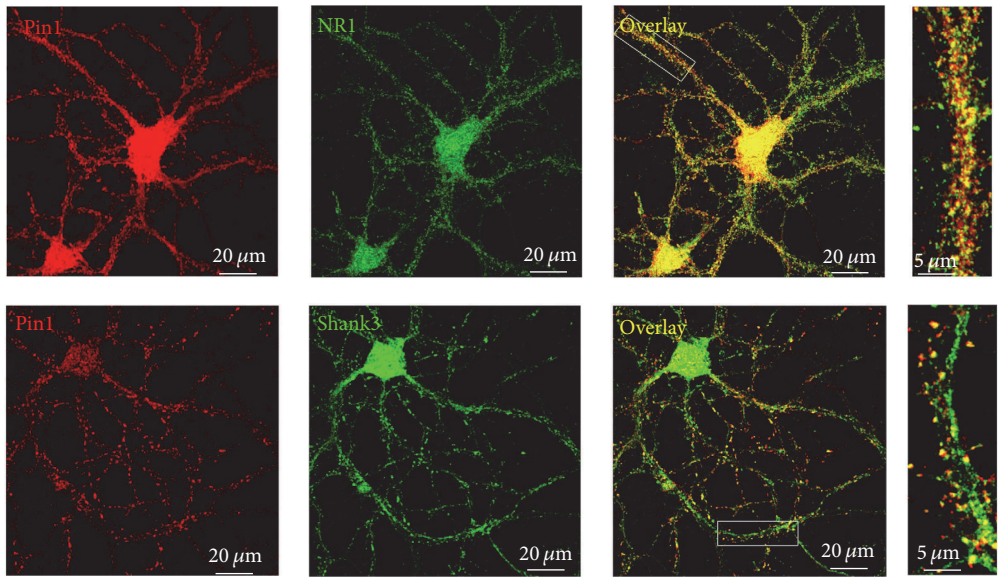

FIGURE 2: Pin1 proteins are partly colocalized with Shank3 and NR1 proteins at dendritic spines of neurons. Cortical neurons at 21 DIV were double immunolabeled for Pin1 (red) and Shank3 (green) or NR1 (green). When the images were merged, the yellow in the overlay showed colocalization of Pin1-immunoreactive puncta with Shank3 and NR1 proteins. Right panels were high-magnification images of selected overlays.

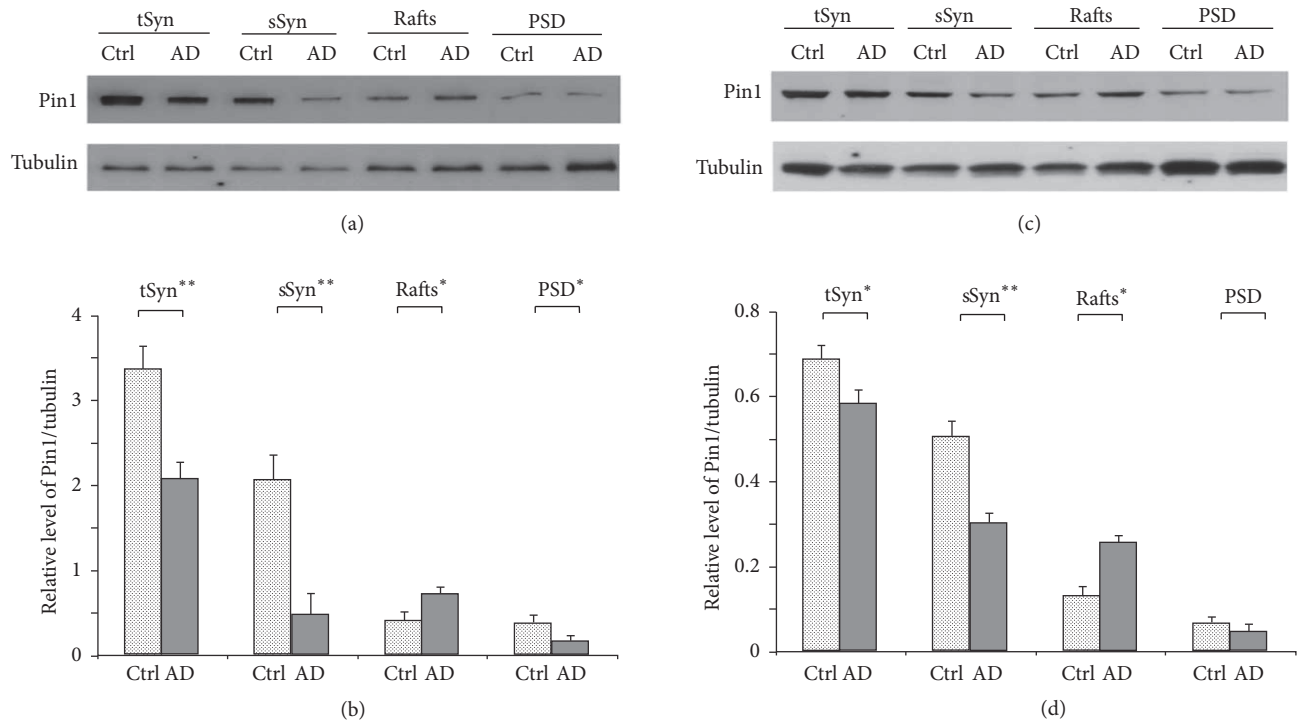

FIGURE 3: Pin1 proteins show pathological loss in the synapses of human AD and Tg2576 AD model mice. The Pin1 proteins in synaptosomes, soluble synaptosomes, dendritic rafts, and PSD fractions were isolated from human frontal cortical tissues (a and b) and from Tg2576 AD model mice cortical tissues (c and d) and were detected by Western blot. (a and c) Representative Western blot experiment. (b and d) Results from densitometric imaging of these same samples (human AD frontal cortical tissues, $n = 8$; human frontal cortical tissues, $n = 5$; Tg2576 mice, $n = 7$; and wild-type mice, $n = 7$; $^{*}p < 0.05$, $^{**}p < 0.01$). Ctrl: human control frontal cortical tissues; AD: human AD frontal cortical tissues; tSyn: the supernatant of synaptosomes extracted by 1% SDS; sSyn: the supernatant of synaptosomes extracted by 0.5% Triton X-100.

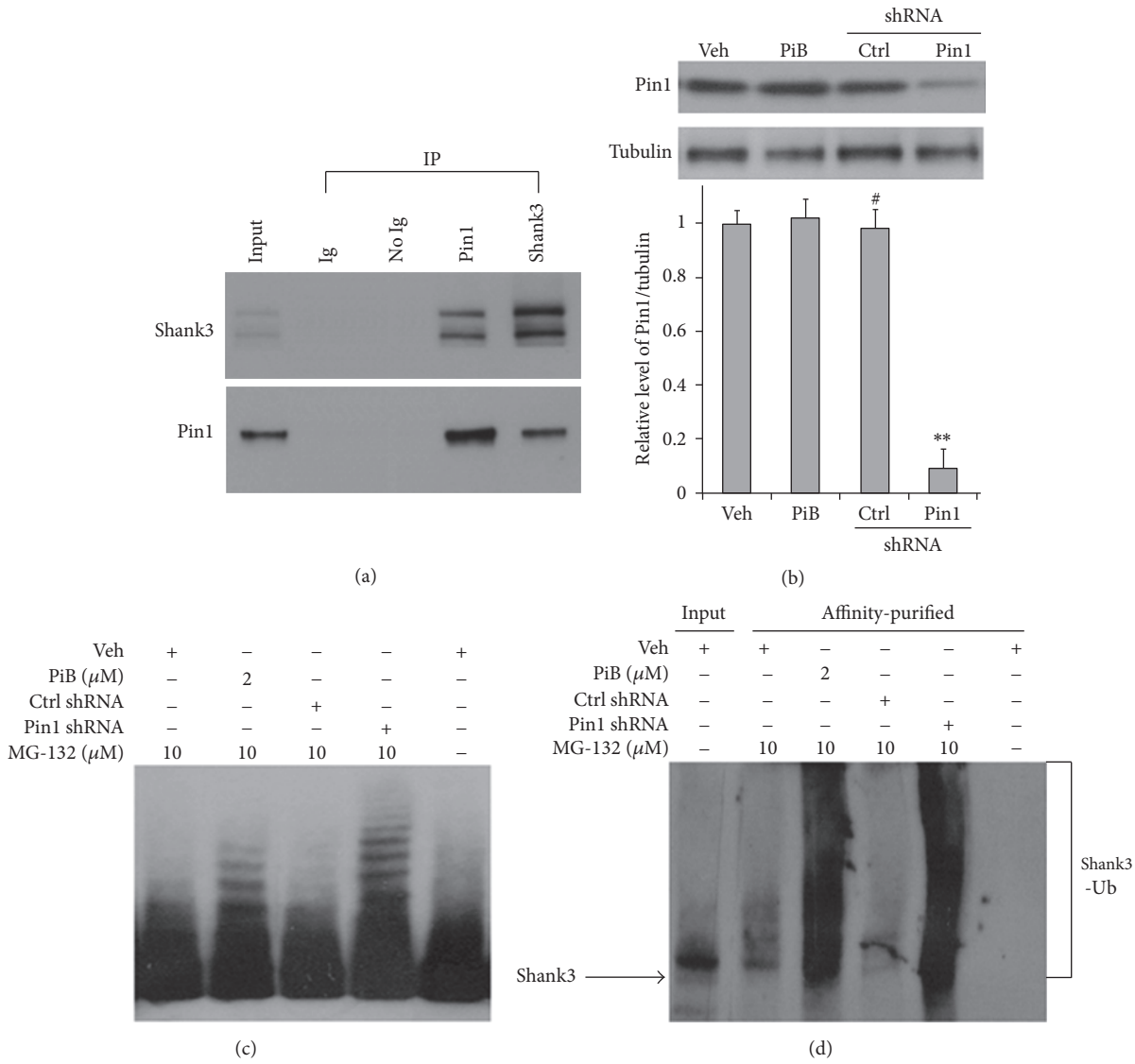

Figure 4: Blocking of Pin1 activity increases the modification of ubiquitin in PSD proteins. C57/BL6 cortical neurons at 21 DIV were incubated with PiB and MG-132 for 24 h and transfected by Pin1 shRNA or control shRNA lentivirus for 48 h, respectively; the PSDs were isolated and analyzed with Western blot. (a) Coimmunoprecipitation between Pin1 and Shank3 proteins. (b) Total Pin1 proteins were knocked down ($n = 7$ dishes for each experimental condition, $^{**}p < 0.01$; $^{\#}p > 0.05$). (c) Ladders of Shank3 proteins after the loss of Pin1 activity. (d) Ubiquitinated Shank3 proteins were enriched by ubiquitin-affinity purification and recognized by Shank3 antibody in Western blot.

plasticity of the PSD. To test this hypothesis, cultured cortical neurons of C57/BL6 mice at 21 DIV were incubated with PiB, the selective inhibitor of Pin1 [33, 34], and MG-132, a proteasome inhibitor, for 24 h at different concentrations (Figure 4(a)). The neurons were collected and PSD fractions were isolated. PSD proteins at equal amounts were analyzed by Western blot. The ubiquitin-labeled PSD proteins were detected by anti-ubiquitin antibodies. Ubiquitin-labeled PSD proteins significantly increased after the cultured neurons were incubated with PiB for 24 h (Figures 4(c) and 4(d)). Because Shank3 protein is a core protein of PSD [23] and Shank3 protein shows polyubiquitination and loss in AD [28, 29], Shank3 protein was analyzed in this test. We observed Pin1 protein and Shank3 protein in synaptosome from cortical tissues of human control brains showed associated together by immunoprecipitation (Figure 4(a)). Meanwhile, Pin1 shRNA was used to knock down Pin1 protein in cultured neurons; the level of Pin1 protein was decreased by about 82% after neurons were transfected by Pin1 shRNA lentivirus for 48 h (Figure 4(b)). We used these test conditions to treat cultured neurons with PiB for 24 h and with Pin1 shRNA for 48 h. The PSD fractions were then isolated. When the amount of PSD protein was increased to 75 μg for Shank3 Western blot, ladders of Shank3 proteins were apparent in the PSD fractions after treatment with Pin1 inhibitor PiB or Pin1 shRNA (Figure 4(c)). To confirm that these ladders of Shank3 proteins contained ubiquitin modification, we enriched the ubiquitinated proteins in isolated PSD using a

polyubiquitin enrichment kit. These ubiquitinated proteins were recognized by Shank3 antibody in Western blot, and Shank3 showed obvious ubiquitination (Figure 4(d)). These results indicate that loss of Pin1 activity may lead to an increase in ubiquitinated proteins in the PSD, which could increase the degradation of Shank3 and other PSD proteins [28, 29], leading to changes in the structure of the PSD in AD development.

2.4. Blocking of Pin1 Activity Disrupts the Structural Plasticity of PSD. Thousands of proteins interact together at the PSD. Shank proteins organize these proteins to form macromolecules including NMDA, AMPA, and mGlu receptors [23]. Because of Shank proteins' large organizational role, the loss of Shank3 proteins and the extensive modification of ubiquitin in Shank3 proteins may result in aberrant PSD structure and glutamate receptor loss [26, 27]. Shank3 proteins show loss and are highly modified by ubiquitin in AD [28, 29]. To evaluate the pathological degradation of PSD proteins after loss of Pin1 activity in AD brain, we selected Shank3 as the functional and structural marker of changes in PSD. The mature synapses at 21 DIV are more sensitive to NMDA and other insults. Cultured neurons of C57/BL6 mice at 21 DIV were treated by PiB at 0.5 μM and 2.0 μM to block Pin1 activity and with control vehicle for 24 h (Figures 5(a)–5(f)), while cultured $Pin1^{+/+}$, $Pin1^{+/-}$, and $Pin1^{-/-}$ neurons at 21 DIV were also examined (Figures 5(g)–5(l)). The neurons on coverslips were analyzed using immunocytochemistry to detect Shank3 protein levels, and the neurons in dishes were used to isolate PSD fractions, which were analyzed by Western blot. We found that C57/BL6 neurons treated with PiB showed significant reduction in Shank3 protein levels (Figures 5(a)–5(f), 5(m), and 5(n)). These results indicated that the loss of Pin1 activity could lead to the loss of Shank3 protein and thus affect the structure of the PSD. The same results were replicated in cultured $Pin1^{-/-}$ neurons, but not in $Pin1^{+/+}$ or $Pin1^{+/-}$ neurons at 21 DIV (Figures 5(g)–5(l), 5(m), and 5(n)). To avoid synaptic degeneration due to the increased Aβ peptide after the loss of Pin1 activity [11], we used cultured cortical neurons from β-amyloid precursor protein $(APP)^{-/-}$ mice to repeat these experiments. The inhibitor of Pin1 and the Pin1 shRNA can also decrease the levels of Shank3 proteins in neurons of $APP^{-/-}$ mice in vitro (data not shown). These results suggest the role of loss of Pin1 activity in reducing levels of Shank3 protein, in addition to direct Aβ peptide toxicity in cultured neurons.

2.5. Inhibition of Pin1 Activity Blocks NMDA Receptor-Mediated Turnover of Shank3 and PSD95 Proteins and Increases NMDA Receptor- and Aβ Oligomer-Mediated Degradation of Shank3 and PSD95 Proteins. The activity of synaptic NMDA receptors regulates the dynamics of proteins in PSD including Shank3 and PSD95 protein [19, 35]. Because the synapses of cortical neurons are functional at 12 DIV and mature at 21 DIV [36] and Pin1 protein is already colocalized with NR1 and Shank3 proteins at dendritic spine at 15 DIV (data not shown), to detect how the loss of Pin1 activity affects levels of Shank and PSD95 proteins in neurons, here we used cortical neurons at 15 DIV to observe NMDA receptor-mediated turnover of Shank3 and PSD95 proteins after the loss of Pin1 activity. Memantine, a noncompetitive antagonist of NMDA receptors, has been used clinically in the treatment of AD to block neuronal oxidative stress [7]. In this test, we selected memantine and another selective competitive antagonist of NMDA receptor AP-5 to block NMDA receptor and observe the effects of Pin1 on levels of Shank3 and PSD95 proteins induced by NMDA at 0.1 μM and 10 μM. According to several rodent studies and human clinical trials, at 10 μM memantine exerts its effect at NMDA receptors [37–39] in addition to other receptors. We selected 0.5 and 5 μM concentrations of memantine for this test. After memantine, NMDA, PiB, and oligomers of Aβ were added to cultured neurons for 24 h (Figure 6), neurons were then collected, and levels of Shank3 and PSD95 proteins were detected by Western blot. 5 μM memantine significantly decreased levels of Shank3 and PSD95 proteins. 50 nM (data not shown) and 100 nM NMDA significantly increased the levels of Shank3 and PSD95 proteins; 5 μM memantine (Figure 6) and 0.5 μM AP-5, a selective antagonist of NMDA receptor (data not shown), blocked the increase of Shank3 and PSD95 proteins in neurons induced by 100 nM NMDA (Figure 6). These results suggest the ability of 50 nM and 100 nM NMDA to induce an increase in Shank3 and PSD95 proteins and to protect synaptic function [36, 40, 41]. After the loss of Pin1 activity in the presence of PiB, the NMDA receptor-mediated increase of Shank3 and PSD95 proteins was significantly blocked (Figure 6). Meanwhile, we found that 10 μM NMDA or 0.5 μM PiB individually did not change the level of Shank3 protein; however when both were incubated with cultured neurons together, levels of Shank3 protein were significantly reduced. 0.5 μM PiB also increased the reduction of Shank3 and PSD95 proteins induced by oligomers of Aβ (Figure 6). These findings indicate that the loss of Pin1 activity could block NMDA receptor-mediated turnover of Shank3 and PSD95 proteins and increase NMDA receptor- and Aβ oligomer-mediated degradation of Shank3 and PSD95 proteins, contributing to synaptic loss in AD development.

3. Discussion

Pin1 protein regulates the function of mitotic phosphoproteins and determines cell-cycle progression [9]. The loss of Pin1 is a common pathological cause linked to the production of Aβ and hyperphosphorylated Tau in AD [10, 11, 42]. Here we identified and showed the association of Pin1 with Shank proteins at dendritic rafts and the PSD, in which both fractions are associated with NR1; this finding suggests Pin1 may regulate signal transduction at dendritic rafts and signal processing at the PSD. The loss of Pin1 activity alters the modification of ubiquitin in PSD proteins and leads to the loss of Shank3 protein. As a result, Pin1 loss may make aberrant synapses more susceptible to the toxic effects of molecules such as oligomers of Aβ and glutamate, thereby inhibiting NMDA receptor-mediated turnover of Shank protein and synaptic generation, and exaggerating NMDA receptor-mediated synaptic degeneration. Pin1 could play a pathological role in synaptic dysfunction in addition

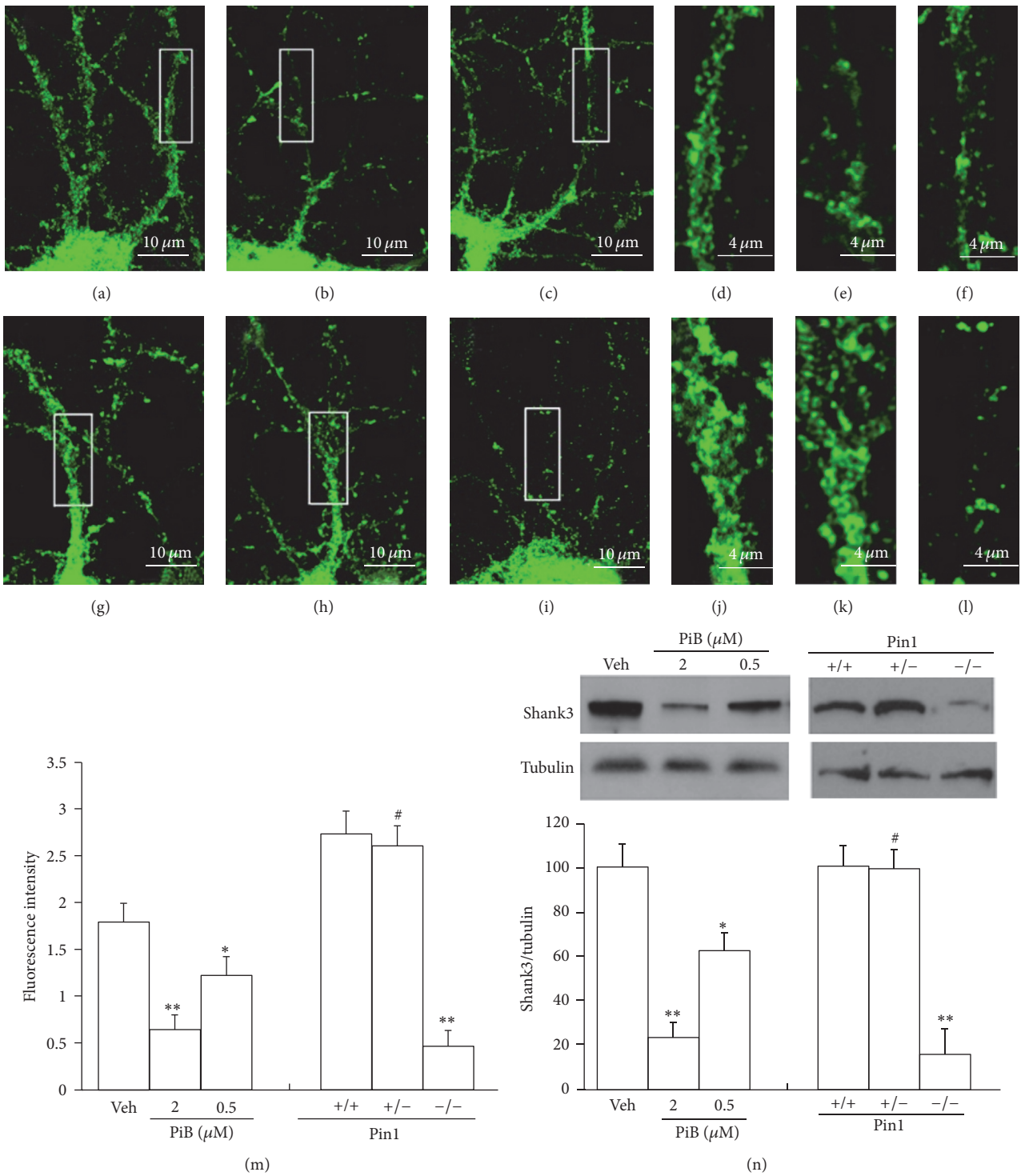

FIGURE 5: Blocking of Pin1 activity leads to degradation of Shank3 proteins in PSD. Cultured cortical neurons at 21 DIV were prepared on coverslips for immunofluorescence detection and in 10 cm dishes for immunoblot assay. Panels (a)–(f) showed the cultured cortical neurons of C57/BL6 mice at 21 DIV treated with vehicle (a and d), 2 μM PiB (b and e), or 0.5 μM PiB (c and f) for 24 h; panels (d), (e), and (f) were the high-magnification images of selected fields. Panels (g)–(l) showed the cultured cortical neurons of Pin1$^{+/+}$ (g and j), Pin1$^{+/-}$ (h and k), and Pin1$^{-/-}$ (i and l) mice at 21 DIV; panels (j), (k), and (l) were the high-magnification images of selected fields. These neurons on coverslips were fixed, permeabilized, and labeled by Shank3 antibody for immunofluorescence detection by immunocytochemistry. (m) Immunofluorescence intensity demonstrated a large PiB-induced decrease in Shank3 proteins from seven independent experiments (~90 neurons for each experimental condition, $^{**}p < 0.01$; $^{*}p < 0.05$). (n) Western blots showed significant decrease in the levels of Shank3 proteins in PiB-treated or in Pin1$^{-/-}$ neurons compared with vehicle-treated or Pin1$^{+/+}$ neuron extracts, respectively ($n = 7$ dishes for each experimental condition, $^{**}p < 0.01$; $^{*}p < 0.05$; $^{\#}p > 0.05$).

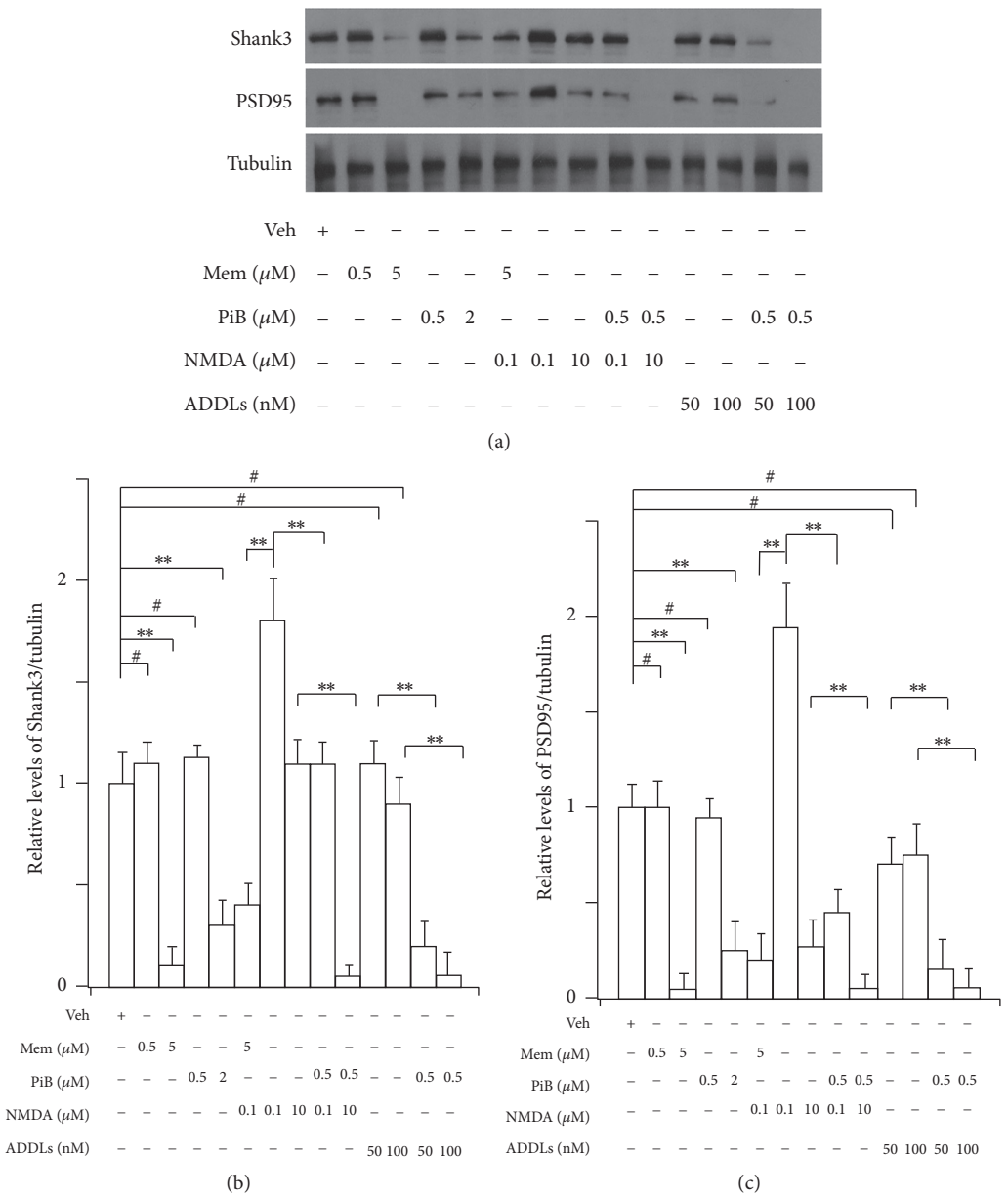

Figure 6: Blocking of Pin1 activity blocks NMDA receptor-mediated turnover of Skank3 and increases degradation of Shank3 and PSD95 induced by oligomers of Aβ and NMDA in cultured neurons. Cortical neurons at 15 DIV were incubated with memantine, NMDA, PiB, and oligomers of Aβ for 24 h. (a) Representative Western blot. (b and c) Results from densitometric imaging of these tests. Memantine 10 μM significantly decreased levels of Shank3 and PSD95 proteins. NMDA 100 nM significantly increased levels of these proteins, and 10 μM memantine significantly inhibited the increase of Shank3 induced by 100 nM NMDA. When 10 μM NMDA and 0.5 μM PiB were incubated with neuron together, these proteins were significantly decreased. The same results were observed between PiB and oligomers of Aβ from seven independent experiments ($n = 7$ dishes for each experimental condition, $^{**}p < 0.001$, $^{\#}p > 0.05$).

to the formation of misfolded proteins in preclinical stages of AD.

With aging, the activity of Pin1 protein may be lost by oxidation in mild cognitive impairment [8, 43], which could lead to the formation of Aβ plaques and hyperphosphorylated Tau in preclinical stages of AD [10–12]. We observed that the levels of Pin1 proteins are significantly lost in the synaptic fractions of AD brain cortical tissues (Figure 3), in addition to the loss of Pin1 protein in total AD brain tissues [10]. In vitro, the loss of Pin1 activity increases the modification of ubiquitination in PSD proteins (Figure 4). Modification of synaptic proteins mediates the protein-protein interactions which are required for structural plasticity of excitatory synapses. The loss of Pin1 activity may be one of the earliest events leading to the pathological modification of synaptic proteins in preclinical AD (Figure 4) [42, 43].

Synaptic NMDA receptors protect synaptic function and stimulate synaptic generation to maintain homeostasis

[36, 40] (Figure 6). Pin1 protein is found in dendritic spines and regulates the synthesis of PSD 95 [30]. Here we found that Pin1 proteins associate with dendritic rafts and the PSD fractions containing NMDA receptors and Shank3 proteins (Figure 1), which suggests that Pin1 may regulate signal transduction at dendritic rafts and may influence the function of Shank3 proteins and other proteins within dendritic rafts and the PSD. The normal level of glutamate in brains is 1–4 μM [44]. The baseline concentration of extracellular glutamate is also reported to be near 25 nM [45]. We selected various concentrations of NMDA to regulate the structural changes in the PSD. Shank proteins have the capability to turn over within minutes [35], organize other scaffolding proteins in addition to glutamate receptors, and induce spine formation [41]. Conversely, the loss of Shank3 protein can lead to aberrant structure of the PSD and loss of NMDA receptors [27]. In our results, 50 nM (data not shown) and 100 nM NMDA increased Shank3 protein levels (Figure 6). Under these conditions, NMDA may protect synapses and increase synaptic formation [36, 40]. On the other hand, memantine and AP-5 blocked the increase of Shank3 proteins induced by NMDA at 100 nM. PiB, the inhibitor of Pin1, also clearly blocked elevations in Shank3 proteins induced by NMDA at 100 nM, which implicates the blocking of Pin1 activity in inhibiting the synthesis of Shank3 induced by NMDA receptor. This confirms that Pin1 may control protein synthesis in dendritic spines [30]. Interestingly, we also found that the inhibitor of Pin1 could increase NMDA receptor-mediated excitotoxicity, leading to the degradation of Shank3 proteins in cultured neurons (Figure 6), which suggests that the loss of Pin1 activity can increase NMDA receptor-mediated excitotoxicity in dendritic spines. To avoid the effects of increased Aβ peptides on the synapse after the loss of Pin1 activity, we used cultured cortical neurons of APP$^{-/-}$ mice and found that PiB or Pin1 shRNA was also capable of inducing Shank3 loss. These results suggest that Pin1 may play a role in the NMDA receptor-mediated functional and structural plasticity of the PSD, and the loss of Pin1 activity may block normal NMDA receptor-mediated synaptic formation thereby increasing the neuron's susceptibility to oligomers of Aβ or other toxic events such as excitation (Figure 6). During this pathological process, the accumulation of modifications at the excitatory synapse may lead to an irreversible synaptic dysfunction and aberration of synaptic structure that cannot be normalized by synaptic NMDA receptors [36, 40], ultimately accelerating synaptic loss.

The PSD is a multiprotein complex organized by Shank proteins [23, 24]. Mutations in this set of proteins are involved in over 133 genetic neurological diseases [24] including Shank-relevant diseases [27]. The loss of Pin1 activity could affect conformational and functional changes in PSD proteins in AD and in other neurological diseases. Pin1 activity often translates to a fate-determining ubiquitination switch, and Pin1 may likewise affect the degree of ubiquitination in the degradation of PSD proteins (Figure 4) including PSD95, GKAP, Shank, and other proteins involved in the disruption of the PSD in AD [21, 28, 46, 47]. Shank3 and other scaffolding proteins, PSD95 and PSD93, undergo proline-directed phosphorylation and share a similar phosphorylation motif [48]. The alteration of Shank protein levels and modification of ubiquitin have been linked to AD [28, 29]. The loss of Pin1 could affect the modification of proteins in the PSD, leading to the degradation of proteins by the UPS (Figure 4) and contributing to the aberrant structure of the PSD in AD. Proteasome activity declines with aging and in AD brains [49], and we found that loss of Pin1 activity can significantly increase the ubiquitin modification and degradation of Shank3 protein in cultured neurons (Figures 4, 5, and 6). These results suggest that the NMDA receptor-mediated activity of the ubiquitin system can be altered, leading to the degradation of PSD proteins after the loss of Pin1 activity in dendritic spine. In addition, Pin1 could also directly bind to phosphorylated Shank3 protein and affect the levels of Shank3 protein in dendritic spine. These relevant molecular mechanisms warrant further investigation.

4. Experimental Procedure

4.1. Human AD and Mice Brain Tissues. Human brain tissues were obtained at autopsy from 8 patients diagnosed clinically and histopathologically with AD (80.9±2.7 years) in the postmortem period (5.5 ± 0.8 h) and from 5 age-matched controls with no clinical or morphologic evidence of brain pathology (81.4 ± 2.0 years) in the postmortem period (5.0 ± 1.0 h). The ages and PMDs of cases were not significantly different between the AD and control group. In this study, we focused on excitatory synapses and the potential effects of medications on glutamate receptor levels. None of our control or AD subjects were on memantine, an antagonist of NMDA receptor, or other NMDA receptor modulators. All tissues were obtained from the DUCOM Memory Disorders brain bank.

Pin1 knockout mice were bred in Flavio Rizzolio's laboratory (Temple University, Philadelphia, PA). Tg2576 mice were bred in the animal facility center at Drexel University College of Medicine.

4.2. Cortical Neuron Culture and Treatment. Cortical neurons of C57/BL6 mice at E18 and Pin1 knockout mice at P0 were cultured on coverslips for immunocytochemical analysis, in 10 cm dishes for dendritic raft or PSD isolation or in 24-well plates for Western blot, as described previously [50, 51]. To culture the neurons of Pin1$^{-/-}$ mice, the cortical neurons of pups at P0 from Pin1$^{+/-}$ mice cross-bred with Pin1$^{+/-}$ mice were cultured individually, and the pups were genotyped. These cultured cortical cells at various times (from 12 to 21 DIV for different tests) were treated with memantine, AP-5, NMDA, PiB, Pin1 shRNA lentivirus particle, control shRNA lentivirus particle, and vehicle as indicated in the figures. PiB, a selective Pin inhibitor [33, 34], was used to block the activity of Pin1. Pin1 shRNA lentivirus particles were used to create Pin1 knockdowns [52].

4.3. Synaptosome, Dendritic Raft, and PSD Preparation. Synaptosomes were prepared from frontal cortical tissues of human brains, from cultured neurons, or from cortical or hippocampal tissues of mice brains [28, 53]. Dendritic rafts fractions were prepared from synaptosomes [15, 54]. PSD fractions were prepared from synaptosomes [31].

4.4. Ubiquitinated-Protein Affinity Isolation. PSD fractions were isolated from cultured neurons with or without treatment of PiB, Pin1 shRNA lentivirus particles, control shRNA lentivirus particles, or vehicle. Proteins from these PSD fractions at equal amounts were solubilized in TBS buffer (10 mM Tris-HCl, 100 mM NaCl) with 0.1% SDS at 70°C for 15 min. The ubiquitinated proteins in supernatant at 100,000 ×g for 30 min were pulled down by ubiquitin-interacting motif affinity gel (polyubiquitin enrichment kit, Pierce Biotechnology) according to the manufacturer's instructions. These gels were washed three times by TBS buffer with 0.1% SDS. Finally, 1% SDS Laemmli sample buffer was used to elute ubiquitinated proteins for Western blot analysis.

4.5. Oligomers of Aβ (ADDLs) Preparation. Oligomers of $A\beta_{1-42}$ peptide were prepared as previously described [50, 55].

4.6. Immunoblot. Western and dot blot analyses were based on published procedures [50]. For Western blot analysis, the samples were separated by 4%–20% glycine-HCl SDS-polyacrylamide gel or 16.5% Tris-tricine SDS-polyacrylamide gel electrophoresis and then transferred to nitrocellulose membrane. For dot blot analysis, the samples of dendritic rafts, PSDs, and synaptosome fractions were treated by 0.1% SDS or by Ham's F-12 medium, and proteins of these samples in equal amounts were dotted on nitrocellulose membrane. The proteins were recognized by specific antibodies and visualized with ECL. Antibodies to flotillin (rabbit), Shank3 (rabbit and goat), NR1 of NMDA receptor subunit (rabbit), PSD95 (goat), Pin1 (mouse and rabbit), calnexin (rabbit), and β-tubulin (rabbit) were from Santa Cruz Biotechnology (Santa Cruz, CA). Antibody A11 to oligomers of Aβ was from Invitrogen [56]. Antibody (rabbit) to Tau [p-231] was from Covance (Emeryville, CA). A polyubiquitin enrichment kit and antibody to ubiquitin (rabbit) were obtained from Pierce, and Alexa-conjugated secondary antibodies were from Invitrogen. Hybond ECL nitrocellulose, HRP-conjugated secondary, and rainbow protein ladders were from Amersham Pharmacia Biosciences.

4.7. Coimmunoprecipitation. IP was carried out by incubation of synapse lysates of human control brain cortical tissues. Synaptosomes containing 200 μg protein were resuspended in buffer A containing 50 mM Tris (pH 7.5), 100 mM NaCl, 1.5 mM EGTA, 0.1% SDS, and 1% Triton X-100 for 1 hour at 4°C. The supernatant from 100,000*g* for 30 minutes was incubated with specific antibodies plus Protein G agarose (Invitrogen) at 4°C overnight, followed by washing 5 times in a buffer B containing 50 mM Tris (pH 7.5), 100 mM NaCl, and 1.5 mM 0.1% Triton X-100. Antibodies used for IP were rabbit polyclonal anti-Pin1 and anti-Shank3 (Santa Cruz) and rabbit IgG (Sigma-Aldrich) as negative controls. The IP was analyzed by Western blot using mouse monoclonal anti-Pin1 and goat polyclonal anti-Shank3 (Santa Cruz).

4.8. Immunocytochemistry. Treated cells were rinsed with neurobasal media and then fixed with 3.7% formaldehyde in neurobasal media (1 : 1 volume) for 20 min followed by an additional 20 min of undiluted fixative. Cells were rinsed extensively in PBS. Coverslips were incubated in blocking solution (10% BSA in PBS with or without 0.1% Triton X-100) for 45 min at room temperature. Antibodies were used against Pin1, NR1, and Shank3. Primary antibodies were diluted in blocking solution and incubated overnight at 4°C. After rinsing with PBS with 1% BSA, coverslips were incubated with appropriate Alexa-conjugated secondary antibodies diluted in PBS plus 1% PBS for 90 min at room temperature, rinsed in PBS three times, and mounted with ProLong Antifade media [51]. Quantitative analysis of the immunofluorescence intensity at dendritic arbors was performed by histogram analysis using ImageJ. Shank3 proteins were expressed in excitatory neurons and at the PSDs of dendritic spines [23]. Cell bodies were digitally removed from images; the Shank3 proteins at dendritic arbors were analyzed. Thirty images were acquired under each experimental condition, and these tests were done in triplicate. The data were pooled for quantitative estimates of changes in Shank3 protein. Three independent experiments were performed for each test [7].

4.9. Statistical Analysis. For each experiment, two or three independent replicated experiments were performed. The densities of immunoblot were acquired with densitometric scan and quantified with ImageJ. Results were expressed as means ± SEM. The data were analyzed with one-way analysis of variance. Statistical significance was determined at $p < 0.05$.

5. Conclusion

Here we found Pin1 proteins exist in detergent-resistant dendritic rafts and PSDs at the precise location of key macromolecules including NMDA, AMPA, mGlu receptors, and Shank proteins for synaptic plasticity. The loss of synaptic Pin1 activity may alter the modifications of ubiquitin in PSD proteins and lead to the loss of Shank3 proteins and formation of aberrant synapses which are more susceptible to toxic effects of molecules such as oligomers of Aβ and glutamate. Toxicity thereby inhibits NMDA receptor-mediated turnover of Shank3 and PSD95 and exaggerates NMDA receptor-mediated loss of Shank3 and PSD95 proteins. These multiple factors could work together to exacerbate synaptic dysfunction in preclinical AD. The loss of Pin1 activity could play an integral role in the pathogenesis of synaptic dysfunction contributing to the onset of clinical AD.

Abbreviations

AD: Alzheimer's disease
Pin1: Peptidyl-prolyl cis-trans isomerase NIMA-interacting 1
PSD: Postsynaptic density
NR1: N-Methyl-D-aspartate (NMDA) receptor 1
UPS: Ubiquitin proteasome system
Aβ: β-Amyloid peptides
ADDLs: Aβ oligomeric ligands

PiB: Benzo[lmn][3,8]phenanthroline-2,7-diacetic acid, 1,3,6,8-tetrahydro-1,3,6,8-tetraoxo-, 2,7-diethyl ester, Pin1 selective inhibitor
MG-132: Z-Leu-Leu-Leu-al, proteasome inhibitor.

Competing Interests

The authors have reported no conflict of interests.

Acknowledgments

This work was financially supported by the Priority Academic Program Development (PAPD) fund of the Jiangsu Higher Education Institution and NIH Grant R21AG031388 (Dr. Gong). The authors would like to thank Robert Schwartzman and Guillermo M. Alexander for their kind help with the experiments. They also would like to thank Diana Winters for her kind help with reading the manuscript.

References

[1] C. Haass and D. J. Selkoe, "Soluble protein oligomers in neurodegeneration: lessons from the Alzheimer's amyloid β-peptide," *Nature Reviews Molecular Cell Biology*, vol. 8, no. 2, pp. 101–112, 2007.

[2] H. Braak and E. Braak, "Diagnostic criteria for neuropathologic assessment of Alzheimer's disease," *Neurobiology of Aging*, vol. 18, no. 4, pp. S85–S88, 1997.

[3] E. Grober, D. Dickson, M. J. Sliwinski et al., "Memory and mental status correlates of modified Braak staging," *Neurobiology of Aging*, vol. 20, no. 6, pp. 573–579, 1999.

[4] T. E. Golde, "Alzheimer disease therapy: can the amyloid cascade be halted?" *Journal of Clinical Investigation*, vol. 111, no. 1, pp. 11–18, 2003.

[5] D. J. Selkoe, "Alzheimer's disease is a synaptic failure," *Science*, vol. 298, no. 5594, pp. 789–791, 2002.

[6] D. J. Selkoe, "Preventing alzheimer's disease," *Science*, vol. 337, no. 6101, pp. 1488–1492, 2012.

[7] F. G. De Felice, P. T. Velasco, M. P. Lambert et al., "Aβ oligomers induce neuronal oxidative stress through an N-methyl-D-aspartate receptor-dependent mechanism that is blocked by the Alzheimer drug memantine," *Journal of Biological Chemistry*, vol. 282, no. 15, pp. 11590–11601, 2007.

[8] R. Sultana, D. Boyd-Kimball, H. F. Poon et al., "Oxidative modification and down-regulation of Pin1 in Alzheimer's disease hippocampus: a redox proteomics analysis," *Neurobiology of Aging*, vol. 27, no. 7, pp. 918–925, 2006.

[9] E. S. Yeh and A. R. Means, "PIN1, the cell cycle and cancer," *Nature Reviews Cancer*, vol. 7, no. 5, pp. 381–388, 2007.

[10] P.-J. Lu, G. Wulf, X. Z. Zhou, P. Davies, and K. P. Lu, "The prolyl isomerase Pin1 restores the function of Alzheimer-associated phosphorylated tau protein," *Nature*, vol. 399, no. 6738, pp. 784–788, 1999.

[11] L. Pastorino, A. Sun, P. J. Lu et al., "The prolyl isomerase Pin1 regulates amyloid precursor protein processing and amyloid-beta production," *Nature*, vol. 440, pp. 528–534, 2006.

[12] A. Maruszak, K. Safranow, K. Gustaw et al., "PIN1 gene variants in Alzheimer's disease," *BMC Medical Genetics*, vol. 10, article 115, 2009.

[13] K. Nakamura, I. Kosugi, D. Y. Lee et al., "Prolyl isomerase pin1 regulates neuronal differentiation via β-catenin," *Molecular and Cellular Biology*, vol. 32, no. 15, pp. 2966–2978, 2012.

[14] Y.-C. Liou, A. Sun, A. Ryo et al., "Role of the prolyl isomerase Pin1 in protecting against age-dependent neurodegeneration," *Nature*, vol. 424, no. 6948, pp. 556–561, 2003.

[15] T. Kawarabayashi, M. Shoji, L. H. Younkin et al., "Dimeric amyloid β protein rapidly accumulates in lipid rafts followed by apolipoprotein E and phosphorylated tau accumulation in the Tg2576 mouse model of Alzheimer's disease," *Journal of Neuroscience*, vol. 24, no. 15, pp. 3801–3809, 2004.

[16] R. M. Koffie, M. Meyer-Luehmann, T. Hashimoto et al., "Oligomeric amyloid β associates with postsynaptic densities and correlates with excitatory synapse loss near senile plaques," *Proceedings of the National Academy of Sciences of the United States of America*, vol. 106, no. 10, pp. 4012–4017, 2009.

[17] M. P. Coba, A. J. Pocklington, M. O. Collins et al., "Neurotransmitters drive combinatorial multistate postsynaptic density networks," *Science Signaling*, vol. 2, no. 68, p. ra19, 2009.

[18] J. C. Trinidad, C. G. Specht, A. Thalhammer, R. Schoepfer, and A. L. Burlingame, "Comprehensive identification of phosphorylation sites in postsynaptic density preparations," *Molecular and Cellular Proteomics*, vol. 5, no. 5, pp. 914–922, 2006.

[19] S. Okabe, H.-D. Kim, A. Miwa, T. Kuriu, and H. Okado, "Continual remodeling of postsynaptic density and its regulation by synaptic activity," *Nature Neuroscience*, vol. 2, no. 9, pp. 804–811, 1999.

[20] G. Wulf, G. Finn, F. Suizu, and K. P. Lu, "Phosphorylation-specific prolyl isomerization: is there an underlying theme?" *Nature Cell Biology*, vol. 7, no. 5, pp. 435–441, 2005.

[21] M. D. Ehlers, "Activity level controls postsynaptic composition and signaling via the ubiquitin-proteasome system," *Nature Neuroscience*, vol. 6, no. 3, pp. 231–242, 2003.

[22] D. Siepe and S. Jentsch, "Prolyl isomerase Pin1 acts as a switch to control the degree of substrate ubiquitylation," *Nature Cell Biology*, vol. 11, no. 8, pp. 967–972, 2009.

[23] T. M. Boeckers, "The postsynaptic density," *Cell and Tissue Research*, vol. 326, no. 2, pp. 409–422, 2006.

[24] Á. Bayés, L. N. Van De Lagemaat, M. O. Collins et al., "Characterization of the proteome, diseases and evolution of the human postsynaptic density," *Nature Neuroscience*, vol. 14, pp. 19–21, 2011.

[25] C. M. Durand, C. Betancur, T. M. Boeckers et al., "Mutations in the gene encoding the synaptic scaffolding protein SHANK3 are associated with autism spectrum disorders," *Nature Genetics*, vol. 39, no. 1, pp. 25–27, 2007.

[26] M. A. Bangash, J. M. Park, T. Melnikova et al., "Enhanced polyubiquitination of shank3 and NMDA receptor in a mouse model of autism," *Cell*, vol. 145, no. 5, pp. 758–772, 2011.

[27] J. Peça, C. Feliciano, J. T. Ting et al., "Shank3 mutant mice display autistic-like behaviours and striatal dysfunction," *Nature*, vol. 472, no. 7344, pp. 437–442, 2011.

[28] Y. Gong, C. F. Lippa, J. Zhu, Q. Lin, and A. L. Rosso, "Disruption of glutamate receptors at Shank-postsynaptic platform in Alzheimer's disease," *Brain Research*, vol. 1292, pp. 191–198, 2009.

[29] E. Pham, L. Crews, K. Ubhi et al., "Progressive accumulation of amyloid-β oligomers in Alzheimer's disease and in amyloid precursor protein transgenic mice is accompanied by selective alterations in synaptic scaffold proteins," *FEBS Journal*, vol. 277, no. 14, pp. 3051–3067, 2010.

[30] P. R. Westmark, C. J. Westmark, S. Wang et al., "Pin1 and PKMζ sequentially control dendritic protein synthesis," *Science Signaling*, vol. 3, no. 112, article ra18, 2010.

[31] K.-O. Cho, C. A. Hunt, and M. B. Kennedy, "The rat brain postsynaptic density fraction contains a homolog of the drosophila discs-large tumor suppressor protein," *Neuron*, vol. 9, no. 5, pp. 929–942, 1992.

[32] D. E. Harrison, R. Strong, Z. D. Sharp et al., "Rapamycin fed late in life extends lifespan in genetically heterogeneous mice," *Nature*, vol. 460, no. 7253, pp. 392–395, 2009.

[33] T. Uchida, M. Takamiya, M. Takahashi et al., "Pin1 and Par14 peptidyl prolyl isomerase inhibitors block cell proliferation," *Chemistry and Biology*, vol. 10, no. 1, pp. 15–24, 2003.

[34] M. Moretto-Zita, H. Jin, Z. Shen, T. Zhao, S. P. Briggs, and Y. Xu, "Phosphorylation stabilizes Nanog by promoting its interaction with Pin1," *Proceedings of the National Academy of Sciences of the United States of America*, vol. 107, no. 30, pp. 13312–13317, 2010.

[35] T. Bresler, M. Shapira, T. Boeckers et al., "Postsynaptic density assembly is fundamentally different from presynaptic active zone assembly," *Journal of Neuroscience*, vol. 24, no. 6, pp. 1507–1520, 2004.

[36] F. X. Soriano, S. Papadia, F. Hofmann, N. R. Hardingham, H. Bading, and G. E. Hardingham, "Preconditioning doses of NMDA promote neuroprotection by enhancing neuronal excitability," *Journal of Neuroscience*, vol. 26, no. 17, pp. 4509–4518, 2006.

[37] H.-S. V. Chen and S. A. Lipton, "Mechanism of memantine block of NMDA-activated channels in rat retinal ganglion cells: uncompetitive antagonism," *Journal of Physiology*, vol. 499, no. 1, pp. 27–46, 1997.

[38] S. A. Lipton, "Paradigm shift in neuroprotection by NMDA receptor blockade: memantine and beyond," *Nature Reviews Drug Discovery*, vol. 5, no. 2, pp. 160–170, 2006.

[39] P. Xia, H.-S. V. Chen, D. Zhang, and S. A. Lipton, "Memantine preferentially blocks extrasynaptic over synaptic NMDA receptor currents in hippocampal autapses," *Journal of Neuroscience*, vol. 30, no. 33, pp. 11246–11250, 2010.

[40] G. E. Hardingham and H. Bading, "Synaptic versus extrasynaptic NMDA receptor signalling: implications for neurodegenerative disorders," *Nature Reviews Neuroscience*, vol. 11, no. 10, pp. 682–696, 2010.

[41] G. Roussignol, F. Ango, S. Romorini et al., "Shank expression is sufficient to induce functional dendritic spine synapses in aspiny neurons," *Journal of Neuroscience*, vol. 25, no. 14, pp. 3560–3570, 2005.

[42] K. P. Lu and X. Z. Zhou, "The prolyl isomerase PIN1: a pivotal new twist in phosphorylation signalling and disease," *Nature Reviews Molecular Cell Biology*, vol. 8, no. 11, pp. 904–916, 2007.

[43] D. A. Butterfield, H. M. Abdul, W. Opii et al., "Pin1 in Alzheimer's disease," *Journal of Neurochemistry*, vol. 98, no. 6, pp. 1697–1706, 2006.

[44] G. Nyitrai, K. A. Kékesi, and G. Juhász, "Extracellular level of GABA and Glu: in vivo microdialysis-HPLC measurements," *Current Topics in Medicinal Chemistry*, vol. 6, no. 10, pp. 935–940, 2006.

[45] M. A. Herman and C. E. Jahr, "Extracellular glutamate concentration in hippocampal slice," *Journal of Neuroscience*, vol. 27, no. 36, pp. 9736–9741, 2007.

[46] M. Colledge, E. M. Snyder, R. A. Crozier et al., "Ubiquitination regulates PSD-95 degradation and AMPA receptor surface expression," *Neuron*, vol. 40, no. 3, pp. 595–607, 2003.

[47] Y. Gong and C. F. Lippa, "Disruption of the postsynaptic density in Alzheimer's disease and other neurodegenerative dementias," *American Journal of Alzheimer's Disease and other Dementias*, vol. 25, no. 7, pp. 547–555, 2010.

[48] H. Jaffe, L. Vinade, and A. Dosemeci, "Identification of novel phosphorylation sites on postsynaptic density proteins," *Biochemical and Biophysical Research Communications*, vol. 321, no. 1, pp. 210–218, 2004.

[49] S. Oh, H. S. Hong, E. Hwang et al., "Amyloid peptide attenuates the proteasome activity in neuronal cells," *Mechanisms of Ageing and Development*, vol. 126, no. 12, pp. 1292–1299, 2005.

[50] Y. Gong, L. Chang, K. L. Viola et al., "Alzheimer's disease-affected brain: presence of oligomeric Aβ ligands (ADDLs) suggests a molecular basis for reversible memory loss," *Proceedings of the National Academy of Sciences of the United States of America*, vol. 100, no. 18, pp. 10417–10422, 2003.

[51] P. N. Lacor, M. C. Buniel, P. W. Furlow et al., "Aβ oligomer-induced aberrations in synapse composition, shape, and density provide a molecular basis for loss of connectivity in Alzheimer's disease," *Journal of Neuroscience*, vol. 27, no. 4, pp. 796–807, 2007.

[52] T. Liu, Y. Huang, R. I. Likhotvorik, L. Keshvara, and D. G. Hoyt, "Protein never in mitosis gene A interacting-1 (PIN1) regulates degradation of inducible nitric oxide synthase in endothelial cells," *American Journal of Physiology—Cell Physiology*, vol. 295, no. 3, pp. C819–C827, 2008.

[53] P. R. Dodd, J. A. Hardy, A. E. Oakley, J. A. Edwardson, E. K. Perry, and J.-P. Delaunoy, "A rapid method for preparing synaptosomes: comparison, with alternative procedures," *Brain Research*, vol. 226, no. 1-2, pp. 107–118, 1981.

[54] T. Suzuki, J. Zhang, S. Miyazawa, Q. Liu, M. R. Farzan, and W.-D. Yao, "Association of membrane rafts and postsynaptic density: proteomics, biochemical, and ultrastructural analyses," *Journal of Neurochemistry*, vol. 119, no. 1, pp. 64–77, 2011.

[55] M. P. Lambert, A. K. Barlow, B. A. Chromy et al., "Diffusible, nonfibrillar ligands derived from Aβ_{1-42} are potent central nervous system neurotoxins," *Proceedings of the National Academy of Sciences of the United States of America*, vol. 95, no. 11, pp. 6448–6453, 1998.

[56] R. Kayed, E. Head, J. L. Thompson et al., "Common structure of soluble amyloid oligomers implies common mechanism of pathogenesis," *Science*, vol. 300, no. 5618, pp. 486–489, 2003.

Hindawi
Neural Plasticity
Volume 2017, Article ID 6537230, 7 pages
https://doi.org/10.1155/2017/6537230

Research Article

Profiling Proteins in the Hypothalamus and Hippocampus of a Rat Model of Premenstrual Syndrome Irritability

Mingqi Qiao,[1] Peng Sun,[1] Yang Wang,[2] Sheng Wei,[1] Xia Wei,[3] Chunhong Song,[1] Fushun Wang,[4] and Jibiao Wu[1]

[1]*Key Laboratory of Traditional Chinese Medicine for Classical Theory, Ministry of Education, Shandong University of Traditional Chinese Medicine, Jinan 250355, China*
[2]*Laboratory of Ethnopharmacology, Institute of Integrated Traditional Chinese and Western Medicine, Xiangya Hospital, Central South University, Changsha 410008, China*
[3]*Technical Office of Pharmacology, Shandong Institute for Food and Drug Control, Jinan 250351, China*
[4]*College of Psychology, Nanjing University of Chinese Medicine, Nanjing 210023, China*

Correspondence should be addressed to Peng Sun; sunpeng369@126.com

Received 23 September 2016; Revised 29 December 2016; Accepted 12 January 2017; Published 31 January 2017

Academic Editor: J. Michael Wyss

Premenstrual syndrome (PMS) refers to several physical and mental symptoms (such as irritability) commonly encountered in clinical gynaecology. The incidence of PMS has been increasing, attracting greater attention from medical fields. However, PMS pathogenesis remains unclear. This study employed two-dimensional gel electrophoresis (2DE) for proteomic map analysis of the hypothalamus and hippocampus of rat models of premenstrual syndrome (PMS) irritability. Matrix-assisted laser desorption/ionisation time of flight mass spectroscopy (MALDI-TOF-MS) was used to identify proteins possibly related with PMS irritability. Baixiangdan, a traditional Chinese medicine effective against PMS irritability, was used in the rat model to study putative target proteins of this medicine. The hypothalamus and hippocampus of each group modelling PMS displayed the following features: decreased expression of Ulip2, tubulin beta chain 15, α actin, and interleukin 1 receptor accessory protein; increased expression of kappa-B motif-binding phosphoprotein; decreased expression of hydrolase at the end of ubiquitin carboxy, albumin, and aldolase protein; and increased expression of M2 pyruvate kinase, panthenol-cytochrome C reductase core protein I, and calcium-binding protein. Contrasting with previous studies, the current study identified new proteins related to PMS irritability. Our findings contribute to understanding the pathogenesis of PMS irritability and could provide a reference point for further studies.

1. Introduction

Premenstrual syndrome (PMS) is a symptom complex that periodically appears during the latter half of the menstrual cycle, accompanied by physical, mental, and behavioural changes [1–3]. It is most commonly seen among women of childbearing age, between 30 and 40 years. Recent literature shows that PMS is a common syndrome among young women and is closely linked with mood, body, and behaviour. PMS has a large coverage of pathogenesis and quite a high morbidity at the same time [4]. The etiology and pathogenesis of PMS are primary aims of basic research in this area; targeted drug research in traditional Chinese and Western medicine has also become a current hotspot.

PMS irritability is a major type of PMS, with features of premenstrual dysphoria, irritability, breast distending pain, and abdominal distension or pain, followed secondarily by insomnia, dreamful sleep, headache, gastral cavity distension, belching, acid regurgitation, premature menstruation, reduced sexual desire, distaste for sexual life, attention-deficit disorder, fatigue, bulimia, diet partiality, lumbago, tendency to tears, and so forth [5] Baixiangdan, a traditional Chinese prescription created by Cyperus (*Cyperus rotundus* L.), Common Peony (*Paeonia lactiflora* Pall.), and Peony bark (*Paeonia suffruticosa* Andr.) (Supplementary Material available online at https://doi.org/10.1155/2017/6537230, Figure S1), have been shown to effectively relieve symptoms of PMS irritability in clinical trials and animal experiments. Studies revealed that

the main active compounds of Baixiangdan were paeoniflorin, paeonol, and alpha-cyperone [6–8], which might have antipyretic, anti-inflammatory, analgesic, and neuroprotective functions [9, 10]. The pathogenesis of PMS irritability, which is very complex, involves the mental, neural, and internal secretion systems. So far, no one has clarified the mechanism therein; hence, no studies have reported will-dominant PMS irritability prevention. Previous studies have revealed that the occurrence of PMS could be related to functional disorders of the hippocampus and the hypothalamus [11–13]. Consequently, the hippocampus and the hypothalamus are the anatomical regions that have been most closely studied regarding the pathogenesis of PMS.

There are changes in the mRNA expression of central monoamine neurotransmitter receptors including 5HT1A, 5HT2A [14], and GABAA [15] receptors and ERα, ERβ, PGR, and central steroidal hormones receptors, in the limbic system of a macaque model with PMS irritability [16]. Aberrant expression of receptor genes could affect their function and further lead to abnormities in the expression of the key protein(s) in downstream signal pathways regulated by these receptors, potentially representing an important link in triggering the disease.

The present study used a rat model of PMS irritability for proteomic screening based on a previous microarray study [16], analysing the differences in expression of the central organization protein linked with this disease in the rat model and a control group, through two-dimensional gel electrophoresis (2DE) and matrix-assisted laser desorption ionisation time of flight mass spectrometry (MALDI-TOF-MS). In addition, the relationship between the protein and the incidence of PMS irritability is discussed below, to explore its mechanism of action. The Baixiangdan capsule was also administered to the rat to determine its possible target protein. The present findings are expected to lay the technical foundation for the proteomic study of this medicine.

2. Materials and Methods

2.1. Laboratory Animals and Ethics Statement. Healthy female SPF Wistar rats weighing 160–180 g were selected. They had ad libitum access to water and food. The feeding room temperature was 24 ± 1°C and the relative humidity was 50 ± 10%. Animals were provided by the Laboratory Animal Center of Shandong Traditional Chinese Medicine University, license number: SCXK (LU) 2011-0003. Laboratory animals were provided care according to "*The Care and Use of Laboratory Animals*" by the Laboratory Animal Center of Shandong University of Traditional Chinese Medicine.

2.2. Drugs. The Baixiangdan capsule was procured from Xiuzheng Pharmaceutical Group Company Limited. It was jointly developed by Qingdao Haichuan Innovative Biological and Natural Medicine Research Center with the batch number: 2007L05105.

2.3. Determination of the Oestrous Cycle. All grouped rats were weighed, recorded, and marked with picric acid, and their oestrous cycle was determined using the vaginal smear (Supplementary Material, Figure S2) microscopic examination method [17, 18]. On a proestrus vaginal smear, epithelial cell nuclei and a few keratinocytes are present, while on an oestrous vaginal smear, enucleate keratinocytes and a few epithelial cells are present. On a postoestrous vaginal smear, leukocytes, keratinocytes, and epithelial cell nuclei are found, and on an anoestrous vaginal smear, there are large numbers of leukocytes, few epithelial cells, and myxocytes. Rats with short estrous cycles (about 3 days) were included in the following experiments.

2.4. Generation of a PMS Irritability Rat Model and Baixiangdan Capsule Treated PMS Irritability Model. Following vaginal smearing [8, 19], 30 rats in the postoestrous period were divided randomly into 3 groups with 10 rats in each: namely, the control group, the group modelling PMS irritability, and the group treated with the Baixiangdan capsule. The PMS irritability group and the group treated with Baixiangdan were connected to ST-A digital pulse stimulators. The stimulation conditions were as follows: voltage 2700–3300 V, pulse width 0.3 s, pulse separation 5 minutes during the daytime and 10 minutes during the night, and continuous stimulation for 5 days. Five-day stimulation covers a dioestrus and a round of the oestrous cycle. As for the group treated with the Baixiangdan capsule, Baixiangdan was intragastrically administered to animals at 0900 hours each day and lasted for 5 days when modelling stimulation was in progress. Drug dosage for the rats was 1 mg/100 g, once each day for 5 days, representing almost 8 times the dose typically taken by human patients.

2.5. Movement and Exploratory Behaviour (Open-Field Test). The field box model number was XR-XZ301 from Shanghai Xinran with dimensions of $50 \times 50 \times 50$ cm^3. Data acquisition software was the animal behaviour trace analysis system XR-Xmaze. The specific operations were the following: the operator held the 1/3 part of the rat's tail and gently placed the rat in the center of the field box, following which the observer recorded the rat's movement trace, modification time, time spent standing in the central grid, number of excrement particles [20–22], and so forth.

To eliminate rat odour, the field box was cleaned with 75% ethanol after each rat was tested. After drying, data acquisition for the next rat was conducted. The grabbing action in this experiment was as gentle as possible to eliminate artificial intervention.

2.6. Attack Behaviour Test. The attack behaviour test [22] was conducted between 1430 and 1730 hours inside the rat housing environment. After day and night inversion, this timeframe was the exciting period for the rats. The specific operations performed were as follows: rats were placed in the cage; an invading rat (which had been spayed) was then placed into the cage after 15 minutes of adaptation, for 10 minutes. Composite aggression was calculated using the following formula: Composite aggression = [(number of attacks) + 0.2 × (attack duration) + (number of bites) + 0.2 × (on-top duration) + (piloerection)].

2.7. Rat Cerebral Tissues Sampling. After decapitation, the operator dissected out the hippocampus and hypothalamus on an ultra-clean platform and placed them in liquid nitrogen immediately for quick cooling. After 30 minutes, they were then stored at −70°C. All operation instruments, watch glasses, and Eppendorf tubes in this experiment were sterilized in an autoclave. The ultra-clean bench surface was wiped with ethanol above 75% and exposed to UV light, to prevent pollution.

2.8. Protein Extraction and Quantification. For protein extracting and quantifying methods, we referred to the literature [23]. The hippocampi and hypothalami were dissected out from the rats; lysate buffer [self-prepared (7 M urea, 2 M thiocarbamide, 4% CHAPS, 1% DTT, 1 mM EDTA, and 40 mM Tris pH 7.4)] was added in a ratio of 150–170 mg : 500 μl (sample : lysate); further, cocktail protease inhibitor (Sigma-Aldrich, St. Louis, MO) was added for oscillating and blowing; freeze-thawing was conducted using liquid nitrogen, which was followed by ultrasonication; DNase I (Sigma-Aldrich) and RNase A (Sigma-Aldrich) were added; centrifugation was conducted at 4°C with 14,000 rpm for 25–30 min; supernatant was then packaged and stored at −80°C, and protein levels were quantified.

2.9. Two-Dimensional Gel Electrophoresis. Two-dimensional gel electrophoresis (2DE) was performed as previously described [24, 25]. Samples were subjected to isoelectric focusing in a 17-cm immobilized pH gradient pH 3–10 (Biorad Inc., Berkeley, CA) overnight, using the Protean Isoelectric Focusing Cell (Biorad). The second-dimensional separation of focused samples on the gel strips was performed through sodium dodecyl sulphate-polyacrylamide electrophoresis (SDS-PAGE) using 13% linear polyacrylamide gels. A previously described silver staining method was used to develop the 2DE gels (Heukeshoven & Dernick, 1988). All samples were analysed in duplicate.

2.10. Image Analysis. Before scanning, bubbles and other impurities were eliminated to ensure there were no water droplets in the photic zone; ImageMaster 2D. v3.01 analytic software was used for protein spot detection. With spot detection guidance, optimal detection results were determined by adjusting sensitivity, and the operator and background factor, to achieve automatic detection. After detection, manual editing, such as the addition, deletion, and splitting of spots was needed for unidentified, wrongly identified, and vaguely identified spots, respectively, caused by congestion due to phosphorylation or other reasons. After manual editing, ImageMaster automatically calculated the number of protein spots. The in-gel digestion method [26] was performed to extract peptide fragments.

2.11. Protein Identification with the MALDI-TOF-MS Technique. The peptide fragment mixture extracted using trypsin needs to be desalted; hence, a 50% (v/v) acetonitrile-containing suction nozzle was used to balance by 0.1% trifluoroacetic acid (TFA) twice; a 0.1% TFA solution was used to dissolve and clean the extracted samples; samples were placed in 5 μl cyano cinnamic acid (CCA) saturated matrix solution; 2 ul treated samples were applied on the target spot on the mass spectroscopy plate. Spectrometric detection was conducted in positive ion reflection: N_2 laser source; wave length, 337 nm; flight tube length, 3 m; accelerating voltage, 20 kV; reflection voltage, 23 kV; and matrix CCA [8]. The matrix peak and the trypsin autolysis peak were considered as the interior standard.

2.12. Database Retrieval. The obtained peptide fragments fingerprint spectrum was retrieved in the Swiss-Prot database (http://www.matrixscience.com).

2.13. Statistical Analysis. Graphpad Prism 5.0 statistical drawing software (Graphpad software Inc., CA) was used to analyse the experimental data. The statistical analysis for the behavioural assays was performed using one-way ANOVA ($n = 10$). All data are shown as the mean ± SD, with the significance level set at $P < 0.05$.

3. Results and Discussions

3.1. Identification of the Rat Model with PMS Irritability and the Effect of the Baixiangdan Capsule. The Baixiangdan capsule is a patented Chinese medicine developed in accordance with the prescription of traditional Chinese medicine. This traditional medicine has been considered effective in treating PMS symptoms, like premenstrual vexation, irritability, headache and distension, breast distending pain, insomnia, dreamful sleep, abdominal distension and pain, and premature menstruation. In addition, the pharmacology and pharmaceutical studies have demonstrated that this medicine has specific active ingredients that can ease PMS [8, 27, 28]. In the current study, emotional stimulation, combined with interference to sleeping, eating, and drinking, was used to generate the rat model in the postoestrous period [7, 8, 27, 29], though such a modelling method was not accepted by all sciences. Further, we administered the Baixiangdan capsule to intervene in the rat model and compared the control group with the model group to identify PMS irritability-related proteins using proteomics.

The field test can be used to evaluate animal excitement, cognition, and interest in the outside world. Two scores are computed on two axes: the horizontal score, reflecting the animal's excitement, and the vertical score, reflecting the animal's tendency to explore an uncertain outside world [30–32]. The total score for the open-field test reflects the exploratory behaviour and excitability of the animals. The results indicate that the horizontal scores, the vertical scores and the total open-field scores of rats in PMS irritability group (Mod) are all significantly increased (Figures 1(a)–1(c), $P < 0.05$), compared with those of the normal group (Ctrl). Combining these results with the macroscopic observation of the rats (for behaviours such as staring angrily, fur standing, chasing, or biting), the prepared model could be considered a successful model of PMS, though the electro-stressing method of modelling was controversial. Compared with the scores of the

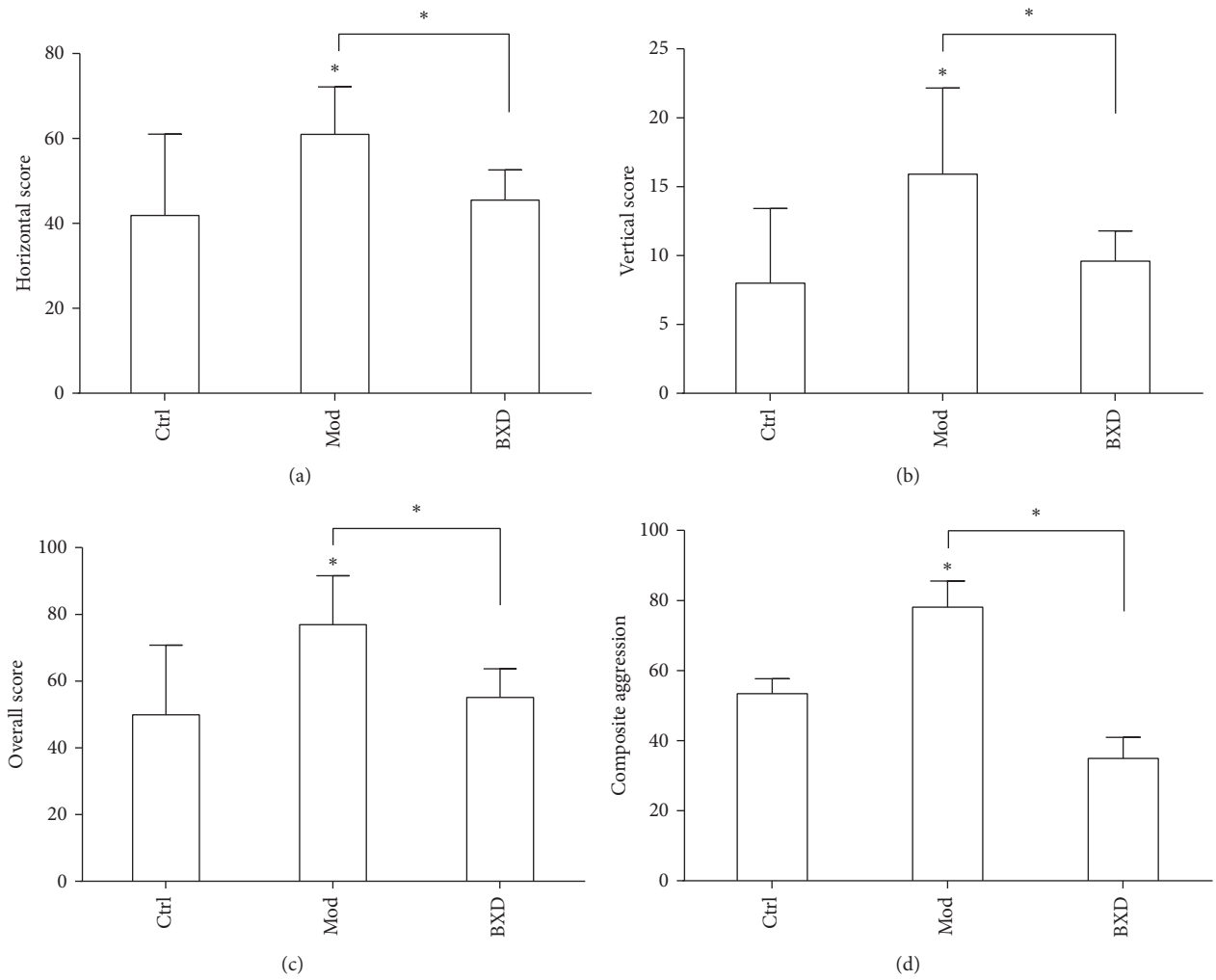

Figure 1: Behavioural assays. (a) Horizontal score in the open-field test, representing the rat's excitability. (b) Vertical score in the open-field test, representing the rat's exploratory behaviour. (c) Overall score in the open-field test. (d) Score in the attack behaviour test. The following groups were analysed: (1) the control/normal group (Ctrl), (2) the PMS irritability model group (Mod), and (3) the group administered with the Baixiangdan capsule (BXD). $^{*}P < 0.05$.

model group (Mod), the horizontal, vertical, and total open-field scores of the rats in the Baixiangdan capsule medication group (BXD) are all significantly decreased (Figures 1(a)–1(c), $P < 0.05$), indicating that the Chinese herbal compound, Baixiangdan, has had a sedative and antianxiety function.

Results for the test of aggressive behaviours are similar to those of the open-field test. Compared with that of the normal group (Ctrl), the score for the rats' aggressive behaviours in the PMS irritability group (Mod) is significantly increased (Figure 1(d), $P < 0.05$). Compared with that of the model group (Mod), the score for the rats' aggressive behaviour in the Baixiangdan capsule medication group (BXD) is significantly decreased (Figure 1(d), $P < 0.05$). For each of the above open-field and aggressive behaviour tests, one experiment was conducted before modelling each group, to act as baseline; there were no statistically significant differences between the groups (not shown, $P > 0.05$).

3.2. Image Analysis of 2DE Serum Protein Profiling. High-resolution serum proteome profiles were obtained from the normal controls (Ctrl), the PMS irritability model rats (Model), and the PMS irritability rats given the Baixiangdan capsule (BXD) through 2DE separation and silver staining of the hypothalami and hippocampi lysates. We analysed the two-dimensional gel electropherograms obtained from the hypothalami and hippocampi tissues in pairs, and obtained 4 overlapping ones: Ctrl versus. Mod hypothalamus (Figure 2(a), 61% matched), Ctrl versus. BXD hypothalamus (Figure 2(b), 72.5% matched), Ctrl versus. Mod hippocampi (Figure 2(c), 56% matched) and Ctrl versus. BXD hippocampi (Figure 2(d), 63.5% matched). In general, after treatment with the Baixiangdan capsule, protein expression approached normal levels or displayed that tendency (Figure 2). The proteins in the rat hippocampus and hypothalamus that were differentially expressed for rats with PMS irritability, control rats, and

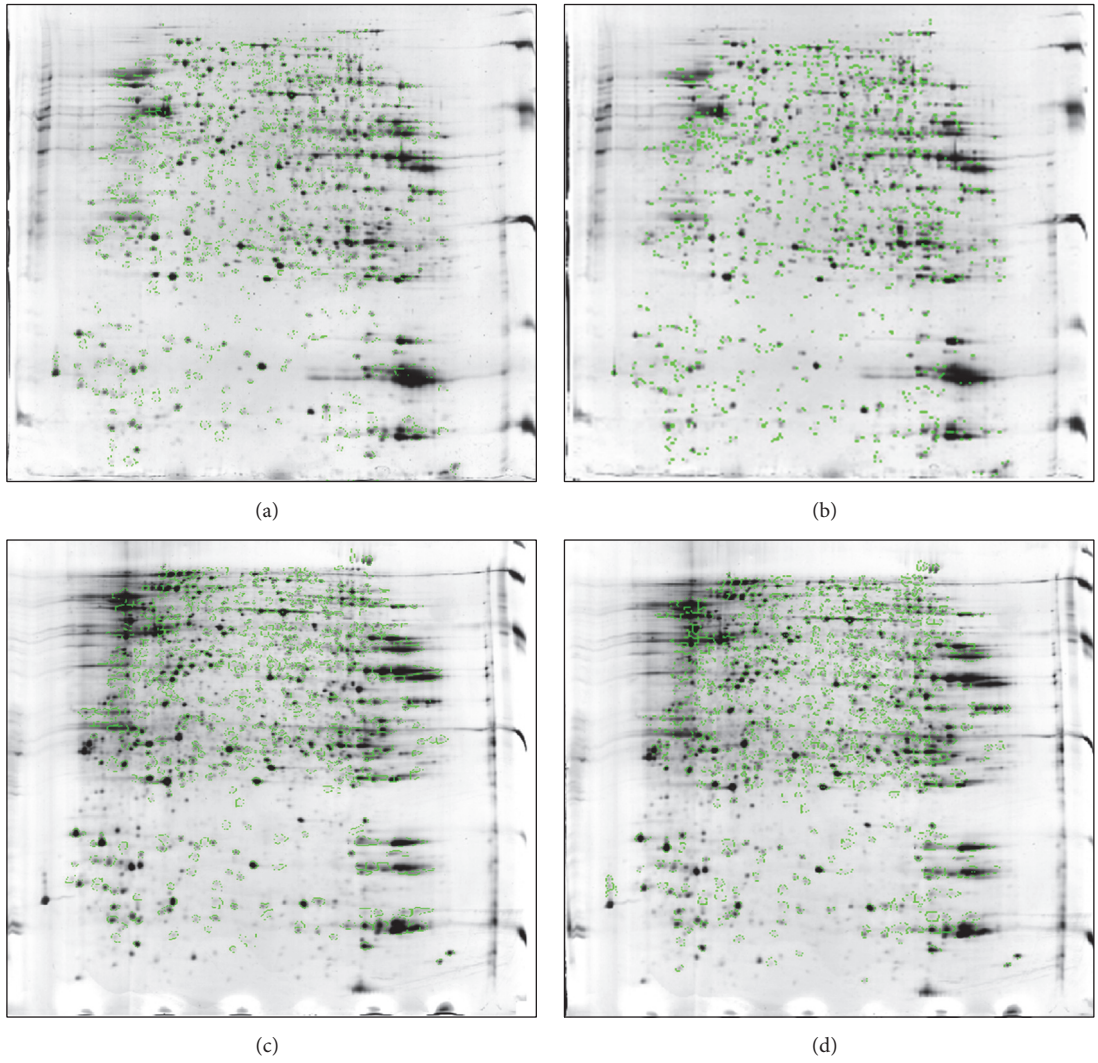

Figure 2: Two-dimensional gel electropherograms obtained from hypothalamus and hippocampi tissues, analysed in pairs. (a) Image overlay of the hypothalamus samples from the control group and the model group. (b) Image overlay of the hypothalamus samples from the control group and the group administered with Baixiangdan. (c) Image overlay of the hippocampi samples from the control group and the model group. (d) Image overlay of the hypothalamus samples from the control group and the group administered with Baixiangdan.

rats given the Baixiangdan capsule were analysed, and there were 22 types of proteins that underwent changes of expression: upregulation of 6 types and downregulation of 16 types.

3.3. Identification of Expressed Biomarkers Using Mass Spectrometry. After in-gel tryptic digestion, MALDI-TOF-MS was used to obtain the peptide mass fingerprint spectrum, with the aid of the website (http://www.matrixscience.com) for identification. Among the 22 proteins, 11 were identified (Table 1); these were Ulip2 protein, tubulin beta chain 15, α actin, aldolase, M2 pyruvate kinase, panthenol-cytochrome C reductase core protein I, hydrolase at the end of ubiquitin carboxy, albumin, interleukin 1 receptor accessory protein, hemoglobin α chain, kappa-B motif-binding phosphoprotein, and calcium-binding protein. When compared with the normal group, the model group displayed the following features of hippocampus organization: decreased level of Ulip2 protein, tubulin beta chain 15, α actin, and interleukin 1 receptor accessory protein and increased level of kappa-B motif-binding phosphoprotein. The hypothalamus organization of the model group, when compared with that of the normal group, displayed the following features: decreased expression of hydrolase at the end of ubiquitin carboxy, albumin and aldolase, and increased expression of M2 pyruvate kinase, panthenol-cytochrome C reductase core protein I and calcium-binding protein. For more information, please check Table 1 for the protein name, molecular weight, the isoelectric point, the protein identification score, and the peptide fragment matching rate.

A preliminary study was conducted on any differences between the normal group and the PMS irritability group in terms of protein expression in the hippocampus and hypothalamus. There were 22 types of proteins with differential expression, 11 of which were subjected to mass spectrum

Table 1: Between-group differences in the expression of proteins in the rat hippocampus and hypothalamus.

Accession	Mr		Cal. PI	Peptides		Sequence coverage
	Theor	Cal				
A25113	49905	2	4.79	21	41	60%
AAA37166	16758	5	5.29	6	11	39%
XP-347150	15275	6	8.45	6	6	58%
A54143	51010	10	5.19	9	12	22%
AAB93667	57744	12	7.15	20	35	44%
XP-217267	52815	13	5.57	8	23	25%
AAH17646	31353	14	4.94	11	17	45%
NP-599153	68674	17	6.09	20	21	44%
NP-036629	39259	18	6.67	13	27	40%
AAH39177	24822	20	5.14	14	20	76%
XP-485555	49754	22	4.73	17	44	39%

identification. Since the enzymes may not digest all the peptide fragments and some hydrophobic and large peptide fragments may get lost, the coverage rate of peptide fragments in this experiment was 22–76%. The identified proteins can be divided into the following types in terms of function: (1) cytoskeletal protein; (2) intermediary metabolic enzyme; (3) ubiquitin path and protein enzyme related protein; (4) signal path protein; (5) transcription, shearing, and extending related protein; and (6) calcium-binding protein. However, this present study did not identify any protein expression changes in central monoamine neurotransmitter receptor and central steroid hormone receptor in the PMS irritability model, which is not consistent with previous research at the mRNA level [16] probably because of the hydrophobic property of these proteins. For example, in enzymolysis, peptide fragments with a hydrophobic property and large molecular weight may get lost, leading to the loss of important information. Another issue is that it is difficult to explain how the particular proteins identified in this study cause PMS irritability, based on our understanding of their functions. The two aforementioned points constitute the main limitations of this study. Nonetheless, this study presents new findings that have not previously been reported, thereby contributing to research on PMS and providing the foundation for further exploration of the aetiology and pathogenesis of PMS. For example, we intend to further investigate the calcium-binding protein, signal path protein, and transcription-related protein, with the administration of more precisely selected chemical compounds in place of Baixiangdan, to more clearly identify the regulatory mechanism. So far, gratifying achievements have been made and future studies would soon follow.

Abbreviations

2DE: Two-dimensional gel electrophoresis
SDS-PAGE: Sodium dodecyl sulphate-polyacrylamide electrophoresis
PMS: Premenstrual syndrome
MALDI-TOF-MS: Matrix-assisted laser desorption ionisation time of flight mass spectrometry
Ctrl: Normal control group
Mod: PMS irritability model group
BXD: PMS irritability rats given Baixiangdan capsule.

Competing Interests

The authors have no conflict of interests to declare.

Authors' Contributions

The manuscript was written through contributions from all the authors. All authors discussed the results and gave full approval to the final version of the manuscript.

Acknowledgments

This work was supported by Special Funds for the Major State Basic Research Programme (2011CB505102).

References

[1] U.-B. Ekholm and T. Backstrom, "Influence of premenstrual syndrome on family, social life, and work performance," *International Journal of Health Services*, vol. 24, no. 4, pp. 629–647, 1994.

[2] M.-C. Hsiao and C.-Y. Liu, "Unusual manifestations of premenstrual syndrome," *Psychiatry and Clinical Neurosciences*, vol. 61, no. 1, pp. 120–123, 2007.

[3] S. S. Sadr, S. M. Samimi Ardestani, K. Razjouyan, M. Daneshvari, and G. Zahed, "Premenstrual syndrome and comorbid depression among medical students in the internship stage: a descriptive study," *Iranian Journal of Psychiatry and Behavioral Sciences*, vol. 8, no. 4, pp. 74–79, 2014.

[4] S. Tabassum, B. Afridi, Z. Aman, W. Tabassum, and R. Durrani, "Premenstrual syndrome: frequency and severity in young college girls," *Journal of the Pakistan Medical Association*, vol. 55, no. 12, pp. 546–549, 2005.

[5] T. Pearlstein, "Selective serotonin reuptake inhibitors for premenstrual dysphoric disorder: the emerging gold standard?" *Drugs*, vol. 62, no. 13, pp. 1869–1885, 2002.

[6] J. Zhou, G. Xie, and X. Yan, *Encyclopedia of Traditional Chinese Medicines—Molecular Structures, Pharmacological Activities, Natural Sources and Applications*, Springer, Berlin, Germany, 2011.

[7] P. Sun, S. Wei, H. Y. Zhang, and M. Q. Qiao, "Metabolic and behavioral patterns in a pre-menstrual syndrome animal model with liver-qi invasion and their reversal by a Chinese traditional formula," *Chinese Medicine*, vol. 1, no. 3, pp. 91–97, 2010.

[8] Y.-Y. Xie, L. Li, Q. Shao et al., "Urinary metabolomics study on an induced-stress rat model using UPLC-QTOF/MS," *RSC Advances*, vol. 5, no. 92, pp. 75111–75120, 2015.

[9] B. Lee, Y.-W. Shin, E.-A. Bae et al., "Antiallergic effect of the root of Paeonia lactiflora and its constituents paeoniflorin and paeonol," *Archives of Pharmacal Research*, vol. 31, no. 4, pp. 445–450, 2008.

[10] I. T. Nizamutdinova, Y. C. Jin, J. S. Kim et al., "Paeonol and paeoniflorin, the main active principles of Paeonia albiflora, protect the heart from myocardial ischemia/reperfusion injury in rats," *Planta Medica*, vol. 74, no. 1, pp. 14–18, 2008.

[11] M. Baroncini, P. Jissendi, S. Catteau-Jonard et al., "Sex steroid hormones-related structural plasticity in the human hypothalamus," *NeuroImage*, vol. 50, no. 2, pp. 428–433, 2010.

[12] F. M. Helmerhorst, L. M. Lopez, and A. A. Kaptein, "Premenstrual syndrome," *The Lancet*, vol. 372, no. 9637, pp. 446–447, 2008.

[13] E. Comasco and I. Sundström-Poromaa, "Neuroimaging the menstrual cycle and premenstrual dysphoric disorder," *Current Psychiatry Reports*, vol. 17, no. 10, article no. 77, 2015.

[14] M. Delgado, A. G. Caicoya, V. Greciano et al., "Anxiolytic-like effect of a serotonergic ligand with high affinity for 5-HT1A, 5-HT2A and 5-HT3 receptors," *European Journal of Pharmacology*, vol. 511, no. 1, pp. 9–19, 2005.

[15] S. Sun, *Effects of Serum from BXD Capsule-Treated PMS Model Rats with Liver-qi Invasion on Neuron Viability and GABAA Receptor-Mediated Currents*, Shandong University of Traditional Chinese Medicine, Jinan, China, 2009.

[16] D. Gao, *Studies on the Underlying Mechanism of Liver-Qi Sthenic Dispersedness—Analyses on the Differential Expression of Sevcral Important Hormone and Neurotransmitter Receptor Genes in the Brain Tissue of Premenstrual Syndrome Liver-Qi Sthenia Symptom*, Shandong University of Traditional Chinese Medicine, 2006.

[17] L. M. Jaramillo, I. B. Balcazar, and C. Duran, "Using vaginal wall impedance to determine estrous cycle phase in Lewis rats," *Lab Animal*, vol. 41, no. 5, pp. 122–128, 2012.

[18] A. B. El-Wishy, "The postpartum buffalo. II. Acyclicity and anestrus," *Animal Reproduction Science*, vol. 97, no. 3-4, pp. 216–236, 2007.

[19] P. M. S. O'Brien, I. E. H. Abukhalil, and C. Henshaw, "Premenstrual syndrome," *Current Obstetrics and Gynaecology*, vol. 5, no. 1, pp. 30–35, 1995.

[20] M. L. Seibenhener and M. C. Wooten, "Use of the open field maze to measure locomotor and anxiety-like behavior in mice," *Journal of Visualized Experiments*, no. 96, Article ID e52434, 2015.

[21] X. Zhu, T. Li, S. Peng, X. Ma, X. Chen, and X. Zhang, "Maternal deprivation-caused behavioral abnormalities in adult rats relate to a non-methylation-regulated D2 receptor levels in the nucleus accumbens," *Behavioural Brain Research*, vol. 209, no. 2, pp. 281–288, 2010.

[22] P. Sun, S. Wei, X. Wei et al., "Anger emotional stress influences VEGF/VEGFR2 and its induced PI3K/AKT/mTOR signaling pathway," *Neural Plasticity*, vol. 2016, Article ID 4129015, 12 pages, 2016.

[23] M. Ahmed, G. R. Srinivasan, E. Theodorsson, A. Bjurholm, and A. Kreicbergs, "Extraction and quantitation of neuropeptides in bone by radioimmunoassay," *Regulatory Peptides*, vol. 51, no. 3, pp. 179–188, 1994.

[24] J. Chen, X. Gao, B. Wang, F. Chen, N. Wu, and Y. Zhang, "Proteomic approach to reveal the proteins associated with encystment of the ciliate *Euplotes encysticus*," *PLoS ONE*, vol. 9, no. 5, Article ID e97362, 2014.

[25] J. Chen, T.-W. Liu, W.-J. Hu et al., "Comparative proteomic analysis of differentially expressed proteins induced by hydrogen sulfide in *Spinacia oleracea* leaves," *PLoS ONE*, vol. 9, no. 9, Article ID e105400, 2014.

[26] P. F. Edgar, S. J. Schonberger, B. Dean, R. L. M. Faull, R. Kydd, and G. J. S. Cooper, "A comparative proteome analysis of hippocampal tissue from schizophrenic and Alzheimer's disease individuals," *Molecular Psychiatry*, vol. 4, no. 2, pp. 173–178, 1999.

[27] Q. Tan, J. Gao, S. Wei, H. Zhang, Y. Su, and X. Liu, "Effect of Baixiangdan capsule on distribution and expression of γ-aminobutyric acid B recepter subunit of premenstrual syndrome rats with liver-qi upward invasion syndrome," *Traditional Chinese Drug Research & Clinical Pharmacology*, vol. 23, no. 4, pp. 378–381, 2012.

[28] Y. Li, B. Zhang, and X. Fan, "Determination of paeoniflorin, paeonol and α-cyperone in Baixiangdan capsule by HPLC," *Chinese Traditional Patent Medicine*, vol. 31, no. 11, pp. 1690–1694, 2009.

[29] Z. Huiyun, W. Sheng, S. Peng, X. Ling, and Q. Mingqi, "Empirical study of changes of pre-menstrual syndrome model rats with liver-qi invasion and liver-qi depression in peripheral blood, sexual hormones, different encephalic regions and accommodate hormones," *World Science & Technology*, vol. 12, no. 1, pp. 51–56, 2010.

[30] R. J. Katz and S. Hersh, "Amitriptyline and scopolamine in an animal model of depression," *Neuroscience and Biobehavioral Reviews*, vol. 5, no. 2, pp. 265–271, 1981.

[31] R. J. Katz, K. A. Roth, and B. J. Carroll, "Acute and chronic stress effects on open field activity in the rat: implications for a model of depression," *Neuroscience and Biobehavioral Reviews*, vol. 5, no. 2, pp. 247–251, 1981.

[32] R. J. Katz, K. A. Roth, and K. Schmaltz, "Amphetamine and tranylcypromine in an animal model of depression: pharmacological specificity of the reversal effect," *Neuroscience and Biobehavioral Reviews*, vol. 5, no. 2, pp. 259–264, 1981.

Hindawi
Neural Plasticity
Volume 2017, Article ID 9382797, 10 pages
https://doi.org/10.1155/2017/9382797

Research Article

Neuroplastic Correlates in the mPFC Underlying the Impairment of Stress-Coping Ability and Cognitive Flexibility in Adult Rats Exposed to Chronic Mild Stress during Adolescence

Yu Zhang,[1,2,3] Feng Shao,[4] Qiong Wang,[4] Xi Xie,[1,2] and Weiwen Wang[1]

[1]*CAS Key Laboratory of Mental Health, Institute of Psychology, Beijing, China*
[2]*The University of Chinese Academy of Sciences, Beijing, China*
[3]*School of Nursing, Binzhou Medical University, Yantai, China*
[4]*School of Psychological and Cognitive Sciences, Beijing Key Laboratory of Behavior and Mental Health, Peking University, Beijing, China*

Correspondence should be addressed to Weiwen Wang; wangww@psych.ac.cn

Received 17 October 2016; Accepted 18 December 2016; Published 15 January 2017

Academic Editor: Fushun Wang

Using a valid chronic mild stress (CMS) model of depression, we found that adolescent (postnatal days [PND] 28–41) CMS induced transient alterations in anhedonia that did not persist into adulthood after a 3-week recovery period. Previously stressed adult rats exhibited more immobility/despair behaviors in the forced swimming test and a greater number of trials to reach criterion in the set-shifting task, suggesting the impaired ability to cope with stressors and the cognitive flexibility that allows adaptation to dynamic environments during adulthood. In addition, adult rat exposure to adolescent CMS had a relatively inhibited activation in ERK signaling and downstream protein expression of phosphorylated cAMP-response element-binding protein (CREB) and brain-derived neurotrophic factor (BDNF) in the medial prefrontal cortex. Further correlation analysis demonstrated that immobility and set-shifting performance were positively correlated with the inhibition of ERK signaling. These results indicated adolescent CMS can be used as an effective stressor to model an increased predisposition to adult depression.

1. Introduction

High plasticity is a fundamental mechanism of brain function for adaptation to dynamic environments. A large body of evidence has demonstrated that neuroplasticity in limbic areas is disrupted in depression, and antidepressant treatment produces therapeutic action by enhancing neuroplasticity [1]. For example, there exists a substantial decrease in the structural and functional plasticity in the prefrontal cortex (PFC) and hippocampus in depression; chronic treatment with antidepressants can reverse this decrease in parallel with the improvement of emotional symptoms [2, 3].

Early adverse experiences significantly increase the incidence of depression during adulthood [4, 5]. However, how stressor exposure during development causes long-term behavioral and physiological consequences is still not fully elucidated. The PFC is a critical brain region involved in the modulation of higher brain functions, including emotion, working memory, and cognitive function [6, 7]. In adolescence (conservatively estimated as the period from postnatal days [PND] 28 to 48 in rodents), the hypothalamic-pituitary-adrenal (HPA) axis is still immature and the PFC undergoes significant and profound development [8]. By causing enhanced and prolonged responses, stressor exposure during this stage may contribute to greater long-term detrimental effects in the development of these systems in adolescents than that in adults [9, 10]. Studies on humans and animals have consistently demonstrated that adverse stressors during adolescence lead to neuroplastic damage, including PFC volume loss, increased neuronal apoptosis, decreased neurogenesis, decreased synaptic transmission, and subsequently emotional and cognitive dysfunctions [11–14].

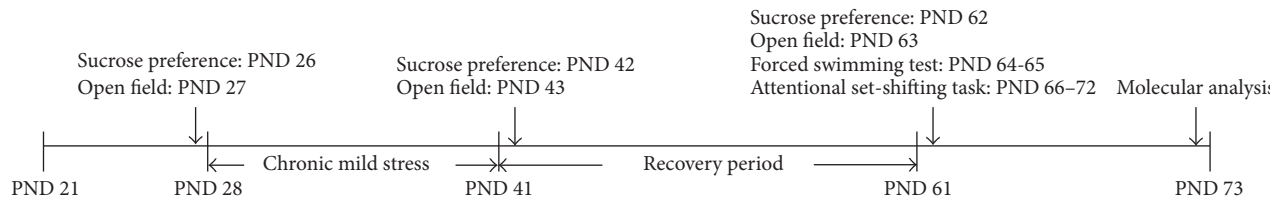

Figure 1: Timeline of procedures. We evaluated the effects of chronic mild stress during adolescence on adult behaviors using the following tests: sucrose preference, open field, forced swimming, and attentional set-shifting task.

Extracellular signal-regulated kinase (ERK), one of the most important members of the mitogen-activated protein kinase (MAPK) family, is highly expressed in the PFC and hippocampus [15]. The activated ERK, phosphorylated ERK (pERK), subsequently modulates downstream nuclear transcription factors, especially cAMP-response element-binding (CREB) protein, which is involved in the transcription of several neurotrophic factors, such as brain-derived neurotrophic factor (BDNF). ERK-CREB signaling exerts extensive effects on behavioral and biological responses to stressors, such as synaptic plasticity, learning and memory, and emotion and cognitive function [16–19]. ERK signaling abnormality exists in the PFC of depressed patients and animals and can be improved by antidepressant treatment [20]. For example, our previous studies indicated that inhibition of ERK signaling in the mPFC and hippocampus was correlated with depressive behaviors induced by chronic cold water swimming stress, and treatment with antidepressant reversed these alterations [21, 22].

Chronic mild stress (CMS), consisting of multiple stressors that are analogous to the continuous and unpredictable life events in humans, is a valid rodent model of depression [23]. In adult rodents, CMS can induce a variety of behavioral and neurobiological changes, including anhedonia, decreased exploratory behavior, and increased immobility/despair behavior when exposed to stressful environments, impaired spatial cognition, and altered expression of ERK, CREB, and BDNF in the PFC [24–26]. Commonly, a longer time (usually 4–6 weeks or longer) is needed to establish this model, and its effects are transient and reversible shortly after the cessation of the stress. A few studies have investigated the long-term effects of CMS delivered during a specific time window, such as adolescence, and the results were inconsistent [12]. For example, Toth et al. reported that CMS from adolescence to early adulthood (PND 30–58) decreased anhedonia when tested 6 weeks after the stress [27], while Pohl et al. reported that CMS during adolescence (PND 23–51, followed by a 3-week no-stress period) increased anhedonia in adult female but not male rats [28]. In addition, predictable and unpredictable CMS during adolescence had protective and detrimental effects, respectively, on emotional and cognitive function in adulthood [29–31]. Thus the long-term effects of stress during adolescence on emotion and cognition are as yet not well characterized.

This study involved a set of behavioral tests to further evaluate the emotional and cognitive profiles of adult rats exposed to CMS solely during adolescence. Instinctive motivations for reward consumption and for exploration were determined, with decreases generally considered typical depressive symptoms. The forced swimming test (FST) was used to assess whether stress-coping ability to subsequent stressors during adulthood was affected by adolescent stress [9, 32, 33]. In addition, an attentional set-shifting task (AST) was performed to evaluate cognitive flexibility, a higher cognitive function that allows adaptation to a dynamic environment for optimized behavioral strategies. Strong evidence suggests that cortically mediated cognitive inflexibility is a core component of depression and is closely linked with attentional bias to negative emotion in depression, efficacy of antidepressant treatment, and recurrence of depression [34–36]. Additionally, the ERK-CREB signaling and downstream BDNF expression in the mPFC, a region involved in stress coping, emotion, and cognitive function, were determined, and the correlations between behavioral and molecular alterations were further analyzed. A dependence of these behavioral and molecular consequences on previous exposure to CMS during adolescence would suggest that exposure to this stressor at this stage can be an effective model to simulate the increased vulnerability to depression in adulthood by reducing neuroplasticity within the mPFC.

2. Methods and Materials

2.1. Animals. Eighteen male Wistar rats were obtained from the Academy of Chinese Military Medical Science (Beijing, China) after weaning (PND 21). Rats were housed individually in stainless steel wire cages and were given 7 days to acclimate to the standard rearing conditions: 12 h light/12 h dark cycle (lights on at 7:00 am), ambient temperature of 20–22°C, and relative humidity of 40–70% with free access to food and water except during the sucrose preference test and the AST. A full timeline of all manipulations and behavioral tests is provided in Figure 1. All experimental procedures were approved by the Institutional Review Board of the Institute of Psychology, Chinese Academy of Sciences, and were in compliance with the National Institutes of Health Guide for the Care and Use of Laboratory Animals.

2.2. Stress Procedure. At PND 28, on the basis of a sucrose preference test, rats were divided into two matched groups and placed in separate rooms: a chronic mild stress (CMS) group ($n = 9$) and a control (CON) group ($n = 9$). Adapted from our previous study [37], the CMS procedure consisted of a variety of unpredictable mild stressors, including 12–24 h

food and/or water deprivation followed in some cases by food restriction, cage tilt, continuous lighting, disrupted light/dark cycle, intermittent white noise, wet bedding, paired housing, flashing light (180 times/min), empty bottle stimulation, and hot or cold air (37°C for 30 min or 8°C for 30 min). Rats in the stress group were randomly exposed to 2–4 stressors every day for 2 weeks (PND 28–41). The controls were left undisturbed under the previously described maintenance conditions. Then, all animals experienced a 3-week no-stress period until adulthood. A series of behavioral tests were performed in sequence as follows to decrease any carry-over effects from one test to the other as much as possible.

2.3. Behavioral Tests

2.3.1. Sucrose Preference Test. This test was performed before, one day after, and three weeks after the CMS exposure (PND 26, 42, and 62, resp.). Briefly, after 20 h of food and water deprivation, rats were offered two bottles containing either tap water or 1.5% sucrose solution. The liquid intake from each bottle was calculated by comparing the differences in bottle weights before and after a 1-h testing window. The sucrose preference was determined as the percentage of sucrose solution intake/total (water + sucrose liquid) intake. Low sucrose preference represented anhedonia, a core symptom of depression. When the preference test ended, rats were given free access to water.

2.3.2. Open Field Test. This test was performed one day after each sucrose preference test (PND 27, 43, and 63). The testing apparatus was a circular arena (diameter × height: 180 cm × 50 cm). Rats were placed individually into the center of the arena and were recorded for 5 min. Exploratory behaviors, including horizontal ambulation and rearing, were determined. The distance of horizontal ambulation was automatically recorded using a computer-based tracking system (Med Associates Inc., USA), while the number of rearing instances was recorded by the experimenter and verified through video recording. The arena was thoroughly cleaned with 75% ethanol between each test to avoid any possible olfactory cues.

2.3.3. Forced Swimming Test. The test was performed one day after the last open field test (PND 64 and 65). The paradigm was similar to that described elsewhere [38]. On the first day, rats were forced to swim in a glass cylinder with water (depth no less than 30 cm, 23-24°C) for 15 min. Then, the rats were dried and transported back to their home cages. On the second day, the rats were allowed to swim for 5 min. The 5-min test session was videotaped from above using a Sony Camcorder. Behavioral analysis proceeded as described in our previous study [39]. Briefly, the immobility time of each rat was measured with a stopwatch by a trained observer who was blind to the experimental treatments. Immobility was defined as a floating state in the water without struggling and making only those movements necessary to keep the head above water.

2.3.4. Attentional Set-Shifting Task. This test was performed for one week from PND 66. The testing apparatus and procedure were introduced in our previous studies [13]. Briefly, rats were restricted to 10–14 g food per day to maintain 80–85% of their original body weight, with free access to water. Rats were trained to obtain a reward (1/4 Honey Nut Cheerios) by digging in two terracotta pots, which were defined by a pair of cues along two stimulus dimensions: the digging medium filling the pots and the odor applied to the inner rim of the pots. The "positive" pot was baited with a reward buried at the bottom of the digging medium. The test contained five successive stages with increased difficulty: the first stage was simple discrimination (SD), which only presented one relevant stimulus dimension (e.g., medium). The second stage was compound discrimination (CD) in which the same relevant stimulus dimension (medium) in SD was required and the second irrelevant dimension (e.g., odor) was presented as a distractor. The third stage was intradimensional shifting (IDS), wherein the medium was still the relevant dimension and the odor was still irrelevant, but new media and new odors were introduced. The fourth stage was reversal learning (RL), in which the same media and odors were used and the relevant dimension (medium) remained, but the negative cue in the IDS stage turned into a positive cue and the positive cue turned into a negative cue. The fifth stage was extradimensional shifting (EDS), in which all new media and odors were again introduced and the relevant dimension was replaced by odor. The test proceeded to the next stage when the rat reached a criterion of six consecutively correct trials. The number of trials to reach the criterion for each stage was recorded.

2.4. Western Blot Analysis

2.4.1. Tissue Collection. The rats were decapitated one day after the behavioral tests. The whole brain was quickly removed, immediately frozen in liquid nitrogen and then stored at −80°C before tissue collection. The tissue collection method was analogous to that in our previous study [40]. In short, according to the rat brain atlas [41], the mPFC (3.20–2.20 mm from the bregma) was bilaterally punched using a stainless steel cannula with an inner diameter of 0.6 mm at −20°C in a cryostat microtome (Leica, CM 3050, Germany).

2.4.2. Western Blotting Analysis. The tissue samples were placed in 50–70 μL precooling lysate buffer (4°C, pH 7.5, containing 5 μg/mL leupeptin, 5 μg/mL aprotinin, 5 μg/mL pepsin inhibitor, 5 μg/mL trypsin inhibitor, 2 mM EDTA, 2 mM EGTA, 1 mM DTT, and 0.5% NP-40) according to their volume and then homogenized using an ultrasonic homogenizer (Sonic Co., Stratford, CT, USA). The protein concentrations in the homogenates were determined by a bicinchoninic acid (BCA) Protein Assay Kit (CW Biotech, Beijing, China). The homogenates were then mixed with 5x sodium dodecyl sulfate (SDS) in proportion to prepare sample solutions with a certain concentration. The prepared sample solutions were denatured at 95°C for 8 min. Denatured proteins (32 μg) were separated by 12% SDS-PAGE and

transferred onto a nitrocellulose (NC) membrane at 230 mA for 1 h. The membrane was blocked with 5% nonfat milk diluted in TBST overnight at 4°C. After being washed in TBST (10 min × 3), the membrane was incubated at RT for 2 h on a shaker with primary antibodies: rabbit monoclonal ERK1/2 antibodies (1 : 1,000, Cell Signaling Technology Inc., Beverly, MA, USA) and rabbit monoclonal pERK1/2 antibodies (1 : 2,000, Cell Signaling Technology Inc.). After further washing in TBST (10 min × 3), the membrane was incubated at RT for 1 h on a shaker with secondary antibodies, HRP-conjugated goat anti-rabbit IgG (1 : 4,000, Zhongshan Golden Bridge Biotechnology, Beijing, China), and then washed again. Bands were detected by enhanced chemiluminescence (ECL, Millipore, Bedford, MA, USA) through a FluorChem E System (ProteinSimple, Santa Clara, CA, USA). After exposure, the membrane was stripped and reprobed with primary mouse monoclonal GAPDH antibodies (1 : 1,000, Zhongshan Golden Bridge Biotechnology) and secondary HRP-conjugated goat anti-mouse IgG (1 : 4,000, Zhongshan Golden Bridge Biotechnology) following the above steps. The pCREB and BDNF levels and the corresponding GAPDH level were determined in a different NC membrane using the same procedures. All bands were quantified using Lab Works TM 4.6 (image acquisition and analysis software). The ratio of each target band intensity to the GAPDH band intensity was used for difference analysis between the CON and CMS groups.

2.5. Data Analysis. All data were presented as the mean ± standard error of the mean (M ± SEM). SPSS 19.0 was employed for statistical analysis. The body weight data, sucrose preference test results, open field test results, and attentional set-shifting task results were analyzed with a mixed model ANOVA with repeated measures (with stress as the between-subjects and time as the within-subjects variable). The remaining behavioral and molecular data were analyzed with a t-test for independent samples. For correlation analyses of mPFC molecular levels and behavioral alterations, Pearson's correlation analysis was adopted. The level of significance for all analyses was set at $p < 0.05$.

3. Results

3.1. Effects of Adolescent CMS on Body Weights. As shown in Figure 2, there were significant main effects for time point ($F_{(2,32)} = 3075.488$, $p < 0.001$) and stress ($F_{(1,16)} = 78.249$, $p < 0.001$) and a significant time point × stress interaction effect ($F_{(2,32)} = 64.527$, $p < 0.001$). Rats that were exposed to CMS during adolescence exhibited lower body weights than the corresponding controls when tested both immediately after the last stressor ($t_{16} = 273.336$, $p < 0.001$) and after a 3-week recovery period ($t_{16} = 25.533$, $p < 0.001$).

3.2. Effects of Adolescent CMS on Depressive Behaviors. For the sucrose preference test, there were significant main effects for time point ($F_{(2,32)} = 19.893$, $p < 0.001$) and stress ($F_{(1,16)} = 6.495$, $p = 0.023$) and a marginally significant time point × stress interaction effect ($F_{(2,32)} = 3.154$, $p = 0.058$; Figure 3(a)). The sucrose preference values were significantly lower in CMS-treated rats than in the corresponding controls one day after the end of CMS ($p < 0.01$), but this decrease did not persist into adulthood after the 3-week recovery period.

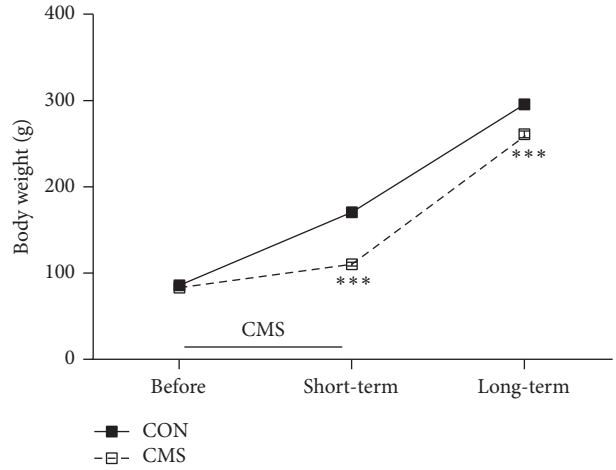

Figure 2: Effects of adolescent CMS on body weight. The body weights were measured on PND 28 (before the initiation of CMS), PND 42 (1 day after the end of CMS, short-term effect), and PND 63 (3 weeks after the end of CMS, long-term effect). $^{***}p < 0.001$ compared to the CON group at the corresponding time points.

In the open field test, there were no significant main effects for time point ($F_{(2,32)} = 0.790$, $p = 0.462$) or stress ($F_{(1,16)} = 0.460$, $p = 0.507$). Likewise, the time point × stress interaction effect ($F_{(2,32)} = 1.982$, $p = 0.153$) for horizontal ambulation was not significant (Figure 3(b)). Similarly, there were no significant main effects for time point ($F_{(2,32)} = 0.479$, $p = 0.623$) or stress ($F_{(1,16)} = 0.804$, $p = 0.382$) and no significant time point × stress interaction effect ($F_{(2,32)} = 0.446$, $p = 0.513$) for the frequency of rearing (Figure 3(c)).

When the FST was conducted during adulthood, CMS-treated adult rats exhibited significantly increased immobility/despair behaviors ($t_{16} = -2.135$, $p = 0.049$; Figure 3(d)).

3.3. Effects of Adolescent CMS on Cognitive Flexibility in the AST. A two-way ANOVA revealed significant main effects for stage ($F_{(4,64)} = 9.884$, $p < 0.001$) and stress ($F_{(1,16)} = 6.939$, $p = 0.022$) but no significant stress × stage interaction effect ($F_{(4,64)} = 1.905$, $p = 0.125$). However, a t-test for each stage in the AST demonstrated a significantly greater number of trials to reach criterion in the EDS stages for the CMS-treated rats than for the controls ($t_{16} = 4.970$, $p = 0.046$). In addition, CMS-treated rats exhibited a moderately increased number of trials to criterion in the RL stages than the controls, but the difference was not significant ($t_{16} = 3.463$, $p = 0.087$) (Figure 4).

3.4. Effects of Adolescent CMS on ERK1/2, pERK1/2, pCREB and BDNF Levels in the mPFC of Adult Rats. Adult rats exposed to adolescent CMS showed significantly increased expression of ERK1 ($t_{16} = -6.087$, $p < 0.001$) and ERK2 ($t_{16} = -4.759$, $p = 0.001$), but the pERK1 and pERK2 levels

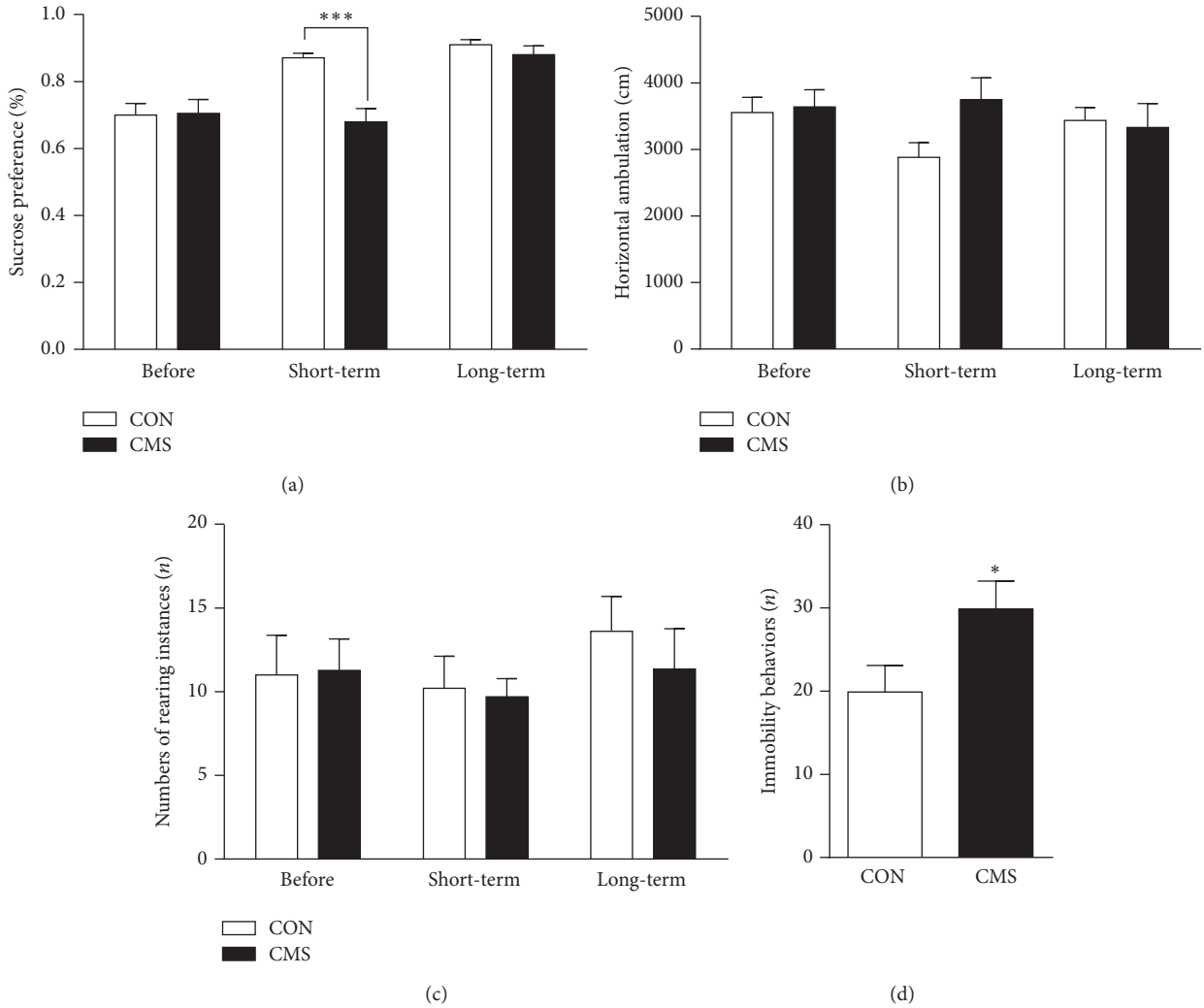

Figure 3: Effects of adolescent CMS on sucrose preference (a), horizontal ambulation (b) and number of rearing instances (c) in the open field test and immobility in the FST (d). Behavioral tests were conducted in sequence as follows: the sucrose preference test was performed before, one day after, and 3 weeks after the end of CMS; the open field test was performed one day after each sucrose preference test; the FST was performed one day after the last open field test in adult rats. $^{*}p < 0.05$ and $^{***}p < 0.001$ compared to the CON group at the corresponding time point.

did not differ between the two groups ($p > 0.05$ for both; Figures 5(a), 5(b), 5(d), and 5(e)). Furthermore, the ratio of pERK1 to ERK1 (pERK1/ERK1, $t_{16} = 2.290$, $p = 0.043$) and the ratio of pERK2 to ERK2 (pERK2/ERK2, $t_{16} = 3.435$ $p = 0.006$) in CMS-treated rats were significantly lower than those of the CON group in adulthood (Figures 5(c) and 5(f)). The level of pCREB, one of the downstream nuclear transcription factors of ERK, and the level of BDNF were likewise decreased in adulthood ($t_{16} = 3.550$, $p = 0.005$ for pCREB; $t_{16} = 2.855$, $p = 0.016$ for BDNF; Figures 5(g) and 5(h)).

3.5. Correlations between Behavioral and Molecular Alterations in Adult Rats. As shown in Table 1, further correlation analysis demonstrated that the increased immobility behaviors in FST were positively associated with the increased ERK1 protein levels in the mPFC ($r = 0.611$, $p = 0.026$). There was a marginally negative correlation between the increased immobility behaviors and the decreased pERK2/ERK2 ratio ($r = -0.535$, $p = 0.060$). In addition, a marginally negative correlation was found between the increased trials to criterion in the EDS stage in AST and the decreased pERK1/ERK1 ratio ($r = -0.557$, $p = 0.057$).

4. Discussion

Adolescent CMS decreased body weight in rats in the current study, even after the 3-week recovery period and into adulthood, reflecting the stressful nature of this paradigm and its prolonged effect. We observed several novel findings in the present study: (1) Adolescent CMS increased immobility in the FST and impaired the set-shifting ability in adult rats even after several weeks of recovery. On the other hand, sucrose preference, while reduced immediately after the CMS, showed recovery and was normal in adulthood.

Table 1: Correlations between behavioral and molecular alterations in adult rats exposed to adolescent CMS.

		ERK1	ERK2	pERK1/ERK1	pERK2/ERK2	pCREB	BDNF
Immobility	r value	0.611	0.454	−0.338	−0.535	−0.468	−0.139
	p value	**0.026***	0.119	0.259	**0.060**	0.106	0.652
EDS	r value	0.142	−0.022	−0.557	−0.350	−0.101	−0.011
	p value	0.659	0.945	**0.057**	0.264	0.754	0.972

* $p < 0.05$.

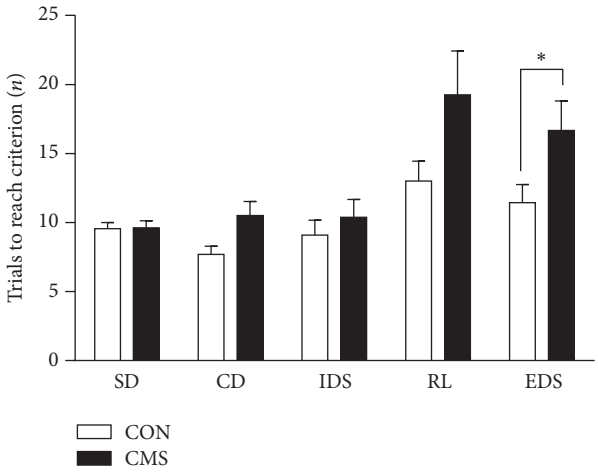

Figure 4: Effects of adolescent CMS on the performance on the AST. Rats were tested 3 weeks after the end of CMS during adulthood. The number of trials to criterion reflected the performance during the 5 stages of the test: simple discrimination (SD), compound discrimination (CD), intradimensional shifting (IDS), reversal learning (RL) and extradimensional set-shifting (EDS). * $p < 0.05$ compared to the CON group at the corresponding stages.

Exploratory activity in the open field test was not affected by the stress exposure during adolescence. (2) Adolescent CMS decreased the relative activation of ERK signaling in the mPFC and the expression of the downstream pCREB and BDNF, which play important roles in brain development and neuroplasticity. (3) Adolescent CMS-induced behavioral alterations were correlated with ERK signaling activities in the mPFC. These results suggested that adolescent CMS did not affect instinctive motivation to consume a reward or exploration but significantly impaired the ability to cope with stressor exposure and cognitive flexibility that allows adaptation to dynamic environments during adulthood. The decreased neuroplasticity of the mPFC may mediate this procedure.

4.1. Effects of Adolescent CMS on the Behaviors of Adult Rats. First, adolescent CMS transiently induced anhedonia shortly after the stress, but this change was reversible, with recovery occurring 3 weeks later. Stress effects on anhedonia can be affected by some experimental factors, such as gender and stress conditions. For example, CMS through childhood and adolescence (PND 23–51) followed by a 3-week no-stress period caused a decrease in sucrose preference and an increase in anxiety behavior in a burying test in female but not male adults [28]. In addition, the unpredictability of the multiple stressors of the CMS presentation is also important because of its effects. Previous research showed that predictable and unpredictable stress during adolescence exerted protective and detrimental effects, respectively, on emotional and cognitive function in adult rats [29–31]. In this study, 2 to 4 types of stressors were randomly delivered at different times every day to maintain a continuous environmental disturbance. On this basis, we found that CMS that was limited to adolescence (PND 28–37) had no effect on the anhedonia of adult rats. Similar results were also observed in exploratory behaviors in the open field test. Fewer attempts to consume a reward and decreased exploration are thought of as typical depressive symptoms. Thus, these results suggested that adolescent CMS did not induce such signs of depression into adulthood.

Second, we found that adult rats with CMS experience during adolescence exhibited more immobility in the FST, suggesting that the animals exposed to adverse events during this period underwent a long-term change in the ability to cope with subsequent challenges during adulthood. The two-stage FST (the first stage was forced swimming training in an unescapable threatening environment; the second stage was a helpless or despair behavior test) has been extensively used to identify an inability to cope with subsequent stressors after excessively adverse experiences, a symptom of depression called helplessness/despair [42]. Thus, our results suggested that previously stressed rats had higher susceptibility to develop despair behavior in a stressful environment during adulthood. Similarly, other studies also showed that the changes induced by stress exposure during adolescence can be long-term but only become apparent after a subsequent stressor is applied, which may contribute to an increased risk for stress-related disorders later in life [9, 43, 44]. In addition, although lower body weight was found in previously stressed rats, there had been similar locomotor activity in open field test in control and stress groups, suggesting that the increased immobility in stress group was unlikely due to deficits in body energy.

Third, we found that adolescent CMS impaired the cognitive flexibility of adult rats, as indicated by the increased number of trials to reach criterion in the EDS stage. Cognitive inflexibility is increasingly recognized as a relatively independent risk factor for the onset of depression, which is closely associated with emotional inflexibility in depression, therapeutic effects on emotional symptoms after antidepressant treatment, and the reoccurrence of depression [34–36].

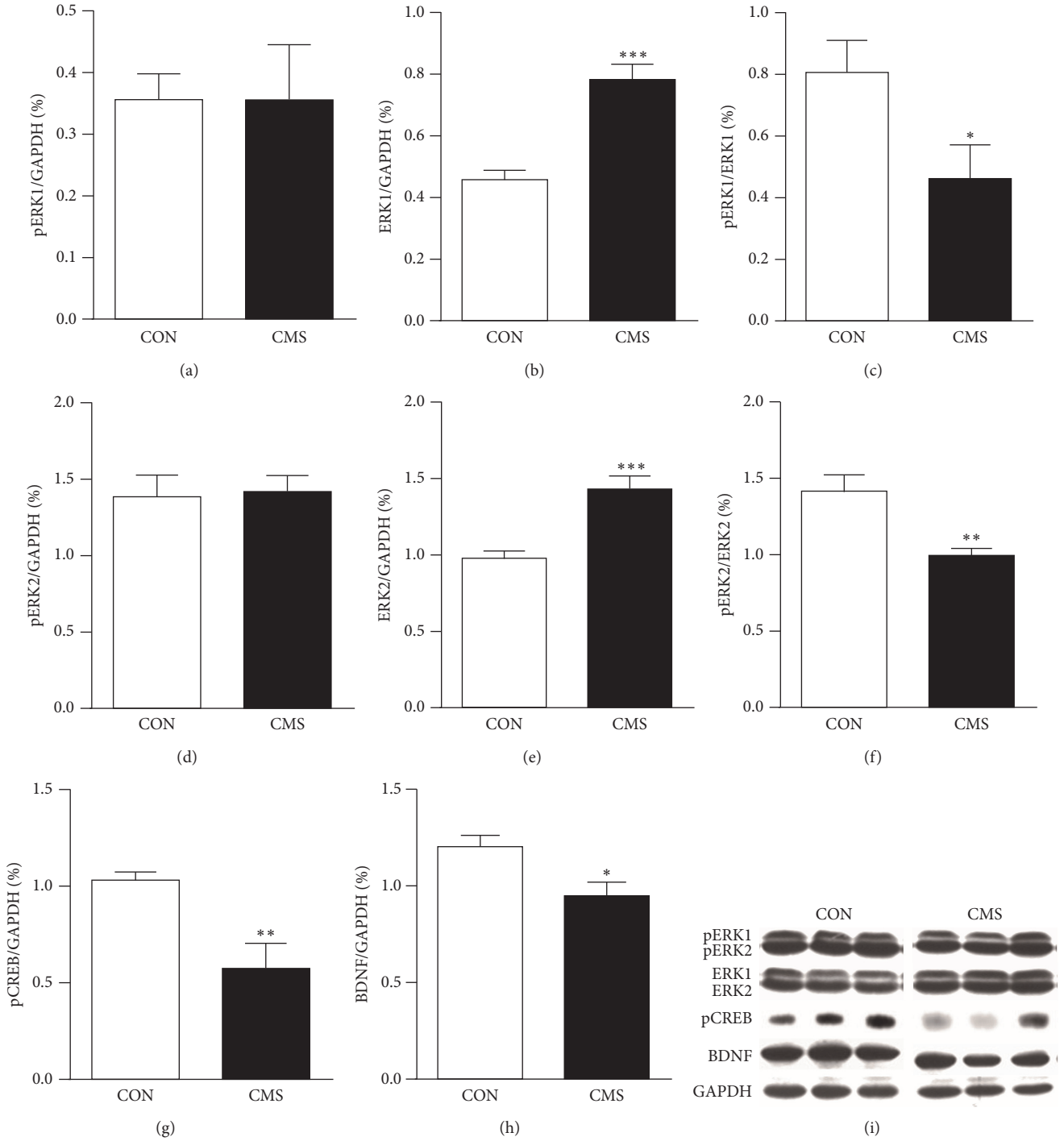

Figure 5: Effects of adolescent CMS on ERK1/2, pERK1/2, pCREB and BDNF levels in the mPFC of adult rats. (a) pERK1; (b) ERK1; (c) pERK1/ERK1; (d) pERK2; (e) ERK2; (f) pERK2/ERK2; (g) pCREB; (h) BDNF; and (i) representative blots for pERK1/2, ERK1/2, pCREB, BDNF and GAPDH. Rats were decapitated for western blot analysis one day after the behavioral tests. The results were calculated as the intensity of the lane of each transcript relative to the intensity of the corresponding GAPDH band and expressed as the mean ± SEM. $^{*}p < 0.05$, $^{**}p < 0.01$, $^{***}p < 0.001$, compared to the CON group.

Normal function of the mPFC is necessary to perform set-shifting [7]. Chronic stress can impair set-shifting performance as a result of the structural and functional effects on the mPFC, which can be ameliorated by antidepressant treatment [45, 46]. Therefore, the impaired EDS performance demonstrated in this study may reflect mPFC dysfunction during adulthood.

4.2. Effects of Adolescent CMS on Neuroplastic Molecules in the mPFC of Adult Rats. We found that adolescent CMS

induced an increase in the expression of ERK1 and ERK2 but not pERK1 and pERK2 in the mPFC of adult rats. Accordingly, the pERK1/ERK1 and pERK2/ERK2 ratios were decreased in previously stressed adult rats compared to controls. Phosphorylated ERK indicates an activated state of ERK, while the pERK1/ERK1 and pERK2/ERK2 ratios reflect the relative activation and actual effects on neural cells [47, 48]. These results suggested that adolescent CMS exerted inhibitory effects on ERK signaling in the mPFC. CREB, a main downstream nuclear transcription factor regulated by ERK signaling, can modulate the transcription of many proteins, such as c-fos and BDNF. The ERK-CREB cascade has been confirmed to be involved in the modulation of neural development, neuroplasticity, stress responses, emotion, and cognition [19, 49]. In line with the inhibition of ERK signaling, there was a long-term decrease in the pCREB and BDNF levels in the mPFC of adult rats subjected to adolescent CMS. Commonly, acute stress increases ERK signaling in the mPFC for adaptation, while chronic stress decreases this signaling and causes functional impairment [22, 47, 50, 51]. Animals with ERK or BDNF gene knockdown also exhibited structural and functional abnormalities in the mPFC [52, 53]. In addition, studies on humans and animals have shown that adolescent stress can cause long-term decreases in the neuroplasticity of the mPFC, which are accompanied by increased depression and anxiety during adulthood [11, 12]. These results suggest that the intracellular ERK-CREB cascade may mediate the decreased neuroplasticity of the mPFC induced by adolescent stress.

4.3. Relationship between Behavioral and Molecular Alterations in Adult Mice Exposed to CMS during Adolescence. Further correlation analysis showed that immobility in the FST was positively correlated with ERK1 protein levels, while there was a marginal negative correlation with the pERK2/ERK2 ratio; the number of trials to criterion in the EDS stage tended to negatively correlate with the pERK1/ERK1 ratio. In adult rats exposed to chronic cold water swimming stress, depressive behaviors including anhedonia and locomotor activity were correlated with changes in the pERK1 and pERK2 and the pERK1/ERK1 and pERK2/ERK2 ratios, which could be reversed by treatment with the antidepressant fluoxetine [22, 51]. Although these studies also suggest that inhibition of ERK signaling in the mPFC is linked with depression, the characteristics of these alterations are different between the two studies. The reasons remain unclear, but the developmental stage when stressors are applied may be an important factor. For example, the mPFC is necessary for juveniles (early stage of adolescence) to process threatening stimuli [54]. In addition, Bingham et al. [55] reported that social defeat during the early adolescent but not late adolescent and adult periods altered the activity of the noradrenergic system and its projecting area, the mPFC, suggesting that the mPFC is an area sensitive to stress during early adolescence, a stage that is similar to that in the present study. Notably, set-shifting performance is specifically regulated by noradrenaline in the mPFC and also involves ERK signaling [7, 56, 57]. For example, the noradrenaline-induced long-term inhibition of pyramidal neuron synapses depends on postsynaptic activation of ERK1 and ERK2 signaling [57]. Imipramine (an antidepressant that can increase brain noradrenaline levels) can improve set-shifting performance, and this effect can be blocked by an inhibitor of ERK1 and ERK2 signaling [58, 59].

Additional Points

Summary. Our results indicate that CMS during adolescence induced long-term behavioral and molecular effects characterized by impairments in stress-coping ability and in cognitive flexibility required for adaptation to dynamic environments during adulthood. The results also indicate that these features may be mediated by decreased neuroplasticity in the mPFC. Thus, adolescent CMS can be used as an effective stressor to model an increased predisposition to adult depression to further elucidate the underlying neurobiological mechanisms of this condition.

Competing Interests

The authors declare no potential conflict of interests in this research.

Authors' Contributions

Weiwen Wang and Feng Shao designed the research; Yu Zhang, Qiong Wang, and Xi Xie performed the research and acquired the data; Yu Zhang, Qiong Wang, and Weiwen Wang interpreted and analyzed the data; Yu Zhang, Feng Shao, and Weiwen Wang drafted, revised, and wrote the paper. Yu Zhang and Feng Shao have contributed equally to this study.

Acknowledgments

The authors would like to thank Dr. Bart Ellenbroek for valuable suggestions regarding the manuscript. This work was supported by the National Natural Science Foundation of China (Grant no. 81471122 and no. 31470988), the Chinese Academy of Sciences (KJZD-EW-L04), and CAS Key Laboratory of Mental Health, Institute of Psychology.

References

[1] C. Pittenger and R. S. Duman, "Stress, depression, and neuroplasticity: a convergence of mechanisms," *Neuropsychopharmacology*, vol. 33, no. 1, pp. 88–109, 2008.

[2] A. V. Kalueff and D. L. Murphy, "The importance of cognitive phenotypes in experimental modeling of animal anxiety and depression," *Neural Plasticity*, vol. 2007, Article ID 52087, 7 pages, 2007.

[3] P. Licznerski and R. S. Duman, "Remodeling of axo-spinous synapses in the pathophysiology and treatment of depression," *Neuroscience*, vol. 251, pp. 33–50, 2013.

[4] B. Buwalda, M. Geerdink, J. Vidal, and J. M. Koolhaas, "Social behavior and social stress in adolescence: a focus on animal models," *Neuroscience & Biobehavioral Reviews*, vol. 35, no. 8, pp. 1713–1721, 2011.

[5] S. J. Lupien, B. S. McEwen, M. R. Gunnar, and C. Heim, "Effects of stress throughout the lifespan on the brain, behaviour and cognition," *Nature Reviews Neuroscience*, vol. 10, no. 6, pp. 434–445, 2009.

[6] J. T. McGuire and M. M. Botvinick, "Prefrontal cortex, cognitive control, and the registration of decision costs," *Proceedings of the National Academy of Sciences of the United States of America*, vol. 107, no. 17, pp. 7922–7926, 2010.

[7] T. W. Robbins and A. F. T. Arnsten, "The neuropsychopharmacology of fronto-executive function: monoaminergic modulation," *Annual Review of Neuroscience*, vol. 32, pp. 267–287, 2009.

[8] L. P. Spear, "Adolescent neurodevelopment," *Journal of Adolescent Health*, vol. 52, no. 2, supplement 2, pp. S7–S13, 2013.

[9] C. M. McCormick, I. Z. Mathews, C. Thomas, and P. Waters, "Investigations of HPA function and the enduring consequences of stressors in adolescence in animal models," *Brain and Cognition*, vol. 72, no. 1, pp. 73–85, 2010.

[10] S. L. Andersen and M. H. Teicher, "Stress, sensitive periods and maturational events in adolescent depression," *Trends in Neurosciences*, vol. 31, no. 4, pp. 183–191, 2008.

[11] M. D. Morrissey, I. Z. Mathews, and C. M. McCormick, "Enduring deficits in contextual and auditory fear conditioning after adolescent, not adult, social instability stress in male rats," *Neurobiology of Learning and Memory*, vol. 95, no. 1, pp. 46–56, 2011.

[12] F. Hollis, C. Isgor, and M. Kabbaj, "The consequences of adolescent chronic unpredictable stress exposure on brain and behavior," *Neuroscience*, vol. 249, pp. 232–241, 2013.

[13] F. Zhang, S. Yuan, F. Shao, and W. Wang, "Adolescent social defeat induced alterations in social behavior and cognitive flexibility in adult mice: effects of developmental stage and social condition," *Frontiers in Behavioral Neuroscience*, vol. 10, article 149, 2016.

[14] T. F. Yuan and G. Hou, "The effects of stress on glutamatergic transmission in the brain," *Molecular Neurobiology*, vol. 51, no. 3, pp. 1139–1143, 2015.

[15] H. Einat, P. Yuan, T. D. Gould et al., "The role of the extracellular signal-regulated kinase signaling pathway in mood modulation," *The Journal of Neuroscience*, vol. 23, no. 19, pp. 7311–7316, 2003.

[16] M. First, I. Gil-Ad, M. Taler, I. Tarasenko, N. Novak, and A. Weizman, "The effects of reboxetine treatment on depression-like behavior, brain neurotrophins, and erk expression in rats exposed to chronic mild stress," *Journal of Molecular Neuroscience*, vol. 50, no. 1, pp. 88–97, 2013.

[17] Y.-H. Leem, S.-S. Yoon, Y.-H. Kim, and S. A. Jo, "Disrupted MEK/ERK signaling in the medial orbital cortex and dorsal endopiriform nuclei of the prefrontal cortex in a chronic restraint stress mouse model of depression," *Neuroscience Letters*, vol. 580, pp. 163–168, 2014.

[18] V. Duric, M. Banasr, P. Licznerski et al., "A negative regulator of MAP kinase causes depressive behavior," *Nature Medicine*, vol. 16, no. 11, pp. 1328–1332, 2010.

[19] I. S. Samuels, J. C. Karlo, A. N. Faruzzi et al., "Deletion of ERK2 mitogen-activated protein kinase identifies its key roles in cortical neurogenesis and cognitive function," *Journal of Neuroscience*, vol. 28, no. 27, pp. 6983–6995, 2008.

[20] R. S. Duman and B. Voleti, "Signaling pathways underlying the pathophysiology and treatment of depression: novel mechanisms for rapid-acting agents," *Trends in Neurosciences*, vol. 35, no. 1, pp. 47–56, 2012.

[21] X. Qi, W. Lin, D. Wang, Y. Pan, W. Wang, and M. Sun, "A role for the extracellular signal-regulated kinase signal pathway in depressive-like behavior," *Behavioural Brain Research*, vol. 199, no. 2, pp. 203–209, 2009.

[22] X. Qi, W. Lin, J. Li, Y. Pan, and W. Wang, "The depressive-like behaviors are correlated with decreased phosphorylation of mitogen-activated protein kinases in rat brain following chronic forced swim stress," *Behavioural Brain Research*, vol. 175, no. 2, pp. 233–240, 2006.

[23] P. Willner, "Chronic mild stress (CMS) revisited: consistency and behavioural-neurobiological concordance in the effects of CMS," *Neuropsychobiology*, vol. 52, no. 2, pp. 90–110, 2005.

[24] M. N. Hill, K. G. C. Hellemans, P. Verma, B. B. Gorzalka, and J. Weinberg, "Neurobiology of chronic mild stress: parallels to major depression," *Neuroscience & Biobehavioral Reviews*, vol. 36, no. 9, pp. 2085–2117, 2012.

[25] D. Liu, Z. Wang, Z. Gao et al., "Effects of curcumin on learning and memory deficits, BDNF, and ERK protein expression in rats exposed to chronic unpredictable stress," *Behavioural Brain Research*, vol. 271, pp. 116–121, 2014.

[26] K. Henningsen, J. T. Andreasen, E. V. Bouzinova et al., "Cognitive deficits in the rat chronic mild stress model for depression: relation to anhedonic-like responses," *Behavioural Brain Research*, vol. 198, no. 1, pp. 136–141, 2009.

[27] E. Toth, R. Gersner, A. Wilf-Yarkoni et al., "Age-dependent effects of chronic stress on brain plasticity and depressive behavior," *Journal of Neurochemistry*, vol. 107, no. 2, pp. 522–532, 2008.

[28] J. Pohl, M. C. Olmstead, K. E. Wynne-Edwards, K. Harkness, and J. L. Menard, "Repeated exposure to stress across the childhood-adolescent period alters rats' anxiety- and depression-like behaviors in adulthood: the importance of stressor type and gender," *Behavioral Neuroscience*, vol. 121, no. 3, pp. 462–474, 2007.

[29] L. E. Chaby, S. A. Cavigelli, A. M. Hirrlinger, M. J. Caruso, and V. A. Braithwaite, "Chronic unpredictable stress during adolescence causes long-term anxiety," *Behavioural Brain Research*, vol. 278, pp. 492–495, 2015.

[30] L. E. Chaby, S. A. Cavigelli, A. White, K. Wang, and V. A. Braithwaite, "Long-term changes in cognitive bias and coping response as a result of chronic unpredictable stress during adolescence," *Frontiers in Human Neuroscience*, 2013.

[31] L. Suo, L. Zhao, J. Si et al., "Predictable chronic mild stress in adolescence increases resilience in adulthood," *Neuropsychopharmacology*, vol. 38, no. 8, pp. 1387–1400, 2013.

[32] I. Z. Mathews, A. Wilton, A. Styles, and C. M. McCormick, "Increased depressive behaviour in females and heightened corticosterone release in males to swim stress after adolescent social stress in rats," *Behavioural Brain Research*, vol. 190, no. 1, pp. 33–40, 2008.

[33] M. Tsoory, H. Cohen, and G. Richter-Levin, "Juvenile stress induces a predisposition to either anxiety or depressive-like symptoms following stress in adulthood," *European Neuropsychopharmacology*, vol. 17, no. 4, pp. 245–256, 2007.

[34] C. Goeldner, T. M. Ballard, F. Knoflach, J. Wichmann, S. Gatti, and D. Umbricht, "Cognitive impairment in major depression and the mGlu2 receptor as a therapeutic target," *Neuropharmacology*, vol. 64, pp. 337–346, 2013.

[35] A. T. Peters, R. H. Jacobs, N. A. Crane et al., "Domain-specific impairment in cognitive control among remitted youth with a history of major depression," *Early Intervention in Psychiatry*, 2015.

[36] M. J. Millan, Y. Agid, M. Brüne et al., "Cognitive dysfunction in psychiatric disorders: characteristics, causes and the quest for improved therapy," *Nature Reviews Drug Discovery*, vol. 11, no. 2, pp. 141–168, 2012.

[37] Q. Wang, X. Luo, F. Shao, and W. Wang, "A comparative study of cognitive functions in two different models of chronic stress in rats," *Chinese Journal of Nervous and Mental Diseases*, vol. 38, no. 8, pp. 449–453, 2012.

[38] I. Lucki, "The forced swimming test as a model for core and component behavioral effects of antidepressant drugs," *Behavioural Pharmacology*, vol. 8, no. 6-7, pp. 523–532, 1997.

[39] X.-T. Guan, F. Shao, X. Xie, L. Chen, and W. Wang, "Effects of aspirin on immobile behavior and endocrine and immune changes in the forced swimming test: comparison to fluoxetine and imipramine," *Pharmacology Biochemistry and Behavior*, vol. 124, pp. 361–366, 2014.

[40] F. Shao, J. Jin, Q. Meng et al., "Pubertal isolation alters latent inhibition and DA in nucleus accumbens of adult rats," *Physiology & Behavior*, vol. 98, no. 3, pp. 251–257, 2009.

[41] G. Paxinos and C. Watson, *The Rat Brain Atlas in Stereotaxic Coordinates*, Academic Press, San Diego, Calif, USA, 1998.

[42] J. F. Cryan, R. J. Valentino, and I. Lucki, "Assessing substrates underlying the behavioral effects of antidepressants using the modified rat forced swimming test," *Neuroscience & Biobehavioral Reviews*, vol. 29, no. 4-5, pp. 547–569, 2005.

[43] C. Pihoker, M. J. Owens, C. M. Kuhn, S. M. Schanberg, and C. B. Nemeroff, "Maternal separation in neonatal rats elicits activation of the hypothalamic-pituitary-adrenocortical axis: a putative role for corticotropin-releasing factor," *Psychoneuroendocrinology*, vol. 18, no. 7, pp. 485–493, 1993.

[44] J. L. Lukkes, M. J. Watt, C. A. Lowry, and G. L. Forster, "Consequences of post-weaning social isolation on anxiety behavior and related neural circuits in rodents," *Frontiers in Behavioral Neuroscience*, vol. 3, article no. 18, 2009.

[45] C. Liston, M. M. Miller, D. S. Goldwater et al., "Stress-induced alterations in prefrontal cortical dendritic morphology predict selective impairments in perceptual attentional set-shifting," *The Journal of Neuroscience*, vol. 26, no. 30, pp. 7870–7874, 2006.

[46] C. O. Bondi, J. D. Jett, and D. A. Morilak, "Beneficial effects of desipramine on cognitive function of chronically stressed rats are mediated by alpha1-adrenergic receptors in medial prefrontal cortex," *Progress in Neuro-Psychopharmacology & Biological Psychiatry*, vol. 34, no. 6, pp. 913–923, 2010.

[47] C.-P. Shen, Y. Tsimberg, C. Salvadore, and E. Meller, "Activation of Erk and JNK MAPK pathways by acute swim stress in rat brain regions," *BMC Neuroscience*, vol. 5, article 36, 2004.

[48] M. H. Greisen, C. A. Altar, T. G. Bolwig, R. Whitehead, and G. Wörtwein, "Increased adult hippocampal brain-derived neurotrophic factor and normal levels of neurogenesis in maternal separation rats," *Journal of Neuroscience Research*, vol. 79, no. 6, pp. 772–778, 2005.

[49] A. Haghparast, Z. Taslimi, M. Ramin, P. Azizi, F. Khodagholi, and M. Hassanpour-Ezatti, "Changes in phosphorylation of CREB, ERK, and c-fos induction in rat ventral tegmental area, hippocampus and prefrontal cortex after conditioned place preference induced by chemical stimulation of lateral hypothalamus," *Behavioural Brain Research*, vol. 220, no. 1, pp. 112–118, 2011.

[50] E. Meller, C. Shen, T. A. Nikolao et al., "Region-specific effects of acute and repeated restraint stress on the phosphorylation of mitogen-activated protein kinases," *Brain Research*, vol. 979, no. 1-2, pp. 57–64, 2003.

[51] X. Qi, W. Lin, J. Li et al., "Fluoxetine increases the activity of the ERK-CREB signal system and alleviates the depressive-like behavior in rats exposed to chronic forced swim stress," *Neurobiology of Disease*, vol. 31, no. 2, pp. 278–285, 2008.

[52] J. D. Runyan and P. K. Dash, "Intra-medial prefrontal administration of SCH-23390 attenuates ERK phosphorylation and long-term memory for trace fear conditioning in rats," *Neurobiology of Learning and Memory*, vol. 82, no. 2, pp. 65–70, 2004.

[53] S. A. Heldt, L. Stanek, J. P. Chhatwal, and K. J. Ressler, "Hippocampus-specific deletion of BDNF in adult mice impairs spatial memory and extinction of aversive memories," *Molecular Psychiatry*, vol. 12, no. 7, pp. 656–670, 2007.

[54] P. A. Kabitzke, G. A. Barr, T. Chan, H. N. Shair, and C. P. Wiedenmayer, "Medial prefrontal cortex processes threatening stimuli in juvenile rats," *Neuropsychopharmacology*, vol. 39, no. 8, pp. 1924–1932, 2014.

[55] B. Bingham, K. McFadden, X. Zhang, S. Bhatnagar, S. Beck, and R. Valentino, "Early adolescence as a critical window during which social stress distinctly alters behavior and brain norepinephrine activity," *Neuropsychopharmacology*, vol. 36, no. 4, pp. 896–909, 2011.

[56] K. Snyder, W.-W. Wang, R. Han, K. McFadden, and R. J. Valentino, "Corticotropin-releasing factor in the norepinephrine nucleus, locus coeruleus, facilitates behavioral flexibility," *Neuropsychopharmacology*, vol. 37, no. 2, pp. 520–530, 2012.

[57] A. Marzo, J. Bai, J. Caboche, P. Vanhoutte, and S. Otani, "Cellular mechanisms of long-term depression induced by noradrenaline in rat prefrontal neurons," *Neuroscience*, vol. 169, no. 1, pp. 74–86, 2010.

[58] C. O. Bondi, G. Rodriguez, G. G. Gould, A. Frazer, and D. A. Morilak, "Chronic unpredictable stress induces a cognitive deficit and anxiety-like behavior in rats that is prevented by chronic antidepressant drug treatment," *Neuropsychopharmacology*, vol. 33, no. 2, pp. 320–331, 2008.

[59] C. H. Duman, L. Schlesinger, M. Kodama, D. S. Russell, and R. S. Duman, "A role for MAP kinase signaling in behavioral models of depression and antidepressant treatment," *Biological Psychiatry*, vol. 61, no. 5, pp. 661–670, 2007.

Hindawi Publishing Corporation
Neural Plasticity
Volume 2016, Article ID 6402942, 9 pages
http://dx.doi.org/10.1155/2016/6402942

Review Article

The Role of Stress Regulation on Neural Plasticity in Pain Chronification

Xiaoyun Li[1] and Li Hu[1,2]

[1]*Key Laboratory of Cognition and Personality, Ministry of Education and Faculty of Psychology, Southwest University, Chongqing, China*
[2]*CAS Key Laboratory of Mental Health, Institute of Psychology, Beijing, China*

Correspondence should be addressed to Li Hu; huli@psych.ac.cn

Received 27 July 2016; Revised 2 November 2016; Accepted 14 November 2016

Academic Editor: Jason Huang

Pain, especially chronic pain, is one of the most common clinical symptoms and has been considered as a worldwide healthcare problem. The transition from acute to chronic pain is accompanied by a chain of alterations in physiology, pathology, and psychology. Increasing clinical studies and complementary animal models have elucidated effects of stress regulation on the pain chronification via investigating activations of the hypothalamic-pituitary-adrenal (HPA) axis and changes in some crucial brain regions, including the amygdala, prefrontal cortex, and hippocampus. Although individuals suffer from acute pain benefit from such physiological alterations, chronic pain is commonly associated with maladaptive responses, like the HPA dysfunction and abnormal brain plasticity. However, the causal relationship among pain chronification, stress regulation, and brain alterations is rarely discussed. To call for more attention on this issue, we review recent findings obtained from clinical populations and animal models, propose an integrated stress model of pain chronification based on the existing models in perspectives of environmental influences and genetic predispositions, and discuss the significance of investigating the role of stress regulation on brain alteration in pain chronification for various clinical applications.

1. Introduction

Chronic pain is a main source of worldwide disability, causing physical and psychological discomforts and rising huge medical expenses [1]. Understanding mechanisms of the development of chronic pain is crucial in monitoring and preventing the progress of pain chronification. In recent decades, increasing clinical studies and complementary animal models contributed to important advances in understanding the transition from acute to chronic pain. Notably, Melzack [2] proposed that stress played an important role in such pain chronification, and accumulating evidence demonstrated that stress regulation (as indexed by the function of hypothalamic-pituitary-adrenal [HPA] axis) consistently engaged in the development of chronic pain [3–5]. In line with these findings, several brain regions, subserving as key candidates for stress regulation [6–8], have been reported to be involved in the transition from acute to chronic pain, including the amygdala, prefrontal cortex (PFC), and hippocampus [9–12]. Therefore, some previous studies hypothesized that these brain regions, especially within the emotional corticolimbic system, acted as the bridge of pain modulation and stress regulation. In this paper, we briefly walk through concepts of pain and stress, review effects of the HPA function on acute and chronic pain, and discuss alterations of stress-associated brain regions in acute and chronic pain. In the following, we discuss two existing stress models of chronic pain in perspectives of environmental influences and genetic predispositions, respectively, and propose an integrated stress model of pain chronification based on previous findings.

2. Acute Pain and Chronic Pain

Pain is a conscious sensation, processing multidimensional information involving sensory, affective, and cognitive components [2]. Acute pain, serving as a warning of injury or

illness, functions to protect the organs from a present or potential damage. If acute pain continues for a long time (e.g., longer than 3 months), it can develop into chronic pain, even after the initial injury or illness has been healed [13]. In addition, the chronic pain itself is usually associated with hyperalgesia and/or allodynia [14] and psychological distress, such as anxiety and depression [15].

3. Stress and the HPA Axis

Stress is a biological reaction [2] that triggers a rapid response by activating the sympathetic nervous system and a relative slower response via evoking the HPA axis [8]. The faster pathway releases catecholamines, such as adrenaline and noradrenaline, priming the body into a classic "fight or flight" mode with enhanced activation of the sympathetic nervous system (e.g., increased heart rate and blood pressure, sweat gland activation). When the slower stress response pathway of the HPA axis is activated, corticotropin-releasing factor (CRF) travels from the paraventricular nucleus (PVN) of the hypothalamus to the pituitary, leading to the release of adrenocorticotropic hormone (ACTH). In turn, ACTH stimulates the adrenal gland to secrete glucocorticoids (cortisol in humans, corticosterone in rodents) that are essential for stress response. This type of hormone can naturally go through the blood-brain barrier and access multiple brain regions, like the amygdala, PFC, and hippocampus, binding with two intracellular receptors, the glucocorticoid receptor and the mineralocorticoid receptor [16]. As such, glucocorticoids can influence neuronal excitability and synaptic and neuronal plasticity [17, 18].

4. The Effect of Stress Regulation on Pain

Studies associated with stress responses have demonstrated that altered activations of the HPA axis are in response to experimental pain [19, 20] and various chronic pain disorders [3, 5]. Conceptually, pain-related activation of the HPA axis has been embedded in an allostatic load model of disease [4, 21]. This model assumes that, in response to acute stress, various physiological activities could be activated to help organism adapt to environmental changes. It has also been proposed that acute pain induced cortisol elevation may reduce pain unpleasantness [22] and increase pain tolerance [23], which provides solid evidence for the transient stress-induced analgesia [24]. However, when stress, induced by physical injury and/or pain-related psychological factors, is prolonged, uncertain, and uncontrollable, the response of such stress becomes maladaptive, entering into a vicious cycle, in which acute pain has evolved into a chronic state with abnormal alterations of brain structures and functions [4, 21]. Meanwhile, cortisol fails to act its protective functions under chronic pain conditions, thereby exaggerating pain severity. In fact, emerging evidence suggests that chronic pain is associated with the dysfunction of cortisol secretion, although the nature of their relationship is not fully elucidated. A majority of previous studies reported reduced cortisol secretions or lower basal levels of cortisol in various chronic pain disorders, such as fibromyalgia [25, 26], chronic whiplash-associated disorder [27], chronic neck pain [28], chronic low back pain [29], chronic fatigue syndrome [30], and chronic pelvic pain [31]. Since the HPA axis is a self-regulating negative feedback system [7], such hypocortisolism is indicative of attenuated activity or impaired feedback sensitivity of the HPA axis. However, a few studies found elevated cortisol levels [32–35], abnormal cortisol diurnal variations [36], and increased feedback sensitivity of the HPA axis [37] in certain chronic pain conditions, like fibromyalgia and chronic back pain. In contrast, several studies reported that the profiles of cortisol secretion in patients suffering with fibromyalgia [38, 39], chronic back pain [40, 41], or chronic temporomandibular disorders [42] did not differ from those in healthy controls. One possible explanation to these conflicting findings is that the HPA axis may be in the state of hyperactivity at the early stage of pain chronification, while, after long-term overt activity, the stress system reaches an exhausted state, thereby turning into the HPA axis hypoactivity [26]. Albeit such explanation requires further verification, it is reasonable to suggest that the HPA axis is involved in the development of chronic pain.

5. Neural Plasticity in Acute and Chronic Pain

The corticolimbic system, including amygdala, PFC, and hippocampus, is a powerful neural network that has been suggested to contribute to the transition from acute to chronic pain [12]. Further, both acute and chronic pain profoundly influence this system, which is also known to relate to stress regulation [8], via structural and functional alterations in the related brain regions. Compelling evidence supporting this conclusion was well documented by various human neuroimaging studies and animal models.

5.1. Brain Responses to Acute Pain. Most human neuroimaging studies on acute pain have revealed consistent activations in the insula and dorsal anterior cingulate cortex [43–45]. Even less consistency, activations in the amygdala, PFC, and hippocampus have been frequently reported in neuroimaging studies of acute pain [46–51]. Specifically, noxious stimulation applied on pain-free individuals evoked stronger Blood-Oxygen-Level-Dependent signals in the PFC [46, 51–53] and hippocampus [46, 48, 54, 55]. Besides, activations of amygdala and hippocampus were observed to be related to pain expectancy [53, 55, 56]. Furthermore, augmented activation of amygdala was induced by pain in depressed individuals [57] and in healthy cohort with greater pain unpleasantness followed by an induction of depressive mood [52], suggesting the role of amygdala in the integration of pain and emotional information. In addition, the HPA axis influences the activations of the abovementioned brain regions under acute pain conditions. For instance, previous studies demonstrated that elevated cortisol levels were (1) associated with reduced pain unpleasantness and decreased pain-related brain activation during constant noxious stimulation [22], (2) linked with lower pain threshold and stronger PFC activity in response to inflammation-induced pain [58], and (3) related

to enhanced hippocampal activation during step-up noxious stimulation (an increasing pattern of noxious stimulation) [59]. These studies suggested that acute pain, acting in a similar way with acute stress, may evoke cortisol levels to boost the survival of the organism by inhibiting and/or facilitating activities of related brain networks. Although no path analysis in these studies was performed to verify the interrelationship among acute pain, stress regulation, and functional changes of the corticolimbic system, it is highly likely that acute pain may evoke an adaptive response to protect the organism via the coinfluence of cortisol elevation and brain responses in the amygdala, PFC, and hippocampus.

In fact, evidence from animal models suggests that this may be the same case. Consistent observations of acute pain-related functional changes in the corticolimbic system have been reported in animal studies. For instance, noxious stimulation induced neuronal excitability in the amygdala [60–62] and PFC [63] and neuronal inhibition in the CA1 hippocampus [64, 65]. In line with the electrophysiological findings, immunohistochemical and fMRI studies also showed similar activation patterns in these brain regions by delivering noxious stimulation on rats [63, 66–69]. These findings confirmed the role of acute pain on brain plasticity. Additionally, it is important to find out the role of stress regulation in the changes of brain responses under acute pain conditions, and evidence from an immunocytochemical study might shed light on this issue [70]. In this study, rats with less pain sensitivity showed less freezing responses, stronger vocalization, and increased PFC activation and plasma corticosterone levels, in response to conditioned aversive stimuli. The authors also found an increased Fos expression (an indicator of neuronal activity in rats) in the hypothalamus and dentate gyrus of the hippocampus in the same group of rats. In contrast, rats with high pain sensitivity responded more passively to aversive events (e.g., more freezing behavior and weaker vocalization), along with increased activation in the amygdala and CA1 hippocampus, but did not show significant changes in corticosterone levels [70]. These findings suggested that enhanced activity of stress axis in rats with low pain sensitivity was due to the role of the PFC and hippocampus in regulation of glucocorticoid release, which was crucial for survival, while such regulation was ineffective in rats with high pain sensitivity [70].

In summary, human and animal studies of acute pain have provided evidence in support of the viewpoint that acute pain, similar to acute stress, increased the release of glucocorticoid. Meanwhile, the above discussed brain regions are highly sensitive to acute painful and stressful stimuli and are highly plastic via regulation of the glucocorticoid negative feedback in the PFC and hippocampus. Therefore, it is conceivable that the whole process can be considered as the reaction in an adaptive and protective response system to aversive stimuli, leading to a better adaptation for survival.

5.2. Brain Alterations in Chronic Pain. Human neuroimaging studies have emphasized the association between chronic pain and abnormal changes in gray matter volume and thickness of the brain in various chronic pain patients [71–73]. Remarkably, a large number of studies have repeatedly showed reduced volumes of the amygdala [12, 74–78], medial prefrontal cortex (mPFC) [71, 74, 79–81], and hippocampus [32, 71, 81–83] in a variety of chronic pain populations. In accordance with the morphological alterations, functional changes of the amygdala, mPFC, and hippocampus were also observed under chronic pain conditions [47, 84, 85]. A meta-analysis study reported that peak activation was found in the basolateral amygdala in clinical populations, suggesting the enhanced cognitive-affective processing among patients suffering from chronic pain [85]. In chronic pain patients, clinical pain intensity appeared to be associated with greater activations in the mPFC [86, 87] and hippocampus [32]. Additionally, under the circumstance of clinical pain fluctuation, greater functional connectivity of mPFC with the limbic system, including the amygdala and hippocampus, was indicative of pain chronification [9, 10, 12, 85, 88]. Although stress regulation and pain chronification are suggested to share a similar mechanism in modulating brain structures and functions [2], how stress regulation plays a role in brain alterations in patients with chronic pain remains unclear. Recently, a clinical study explored the influence of maladaptive stress response on pain state of patients, such as elevated cortisol levels that were associated with enhanced clinical pain intensity, smaller hippocampal volume, and stronger hippocampal activations [32], which provided strong evidence to demonstrate the important role of the maladaptive stress response on the transition from acute to chronic pain [4]. Interestingly, a recent study of chronic myofascial pain reported that gray matter atrophy in the PFC and hippocampus was independent of the cortisol levels. They also reported that only the gray matter density of PFC was negatively correlated with pain thresholds in patients, suggesting the presence of pain disinhibition [89]. Despite these findings are contradictive, it can be imaginable that dysfunction of the HPA axis and abnormal brain alterations may be caused by maladaptive responses to chronic pain.

In support of the above viewpoints, evidence from animal studies has unraveled the role of chronic pain in altering the structure and function of the corticolimbic system. The long-lasting sympathic pain increased neuronal excitability and dendritic branching of amygdala in rodents [90, 91], resulting in an enlarged amygdala volume [92]. Spared nerve injury sympathic pain induced alterations of dendritic length, spine density, and neuronal activity in the mPFC [93, 94], and long-term neuropathic pain reduced prefrontal volumes in rodents [95]. Moreover, hippocampal neurogenesis appeared to be suppressed in a rat model of neuropathic pain, subserving a possible mechanism of pain chronification [83, 96]. Additionally, since the mPFC receives inputs from both amygdala and hippocampus [97], pain-related amygdala hyperactivity inhibited the mPFC activation and impaired functions related to decision-making in an arthritis pain model [98, 99], whereas reduced hippocampus-prefrontal connectivity was associated with impaired spatial memory performance in rats with neuropathic pain [100]. Yet the knowledge of influence of stress regulation on brain alterations in chronic pain is very limited. An animal study of chronic neuropathic pain reported that enhanced nociceptive sensitivity during chronic pain was associated with increased activation in the

amygdala and decreased activation in the hippocampus but failed to influence activation of the HPA axis [101]. Interestingly, such dissociation between pain sensitivity and stress response in rats implicated that the HPA axis dysfunction in chronic pain patients might not originate from pain itself, but rather from other factors associated with repeated painful stimuli (e.g., experimental cues and an inability to escape from pain).

In summary, human neuroimaging studies and animal models of chronic pain have suggested that chronic pain could induce a chronic stress-like alteration in the HPA axis and the corticolimbic system, with dysregulation of the HPA axis, and dysfunction and reorganization of the corticolimbic system. It is reasonable to conclude that such maladaptive responses are likely to contribute to the development of chronic pain.

6. Stress Models of Pain Chronification

Given that activation of the HPA axis influences neural alterations, both structurally and functionally, the role of stress regulation becomes critical in the understanding of brain mechanisms in the evolution of acute pain into chronic pain.

From the perspective of stress regulation, human and animal studies suggest that chronic stress has an enduring and destructive effect on the brain via activation of the HPA axis, particularly the glucocorticoid secretion [102]. To explain this phenomenon, two different hypotheses have been proposed: the neurotoxicity hypothesis and the vulnerability hypothesis. The neurotoxicity hypothesis suggests that prolonged release of glucocorticoid impairs the neuronal capacity to resist toxic invasion or normal attrition, leading to the reduction of hippocampal volume in populations with chronic stress, including posttraumatic stress disorder (PTSD) and depression [103]. In contrast, the vulnerability hypothesis points out that small hippocampal volume is a predetermine risk factor for chronic stress that is shaped by genetic predispositions and/or early life stress [104], as evidenced in the studies of stress [105], anxiety [106], and PTSD [104].

Accordingly, two stress models of chronic pain have also been proposed, from environmental influence and genetic predisposition perspectives, respectively: a "neurotoxic model" and a "vulnerability model." The "neurotoxic model" suggests that persistent pain may lead to the maladaptive stress response, such as dysfunction of the HPA axis, affecting the alterations in brain structure and function [6, 107]. In line with this model, chronic pain-related changes in the corticolimbic system, including the amygdala, PFC, and hippocampus [47, 71, 73, 108], have been considered as a consequence of allostatic load of chronic disease, in which prolonged pain dysregulates the HPA axis, thereby impairing brain structures and functions [4]. In contrast, the "vulnerability model" proposes that the characteristics of some particular brain structures, such as the volume of the brain regions within the corticolimbic system [109], may contribute to the vulnerability of development from acute to chronic pain, thus affecting the activation of the HPA axis and brain functions [105, 110]. For example, a longitudinal study tracked brain alterations for 3 years in patients with subacute back pain as they gradually evolved to chronic pain states and found that small sizes of amygdala and hippocampus were the preexisting risk factors in the development of chronic back pain [12].

It is of interest to note that a recent study of chronic back pain using path analysis has suggested that small hippocampal volume has represented a risk factor of vulnerability to persist pain in a maladaptive stress response manner (the "vulnerability model") [32]. However, their observation cannot disprove the "neurotoxic model" because the development of chronic back pain, similar to other chronic pain diseases, is a dynamic process, and any cross-sectional study cannot track the causal relationship among pain chronification, stress regulation, and brain alterations during the whole process. Indeed, we are not able to rule out the possibility that the influence of stress response in pain chronification is driven by the combination of both environmental and genetic factors. It should be noted that emerging studies in the perspectives of stress regulation or pain chronification support this possibility [102, 111]. We presume that the level of activation of the HPA axis is determined by the combination of vulnerable factors (e.g., structural characteristics of the corticolimbic system) and environmental factors (e.g., pain caused by an injury) and influences the alterations of the structure and function of the corticolimbic system. Subsequently, these physiological responses would lead to either the recovery of health or the persistence of pain state that in turn strengthens brain reorganizations and eventually develops into a chronic pain state (Figure 1). Besides, the proposed stress model of pain chronification should be verified in a longitudinal design by tracking the alterations of all physiological responses, including brain structures and functions, and glucocorticoid levels. We foresee that unraveling the stress effect on brain mechanisms in pain chronification will be of great importance to predict the development of chronic pain [9–12], thus having important clinical significance.

7. Conclusion

We have provided a broad range of compelling evidence that pain modulation and stress regulation can be considered as an integrated processing [2], within the framework of corticolimbic system. Human neuroimaging studies and animal models have unfolded a field of vision in the mechanism that drives the development of chronic pain under the HPA axis regulation. In contrast to the fact that activations of the HPA axis and the corticolimbic system show an adaptive manner to the perceived danger in acute pain, chronic pain is commonly associated with dysfunction of the HPA axis and brain reorganizations. Based on the two existing stress models of chronic pain, we propose an integrated stress model of pain chronification, emphasizing the integration of contingent environmental influences and genetic predispositions in the

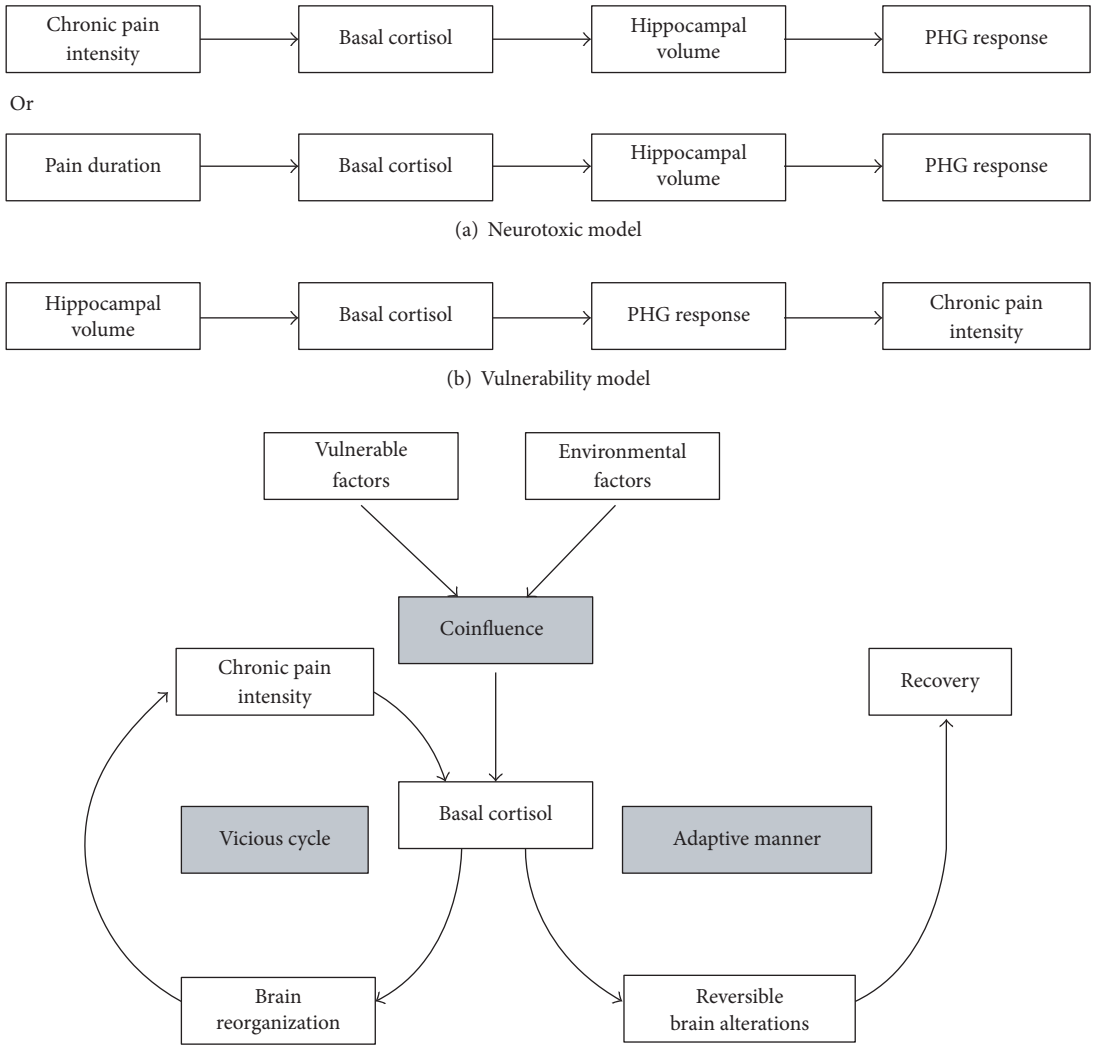

(a) Neurotoxic model

(b) Vulnerability model

(c) Proposed model of pain chronification

Figure 1: Stress models of chronic pain. (a) The neurotoxic model, from the perspective of environmental influences, conceptualizes that chronic pain intensity or pain duration may lead to the maladaptive stress response, affecting the structure and function of the hippocampal formation and the parahippocampal gyrus (PHG) [32]. (b) The vulnerability model, from the perspective of genetic predispositions, conceptualizes that the small hippocampal volume as a vulnerable factor affects the levels of stress hormones, which in turn lead to enhanced activations of the parahippocampal gyrus and increased persistent pain intensity [32]. (c) The proposed integrated model, from the perspective of the combination of environmental influences and genetic predispositions, conceptualizes that vulnerable factors (e.g., properties of particular brain structures) and environmental factors (e.g., injury) codetermine the levels of basal cortisol, which result in the brain alterations. Thereafter, these physiological responses either return to normal levels with an adaptive manner or initiate a vicious cycle of cortisol dysfunction, brain reorganizations, and persistent pain state.

transition from acute to chronic pain. However, the precise mechanism of this integrated model remains to be investigated. Hopefully, future studies can determine physiological responses in relation to activation of the HPA axis and alterations of the corticolimbic system as the specific biomarkers of pain chronification, for monitoring and preventing the transition to chronic pain. The identification of these biomarkers in patients suffering from acute and chronic pain is important, as it can help facilitate the effective pain rehabilitation, reduce pain-related disability, and improve quality of life.

Competing Interests

The authors declare that there are no competing interests regarding the publication of this paper.

Acknowledgments

Li Hu is supported by the National Natural Science Foundation of China (nos. 31471082 and 31671141), Chongqing Research Program of Basic Research and Frontier Technology (no. cstc2015jcyjBX0050), and the Scientific Foundation

Project of Institute of Psychology, Chinese Academy of Sciences (no. Y6CX021008).

References

[1] C. J. L. Murray and A. D. Lopez, "Measuring the global burden of disease," *New England Journal of Medicine*, vol. 369, no. 5, pp. 448–457, 2013.

[2] R. Melzack, "Pain and stress: a new perspective," in *Psychological Factors in Pain*, R. J. Gatchel and D. C. Turk, Eds., pp. 89–106, Guildford Press, New York, NY, USA, 1999.

[3] G. Blackburn-Munro and R. E. Blackburn-Munro, "Chronic pain, chronic stress and depression: coincidence or consequence?" *Journal of Neuroendocrinology*, vol. 13, no. 12, pp. 1009–1023, 2001.

[4] D. Borsook, N. Maleki, L. Becerra, and B. McEwen, "Understanding migraine through the lens of maladaptive stress responses: a model disease of allostatic load," *Neuron*, vol. 73, no. 2, pp. 219–234, 2012.

[5] B. S. McEwen and M. Kalia, "The role of corticosteroids and stress in chronic pain conditions," *Metabolism: Clinical and Experimental*, vol. 59, no. 1, p. -S15, 2010.

[6] E. R. de Kloet, M. Joëls, and F. Holsboer, "Stress and the brain: from adaptation to disease," *Nature Reviews Neuroscience*, vol. 6, no. 6, pp. 463–475, 2005.

[7] J. P. Herman, M. M. Ostrander, N. K. Mueller, and H. Figueiredo, "Limbic system mechanisms of stress regulation: hypothalamo-pituitary- adrenocortical axis," *Progress in Neuro-Psychopharmacology and Biological Psychiatry*, vol. 29, no. 8, pp. 1201–1213, 2005.

[8] B. S. McEwen, "Physiology and neurobiology of stress and adaptation: central role of the brain," *Physiological Reviews*, vol. 87, no. 3, pp. 873–904, 2007.

[9] M. N. Baliki, B. Petre, S. Torbey et al., "Corticostriatal functional connectivity predicts transition to chronic back pain," *Nature Neuroscience*, vol. 15, no. 8, pp. 1117–1119, 2012.

[10] J. A. Hashmi, M. N. Baliki, L. Huang et al., "Shape shifting pain: chronification of back pain shifts brain representation from nociceptive to emotional circuits," *Brain*, vol. 136, no. 9, pp. 2751–2768, 2013.

[11] A. R. Mansour, M. N. Baliki, L. Huang et al., "Brain white matter structural properties predict transition to chronic pain," *Pain*, vol. 154, no. 10, pp. 2160–2168, 2013.

[12] E. Vachon-Presseau, P. Tétreault, B. Petre et al., "Corticolimbic anatomical characteristics predetermine risk for chronic pain," *Brain*, vol. 139, no. 7, pp. 1958–1970, 2016.

[13] H. Merskey and N. Bogduk, *Classification of Chronic Pain: Descriptions of Chronic Pain Syndromes and Definitions of Pain Terms*, IASP Press, Seattle, Wash, USA, 2nd edition, 1994.

[14] M. J. Millan, "The induction of pain: an integrative review," *Progress in Neurobiology*, vol. 57, no. 1, pp. 1–164, 1999.

[15] S. J. Linton, "A review of psychological risk factors in back and neck pain," *Spine*, vol. 25, no. 9, pp. 1148–1156, 2000.

[16] M. Joëls, H. Karst, R. DeRijk, and E. R. de Kloet, "The coming out of the brain mineralocorticoid receptor," *Trends in Neurosciences*, vol. 31, no. 1, pp. 1–7, 2008.

[17] B. S. McEwen, "Plasticity of the hippocampus: adaptation to chronic stress and allostatic load," *Annals of the New York Academy of Sciences*, vol. 933, pp. 265–277, 2001.

[18] B. Roozendaal, B. S. McEwen, and S. Chattarji, "Stress, memory and the amygdala," *Nature Reviews Neuroscience*, vol. 10, no. 6, pp. 423–433, 2009.

[19] M. Al'Absi, K. L. Petersen, and L. E. Wittmers, "Adrenocortical and hemodynamic predictors of pain perception in men and women," *Pain*, vol. 96, no. 1-2, pp. 197–204, 2002.

[20] C. Zimmer, H.-D. Basler, H. Vedder, and S. Lautenbacher, "Sex differences in cortisol response to noxious stress," *Clinical Journal of Pain*, vol. 19, no. 4, pp. 233–239, 2003.

[21] B. S. McEwen, "Stress, adaptation, and disease: allostasis and allostatic load," *Annals of the New York Academy of Sciences*, vol. 840, pp. 33–44, 1998.

[22] E. Vachon-Presseau, M.-O. Martel, M. Roy et al., "Acute stress contributes to individual differences in pain and pain-related brain activity in healthy and chronic pain patients," *The Journal of Neuroscience*, vol. 33, no. 16, pp. 6826–6833, 2013.

[23] K. E. Dixon, B. E. Thorn, and L. C. Ward, "An evaluation of sex differences in psychological and physiological responses to experimentally-induced pain: a path analytic description," *Pain*, vol. 112, no. 1-2, pp. 188–196, 2004.

[24] N. I. Yarushkina, T. R. Bagaeva, and L. P. Filaretova, "Central corticotropin-releasing factor (CRF) may attenuate somatic pain sensitivity through involvement of glucocorticoids," *Journal of Physiology & Pharmacology*, vol. 62, no. 5, pp. 541–548, 2011.

[25] L. J. Crofford, "The hypothalamic-pituitary-adrenal stress axis in fibromyalgia and chronic fatigue syndrome," *Zeitschrift fur Rheumatologie*, vol. 57, S2, pp. S67–S71, 1998.

[26] R. Riva, P. J. Mork, R. H. Westgaard, and U. Lundberg, "Comparison of the cortisol awakening response in women with shoulder and neck pain and women with fibromyalgia," *Psychoneuroendocrinology*, vol. 37, no. 2, pp. 299–306, 2012.

[27] J. Gaab, S. Baumann, A. Budnoik, H. Gmünder, N. Hottinger, and U. Ehlert, "Reduced reactivity and enhanced negative feedback sensitivity of the hypothalamus–pituitary–adrenal axis in chronic whiplash-associated disorder," *Pain*, vol. 119, no. 1–3, pp. 219–224, 2005.

[28] L. Karlsson, B. Gerdle, B. Ghafouri et al., "Intramuscular pain modulatory substances before and after exercise in women with chronic neck pain," *European Journal of Pain*, vol. 19, no. 8, pp. 1075–1085, 2015.

[29] C. Muhtz, R. Rodriguez-Raecke, K. Hinkelmann et al., "Cortisol Response to Experimental Pain in Patients with Chronic Low Back Pain and Patients with Major Depression," *Pain Medicine (United States)*, vol. 14, no. 4, pp. 498–503, 2013.

[30] S. L. Nijhof, J. M. T. M. Rutten, C. S. P. M. Uiterwaal, G. Bleijenberg, J. L. L. Kimpen, and E. M. V. D. Putte, "The role of hypocortisolism in chronic fatigue syndrome," *Psychoneuroendocrinology*, vol. 42, pp. 199–206, 2014.

[31] K. F. S. Petrelluzzi, M. C. Garcia, C. A. Petta, D. M. Grassi-Kassisse, and R. C. Spadari-Bratfisch, "Salivary cortisol concentrations, stress and quality of life in women with endometriosis and chronic pelvic pain," *Stress*, vol. 11, no. 5, pp. 390–397, 2008.

[32] E. Vachon-Presseau, M. Roy, M.-O. Martel et al., "The stress model of chronic pain: evidence from basal cortisol and hippocampal structure and function in humans," *Brain*, vol. 136, no. 3, pp. 815–827, 2013.

[33] D. Catley, A. T. Kaell, C. Kirschbaum, and A. A. Stone, "A naturalistic evaluation of cortisol secretion in persons with fibromyalgia and rheumatoid arthritis," *Arthritis Care & Research*, vol. 13, no. 1, pp. 51–61, 2000.

[34] L. J. Crofford, S. R. Pillemer, K. T. Kalogeras et al., "Hypothalamic-pituitary-adrenal axis perturbations in patients with fibromyalgia," *Arthritis & Rheumatism*, vol. 37, no. 11, pp. 1583–1592, 1994.

[35] G. Neeck and W. Riedel, "Hormonal pertubations in fibromyalgia syndrome," *Annals of the New York Academy of Sciences*, vol. 876, pp. 325–339, 1999.

[36] G. A. McCain and K. S. Tilbe, "Diurnal hormone variation in fibromyalgia syndrome: a comparison with rheumatoid arthritis," *The Journal of Rheumatology*, vol. 16, no. 19, pp. 154–157, 1989.

[37] K. Wingenfeld, D. Wagner, I. Schmidt, G. Meinlschmidt, D. H. Hellhammer, and C. Heim, "The low-dose dexamethasone suppression test in fibromyalgia," *Journal of Psychosomatic Research*, vol. 62, no. 1, pp. 85–91, 2007.

[38] J. A. Macedo, J. Hesse, J. D. Turner, J. Meyer, D. H. Hellhammer, and C. P. Muller, "Glucocorticoid sensitivity in fibromyalgia patients: decreased expression of corticosteroid receptors and glucocorticoid-induced leucine zipper," *Psychoneuroendocrinology*, vol. 33, no. 6, pp. 799–809, 2008.

[39] K. Wingenfeld, C. Heim, I. Schmidt, D. Wagner, G. Meinlschmidt, and D. H. Hellhammer, "HPA axis reactivity and lymphocyte glucocorticoid sensitivity in fibromyalgia syndrome and chronic pelvic pain," *Psychosomatic Medicine*, vol. 70, no. 1, pp. 65–72, 2008.

[40] S. Sudhaus, B. Fricke, S. Schneider et al., "The cortisol awakening response in patients with acute and chronic low back pain: relations with psychological risk factors of pain chronicity," *Schmerz*, vol. 21, no. 3, pp. 202–211, 2007.

[41] V. Sveinsdottir, H. R. Eriksen, H. Ursin, Å. M. Hansen, and A. Harris, "Cortisol, health, and coping in patients with nonspecific low back pain," *Applied Psychophysiology Biofeedback*, vol. 41, no. 1, pp. 9–16, 2016.

[42] K. B. Jo, Y. J. Lee, I. G. Lee, S. C. Lee, J. Y. Park, and R. S. Ahn, "Association of pain intensity, pain-related disability, and depression with hypothalamus–pituitary–adrenal axis function in female patients with chronic temporomandibular disorders," *Psychoneuroendocrinology*, vol. 69, pp. 106–115, 2016.

[43] A. V. Apkarian, M. C. Bushnell, R.-D. Treede, and J.-K. Zubieta, "Human brain mechanisms of pain perception and regulation in health and disease," *European Journal of Pain*, vol. 9, no. 4, pp. 463–484, 2005.

[44] M. C. Bushnell, M. Čeko, and L. A. Low, "Cognitive and emotional control of pain and its disruption in chronic pain," *Nature Reviews Neuroscience*, vol. 14, no. 7, pp. 502–511, 2013.

[45] R. Peyron, B. Laurent, and L. García-Larrea, "Functional imaging of brain responses to pain. A review and meta-analysis (2000)," *Clinical Neurophysiology*, vol. 30, no. 5, pp. 263–288, 2000.

[46] S. W. G. Derbyshire, A. K. P. Jones, F. Gyulai, S. Clark, D. Townsend, and L. L. Firestone, "Pain processing during three levels of noxious stimulation produces differential patterns of central activity," *Pain*, vol. 73, no. 3, pp. 431–445, 1997.

[47] N. Maleki, L. Becerra, J. Brawn, B. McEwen, R. Burstein, and D. Borsook, "Common hippocampal structural and functional changes in migraine," *Brain Structure & Function*, vol. 218, no. 4, pp. 903–912, 2013.

[48] D. A. Matre, L. Hernandez-Garcia, T. D. Tran, and K. L. Casey, "'First pain' in humans: convergent and specific forebrain responses," *Molecular Pain*, vol. 6, no. 1, article 81, 2010.

[49] A. R. Segerdahl, M. Mezue, T. W. Okell, J. T. Farrar, and I. Tracey, "The dorsal posterior insula subserves a fundamental role in human pain," *Nature Neuroscience*, vol. 18, no. 4, pp. 499–500, 2015.

[50] T. D. Tran, H. Wang, A. Tandon, L. Hernandez-Garcia, and K. L. Casey, "Temporal summation of heat pain in humans: evidence supporting thalamocortical modulation," *Pain*, vol. 150, no. 1, pp. 93–102, 2010.

[51] C. H. Wilder-Smith, D. Schindler, K. Lovblad, S. M. Redmond, and A. Nirkko, "Brain functional magnetic resonance imaging of rectal pain and activation of endogenous inhibitory mechanisms in irritable bowel syndrome patient subgroups and healthy controls," *Gut*, vol. 53, no. 11, pp. 1595–1601, 2004.

[52] C. Berna, S. Leknes, E. A. Holmes, R. R. Edwards, G. M. Goodwin, and I. Tracey, "Induction of depressed mood disrupts emotion regulation neurocircuitry and enhances pain unpleasantness," *Biological Psychiatry*, vol. 67, no. 11, pp. 1083–1090, 2010.

[53] K. Bornhövd, M. Quante, V. Glauche, B. Bromm, C. Weiller, and C. Büchel, "Painful stimuli evoke different stimulus-response functions in the amygdala, prefrontal, insula and somatosensory cortex: a single-trial fMRI study," *Brain*, vol. 125, no. 6, pp. 1326–1336, 2002.

[54] U. Bingel, M. Quante, R. Knab, B. Bromm, C. Weiller, and C. Büchel, "Subcortical structures involved in pain processing: evidence from single-trial fMRI," *Pain*, vol. 99, no. 1-2, pp. 313–321, 2002.

[55] M. Ziv, R. Tomer, R. Defrin, and T. Hendler, "Individual sensitivity to pain expectancy is related to differential activation of the hippocampus and amygdala," *Human Brain Mapping*, vol. 31, no. 2, pp. 326–338, 2010.

[56] A. Ploghaus, I. Tracey, J. S. Gati et al., "Dissociating pain from its anticipation in the human brain," *Science*, vol. 284, no. 5422, pp. 1979–1981, 1999.

[57] I. A. Strigo, A. N. Simmons, S. C. Matthews, A. D. Craig, and M. P. Paulus, "Increased affective bias revealed using experimental graded heat stimuli in young depressed adults: evidence of "emotional allodynia"," *Psychosomatic Medicine*, vol. 70, no. 3, pp. 338–344, 2008.

[58] S. Benson, L. Rebernik, A. Wegner et al., "Neural circuitry mediating inflammation-induced central pain amplification in human experimental endotoxemia," *Brain, Behavior, & Immunity*, vol. 48, no. 1, pp. 222–231, 2015.

[59] J. C. Choi, J. Kim, E. Kang et al., "Step-down vs. step-up noxious stimulation: differential effects on pain perception and patterns of brain activation," *Acta Anaesthesiologica Scandinavica*, vol. 60, no. 1, pp. 117–127, 2016.

[60] J. F. Bernard, G. F. Huang, and J. M. Besson, "Nucleus centralis of the amygdala and the globus pallidus ventralis: electrophysiological evidence for an involvement in pain processes," *Journal of Neurophysiology*, vol. 68, no. 2, pp. 551–569, 1992.

[61] W. Li and V. Neugebauer, "Differential roles of mGluR1 and mGluR5 in brief and prolonged nociceptive processing in central amygdala neurons,," *Journal of Neurophysiology*, vol. 91, no. 1, pp. 13–24, 2004.

[62] V. Neugebauer and W. Li, "Differential sensitization of amygdala neurons to afferent inputs in a model of arthritic pain," *Journal of Neurophysiology*, vol. 89, no. 2, pp. 716–727, 2003.

[63] R. Zhang, M. Tomida, Y. Katayama, and Y. Kawakami, "Response durations encode nociceptive stimulus intensity in the rat medial prefrontal cortex," *Neuroscience*, vol. 125, no. 3, pp. 777–785, 2004.

[64] S. Khanna, "Dorsal hippocampus field CA1 pyramidal cell responses to a persistent versus an acute nociceptive stimulus and

their septal modulation," *Neuroscience*, vol. 77, no. 3, pp. 713–721, 1997.

[65] S. Khanna and J. G. Sinclair, "Noxious stimuli produce prolonged changes in the CA1 region of the rat hippocampus," *Pain*, vol. 39, no. 3, pp. 337–343, 1989.

[66] Z. Wang, S. Bradesi, J.-M. I. Maarek et al., "Regional brain activation in conscious, nonrestrained rats in response to noxious visceral stimulation," *Pain*, vol. 138, no. 1, pp. 233–243, 2008.

[67] T. Hayashi, M. Miyata, T. Nagata, Y. Izawa, and Y. Kawakami, "Intracerebroventricular fluvoxamine administration inhibited pain behavior but increased Fos expression in affective pain pathways," *Pharmacology Biochemistry & Behavior*, vol. 91, no. 3, pp. 441–446, 2009.

[68] S. Khanna, L. S. Chang, F. Jiang, and H. C. Koh, "Nociception-driven decreased induction of Fos protein in ventral hippocampus field CA1 of the rat," *Brain Research*, vol. 1004, no. 1-2, pp. 167–176, 2004.

[69] T. Nakagawa, A. Katsuya, S. Tanimoto et al., "Differential patterns of c-fos mRNA expression in the amygdaloid nuclei induced by chemical somatic and visceral noxious stimuli in rats," *Neuroscience Letters*, vol. 344, no. 3, pp. 197–200, 2003.

[70] M. Lehner, E. Taracha, A. Skórzewska et al., "Behavioral, immunocytochemical and biochemical studies in rats differing in their sensitivity to pain," *Behavioural Brain Research*, vol. 171, no. 2, pp. 189–198, 2006.

[71] A. V. Apkarian, Y. Sosa, S. Sonty et al., "Chronic back pain is associated with decreased prefrontal and thalamic gray matter density," *The Journal of Neuroscience*, vol. 24, no. 46, pp. 10410–10415, 2004.

[72] A. May, "Chronic pain may change the structure of the brain," *Pain*, vol. 137, no. 1, pp. 7–15, 2008.

[73] R. F. Smallwood, A. R. Laird, A. E. Ramage et al., "Structural brain anomalies and chronic pain: a quantitative meta-analysis of gray matter volume," *Journal of Pain*, vol. 14, no. 7, pp. 663–675, 2013.

[74] M. Burgmer, M. Gaubitz, C. Konrad et al., "Decreased gray matter volumes in the cingulo-frontal cortex and the amygdala in patients with fibromyalgia," *Psychosomatic Medicine*, vol. 71, no. 5, pp. 566–573, 2009.

[75] J. S. Labus, I. D. Dinov, Z. Jiang et al., "Irritable bowel syndrome in female patients is associated with alterations in structural brain networks," *Pain*, vol. 155, no. 1, pp. 137–149, 2014.

[76] C. P. Mao and H. J. Yang, "Smaller amygdala volumes in patients with chronic low back pain compared with healthy control individuals," *Journal of Pain*, vol. 16, no. 12, pp. 1366–1376, 2015.

[77] R. Rodriguez-Raecke, A. Niemeier, K. Ihle, W. Ruether, and A. May, "Brain gray matter decrease in chronic pain is the consequence and not the cause of pain," *The Journal of Neuroscience*, vol. 29, no. 44, pp. 13746–13750, 2009.

[78] W. Valfrè, I. Rainero, M. Bergui, and L. Pinessi, "Voxel-based morphometry reveals gray matter abnormalities in migraine," *Headache*, vol. 48, no. 1, pp. 109–117, 2008.

[79] U. Blankstein, J. Chen, N. E. Diamant, and K. D. Davis, "Altered brain structure in irritable bowel syndrome: potential contributions of pre-existing and disease-driven factors," *Gastroenterology*, vol. 138, no. 5, pp. 1783–1789, 2010.

[80] P. Y. Geha, M. N. Baliki, R. N. Harden, W. R. Bauer, T. B. Parrish, and A. V. Apkarian, "The brain in chronic CRPS pain: abnormal gray-white matter interactions in emotional and autonomic regions," *Neuron*, vol. 60, no. 4, pp. 570–581, 2008.

[81] T. Schmidt-Wilcke, E. Leinisch, A. Straube et al., "Gray matter decrease in patients with chronic tension type headache," *Neurology*, vol. 65, no. 9, pp. 1483–1486, 2005.

[82] J. S. Labus, C. S. Hubbard, J. Bueller et al., "Impaired emotional learning and involvement of the corticotropin-releasing factor signaling system in patients with irritable bowel syndrome," *Gastroenterology*, vol. 145, no. 6, pp. 1253–1261.e3, 2013.

[83] A. A. Mutso, D. Radzicki, M. N. Baliki et al., "Abnormalities in hippocampal functioning with persistent pain," *The Journal of Neuroscience*, vol. 32, no. 17, pp. 5747–5756, 2012.

[84] A. V. Apkarian, P. S. Thomas, B. R. Krauss, and N. M. Szeverenyi, "Prefrontal cortical hyperactivity in patients with sympathetically mediated chronic pain," *Neuroscience Letters*, vol. 311, no. 3, pp. 193–197, 2001.

[85] L. E. Simons, E. A. Moulton, C. Linnman, E. Carpino, L. Becerra, and D. Borsook, "The human amygdala and pain: evidence from neuroimaging," *Human Brain Mapping*, vol. 35, no. 2, pp. 527–538, 2014.

[86] M. N. Baliki, D. R. Chialvo, P. Y. Geha et al., "Chronic pain and the emotional brain: specific brain activity associated with spontaneous fluctuations of intensity of chronic back pain," *The Journal of Neuroscience*, vol. 26, no. 47, pp. 12165–12173, 2006.

[87] P. Schweinhardt, C. Glynn, J. Brooks et al., "An fMRI study of cerebral processing of brush-evoked allodynia in neuropathic pain patients," *NeuroImage*, vol. 32, no. 1, pp. 256–265, 2006.

[88] A. A. Mutso, B. Petre, L. Huang et al., "Reorganization of hippocampal functional connectivity with transition to chronic back pain," *Journal of Neurophysiology*, vol. 111, no. 5, pp. 1065–1076, 2014.

[89] D. Niddam, S. Lee, Y. Su, and R. Chan, "Brain structural changes in patients with chronic myofascial pain," *European Journal of Pain*, 2016.

[90] R. Ikeda, Y. Takahashi, K. Inoue, and F. Kato, "NMDA receptor-independent synaptic plasticity in the central amygdala in the rat model of neuropathic pain," *Pain*, vol. 127, no. 1-2, pp. 161–172, 2007.

[91] M. Tajerian, D. Leu, Y. Zou et al., "Brain neuroplastic changes accompany anxiety and memory deficits in a model of complex regional pain syndrome," *Anesthesiology*, vol. 121, no. 4, pp. 852–865, 2014.

[92] L. Gonçalves, R. Silva, F. Pinto-Ribeiro et al., "Neuropathic pain is associated with depressive behaviour and induces neuroplasticity in the amygdala of the rat," *Experimental Neurology*, vol. 213, no. 1, pp. 48–56, 2008.

[93] T. Kiritoshi and V. Neugebauer, "Group II mGluRs modulate baseline and arthritis pain-related synaptic transmission in the rat medial prefrontal cortex," *Neuropharmacology*, vol. 95, pp. 388–394, 2015.

[94] A. E. Metz, H.-J. Yau, M. V. Centeno, A. V. Apkarian, and M. Martina, "Morphological and functional reorganization of rat medial prefrontal cortex in neuropathic pain," *Proceedings of the National Academy of Sciences of the United States of America*, vol. 106, no. 7, pp. 2423–2428, 2009.

[95] P. Schweinhardt, D. A. Seminowicz, E. Jaeger, G. H. Duncan, and M. C. Bushnell, "The anatomy of the mesolimbic reward System: a link between personality and the placebo analgesic response," *Journal of Neuroscience*, vol. 29, no. 15, pp. 4882–4887, 2009.

[96] M. Terada, N. Kuzumaki, N. Hareyama et al., "Suppression of enriched environment-induced neurogenesis in a rodent model of neuropathic pain," *Neuroscience Letters*, vol. 440, no. 3, pp. 314–318, 2008.

[97] W. B. Hoover and R. P. Vertes, "Anatomical analysis of afferent projections to the medial prefrontal cortex in the rat," *Brain Structure & Function*, vol. 212, no. 2, pp. 149–179, 2007.

[98] G. Ji and V. Neugebauer, "CB1 augments mGluR5 function in medial prefrontal cortical neurons to inhibit amygdala hyperactivity in an arthritis pain model," *European Journal of Neuroscience*, vol. 39, no. 3, pp. 455–466, 2014.

[99] G. Ji, H. Sun, Y. Fu et al., "Cognitive impairment in pain through amygdala-driven prefrontal cortical deactivation," *The Journal of Neuroscience*, vol. 30, no. 15, pp. 5451–5464, 2010.

[100] H. Cardoso-Cruz, D. Lima, and V. Galhardo, "Impaired spatial memory performance in a rat model of neuropathic pain is associated with reduced hippocampus-prefrontal cortex connectivity," *The Journal of Neuroscience*, vol. 33, no. 6, pp. 2465–2480, 2013.

[101] Y. M. Ulrich-Lai, W. Xie, J. T. A. Meij, C. M. Dolgas, L. Yu, and J. P. Herman, "Limbic and HPA axis function in an animal model of chronic neuropathic pain," *Physiology & Behavior*, vol. 88, no. 1-2, pp. 67–76, 2006.

[102] S. J. Lupien, B. S. McEwen, M. R. Gunnar, and C. Heim, "Effects of stress throughout the lifespan on the brain, behaviour and cognition," *Nature Reviews Neuroscience*, vol. 10, no. 6, pp. 434–445, 2009.

[103] R. M. Sapolsky, L. C. Krey, and B. S. Mcewen, "The neuroendocrinology of stress and aging: the glucocorticoid cascade hypothesis," *Endocrine Reviews*, vol. 7, no. 3, pp. 284–301, 1986.

[104] M. W. Gilbertson, M. E. Shenton, A. Ciszewski et al., "Smaller hippocampal volume predicts pathologic vulnerability to psychological trauma," *Nature Neuroscience*, vol. 5, no. 11, pp. 1242–1247, 2002.

[105] D. M. Lyons, C. Yang, A. M. Sawyer-Glover, M. E. Moseley, and A. F. Schatzberg, "Early life stress and inherited variation in monkey hippocampal volumes," *Archives of General Psychiatry*, vol. 58, no. 12, pp. 1145–1151, 2001.

[106] I. N. Karatsoreos and B. S. McEwen, "Psychobiological allostasis: resistance, resilience and vulnerability," *Trends in Cognitive Sciences*, vol. 15, no. 12, pp. 576–584, 2011.

[107] R. M. Sapolsky, H. Uno, C. S. Rebert, and C. E. Finch, "Hippocampal damage associated with prolonged glucocorticoid exposure in primates," *Journal of Neuroscience*, vol. 10, no. 9, pp. 2897–2902, 1990.

[108] L. E. Simons, I. Elman, and D. Borsook, "Psychological processing in chronic pain: a neural systems approach," *Neuroscience and Biobehavioral Reviews*, vol. 39, pp. 61–78, 2014.

[109] D. P. Hibar, J. L. Stein, M. E. Renteria et al., "Common genetic variants influence human subcortical brain structures," *Nature*, vol. 520, no. 7546, pp. 224–229, 2015.

[110] S. J. Lupien, F. Maheu, M. Tu, A. Fiocco, and T. E. Schramek, "The effects of stress and stress hormones on human cognition: implications for the field of brain and cognition," *Brain and Cognition*, vol. 65, no. 3, pp. 209–237, 2007.

[111] M. N. Baliki and A. V. Apkarian, "Nociception, pain, negative moods, and behavior selection," *Neuron*, vol. 87, no. 3, pp. 474–491, 2015.

Hindawi Publishing Corporation
Neural Plasticity
Volume 2016, Article ID 8072156, 13 pages
http://dx.doi.org/10.1155/2016/8072156

Research Article

Activation of Sphingosine 1-Phosphate Receptor 1 Enhances Hippocampus Neurogenesis in a Rat Model of Traumatic Brain Injury: An Involvement of MEK/Erk Signaling Pathway

Yuqin Ye,[1,2] Zhenyu Zhao,[3] Hongyu Xu,[1] Xin Zhang,[1] Xinhong Su,[1] Yongxiang Yang,[1] Xinguang Yu,[3] and Xiaosheng He[1]

[1]*Department of Neurosurgery, Xijing Hospital, Fourth Military Medical University, Xi'an 710032, China*
[2]*Department of Neurosurgery, PLA 163rd Hospital (Second Affiliated Hospital of Hunan Normal University), Changsha 410000, China*
[3]*Department of Neurosurgery, PLA General Hospital, Beijing 100853, China*

Correspondence should be addressed to Xiaosheng He; hexiaos@fmmu.edu.cn

Received 23 July 2016; Accepted 31 October 2016

Academic Editor: Fang Pan

Among sphingosine 1-phosphate receptors (S1PRs) family, S1PR1 has been shown to be the most highly expressed subtype in neural stem cells (NSCs) and plays a crucial role in the migratory property of NSCs. Recent studies suggested that S1PR1 was expressed abundantly in the hippocampus, a specific neurogenic region in rodent brain for endogenous neurogenesis throughout life. However, the potential association between S1PR1 and neurogenesis in hippocampus following traumatic brain injury (TBI) remains unknown. In this study, the changes of hippocampal S1PR1 expression after TBI and their effects on neurogenesis and neurocognitive function were investigated, focusing on particularly the extracellular signal-regulated kinase (Erk) signaling pathway which had been found to regulate multiple properties of NSCs. The results showed that a marked upregulation of S1PR1 occurred with a peak at 7 days after trauma, revealing an enhancement of proliferation and neuronal differentiation of NSCs in hippocampus due to S1PR1 activation. More importantly, it was suggested that mitogen-activated protein kinase-Erk kinase (MEK)/Erk cascade was required for S1PR1-meidated neurogenesis and neurocognitive recovery following TBI. This study lays a preliminary foundation for future research on promoting hippocampal neurogenesis and improving TBI outcome.

1. Introduction

Traumatic brain injury (TBI) is a commonly-seen cause of brain damage and often results in a series of nonreversible neuronal loss and neurological deficits [1, 2]. Neural stem cells (NSCs), located in the subgranular zone (SGZ) of hippocampal dentate gyrus (DG), are capable of proliferating, differentiating, and integrating into the existing neuronal circuits that play a pivotal role in neurogenesis throughout life in mammalian brain [3, 4]. These self-renewing cells contribute not only to embryonic brain development, but also to neural regeneration after TBI in adults [3, 5, 6]. Endogenous neural regeneration in hippocampus represents a special type of neural plasticity that has huge potential to replenish neural loss and restore neurological function after TBI [5]. However, severe and permanent functional disability in TBI often occurred due to limited endogenous neurogenesis capacity of adult brain [4, 7]. Therefore, activating endogenous NSCs to enhance neurogenesis in hippocampus is considered to be one of the promising strategies for TBI rehabilitation. As a matter of fact, the details of NSCs proliferation and differentiation remain not to be fully elucidated since there are a variety of complex regulatory factors found to be involved in endogenous neurogenesis process [3, 8]. Hence, identification of these unknown factors would help us understand more about hippocampal neurogenesis and provide new clues in order to improve neural repair after TBI.

As classical G-protein-coupled receptors, sphingosine 1-phosphate receptors (S1PRs) are a critical immune-modulatory receptor family that consists of S1PR1, S1PR2, S1PR3,

S1PR4, and S1PR5 [9]. S1PRs family is enriched in central nervous system (CNS) and recognizes lots of bioactive signaling ligands including lipid mediator sphingosine 1-phosphate (S1P) to regulate neuronal survival, gliosis, astrocyte migration, and other biological processes in both physiological and pathological circumstances [10–12]. Of the five known S1PRs, S1PR1 expressed in hippocampal primordium and subventricular zone (SVZ) could be detected as early as E14 during CNS development [13]. In particular, increasing evidence suggested that NSCs harvested all subtypes of S1PRs, in which S1PR1 was the most highly expressed [14, 15]. And S1PR1 might be a presumed S1PRs subtype responsible for the proliferation and morphological changes of NSCs induced by S1P *in vitro* [16]. Recently, it has been demonstrated that S1PR1 plays an important role in the transplanted NSCs migration toward injured area of spinal cord for rebuilding [15]. However, little is known about the potential *in vivo* effect of S1PR1 on the proliferation and differentiation of NSCs in hippocampus following TBI. The mitogen-activated protein kinases (MAPK)/extracellular signal-regulated kinase (Erk) signaling pathway is a pivotal cell cascade that takes a crucial role in multiple factors involved in hippocampal neurogenesis [16–18]. Till today, whether and how MAPK-Erk kinase (MEK)/Erk cascade is implicated in the presumed S1PR1-assicoated neurogenesis after TBI remain poorly understood. The present study aims to clarify the potential role of S1PR1 in hippocampal NSCs proliferation and differentiation in response to TBI, and its underlying link with MEK/Erk cascade.

2. Materials and Methods

2.1. Animals and Experimental Groups. Healthy male Sprague-Dawley rats (weighing 250–300 g) were provided by Laboratory Animal Center of Fourth Military Medical University. The animals were maintained under an environment with 24–27°C, 60% humidity, a 12-hour light/dark cycle (light on from 07:00 to 19:00), and enough food and water. All the experimental procedures were carried out in accordance with the National Experimental Animals Guidelines and approved by the Institutional Animal Care and Use Committee of Fourth Military Medical University, Xi'an, China. All measures were taken to minimize animal suffering.

One hundred and sixty-five rats were randomly assigned to eight groups as below: sham group ($n = 15$), TBI group ($n = 35$), TBI-treated with vehicle 1% dimethyl sulfoxide (DMSO) group (TBI+Vehicle group, $n = 23$), TBI-treated with selective S1PR1 agonist SEW2871 group (TBI+SEW group, $n = 23$), TBI-treated with SEW2871 and S1PR1 antagonist VPC23019 group (TBI+SEW+VPC group, $n = 18$), TBI-treated with SEW2871 and MEK/Erk inhibitor U0126 (TBI+SEW+U0126 group, $n = 17$), TBI-treated with VPC23019 (TBI+VPC group, $n = 17$), and TBI-treated with MEK/Erk activator erucin (ERN) and VPC23019 (TBI+VPC+ERN group, $n = 17$).

2.2. TBI Model Establishment. TBI was induced by a controlled cortical impact (CCI) device (Hatteras Instruments, Cary, NC, USA). All animals were anesthetized by intraperitoneal (i.p.) injection of sodium pentobarbital (60 mg/kg) and were placed on the stereotaxic frame (Kopf Instruments, Tujunga, CA, USA) of injury device. The rat head was horizontally secured by two lateral ear pins and an incisor bar. After a sagittal incision was performed on the scalp, a 4.0 mm diameter craniotomy was made between lambda and bregma sutures and 3.0 mm lateral to the sagittal suture on the right. The skull flap was removed to expose the dura, on which a perpendicular impact was performed by a piston rod with its contact surface of 3.0 mm diameter. The brain injury was conducted in accordance with the following biomechanical parameters: 1.5 mm for vertical dura shift, 100.0 ms for contact time, and 3.0 m/s for piston velocity. Then, the skull flap was restored and the scalp was sutured. Rats in sham surgery group were subjected only to craniotomy without cortical impact. During the surgical procedure and recovery period, a heating pad was used to keep the rat body temperature at 36.0–37.0°C. All TBI rats appeared with arched back, erect hair, unconsciousness, and slow respiration but recovered to normal within the following 2 hours. No rats died in all groups.

2.3. Drugs and 5-Bromo-2-deoxyuridine (BrdU) Administration. For administration of S1PR1 agonist or antagonist (Figures 1(a) and 1(b)), SEW2871 (Cayman Chemical, 10006440, Ann Arbor, MI, USA) and VPC23019 (Cayman Chemical, 13240, Ann Arbor, MI, USA) were, respectively, dissolved in DMSO (5% DMSO in 0.05 M PBS), making each individual concentration as 1 mg/mL and 0.25 mg/mL. The dosage of SEW2871 and VPC23019 used in this study was a slight modification to that reported by other authors [19–21]. In the consecutive 7 days after TBI, rats in TBI+Vehicle, TBI+SEW, TBI+VPC group, together with TBI+SEW+VPC group were treated, respectively, with an i.p. injection of DMSO (0.5 mL/kg/day), SEW2871 (1.0 mg/kg/day), VPC23019 (0.5 mg/kg/day), and a combination of SEW2871 and VPC23019.

For administration of the MEK/Erk inhibitor (Figures 1(a) and 1(b)), U0126 (Cell Signaling, 9903, Beverly, MA, USA) was dissolved in DMSO to a final concentration of 0.4 mg/mL. The dosage of U0126 followed that in previous studies with some modification [22, 23]. Rats in TBI+SEW+U0126 group were not only treated with i.p. injection of SEW2871 in the same way as described above, but also given to with intravenous (i.v.) injection of U0126 (0.2 mg/kg) via the tail vein twenty minutes before induction of TBI (while the rats were anesthetized). ERN, a bioactive compound from cruciferous vegetables, has been found to be an effective activator of MEK/Erk [24, 25]. Before administration of ERN (Figures 1(a) and 1(b)), its stock solution (Santa Cruz Biotechnology, sc-204741, Dallas, TX, USA) was diluted to a final concentration of 75 mmol/L with DMSO. Rats in TBI+VPC+ERN group received both VPC23019 treatment in the same way as described above and i.p. injection of ERN (12.5 mg/kg) twenty minutes before inducing TBI.

For administration of a thymidine analog to label the endogenous NSCs in hippocampus, BrdU (Sigma-Aldrich, B9285, St. Louis, MO, USA) was dissolved in 0.1 M sterile

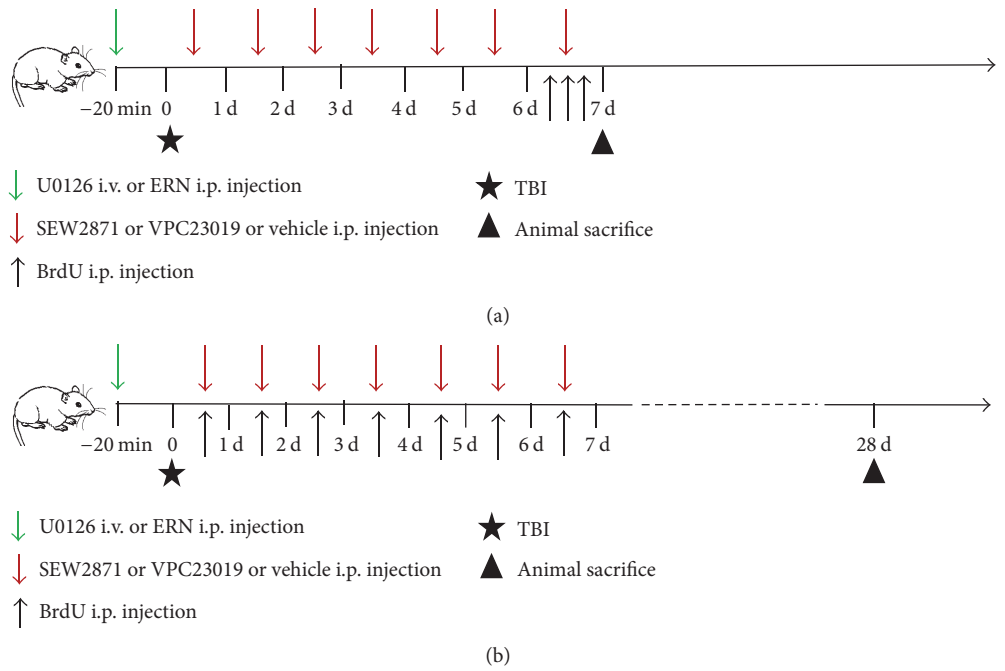

Figure 1: Schematic diagram of drugs and 5-bromo-2-deoxyuridine (BrdU) administration. The time-point of traumatic brain injury (TBI) model establishment was defined as zero point (indicated by black pentagram). (a) For the assay of neural stem cells (NSCs) proliferation, BrdU (100 mg/kg) was injected intraperitoneally (i.p.) three times with 8-hour interval at 6 days after TBI (indicated by black arrow) and the animals were sacrificed for perfusion at 7 days after TBI (indicated by black triangle). (b) For the analysis of NSCs differentiation, BrdU (100 mg/kg) was injected i.p. seven times with 24-hour interval 1–7 days after TBI (indicated by black arrow) and the animals were sacrificed for perfusion at 28 days after TBI (indicated by black triangle). SEW2871 (1.0 mg/kg/day) or VPC23019 (0.5 mg/kg/day) or vehicle (0.5 mL/kg/day) was administrated i.p. in rats of the corresponding group seven times within 24-hour interval 1–7 days after TBI (indicated by red arrow in (a) and (b)). Erucin (ERN, 12.5 mg/kg) or U0126 (0.2 mg/kg) was administrated i.p. or intravenously (i.v.) in rats of TBI+SEW+U0126 group 20 minutes before TBI (indicated by green arrow in (a) and (b)).

phosphate-buffered saline (PBS) to a final concentration of 10 mg/mL. On one hand, rats for the assessment of NSCs proliferation received three times i.p. injection of BrdU (100 mg/kg) with an 8-hour interval at the sixth day after TBI and were sacrificed for perfusion at the seventh day (Figure 1(a)). On the other hand, rats for the evaluation of NSCs neuronal differentiation were treated with an i.p. injection of BrdU (100 mg/kg) once per day from 1 to 7 days after TBI, and these rats were sacrificed for perfusion at 28 days after injury (Figure 1(b)).

2.4. Brain Tissue Preparation. At the scheduled time-points, rats were deeply anesthetized with sodium pentobarbital (60 mg/kg) and perfused with 50 mL of 0.9% saline through the left ventricle, and then by 4% paraformaldehyde in 0.1 M phosphate buffer saline (PBS) for 2 hours. The brains were removed and immersed in 4% paraformaldehyde in PBS (pH = 7.4) at 4°C overnight and then dehydrated by alcohol and embedded in paraffin. Coronal, 5 μm thick brain sections containing the entire DG of hippocampus (from bregma −2.40 mm to −4.68 mm) were prepared by a microtome (Leica, Nussloch, Germany) and dried at 92°C overnight for immunofluorescence (IF). To assess the NSCs proliferation at 7 days after injury, a series of ten sections (120 μm apart) from each rat brain were processed for BrdU/sex determining region Y-box 2 (SOX2) double-labeling IF. To assay the NSCs neuronal differentiation at 28 days after injury, another series of ten sections (120 μm apart) parallel to the above ten from each brain were processed for BrdU/NeuN double-labeling IF.

2.5. IF. For DNA denaturation, brain sections were deparaffinized by alcohol and dimethylbenzene and then were incubated in the citric acid antigen retrieval buffer (pH = 6.0) at 95°C for 15 min. After that, the sections were incubated in PBS with 1% donkey serum albumin and 0.3% Triton X-100 at room temperature for 30 min to block nonspecific signals. For visualization of BrdU, SOX2, and NeuN, the sections were incubated in relevant primary antibodies, respectively, as follows: sheep anti-BrdU antibody (1 : 200, GeneTex, GTX21893, Irvine, CA, USA), rabbit anti-rat SOX2 antibody (1 : 500, GeneTex, GTX101507, Irvine, CA, USA), and mouse anti-rat NeuN antibody (1 : 500, Merck Millipore, MAB377, Billerica, MA, USA) in PBS overnight at 4°C. After three washes in PBS, the sections were incubated in relevant secondary antibodies as follows: Alexa fluor 594-labeled donkey anti-sheep IgG antibody (1 : 2000, Molecular Probes, A-11016, Eugene, OR, USA), Alexa fluor 488-labeled goat anti-rabbit IgG antibody (1 : 1000, Molecular Probes, A-11008, Eugene, OR, USA), and Alexa fluor 488-labeled

goat anti-mouse IgG antibody (1 : 2000, Molecular Probes, A-11029, Eugene, OR, USA) in PBS for 1 hour at room temperature. Finally, the sections were washed 3 times in PBS, mounted with an anti-fade mounting medium containing 1, 4-Diazobicyclo (Electron Microscopy Sciences, CAT17895-01, Hatfield, PA, USA), and cover-slipped. All the procedures were performed in a manner that minimized light exposure to the tissue.

2.6. Microscopic Cell Counting. A confocal laser scanning microscope (FV1000, Olympus, Tokyo, Japan) with a FLUOVIEW image system (v.1.4a, Olympus, Tokyo, Japan) was used to capture the immunolabeled cells in hippocampus. $BrdU^+/SOX2^+$ cells and $BrdU^+/NeuN^+$ cells of five consecutive visual fields (24.41 μm^2 each, magnified by 400x) at DG in each section were counted; the value was averaged across the five visual fields and was thought to be the number of double-labeled cells for each section. Then, the average across the 10 sections was considered as the final number of double-labeled cells for each brain sample. The data were expressed as Mean ± SD. Images were assembled and labeled in Photoshop 7.0 (Adobe Systems, San Jose, CA, USA).

2.7. Western Blotting (WB). Rats for the determination of S1PR1 protein were sacrificed at scheduled time-points and the brains were removed in the same way as described above. After split from brain on ice, the hippocampal tissues were homogenized and digested in a homogenizer with a lysis buffer (1% NP-40, 150 mM NaCl, 50 mM Tris (pH = 7.4), 1% Triton X-100, 0.5 mM EDTA, 1 mg/mL aprotinin, 1% deoxycholate, 10 mg/mL leupeptin, and 1 mM phenylmethylsulfonyl fluoride). The lysates were incubated on ice for 15 min and then centrifuged at 12,000 rpm for 30 min at 4°C. The protein concentration was examined by bicinchoninic acid Protein Assay kit (Beyotime, P0011, Shanghai, China). Then, sodium dodecyl sulfate (SDS) sample loading buffer was added in the supernatant and the mixture was boiled at 100°C for 5 min. Samples containing 40 μg protein were resolved on 10% sodium dodecyl sulfate-polyacrylamide gel electrophoresis (SDS-PAGE) and electroblotted at 4°C for 50 minutes to nitrocellulose membrane. Following blocked by 5% skim milk in Tris-buffered saline solution containing 0.1% Tween-20 (TBST), the membranes were incubated overnight at 4°C with the following primary antibodies: rabbit anti-rat S1PR1 antibody (1 : 500, Prosci, 4809, Poway, CA, USA), rabbit anti-rat phosphate Erk (pErk) antibody (1 : 1000, Cell Signaling, 9101, Beverly, MA, USA), rabbit anti-rat total Erk (tErk) antibody (1 : 1000, Cell Signaling, 9102, Beverly, MA, USA), rabbit anti-rat phosphate MEK (pMEK) antibody (1 : 1000, Cell Signaling, 9154, Beverly, MA, USA), and rabbit anti-rat total MEK (tMEK) antibody (1 : 1000, Cell Signaling, 9126, Beverly, MA, USA). Rabbit anti-β-actin antibody (1 : 1500, Cwbiotech, CW0097, Beijing, China) was used as internal control for the concentration of immunoreactive proteins loaded.

After three washes in TBST, the membranes were incubated with horse radish peroxidase- (HRP-) conjugated goat anti-rabbit IgG antibody (1 : 20000, Cell Signaling Technology, 7074, Boston, MA, USA) for 1 hour at room temperature. The immunoreactive protein bands were visualized in Western Bright enhanced chemiluminescence reagents (K12045-d20, Advansta, Menlo Park, CA, USA). The immunoblots were analyzed by Gel-Pro Analyzer software (version 6.0, Media Cybernetics, Rockville, MD, USA). The ratio of S1PR1, pErk, tErk, pMEK, and tMEK to β-actin in gray scale (optical density value) was taken as the expression values, respectively.

2.8. Morris Water Maze (MWM) Test. At 24–28 days after injury, rats for spatial learning and memory test were performed with MWM trials [26]. A circular pool (160 cm diameter and 50 cm depth) filled with water (23 ± 2°C and 30 cm deep) was divided into four equal quadrants. There were 4 black plastic panels in different shape placed above the water surface serving as spatial cues for rat. All the objects in the experimental room remained at a constant position during testing process. A black circular platform (12 cm diameter) for rat escaping from water was submerged 1 cm under water surface in one of the four quadrants. The rat movements were recorded by a video tracking system placed 2 m above the pool center and analyzed by a data analysis system (DigBehMR, Shanghai Auspicious Software Technology Company Limited, China).

At 24–27 days after TBI, each rat performed four consecutive hidden platform trials per day in the maze with a trial-trial interval of 60 s. For each trial, rat was randomly placed into water facing the inside of the pool wall at one of the four quadrants and was freed to swim to find the hidden platform to escape from water. Each rat was given a maximum of 120 s to reach the platform and was allowed to remain on it for 15 s. If the rat failed to find the platform within 120 s, it was taken and placed onto the platform for 15 s. The time between rat being placed into water and reaching platform was recorded as escape latency. Average escape latency over the four consecutive days was regarded as the index of rat spatial learning capacity.

On 28 days after TBI, the platform was removed from the pool, and probe trails were conducted to assess spatial memory capacity of rats. Animals were allowed to swim freely for 120 s to find the previous platform which had been removed. "Platform crossing" referred to the times a rat swam over the location at which the platform was originally set in the hidden platform trials. Times of platform crossing and duration time spent in target quadrant were recorded. These two parameters were averaged and considered as the index of rat spatial memory capacity.

Following probe trails, visible platform trials were performed to assess swim capacity of each rat. A visible platform was placed above water surface in the pool, and rats were allowed swim freely to find the visible platform. Swim speed was recorded to assess rat motor activity in MWM test.

2.9. Statistical Analysis. Data was expressed as Mean ± SD and statistical analysis was processed by Graphpad Prisom software (v.6.01, Graphpad software, San Diego, CA, USA). Difference between groups was processed with one-way analysis of variance (ANOVA) and Tukey HSD *post hoc* test. The difference was considered statistically significant at $P < 0.05$.

3. Result

3.1. Expression of S1PR1 in Hippocampus Was Significantly Increased after TBI. The expression of S1PR1 in hippocampus at 12 hours, 1 day, 3 days, 7 days, 14 days, 21 days, and 28 days after TBI was determined by WB (Figure 2(a)). In the observed period, upregulated level of S1PR1 occurred from 12 hours after trauma, reached the peak at 7 days, and remained at a higher level than the sham at least 28 days ($P < 0.05$) (Figure 2(b)). Further analysis revealed that an obvious difference existed between any two time-point groups after trauma ($P < 0.05$) (Figure 2(b)). The data suggested that the hippocampal S1PR1 level was significantly increased after TBI.

3.2. S1PR1 Activation Enhanced NSCs Proliferation in Hippocampus after TBI. The anatomic boundary of DG was identified as described previously [27] (Figure 3(a)). To investigate the influence of S1PR1 activation upon hippocampal neurogenesis after TBI, SEW2871 and/or VPC23019 was administrated to intervene the activity of S1PR1 in rats of corresponding groups. BrdU/SOX2 double-labeling IF was used to assess NSCs proliferation in DG at 7 days after injury (Figures 3(b) and 3(d)). As compared with sham group, the number of $BrdU^+$ (red)/$SOX2^+$ (green) cells in TBI+Vehicle group significantly increased at 7 days after TBI ($P < 0.05$). In addition, there were obviously more $BrdU^+/SOX2^+$ cells in TBI+SEW group than TBI+Vehicle group ($P < 0.05$). Statistical analysis showed that SEW2871 triggered an increase of NSCs proliferation by 62.31%. The results showed that TBI-induced NSCs proliferation in DG, and S1PR1 agonist further enhanced the TBI-induced NSCs proliferation. However, TBI+SEW+VPC group exhibited a decreased number of $BrdU^+/SOX2^+$ cells compared to that in TBI+SEW group ($P < 0.05$). The results suggested that application of S1PR1 antagonist reduced the effect of S1PR1 on NSCs proliferation. Taken together, all the above data indicated that S1PR1 activity was correlated with hippocampal NSCs proliferation after TBI.

3.3. S1PR1 Activation Promoted NSCs Differentiated into Neurons in Hippocampus after TBI. After understanding the effect of S1PR1 on NSCs proliferation in hippocampus, the potential association between S1PR1 expression and NSCs neuronal differentiation was then investigated. BrdU/NeuN double-labeling IF was performed to identify the hippocampal newly generated neurons, which were thought to be a main type of NSCs offspring for posttraumatic brain repair [3–5] (Figures 3(c) and 3(e)). Obviously, there were more $BrdU^+$ (red)/$NeuN^+$ (green) cells in TBI+Vehicle group than sham group at 28 days after trauma ($P < 0.05$). Moreover, the administration of S1PR1 agonist in the rats of TBI+SEW group markedly increased the number of $BrdU^+/NeuN^+$ cells compared to TBI+Vehicle group ($P < 0.05$). Nevertheless, the S1PR1-mediated neuronal differentiation of NSCs was abrogated by S1PR1 antagonist shown by a significant reduction of $BrdU^+/NeuN^+$ cells in TBI+SEW+VPC group ($P < 0.05$). The above data suggested that S1PR1 activation promoted the neuronal differentiation of NSCs in hippocampus after TBI.

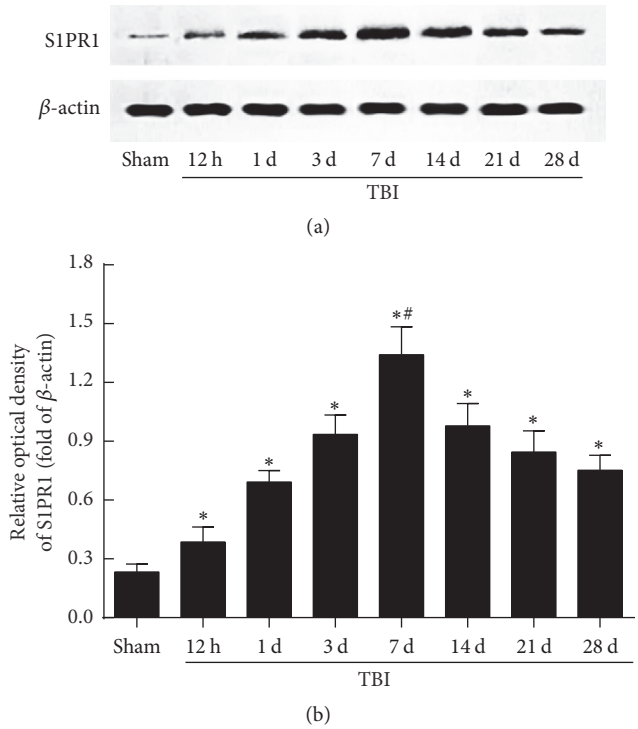

Figure 2: Hippocampal sphingosine 1-phosphate receptor 1 (S1PR1) expression increased markedly after TBI. (a) The level of S1PR1 protein in hippocampus was detected by western blotting (WB) at 12 hours, 1, 3, 7, 14, 21, and 28 days after trauma. (b) Quantitative analysis indicated that upregulated expression of hippocampal S1PR1 occurred from 12 hours, peaked at 7 days, and remained at a relatively higher level for at least 28 days after TBI ($n = 3$, sham group; $n = 5$ each time-point group of TBI). Further analysis revealed that there was a statistical difference between any two time-point groups after trauma. $^*P < 0.05$ versus sham group; $^\#P < 0.05$ versus other time-point groups of TBI.

3.4. MEK/Erk Signaling Pathway Was Activated in Response to the Upregulated S1PR1 after TBI. It was well acknowledged that MEK/Erk cascade played a key role in multiple functions of neurogenesis, such as NSCs survival, proliferation, and differentiation. Hence, an investigation of the activity of MEK/Erk cascade in S1PR1-mediated NSCs proliferation and differentiation after TBI was performed by detecting S1PR1, pMEK, tMEK, pErk, and tErk expression in hippocampus with WB at day 7 after trauma (Figure 4(a)). As shown in Figures 4(b), 4(c), and 4(e), the levels of S1PR1, pMEK, and pErk in TBI+Vehicle group were dramatically increased compared with sham group ($P < 0.05$), and the TBI-induced S1PR1, pMEK, and pErk upregulation was further enhanced by the administration of S1PR1 agonist in TBI+SEW group ($P < 0.05$). However, this enhancement was attenuated by treatment with S1PR1 antagonist in TBI+SEW+VPC group ($P < 0.05$). Quantitation analysis revealed that there was no statistical difference in the level of tMEK and tErk between the four groups ($P > 0.05$) (Figures 4(d) and 4(f)). Taken together, the data revealed that the phosphorylation of MEK

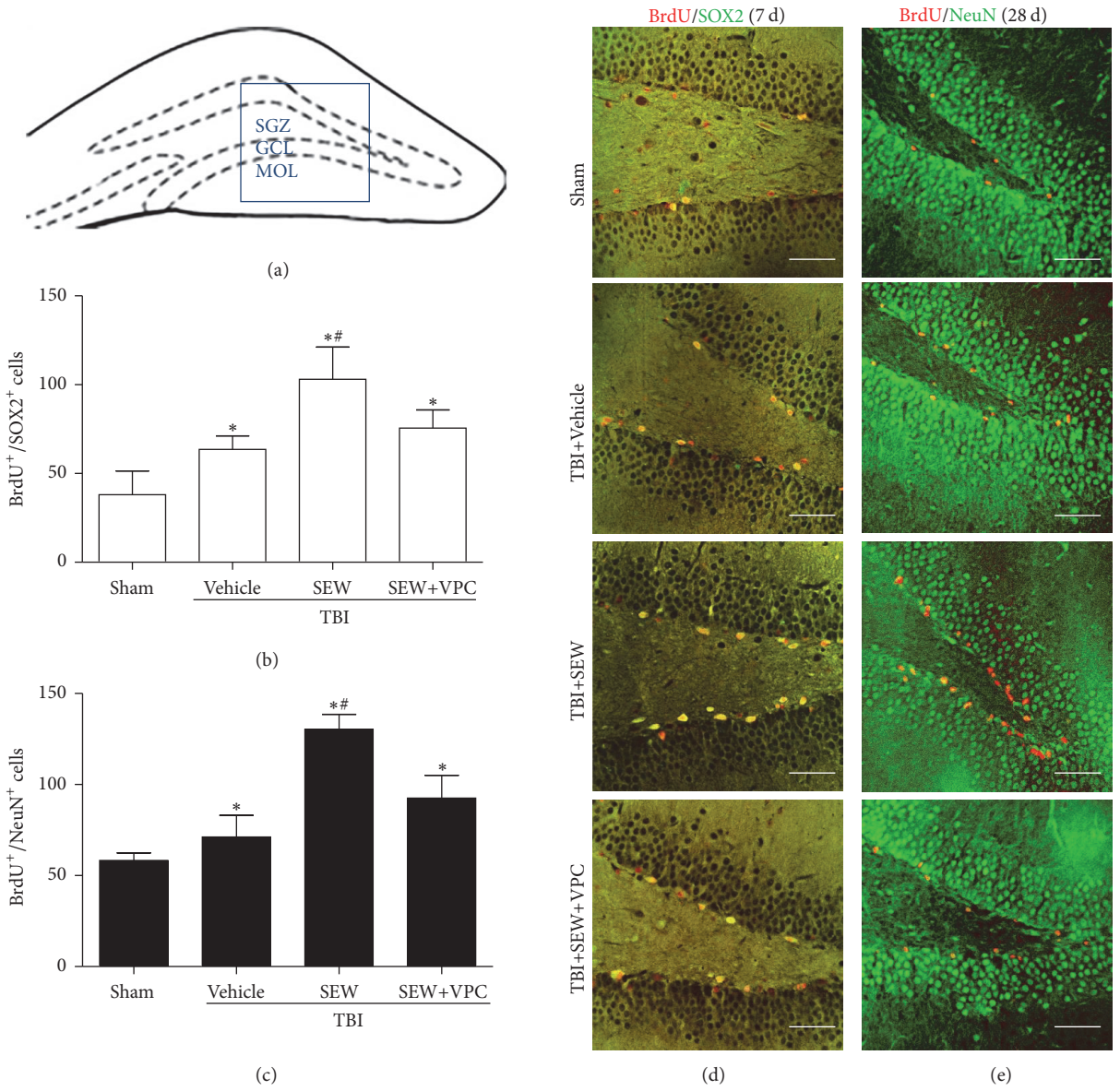

Figure 3: S1PR1 activation enhanced NSCs proliferation and neuronal differentiation in hippocampal dentate gyrus (DG) after TBI. (a) Coronal diagram of rat hippocampus, the subgranular zone, granular cells layer, and molecular layer of DG were, respectively, marked by SGZ, GCL, and MOL, the blue pane representing one of microscopic visual fields for counting immunolabeled cells of immunofluorescence (IF). (b) NSCs proliferation in SGZ at 7 days after TBI was assessed by BrdU/SOX2 double-labeling IF. Quantitation analysis showed that, relative to sham group ($n = 3$), brain injury induced more double-positive cells in TBI+Vehicle group ($n = 6$). Following the treatment of SEW2871, the number of $BrdU^+/SOX2^+$ cells further increased in TBI+SEW group ($n = 6$). Reversely, administration of VPC23019 resulted in a significant reduction of $BrdU^+/SOX2^+$ cells in TBI+SEW+VPC group ($n = 6$). (c) Neuronal differentiation of NSCs in SGZ at 28 days after TBI was assessed by BrdU/NeuN double-labeling IF. Statistical data indicated that $BrdU^+/NeuN^+$ cells increased in TBI+Vehicle group ($n = 6$) compared with sham group ($n = 3$). And the double-positive cells increased at even higher level after SEW2871 treatment in TBI+SEW group ($n = 6$). However, VPC23019 administration caused an evident decrease of $BrdU^+/NeuN^+$ cells in TBI+SEW+VPC group ($n = 6$). (d) and (e) Representative IF microphotographs of hippocampus immunolabeled with BrdU/SOX2 and BrdU/NeuN in all the above four groups at 7 days and 28 days after trauma. Scale bar: 50 μm. $^*P < 0.05$ versus sham group; $^\#P < 0.05$ versus TBI+Vehicle group or TBI+SEW+VPC group.

and Erk was activated in response to the increased S1PR1 after trauma. It was suggested that MEK/Erk signaling pathway might be the underlying downstream cascade to mediate S1PR1-associated hippocampal neurogenesis after TBI.

3.5. S1PR1 Induced Neurogenesis in Hippocampus Though MEK/Erk Cascade following TBI. To further demonstrate MEK/Erk signaling pathway contributing to S1PR1-associated neurogenesis after trauma, the effect of MEK/Erk

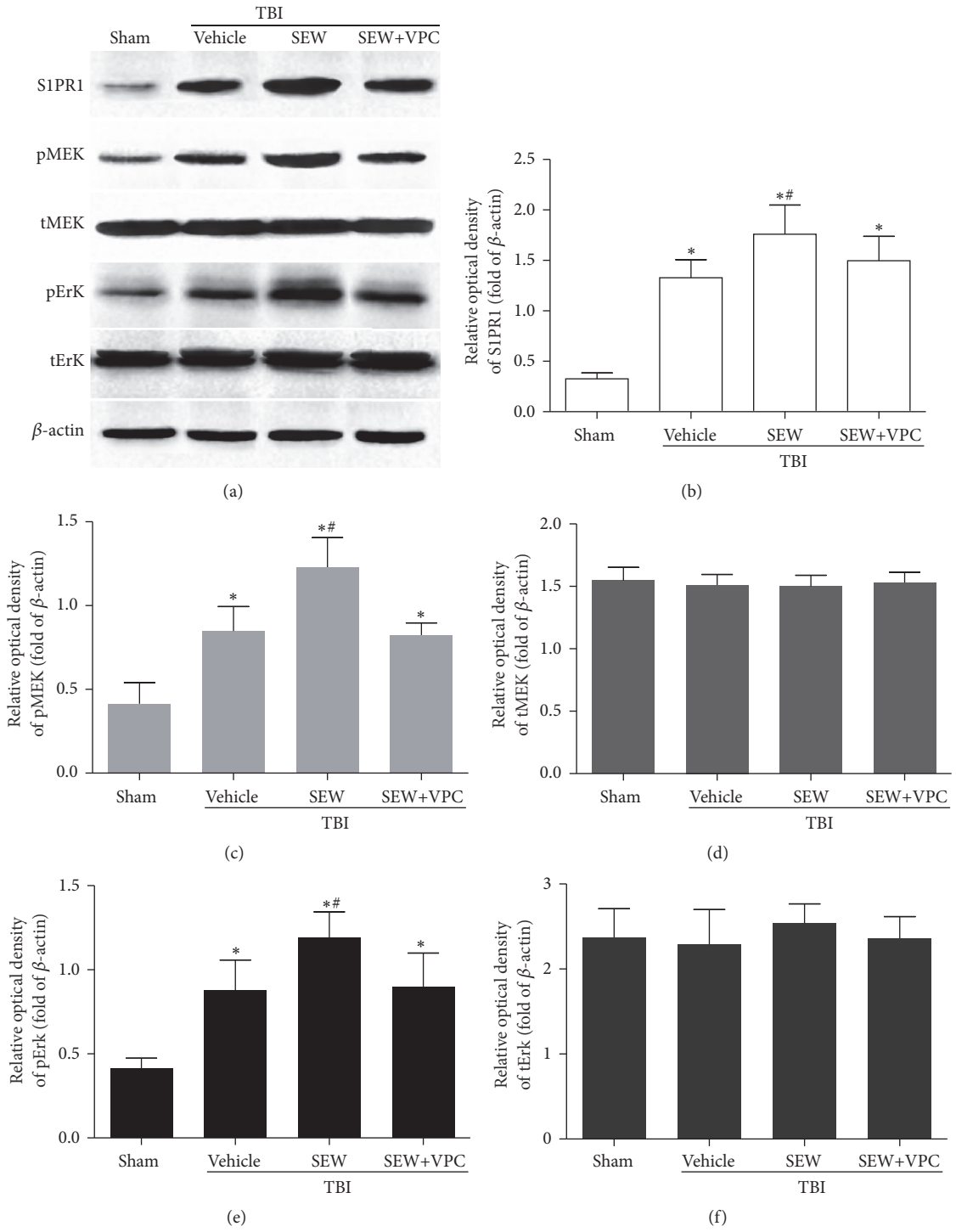

Figure 4: Activation of S1PR1 triggered MEK/Erk pathway phosphorylation in hippocampus at 7 days after TBI. (a) WB was performed to determine hippocampal S1PR1, pMEK, tMEK, pErk, and tErk expression in groups of sham, TBI+Vehicle, TBI+SEW, and TBI+SEW+VPC group ($n = 3$ in sham and $n = 6$ in other groups). (b, c, and e) The level of S1PR1, pMEK, and pErk significantly increased after trauma. SEW2871 induced further upregulation of S1PR1, pMEK, and pErk. However, the effect was attenuated by administration of VPC23019. (d, f) Neither S1PR1 agonism nor antagonism had effect on tMEK and tErk expression in hippocampus after TBI. $^{*}P < 0.05$ versus sham group; $^{\#}P < 0.05$ versus TBI+Vehicle group or TBI+SEW+VPC group.

inhibitor and activator upon NSCs proliferation at 7 days and NSCs neuronal differentiation at 28 days after TBI was studied (Figures 5(a) and 5(b)). On one hand, in comparison with TBI+SEW group, the number of $BrdU^+/SOX2^+$ cells and $BrdU^+/NeuN^+$ cells in TBI+SEW+U1026 group was decreased by 42.50% and 24.98%, respectively ($P < 0.05$) (Figures 5(c) and 5(d)); this data suggested that MEK/Erk inhibition mitigated the S1PR1-induced neurogenesis in hippocampus after TBI. On the other hand, the double-labeled cells in TBI+VPC+ERN group were significantly increased compared to TBI+VPC group at 7 and 28 days after trauma ($P < 0.05$) (Figures 5(c) and 5(d)), indicating that the detrimental effect of VPC231019 on NSCs proliferation and neuronal differentiation was rescued by ERN. Consequently, the above results implied that S1PR1 induced hippocampal neurogenesis via MEK/Erk pathway following TBI.

3.6. MEK/Erk Activity Contributed to S1PR1-Mediated Learning and Memory Performance in MWM Test. Since there was a close connection between hippocampal neurogenesis and cognitive function, the involvement of MEK/Erk signaling pathway in the S1PR1-mediated hippocampal learning and memory function was investigated by MWM test from 24 to 28 days following TBI.

In hidden platform trials, a gradual decrease in rat escape latency across 24, 25, 26, and 27 days after trauma was presented in Figure 6(a). It was clear that the daily escape latency of TBI+Vehicle group was significantly longer than sham group ($P < 0.05$), indicating that rat learning function was impaired by TBI. TBI+SEW group showed a much shorter latency than TBI+Vehicle group ($P < 0.05$), suggesting that administration of SEW2871 improved the impaired learning performance after TBI. In addition, the rats in TBI+SEW+U0126 group spent longer escape latency searching the hidden platform compared with rats in TBI+SEW group ($P < 0.05$). Moreover, the latency of TBI+VPC+ERN group was obviously less than that of TBI+VPC group ($P < 0.05$). These data implied that S1PR1-mediated learning function was affected by MEK/Erk activity after TBI.

In probe trails, platform crossing times and duration spent in target quadrant at 28 days after injury were shown in Figures 6(b) and 6(c), respectively. These two indexes of TBI+Vehicle group were less than those of sham group ($P < 0.05$). Compared with TBI+Vehicle group, rats in TBI+SEW group exhibited better performance in probe trails ($P < 0.05$). In addition, TBI+SEW+U0126 group presented evidently decreased times and duration compared to TBI+SEW group ($P < 0.05$). Furthermore, the platform crossing times and target quadrant duration of TBI+VPC+ERN group were significant below those of TBI+SEW group ($P < 0.05$). Taken together, the above data indicated that S1PR1 activation improved memory impairment caused by TBI via MEK/Erk pathway.

In visible platform trials, all rats swam and found the platform normally. The average swimming speed of the rats in each group was 19.34±0.77 cm/s, 18.15±1.24 cm/s, 18.88± 1.64 cm/s, 18.90 ± 1.82 cm/s, 18.51 ± 3.08 cm/s, and 17.73 ± 0.90 cm/s, respectively (Figure 6(d)); the difference between groups did not reach a statistically significant level ($P > 0.05$). This data indicated that rat swimming speed of each group was at the same level, suggesting that the swimming speed exerted no impact on the above results in MWM test. In addition, the statistic difference between TBI+SEW group and sham group in the above trails was not observed ($P > 0.05$) (Figure 6), further implying that activation of S1PR1 facilitated learning and memory recovery after TBI.

4. Discussion

Increasing evidence suggests that brain injury is capable of stimulating hippocampal NSCs to divide and generate new neurons for repairing [3, 7]. However, the level of hippocampal neurogenesis after TBI is inadequate to meet the needs of injury repairing and neurological function recovery [3, 6]. Thus, it is valuable to effectively boost neurogenesis for traumatic brain rehabilitation by uncovering the potential molecule and the underlying mechanisms. The present study pointed out that activation of S1PR1 improved rat hippocampal neurogenesis via MEK/Erk signaling pathway after TBI. Initially, we confirmed that TBI could trigger NSCs proliferation and neuronal differentiation in hippocampus. Afterwards, we found that S1PR1 activation further promoted the hippocampal neurogenesis induced by TBI, and the enhancement could be attenuated by the antagonism of S1PR1. Moreover, it was revealed that MEK and Erk phosphorylation was activated in the S1PR1-mediated neurogenesis after TBI. Inhibition of MEK/Erk abolished the neurogenesis improved by S1PR1 activation. Reversely, the unfavorable effect of S1PR1 antagonism on posttraumatic neurogenesis and cognition recovery was rescued by the activation of MEK/Erk.

Recent studies demonstrated that S1PR1 was highly expressed in NSCs, and S1PR1 activation was involved in NSCs migration induced by high S1P concentration *in vitro* [14, 15]. In particular, S1PR1 contributed much to the migration of transplanted NSCs toward the injured site of spinal cord [15]. The study by Harada et al. suggested that S1P was essential for NSCs proliferation and morphological changes during brain development, but the subtype of S1PRs family contributed to S1P-induced NSCs activity was not clearly defined [16]. According to [35S]GTPγS autoradiography map of embryonic brain, the authors speculated that S1P1 might be the subtype receptor mediating the effect of S1P on NSCs proliferation and morphological changes [16]. In addition, it has been documented that S1PR1 is expressed abundantly in both hippocampus and SVZ, which are two specific regions responsible for neurogenesis throughout life in rodent brain [13, 28]. However, the effect of S1PR1 on endogenous NSCs properties in hippocampus after CNS trauma remains poorly understood.

In this study, it was shown that S1PR1 expression in hippocampus increased significantly with a maximal level at 7 days and remained at a higher level than sham at 28 days after TBI. Hippocampal NSCs proliferation after TBI also peaked at 7 days after trauma, as demonstrated in numerous previous studies [3, 29, 30]. Accordingly, it can be considered that TBI-induced neurogenesis might correlate with the upregulation of S1PR1 protein in hippocampus. More importantly, through

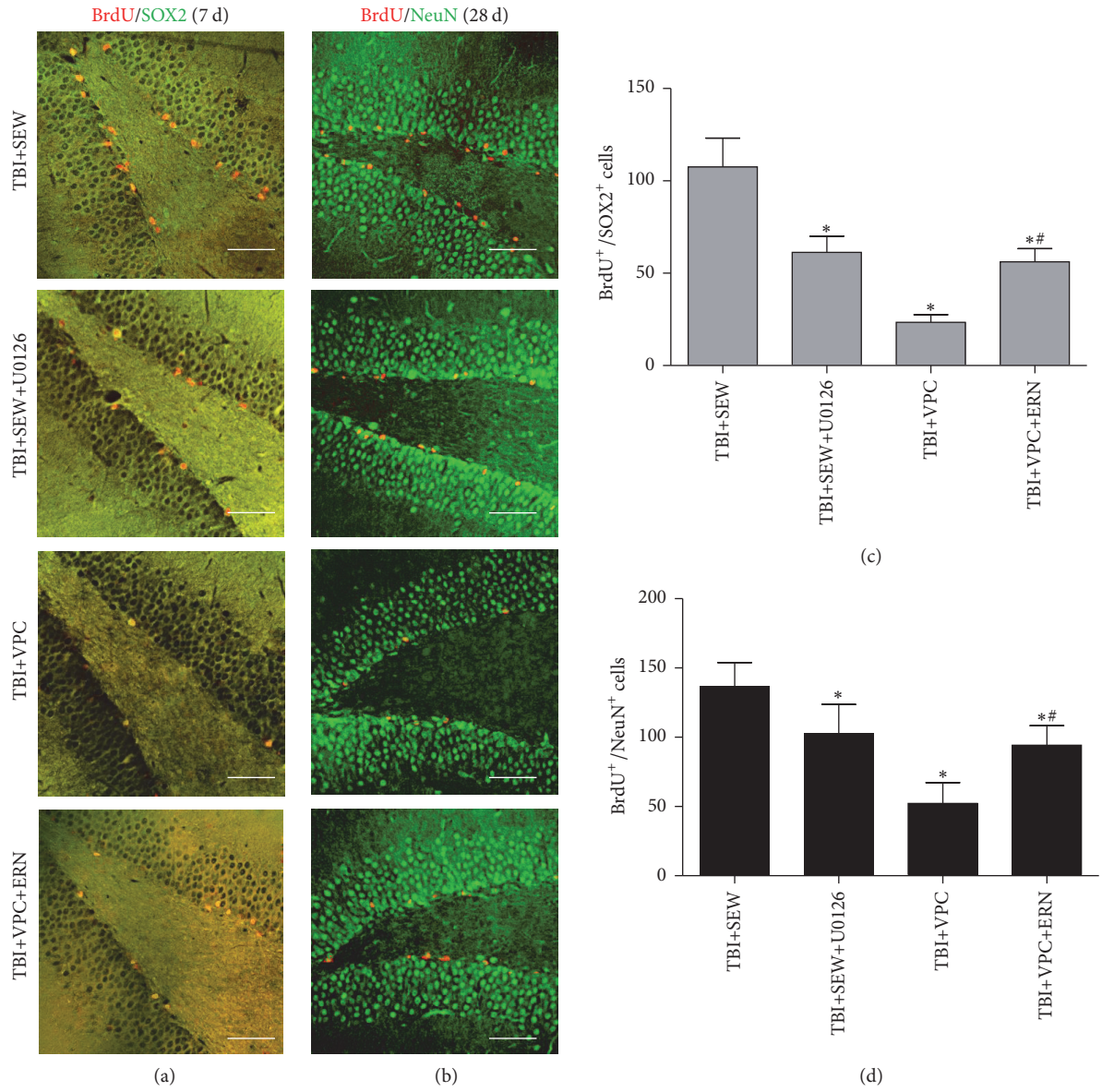

Figure 5: S1PR1-induced NSCs proliferation and neuronal differentiation in TBI rats were affected by MEK/Erk activity. (a, b) Representative IF microphotographs of hippocampus immunolabeled with BrdU/SOX2 and BrdU/NeuN in TBI+SEW, TBI+SEW+U0126, TBI+VPC, and TBI+VPC+ERN groups at 7 days and 28 days after trauma ($n = 6$ in each group). (c, d) Statistical analysis showed that, compared to TBI+SEW group, administration of U0126 significantly decreased the number of BrdU+/SOX2+ cells and BrdU+/NeuN+ cells in TBI+SEW+U0126 group. Reversely, the double-labeled cells in TBI+VPC+ERN group were significantly increased compared with TBI+VPC group. Scale bar: 50 μm. $^{*}P < 0.05$ versus TBI+SEW group; $^{\#}P < 0.05$ versus TBI+VPC group.

i.p. administration of S1PR1 agonist in rats, we found the activated S1PR1 could further promote NSCs proliferation and neuronal differentiation in hippocampus after TBI, and the effect was abolished by antagonism of S1PR1. These results indicated that S1PR1 activation facilitated posttraumatic neurogenesis in hippocampus, which might provide a clue to develop new strategies for brain repairing and functional recovery after TBI.

In several previous studies, it was well acknowledged that MEK/Erk cascade was critical for the activation of transcription factors and genes to regulate NSCs proliferation and differentiation, as well as the maturation of NSCs-derived neuronal cells [18, 31, 32]. Recently, growing researches have demonstrated an involvement of MEK/Erk cascade in neurogenesis induced by diverse growth factors, such as neurotrophin-3 and vascular endothelial growth factor (VEGF) [33–35]. Particularly, Ge and his colleagues found that MEK/Erk pathway was required for the neuronal differentiation but not for the oligodentrocytic differentiation of NSCs induced by poly-L-ornithine *in vitro* [36]. Furthermore, MEK/Erk pathway has been reported to play protective roles for neurons survival in DG [17, 32] and also contribute to the antiapoptotic effect of S1PR1 on neurons in injured cortex after cerebral ischemia [19].

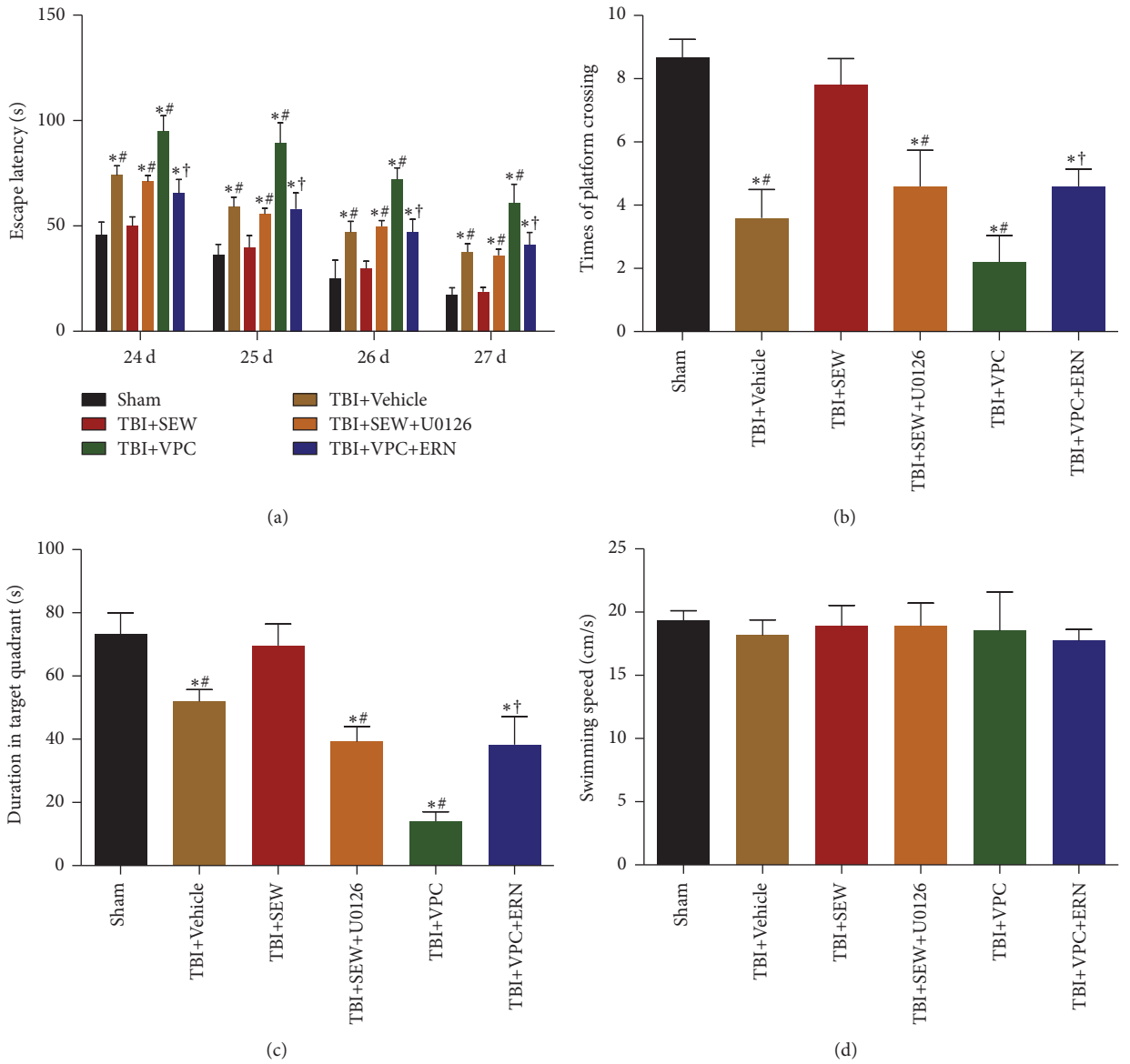

Figure 6: Cognitive function of rats in sham, TBI+Vehicle, TBI+SEW, TBI+SEW+U0126, TBI+VPC, and TBI+VPC+ERN group ($n = 3$ in sham and $n = 5$ in other groups) were evaluated by Morris water maze (MWM) test. (a) Escape latency in hidden platform trial exhibited a gradual reduction tendency from 24 to 27 days after trauma. Daily escape latency of TBI+Vehicle group was longer than that of sham group. Use of S1PR1 agonist in TBI+SEW group significantly shorten the latency, but the effect was eliminated in TBI+SEW+U0126 group. In addition, the escape latency of TBI+VPC+ERN group decreased compared with TBI+VPC group. (b, c) Platform crossing times and target quadrant duration in probe trial revealed that, relative to sham group, TBI+Vehicle group presented less times and shorter duration at 28 days after TBI. S1PR1 activation significantly increased the two indexes of TBI+SEW group, but the favorable effect was blocked by U0126 treatment in TBI+SEW+U0126 group. Moreover, the times of platform crossing and duration in target quadrant of TBI+VPC group were lower than those of TBI+VPC+ERN group. (d) Rat swimming speed of the six groups did not show any statistical difference. $^{*}P < 0.05$ versus sham group; $^{\#}P < 0.05$ versus TBI+SEW group, $^{\dagger}P < 0.05$ versus TBI+VPC group.

In this study, it was observed that the levels of hippocampal S1PR1, pMEK, and pErk in TBI group were higher at 7 days after trauma compared with sham group, and that activation of S1PR1 by SEW2871 further increased the hippocampal pMEK and pErk expression. Consistently, this effect could be eliminated by antagonism of S1PR1. The results implied that a potential association might exist between S1PR1 activation and MEK/Erk cascade phosphorylation in hippocampal neurogenesis after TBI. In addition to our findings, other studies have shown that the upregulated expression of pErk at 8 hours, 1 day, and even 14 days after CNS injury also played a positive role in hippocampal neurogenesis [31, 32, 37]. Accordingly, these evidences collectively provided an insight into the regulatory role of MEK/Erk signaling in neurogenesis after TBI.

Moreover, MEK/Erk pathway has been implicated in S1P-associated survival and proliferation of human embryonic stem cells, though the subtype of S1PRs accounting for

the process remains to be determined [38]. In our study, following administration of MEK/Erk inhibitor in TBI rats, a significant decrease of the proliferation and neuronal differentiation of NSCs was observed in hippocampus, indicating that MEK/Erk signaling pathway was indeed essential for S1PR1-mediated hippocampal neurogenesis after TBI. However, the underlying mechanisms in which S1PR1 triggers the phosphorylation of MEK and Erk in posttraumatic neurogenesis require further investigation.

It was noteworthy that a lot of past studies highlighted the influence of MEK/Erk pathway on NSCs properties such as proliferation and survival, whereas the effect of MEK/Erk on NSCs differentiation in hippocampal neurogenesis after TBI was not fully elaborated [16, 18, 35]. In the present study, besides probing the involvement of MEK/Erk signaling in S1PR1-associated NSCs proliferation, we extended our investigation on the role of MEK/Erk cascade in S1PR1-associated neuronal differentiation of NSCs at 28 days after TBI. The data showed that S1PR1 agonist via i.p. injection significantly increased the number of NSCs-derived newborn neurons in DG. And inhibition of MEK/Erk signaling resulted in a marked suppression in the S1PR1-induced neuronal differentiation of NSCs. Moreover, activation of MEK/Erk restored the diminished hippocampal neurogenesis caused by S1PR1 antagonist after TBI. Therefore, it can be inferred that activation of S1PR1 enhances hippocampal NSCs differentiate into neurons though MEK/Erk pathway after TBI. However, the precise downstream cascade of MEK/Erk responsible for S1PR1-meidated NSCs differentiation remains elusive. Most recently, quite a few evidences pointed out that cAMP-response element binding protein (CREB) was the principal downstream target of MEK/Erk signaling to regulate hippocampal plasticity [35, 37, 39]. Our research team is on the way to explore the presumed role of MEK/Erk/CREB cascade in multidirectional differentiation of NSCs induced by S1PR1.

As the paramount structure of limbic system, hippocampus links closely to cognitive and behavioral formation, which is easily impaired by brain injury [40]. Accumulative evidence supported that the newborn neurons in the posttraumatic neurogenesis could functionally integrate into the injured neural network and facilitate hippocampus-dependent neurocognitive recovery [6, 7, 41]. It has been reported that S1PR1 activation was in a position to ameliorate hippocampal damage and spatial memory deficits of Alzheimer's disease rats [42]. In addition, a recent study revealed that a known S1PRs agonist, FTY720, could ameliorate sevoflurane-induced neurocognitive impairment by distinctively binding to S1PR1 and activating the downstream pathway [43]. These findings indicated that the activity of S1PR1 indeed correlated with hippocampus-dependent cognitive function in a variety of neurological diseases, such as neurotoxicity and neurodegeneration [42, 43]. Here, we found that the learning and memory performance was improved by S1PR1 activation in neurotrauma, inhibition of MEK/Erk cascade worsened the learning and memory performance elicited by S1PR1 agonist after TBI. Furthermore, the adverse effect of S1PR1 antagonism on neurocognition after TBI was meliorated by MEK/Erk activation. It indicates that MEK/Erk signaling pathway is critical to S1PR1-mediated hippocampal neurogenesis for posttraumatic neurocognitive recovery.

5. Conclusion

In summary, our results indicated that S1PR1 produced a favorable effect of activation on NSCs proliferation and neuronal differentiation in hippocampus after TBI, and MEK/Erk signaling pathway played a key role in the S1PR1-mediated hippocampal neurogenesis. In the future, a deep exploration into the underlying mechanism will be required before S1PR1 was considered as a promising target for strategies to promote hippocampal neurogenesis for TBI repairing.

Competing Interests

The authors declare that there is no conflict of interests regarding the publication of this paper.

Authors' Contributions

Yuqin Ye, Zhenyu Zhao, Hongyu Xu, and Xin Zhang contributed equally to this work.

Acknowledgments

The present work was supported by grants from the National Natural Science Foundation of China (81171155 and 81471264) and Scientific Research Foundation of Hunan Provincial Education Department (13B067). The authors would like to thank Dr. Chen Chen from Department of Psychology and Dr. Jing Chang from Department of Biochemistry and Molecular Biology for their technical support throughout the study.

References

[1] R. Ślusarz, R. Jabłońska, A. Królikowska et al., "Measuring scales used for assessment of patients with traumatic brain injury: multicenter studies," *Patient Preference and Adherence*, vol. 9, pp. 869–875, 2015.

[2] D. J. Sharp, G. Scott, and R. Leech, "Network dysfunction after traumatic brain injury," *Nature Reviews Neurology*, vol. 10, no. 3, pp. 156–166, 2014.

[3] L. E. Villasana, K. N. Kim, G. L. Westbrook, and E. Schnell, "Functional integration of adult-born hippocampal neurons after traumatic brain injury," *Eneuro*, vol. 2, no. 5, Article ID 0056-15, 2015.

[4] D. K. Ma, M. A. Bonaguidi, G.-L. Ming, and H. Song, "Adult neural stem cells in the mammalian central nervous system," *Cell Research*, vol. 19, no. 6, pp. 672–682, 2009.

[5] M. Yamaguchi, T. Seki, I. Imayoshi et al., "Neural stem cells and neuro/gliogenesis in the central nervous system: understanding the structural and functional plasticity of the developing, mature, and diseased brain," *Journal of Physiological Sciences*, vol. 66, no. 3, pp. 179–206, 2016.

[6] T.-S. Yu, P. M. Washington, and S. G. Kernie, "Injury-induced neurogenesis: mechanisms and relevance," *Neuroscientist*, vol. 22, no. 1, pp. 61–71, 2016.

[7] R. M. Richardson, D. Sun, and M. R. Bullock, "Neurogenesis After Traumatic Brain Injury," *Neurosurgery Clinics of North America*, vol. 18, no. 1, pp. 169–181, 2007.

[8] H. Okano, "Adult neural stem cells and central nervous system repair," *Ernst Schering Research Foundation Workshop*, no. 60, pp. 215–228, 2006.

[9] M.-J. Lee, J. R. Van Brocklyn, S. Thangada et al., "Sphingosine-1-phosphate as a ligand for the G protein-coupled receptor EDG-1," *Science*, vol. 279, no. 5356, pp. 1552–1555, 1998.

[10] H. Nishimura, T. Akiyama, I. Irei, S. Hamazaki, and Y. Sadahira, "Cellular localization of sphingosine-1-phosphate receptor 1 expression in the human central nervous system," *Journal of Histochemistry and Cytochemistry*, vol. 58, no. 9, pp. 847–856, 2010.

[11] R. E. Toman and S. Spiegel, "Lysophospholipid receptors in the nervous system," *Neurochemical Research*, vol. 27, no. 7-8, pp. 619–627, 2002.

[12] S. Milstien, D. Gude, and S. Spiegel, "Sphingosine 1-phosphate in neural signalling and function," *Acta Paediatrica*, vol. 96, no. 455, pp. 40–43, 2007.

[13] C. McGiffert, J. J. A. Contos, B. Friedman, and J. Chun, "Embryonic brain expression analysis of lysophospholipid receptor genes suggests roles for s1p1 in neurogenesis and s1p1-3 in angiogenesis," *FEBS Letters*, vol. 531, no. 1, pp. 103–108, 2002.

[14] A. Kimura, T. Ohmori, Y. Kashiwakura et al., "Antagonism of sphingosine 1-phosphate receptor-2 enhances migration of neural progenitor cells toward an area of brain infarction," *Stroke*, vol. 39, no. 12, pp. 3411–3417, 2008.

[15] A. Kimura, T. Ohmori, R. Ohkawa et al., "Essential roles of sphingosine 1-phosphate/S1P1 receptor axis in the migration of neural stem cells toward a site of spinal cord injury," *Stem Cells*, vol. 25, no. 1, pp. 115–124, 2007.

[16] J. Harada, M. Foley, M. A. Moskowitz, and C. Waeber, "Sphingosine-1-phosphate induces proliferation and morphological changes of neural progenitor cells," *Journal of Neurochemistry*, vol. 88, no. 4, pp. 1026–1039, 2004.

[17] Y. N. Zhao, J. M. Li, Q. Q. Tang et al., "Regulation of extracellular signal-regulated kinase 1/2 influences hippocampal neuronal survival in a rat model of diabetic cerebral ischemia," *Neural Regeneration Research*, vol. 9, no. 7, pp. 749–756, 2014.

[18] N. Shioda, F. Han, and K. Fukunaga, "Role of Akt and Erk signaling in the neurogenesis following brain ischemia," *International Review of Neurobiology*, vol. 85, pp. 375–387, 2009.

[19] Y. Hasegawa, H. Suzuki, T. Sozen, W. Rolland, and J. H. Zhang, "Activation of sphingosine 1-phosphate receptor-1 by FTY720 is neuroprotective after ischemic stroke in rats," *Stroke*, vol. 41, no. 2, pp. 368–374, 2010.

[20] A. S. Awad, H. Ye, L. Huang et al., "Selective sphingosine 1-phosphate 1 receptor activation reduces ischemia-reperfusion injury in mouse kidney," *American Journal of Physiology-Renal Physiology*, vol. 290, no. 6, pp. F1516–F1524, 2006.

[21] Z. Kolahdooz, S. Nasoohi, M. Asle-Rousta, A. Ahmadiani, and L. Dargahi, "Sphingosin-1-phosphate receptor 1: a potential target to inhibit neuroinflammation and restore the sphingosin-1-phosphate metabolism," *Canadian Journal of Neurological Sciences*, vol. 42, no. 3, pp. 195–202, 2015.

[22] G. Ashabi, M. Ramin, P. Azizi et al., "ERK and p38 inhibitors attenuate memory deficits and increase CREB phosphorylation and PGC-1α levels in Aβ-injected rats," *Behavioural Brain Research*, vol. 232, no. 1, pp. 165–173, 2012.

[23] J. V. Duncia, J. B. Santella III, C. A. Higley et al., "MEK inhibitors: the chemistry and biological activity of U0126, its analogs, and cyclization products," *Bioorganic and Medicinal Chemistry Letters*, vol. 8, no. 20, pp. 2839–2844, 1998.

[24] A. Melchini, M. H. Traka, S. Catania et al., "Antiproliferative activity of the dietary isothiocyanate erucin, a bioactive compound from cruciferous vegetables, on human prostate cancer cells," *Nutrition and Cancer*, vol. 65, no. 1, pp. 132–138, 2013.

[25] J. Jakubíková, J. Sedlák, R. Mithen, and Y. Bao, "Role of PI3K/Akt and MEK/ERK signaling pathways in sulforaphane- and erucin-induced phase II enzymes and MRP2 transcription, G2/M arrest and cell death in Caco-2 cells," *Biochemical Pharmacology*, vol. 69, no. 11, pp. 1543–1552, 2005.

[26] C. V. Vorhees and M. T. Williams, "Morris water maze: procedures for assessing spatial and related forms of learning and memory," *Nature Protocols*, vol. 1, no. 2, pp. 848–858, 2006.

[27] D. G. Amaral, H. E. Scharfman, and P. Lavenex, "The dentate gyrus: fundamental neuroanatomical organization (dentate gyrus for dummies)," *Progress in Brain Research*, vol. 163, pp. 3–22, 2007.

[28] D. H. Lee, B. T. Jeon, E. A. Jeong et al., "Altered expression of sphingosine kinase 1 and sphingosine-1-phosphate receptor 1 in mouse hippocampus after kainic acid treatment," *Biochemical and Biophysical Research Communications*, vol. 393, no. 3, pp. 476–480, 2010.

[29] Y. Ye, H. Xu, X. Zhang et al., "Association between toll-like receptor 4 expression and neural stem cell proliferation in the hippocampus following traumatic brain injury in mice," *International Journal of Molecular Sciences*, vol. 15, no. 7, pp. 12651–12664, 2014.

[30] S. Chirumamilla, D. Sun, M. R. Bullock, and R. J. Colello, "Traumatic brain injury induced cell proliferation in the adult mammalian central nervous system," *Journal of Neurotrauma*, vol. 19, no. 6, pp. 693–703, 2002.

[31] N. Shioda, F. Han, M. Morioka, and K. Fukunaga, "Bis(1-oxy-2-pyridinethiolato)oxovanadium(IV) enhances neurogenesis via phosphatidylinositol 3-kinase/Akt and extracellular signal regulated kinase activation in the hippocampal subgranular zone after mouse focal cerebral ischemia," *Neuroscience*, vol. 155, no. 3, pp. 876–887, 2008.

[32] G. Umschweif, S. Liraz-Zaltsman, D. Shabashov et al., "Angiotensin receptor type 2 activation induces neuroprotection and neurogenesis after traumatic brain injury," *Neurotherapeutics*, vol. 11, no. 3, pp. 665–678, 2014.

[33] M. Ohtsuka, H. Fukumitsu, and S. Furukawa, "Neurotrophin-3 stimulates neurogenetic proliferation via the extracellular signal-regulated kinase pathway," *Journal of Neuroscience Research*, vol. 87, no. 2, pp. 301–306, 2009.

[34] K.-T. Lu, C.-L. Sun, P. Y. Y. Wo et al., "Hippocampal neurogenesis after traumatic brain injury is mediated by vascular endothelial growth factor receptor-2 and the Raf/MEK/ERK cascade," *Journal of Neurotrauma*, vol. 28, no. 3, pp. 441–450, 2011.

[35] N. M. Fournier, B. Lee, M. Banasr, M. Elsayed, and R. S. Duman, "Vascular endothelial growth factor regulates adult hippocampal cell proliferation through MEK/ERK- and PI3K/Akt-dependent signaling," *Neuropharmacology*, vol. 63, no. 4, pp. 642–652, 2012.

[36] H. Ge, L. Tan, P. Wu et al., "Poly-L-ornithine promotes preferred differentiation of neural stem/progenitor cells via ERK signalling pathway," *Scientific Reports*, vol. 5, Article ID 15535, 2015.

[37] K.-T. Lu, T.-C. Huang, J.-Y. Wang et al., "NKCC1 mediates traumatic brain injury-induced hippocampal neurogenesis through CREB phosphorylation and HIF-1α expression," *Pflügers Archiv European Journal of Physiology*, vol. 467, no. 8, pp. 1651–1661, 2015.

[38] K. Avery, S. Avery, J. Shepherd, P. R. Heath, and H. Moore, "Sphingosine-1-phosphate mediates transcriptional regulation of key targets associated with survival, proliferation, and pluripotency in human embryonic stem cells," *Stem Cells and Development*, vol. 17, no. 6, pp. 1195–1205, 2008.

[39] K. Merz, S. Herold, and D. C. Lie, "CREB in adult neurogenesis—master and partner in the development of adult-born neurons?" *European Journal of Neuroscience*, vol. 33, no. 6, pp. 1078–1086, 2011.

[40] H. van Praag, A. F. Schinder, B. R. Christle, N. Toni, T. D. Palmer, and F. H. Gage, "Functional neurogenesis in the adult hippocampus," *Nature*, vol. 415, no. 6875, pp. 1030–1034, 2002.

[41] R. A. Kohman and J. S. Rhodes, "Neurogenesis, inflammation and behavior," *Brain, Behavior, and Immunity*, vol. 27, no. 1, pp. 22–32, 2013.

[42] M. Asle-Rousta, S. Oryan, A. Ahmadiani, and M. Rahnema, "Activation of sphingosine 1-phosphate receptor-1 by SEW2871 improves cognitive function in Alzheimer's disease model rats," *EXCLI Journal*, vol. 12, pp. 449–461, 2013.

[43] H. Zhou, S. Li, X. Niu, P. Wang, J. Wang, and M. Zhang, "Protective effect of FTY720 against sevoflurane-induced developmental neurotoxicity in rats," *Cell Biochemistry and Biophysics*, vol. 67, no. 2, pp. 591–598, 2013.

Hindawi Publishing Corporation
Neural Plasticity
Volume 2016, Article ID 8928530, 12 pages
http://dx.doi.org/10.1155/2016/8928530

Research Article

ATP Induces Disruption of Tight Junction Proteins via IL-1 Beta-Dependent MMP-9 Activation of Human Blood-Brain Barrier *In Vitro*

Fuxing Yang,[1,2] Kai Zhao,[1] Xiufeng Zhang,[1,3] Jun Zhang,[1] and Bainan Xu[1]

[1]*Department of Neurosurgery, Chinese PLA General Hospital, 28 Fuxing Road, Haidian District, Beijing 100853, China*
[2]*Department of Neurosurgery, 2nd Affiliated Hospital of Fujian Medical University, 34 Zhongshan Northern Road, Quanzhou 362000, China*
[3]*Medical College, Nankai University, 94 Weijin Road, Tianjin 300071, China*

Correspondence should be addressed to Jun Zhang; junzhang301@163.com and Bainan Xu; xbn301@126.com

Received 21 June 2016; Revised 29 August 2016; Accepted 8 September 2016

Academic Editor: Fushun Wang

Disruption of blood-brain barrier (BBB) follows brain trauma or central nervous system (CNS) stress. However, the mechanisms leading to this process or the underlying neural plasticity are not clearly known. We hypothesized that ATP/P2X7R signaling regulates the integrity of BBB. Activation of P2X7 receptor (P2X7R) by ATP induces the release of interleukin-1β (IL-1β), which in turn enhances the activity of matrix metalloproteinase-9 (MMP-9). Degradation of tight junction proteins (TJPs) such as ZO-1 and occludin occurs, which finally contributes to disruption of BBB. A contact coculture system using human astrocytes and hCMEC/D3, an immortalized human brain endothelial cell line, was used to mimic BBB *in vitro*. Permeability was used to evaluate changes in the integrity of TJPs. ELISA, Western blot, and immunofluorescent staining procedures were used. Our data demonstrated that exposure to the photoreactive ATP analog, 3′-O-(4-benzoyl)benzoyl adenosine 5′-triphosphate (BzATP), induced a significant decrease in ZO-1 and occludin expression. Meanwhile, the decrease of ZO-1 and occludin was significantly attenuated by P2X7R inhibitors, as well as IL-1R and MMP antagonists. Further, the induction of IL-1β and MMP-9 was closely linked to ATP/P2X7R-associated BBB leakage. In conclusion, our study explored the mechanism of ATP/P2X7R signaling in the disruption of BBB following brain trauma/stress injury, especially focusing on the relationship with IL-1β and MMP-9.

1. Introduction

Traumatic brain injury (TBI) often coexists with acute stress disorder (ASD) or post-traumatic stress disorder (PTSD) [1]. TBI is one of the major health problems that account for high mortality worldwide. According to the World Health Organization, TBI is expected to become the third leading cause of death and disability worldwide by 2020 [2]. TBI/PTSD or TBI/ASD are public health concerns warranting advanced investigation into the underlying mechanisms for appropriate therapeutic intervention [3]. Disruption of blood-brain barrier (BBB) is a common result following brain trauma/stress injury, and little is known about the changes in neural plasticity following brain injury and subsequent cellular responses. Currently, there is no effective neuroprotective agent that is available clinically, to prevent the damage to BBB following CNS trauma/stress injury [4, 5].

Extracellular ATP, which is dramatically increased after acute injury or stress to the central nervous system, is considered an initiator of secondary brain injury by activating a wide variety of purinergic receptors [6]. P2X7 is a unique purinergic receptor. In addition to the rapid opening of the cation channels, with prolonged exposure to high concentrations of ATP, it triggers a membrane pore facilitating the passage of large molecules, which suggests that P2X7 receptors may play a crucial role in the pathophysiology of brain trauma [7, 8]. It is reported that activation of P2X7 receptor resulted in the release of IL-1β [9, 10], which is an important proinflammatory cytokine. Furthermore, activation of IL-1β leads to the production of MMP-9 [11], which affects the

tight junction proteins including ZO-1, and in turn, leads to disruption of blood-brain barrier [12, 13]. Overall, the ATP/P2X7R signaling pathway may be implicated in the process of BBB leakage following CNS trauma/stress injury. However, the underlying physiologic mechanisms following ATP-associated BBB damage and their relationship with IL-1β and MMP-9 are still unknown.

In this study, we used a coculture model *in vitro* comprising an immortal human cell line hCMEC/D3 expressing endothelial and BBB markers and human astrocytes to investigate the role of ATP/P2X7R signaling in the disruption of tight junction proteins [14]. We demonstrated that ATP/P2X7R signaling regulates the integrity of BBB. Activation of P2X7 receptor by ATP induces the release of IL-1β, which in turn enhances the production of MMP-9, leading to degradation of tight junction proteins, such as ZO-1 and occludin, resulting in the disruption of BBB.

2. Materials and Methods

2.1. Materials. Human astrocytes (HAs) were obtained from Jiamay Biolab (Beijing, China); hCMEC/D3 cell lines were purchased from Jiangyin Yuxi Biotechnology (Jiangsu, China); polyclonal anti-ZO-1 and anti-occludin antibodies were acquired from Biorbyt (Cambridge, UK, cat: orb11587, orb11181); Alexa Fluor 594-conjugated AffiniPure donkey anti-rabbit IgG was obtained from Jackson ImmunoResearch Inc. (West Grove, PA, USA, cat: 711-585-152); human interleukin-1β ELISA kit and human MMP-9 ELISA kit were purchased from Jiamay (Beijing, China, cat: FHK0016, FHK0144); high glucose Dulbecco's Modified Eagle's Medium (DMEM) basal medium was obtained from Hyclone (Logan, UT, United States); and EBM-2 basal medium was purchased from Lonza (Walkersville, MD, USA). Fetal bovine serum (FBS) was obtained from GIBCO (Rockville, MD, USA); phenylmethanesulfonyl fluoride (PMSF) was acquired from Amresco (Solon, OH, USA); the different cocktails were purchased from Yuanye Biotech (Shanghai, China); skimmed milk was obtained from Yili Industrial Group Co. Ltd. (Beijing, China); and anti-β-actin and other materials were purchased from Jiamay Biolab (Beijing, China).

2.2. In Vitro Model of Human BBB. The hCMEC/D3 cells and HAs were cultured as described in a previous study [15]. Briefly, hCMEC/D3 cells were cultured in EBM-2 basal medium supplemented with 5% FBS, growth factors, 100 U/mL of penicillin, and 100 μg/mL of streptomycin. HAs were cultured in high glucose DMEM supplemented with 10% FBS, 100 U/mL of penicillin, and 100 μg/mL streptomycin. Cells were maintained at 37°C in the presence of 5% CO_2.

The contact coculture model of hCMEC/D3 and astrocytes was used as an *in vitro* model of human BBB [16]. Briefly, HAs (5×10^3 cells/cm^2) were seeded externally on Transwell inserts (polyester membranes, 6.5 mm diameter, 0.4 μm pore size, Corning Costar) in an inverted position and allowed to adhere to the membrane overnight. After incubation, the hCMEC/D3 cells (2×10^5 cells/cm^2) were added to the interior of the inserts and both the cell layers were grown to confluence.

2.3. ELISA for IL-1β and MMP-9. Enzyme-linked immunosorbent assay (ELISA) was used to determine the levels of IL-1β and MMP-9. The hCMEC/D3 cells and HAs grown on Transwell insert were treated with A438079 (a selective P2X7 receptor antagonist, 10 μM), or IL-1RA (an IL-1R antagonist, which competitively blocked the binding to IL-1 receptors, 100 μg/mL), or batimastat (a MMP antagonist, 5 μM) 30 min prior to the addition of BzATP (100 μg/mL). The cells were exposed to photoreactive ATP analog, 3′-O-(4-benzoyl)benzoyl adenosine 5′-triphosphate (BzATP), for 2 h and their specific vehicles as control. After brief centrifugation, 100 μL of cell culture supernatant samples was analyzed using human IL-1β ELISA kit/human MMP-9 ELISA kit according to the manufacturer's instructions. Quantitative analysis was performed on a microplate reader (Thermo fisher, Multiskan MK3).

2.4. Permeability of the Coculture System. The hCMEC/D3 cells and HAs were cocultured on Transwell insert. Cells were pretreated with inhibitors (A438079 10 μM, or IL-1RA 100 μg/mL, or batimastat 5 μM) for 30 min followed by BzATP (100 μg/mL) for 2 h. To characterize the changes in structural integrity of BBB models *in vitro*, we measured the permeability of the coculture system to FITC-dextran, as reported in a previous study [17]. Fluorescein isothiocyanate-labeled dextran (FITC-dextran, 10 KDa, 10 μM) was added to the apical compartment. After 30 min, 100 μL of the medium was removed from the basal compartment. The fluorescence of the collected samples was measured at 485 nm/520 nm using a Fluorescence Microplate Reader (Thermo Fisher, Fluoroskan Ascent FL).

2.5. Immunofluorescence Staining of Tight Junction Proteins. After treatment with inhibitors (A438079 10 μM, or IL-1RA 100 μg/mL, or batimastat 5 μM) for 30 min prior to exposure to BzATP (100 μg/mL) for 2 h, cells were washed twice with PBS and fixed using 4% PFA at room temperature for 30 min. Excess PFA was removed with PBS three times. The cells were permeabilized with 0.1% Triton X-100 in PBS for 10 min. After washing three times with PBS, the cells were incubated with 3% H_2O_2 for 10 min, followed by PBS three times. After blocking for 30 min with 10% FBS and three times with PBS, cells were incubated with polyclonal anti-occludin antibody (1 : 200) or polyclonal anti-ZO-1 antibody (1 : 200) at 4°C overnight. Unbound antibodies were removed using PBS. Alexa Fluor 594-conjugated AffiniPure donkey anti-rabbit IgG (1 : 500) was used as a secondary antibody and incubated with cells for 2 h at room temperature. Similarly, unbound antibodies were removed with PBS. Analysis and imaging were performed using a confocal laser-scanning microscope (TSC-SP2, Leica, Germany).

2.6. Western Blot of Tight Junction Proteins. Western blot was used to detect the expressions of occludin and ZO-1. The hCMEC/D3 cells were washed with PBS and harvested

with 0.25% trypsin. The cells were suspended in 150 μL ice-cold RIPA lysis buffer, sonicated 10 times for 5 s with 10 s pauses in an ice-water bath, and centrifuged at 12,000 rpm for 5 min at 4°C. Protein quantity was detected using a BCA assay kit, and equal amounts of protein were used for Western blot analysis. Next, the protein was separated by SDS-PAGE and transferred to PVDF membranes using semidry methods. Membranes were blocked in TBST + 5% skimmed milk for 2 h at room temperature. Membranes were incubated overnight at 4°C with the primary antibodies: rabbit polyclonal anti-ZO-1 antibody (1 : 100) or polyclonal anti-occludin antibody (1 : 100). The membranes were washed for 10 min with TBST buffer three times. Immunoblots were processed with secondary antibodies (1 : 2000~1 : 5000) for 1 h at room temperature. β-Actin was blotted on the same membrane as the internal control. Blots were quantified using Image J software (NIH).

2.7. Statistical Analysis. All the experiments were repeated three times and similar results were obtained. Statistical analysis was performed by one-way ANOVA (multiple comparisons) using the SPSS 16.0 statistics software (SPSS, Chicago, IL). P value less than 0.05 was considered statistically significant.

3. Results

3.1. A438079 Attenuated BzATP-Induced Disruption of BBB In Vitro

3.1.1. Effect of BzATP/BzATP + A438079 on IL-1β and MMP-9 Induction. In this study, we investigated the effects of BzATP on the TJPs of blood-brain barrier and correlated the expression of IL-1β and MMP-9. First, we evaluated the role of BzATP in the induction of IL-1β and MMP-9. ELISA results showed that the levels of IL-1β and MMP-9 were significantly higher in the BzATP group than in the control group without BzATP ($P < 0.05$; Figures 1(a) and 1(b)). Second, A438079 treatment significantly attenuated the increase in IL-1β and MMP-9, compared with the vehicle group ($P < 0.05$, Figures 1(a) and 1(b)). Furthermore, administration of A438079 alone did not significantly affect the levels of IL-1β and MMP-9, compared with the blank control group ($P < 0.05$, Figures 1(a) and 1(b)).

3.1.2. Effect of A438079 on Permeability of Endothelial Coculture System. To determine the altered permeability of BBB model, we measured the fluorescence of FITC-dextran diffused through the coculture system. FITC-dextran (10 KDa, 10 μM) diffused across BBB from the apical to the basal compartment. The fluorescence intensity of samples collected basally was measured. As shown in Figure 1(c), exposure to BzATP significantly increased permeability to FITC-dextran compared with the control group ($P < 0.05$, Figure 1(c)). Inhibition of P2X7R abolished BzATP-induced paracellular permeability, while A438079 alone did not affect basal permeability levels ($P < 0.05$, Figure 1(c)).

3.1.3. Effect of A438079 on TJPs Degradation. In an attempt to determine whether ATP-induced increase in BBB permeability was due to the altered levels of TJPs, the protein expression of occludin and ZO-1 was evaluated via immunofluorescence staining and Western blot. As shown in Figure 2, BzATP-treated cells showed significantly decreased staining of ZO-1 and occludin, which was significantly attenuated by A438079. Furthermore, Western blot analysis confirmed the decrease in the expression of ZO-1 and occludin in BzATP groups compared with the controls. Treatment with A438079 enhanced the levels of ZO-1 and occludin compared with BzATP alone ($P < 0.05$, Figure 1(d)). The results of Western blot were similar to immunofluorescence staining of occludin and ZO-1 in the following experiments.

3.2. IL-1β Inhibition Attenuated BzATP-Induced Tight Junction Disruption and Endothelial Coculture Hyperpermeability

3.2.1. BzATP-Induced MMP-9 Induction Was Attenuated by IL-1RA. As discussed in Section 3.1.1, BzATP induced the release of IL-1β and MMP-9 in the BBB model. In order to correlate IL-1β and MMP-9, we designed two experiments (Sections 3.2 and 3.3), using their inhibitors, respectively. First, we investigated whether IL-1RA inhibited the BzATP-induced increase in MMP-9. As shown in Figure 3, IL-1RA treatment significantly attenuated the increase in MMP-9 levels triggered by BzATP compared with the vehicle group ($P < 0.05$, Figure 3(a)).

3.2.2. IL-1RA Attenuated Hyperpermeability of BzATP-Induced Endothelial Coculture System. Exposure to BzATP significantly increased the permeability to FITC-dextran compared with control group ($P < 0.05$, Figure 3(b)). IL-1RA attenuated BzATP-induced paracellular permeability. However, IL-1RA alone did not affect basal permeability levels ($P < 0.05$, Figure 3(b)).

3.2.3. BzATP-Induced TJP Disruption Was Attenuated by IL-1RA. Immunofluorescence staining showed that the expression of ZO-1 and occludin in BzATP groups was significantly decreased compared with controls, while treatment with IL-1RA and BzATP significantly increased the levels of the two tight junction proteins, indicating that the treatment reversed the degradation of TJPs (Figure 3(c)).

3.3. BzATP-Induced Tight Junction Disruption and Hyperpermeability of the Endothelial Coculture System Were Attenuated by MMP

3.3.1. BzATP-Induced IL-1β Induction Was Not Attenuated by MMP-9 Inhibition. ELISA showed that the levels of IL-1β were significantly higher in the BzATP-treated groups than in the control group without BzATP. However, batimastat treatment did not alter the level of IL-1β ($P > 0.05$, Figure 4(a)).

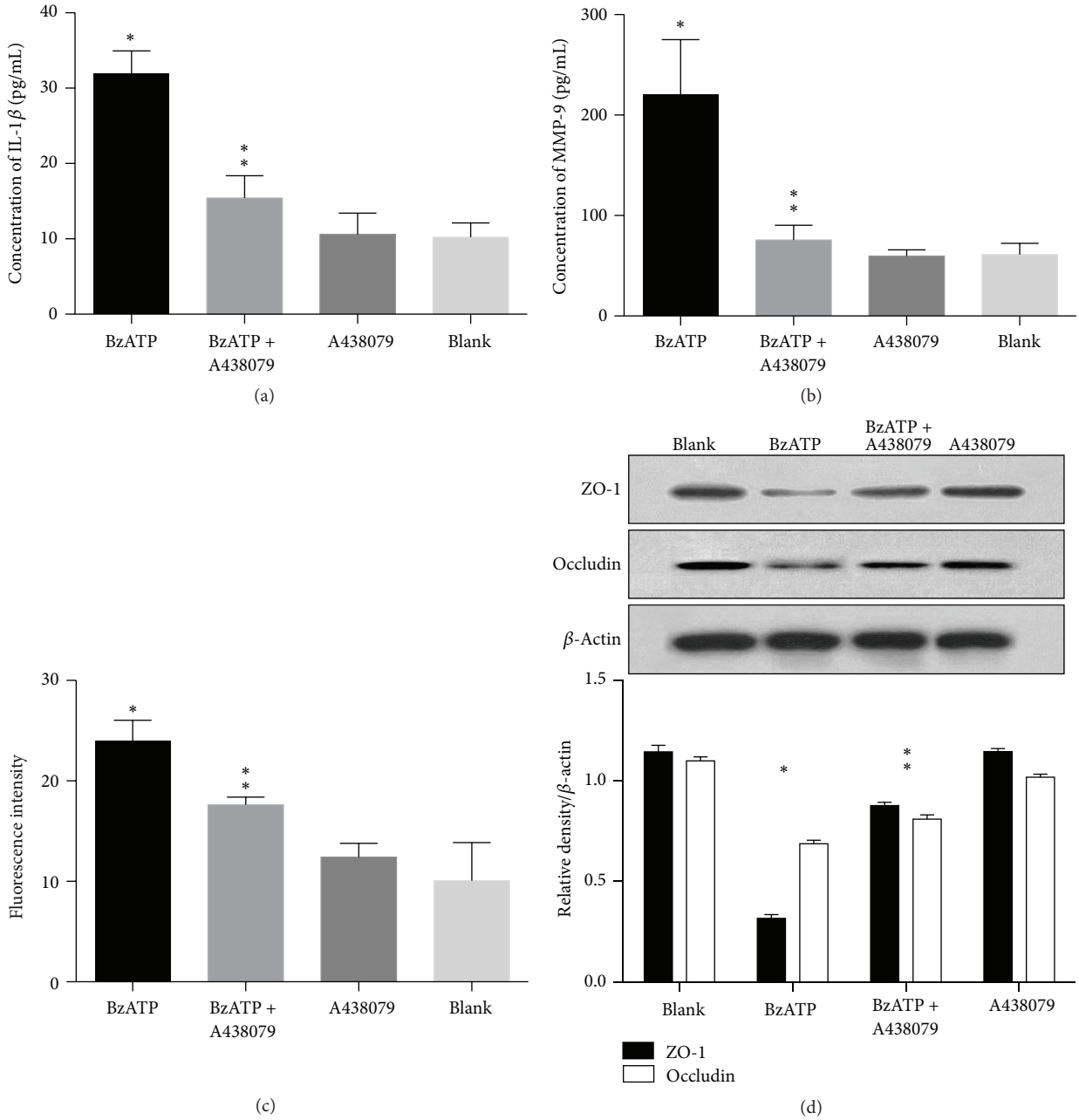

Figure 1: A438079 attenuates BzATP-induced disruption of blood-brain barrier *in vitro*. (a) The IL-1β level was significantly higher in BzATP groups than in control groups ($^{*}P < 0.05$). A438079 treatment significantly reduced the levels of IL-1β compared with the vehicle group ($^{**}P < 0.05$). (b) The level of MMP-9 was significantly higher in BzATP groups than in control groups ($^{*}P < 0.05$). A438079 treatment significantly reduced the level of MMP-9 compared with the vehicle group ($^{**}P < 0.05$). (c) BzATP induced hyperpermeability compared with the control groups ($^{*}P < 0.05$), which was decreased by the P2X7 inhibitor A438079 in the coculture system ($^{**}P < 0.05$). (d) Western blot analysis showed that the expression of ZO-1 and occludin in the BzATP groups was decreased compared with the controls ($^{*}P < 0.05$), while A438079 treatment significantly attenuated the disruptions of ZO-1 and occludin ($^{**}P < 0.05$).

3.3.2. MMP Inhibition Attenuated Hyperpermeability of BzATP-Induced Endothelial Coculture System. Exposure to BzATP significantly increased the permeability to FITC-dextran compared with the control group ($P < 0.05$, Figure 4(b)). Batimastat attenuated BzATP-induced paracellular permeability, while batimastat alone did not affect the basal permeability levels ($P < 0.05$, Figure 4(b)).

3.3.3. BzATP-Induced TJP Disruption Was Attenuated by MMP Inhibition. Immunofluorescence staining showed that

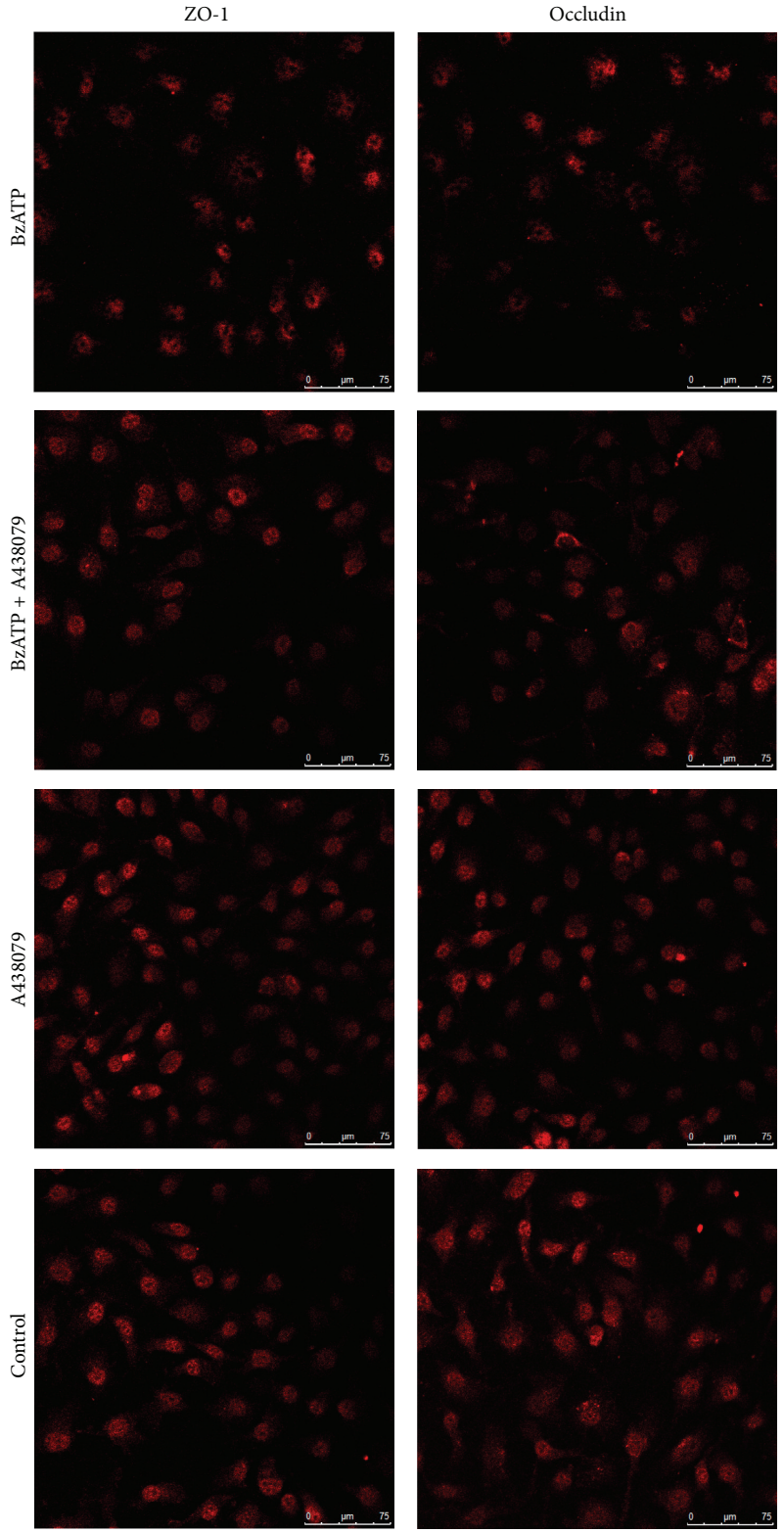

Figure 2: Confocal microscopy images of immunofluorescence staining of ZO-1 and occludin in hCMEC/D3 cells demonstrating the protective effect of A438079 against BzATP-induced tight junction disruption.

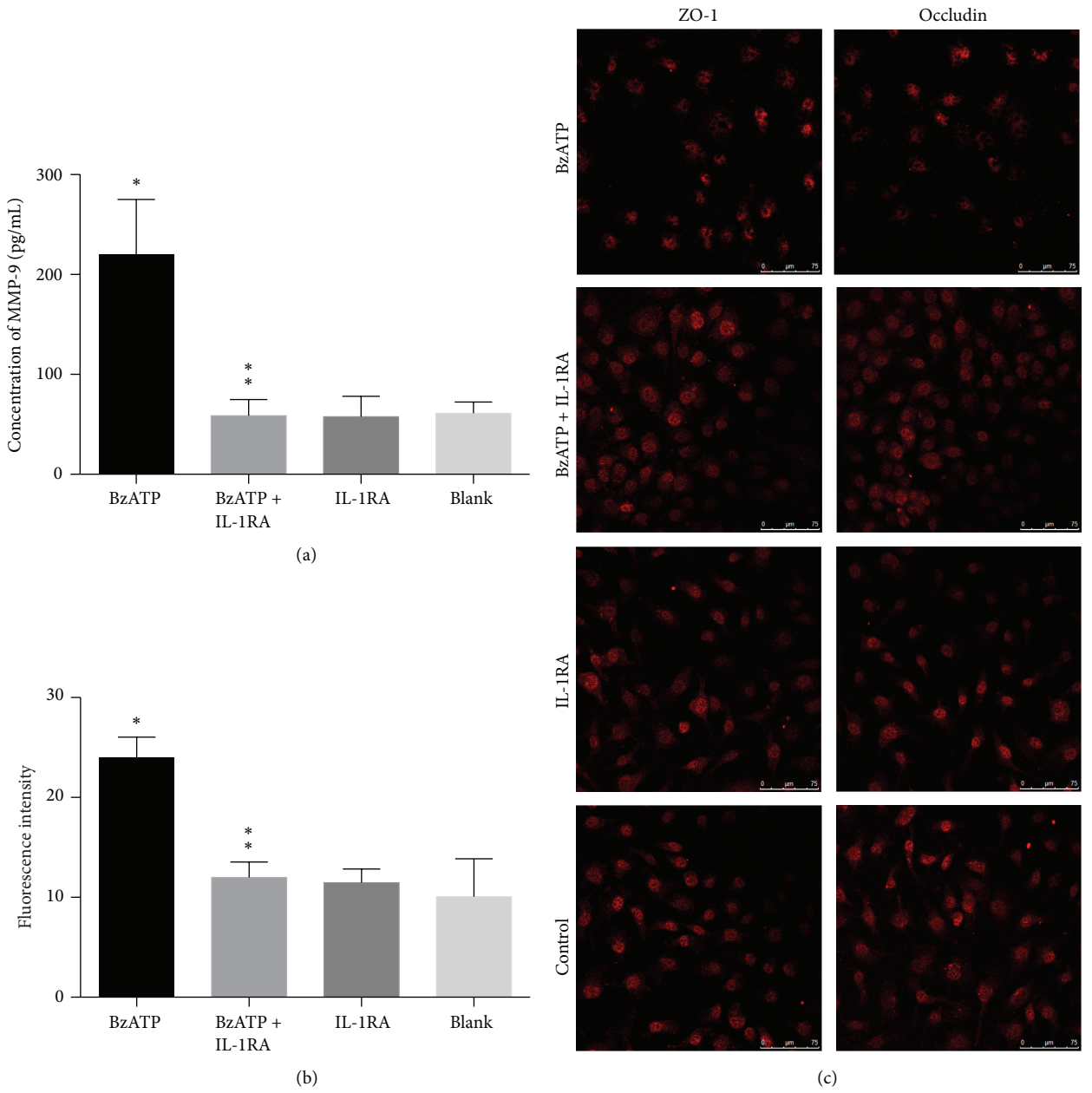

Figure 3: BzATP-induced tight junction disruption and hyperpermeability of endothelial coculture system were attenuated by IL-1β inhibition. (a) The levels of MMP-9 were significantly higher in the BzATP groups than in the control groups ($^{*}P < 0.05$). IL-1RA treatment significantly reduced the level of MMP-9 versus vehicle group ($^{**}P < 0.05$). (b) BzATP induces hyperpermeability versus control groups ($^{*}P < 0.05$), which was decreased by IL-1RA in the coculture system ($^{**}P < 0.05$). (c) Confocal microscopy images of immunofluorescence staining of ZO-1 and occludin demonstrating the protective effect of IL-1RA against BzATP-induced tight junction disruption.

the expression of ZO-1 and occludin in the BzATP group was significantly decreased compared with that of the controls. In contrast, treatment with batimastat combined with BzATP significantly increased the levels of the two tight junction proteins, indicating that batimastat treatment reversed the degradation of TJPs (Figure 4(c)).

3.4. IL-1β-Induced Tight Junction Disruption and Hyperpermeability of Endothelial Coculture System Were Attenuated by MMP-9 Inhibition

3.4.1. IL-1β-Induced MMP-9 Induction Was Attenuated by MMP-9 Inhibition. We investigated the association between

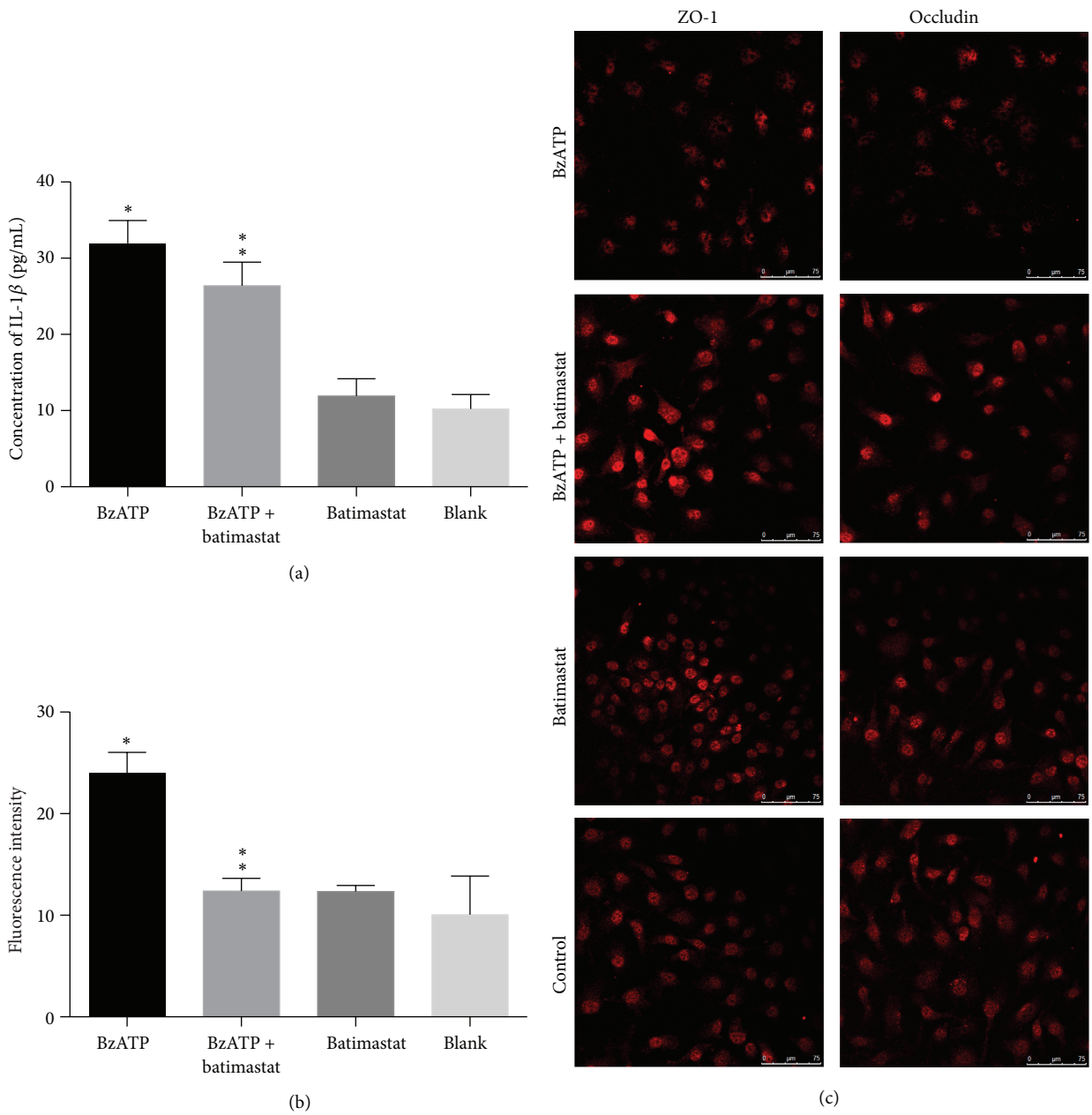

Figure 4: MMP-9-induced tight junction disruption and endothelial coculture system hyperpermeability were not attenuated by IL-1β inhibition. (a) The levels of IL-1β were significantly higher in BzATP groups than in control groups ($^{*}P < 0.05$). However, batimastat + BzATP treatment did not alter the level of IL-1β versus BzATP group ($^{**}P > 0.05$). (b) Exposure to BzATP significantly increased the permeability to FITC-dextran compared with the control groups ($^{*}P < 0.05$). Batimastat attenuated BzATP-induced paracellular permeability versus BzATP group ($^{**}P < 0.05$). (c) Confocal microscopy images of immunofluorescence staining of ZO-1 and occludin demonstrating the protective effect of batimastat against BzATP-induced tight junction disruption.

IL-1β and MMP-9 in the absence of BzATP. Our study showed that IL-1β treatment significantly increased the levels of MMP-9, compared with the vehicle group ($P < 0.05$, Figure 5(a)). Apparently, administration of batimastat significantly attenuated the levels of MMP-9 ($P < 0.05$, Figure 5(a)). However, MMP-9 did not significantly affect the level of IL-1β, as discussed in Section 3.5.1.

3.4.2. MMP-9 Inhibition Attenuated Hyperpermeability of IL-1β-Induced Endothelial Coculture System. Exposure to IL-1β significantly increased the permeability to FITC-dextran compared with control group ($P < 0.05$, Figure 5(b)). Batimastat attenuated IL-1β-induced paracellular permeability, while batimastat alone did not affect the basal permeability levels ($P < 0.05$, Figure 5(b)).

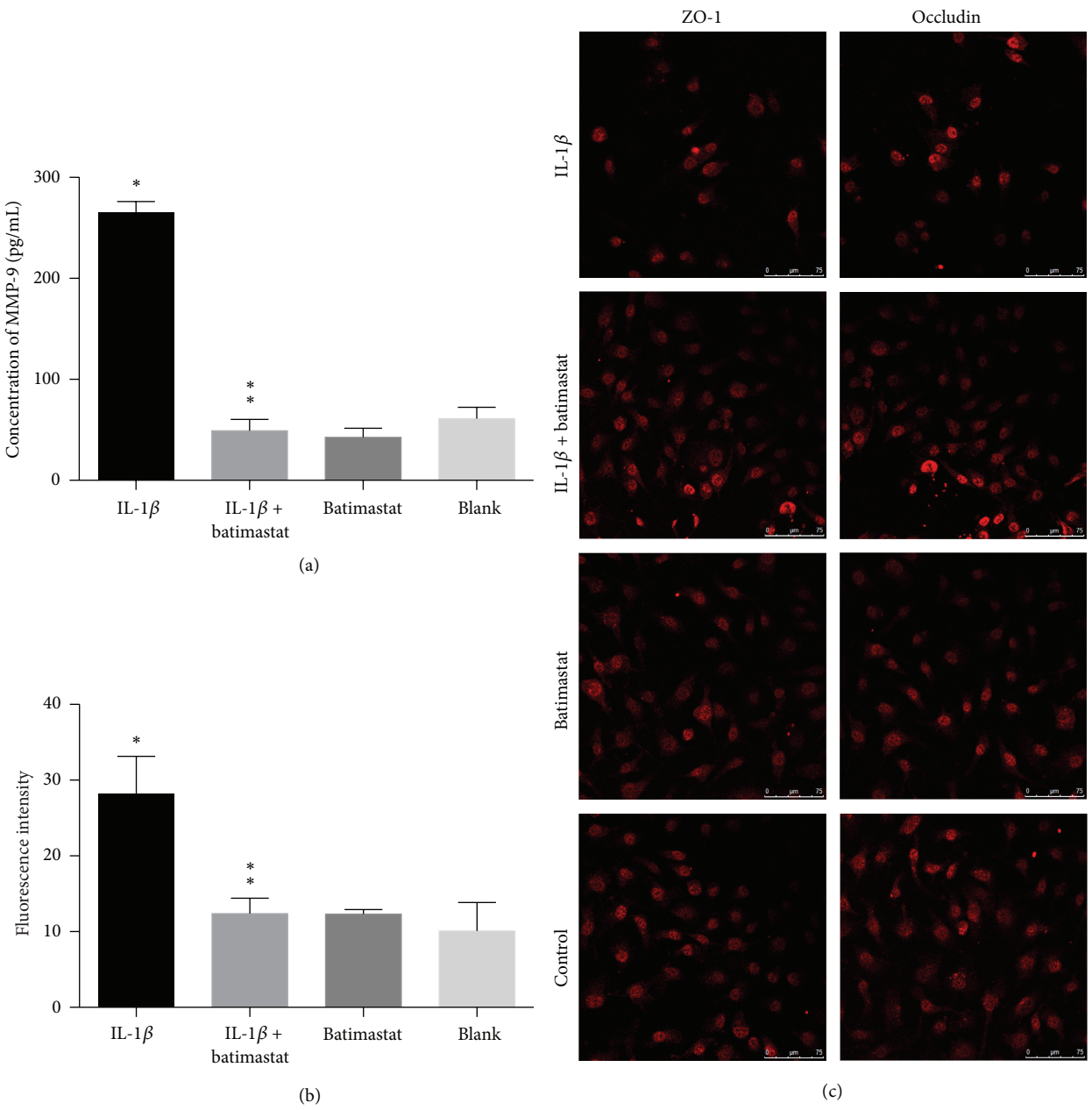

FIGURE 5: IL-1β-induced tight junction disruption and endothelial coculture system hyperpermeability were attenuated by MMP-9 inhibition. (a) The levels of MMP-9 were significantly higher in IL-1β groups than in control groups ($^{*}P < 0.05$). Batimastat treatment significantly reduced the level of MMP-9 versus vehicle group ($^{**}P < 0.05$). (b) Exposure to IL-1β significantly increased the permeability to FITC-dextran compared with the control groups ($^{*}P < 0.05$), which was decreased by batimastat in coculture system ($^{**}P < 0.05$). (c) Confocal microscopy images of immunofluorescence staining of ZO-1 and occludin demonstrating the protective effect of batimastat against IL-1β-induced tight junction disruption.

3.4.3. IL-1β-Induced TJP Disruption Was Attenuated by MMP-9 Inhibition. Immunofluorescence staining showed that the expression of ZO-1 and occludin in the IL-1β groups was significantly decreased compared with the controls, while batimastat + IL-1β groups showed a significant increase in the levels of the two tight junction proteins, indicating that batimastat treatment reversed the degradation of TJPs (Figure 5(c)).

3.5. MMP-9-Induced Tight Junction Disruption and Hyperpermeability of Endothelial Coculture System Were Not Attenuated by IL-1β Inhibition

3.5.1. MMP-9 Has No Effect on IL-1β Induction. To further confirm the relationship between IL-1β and MMP-9, we investigated whether MMP-9 elevated the levels of IL-1β. ELISA analysis showed that the levels of IL-1β were not

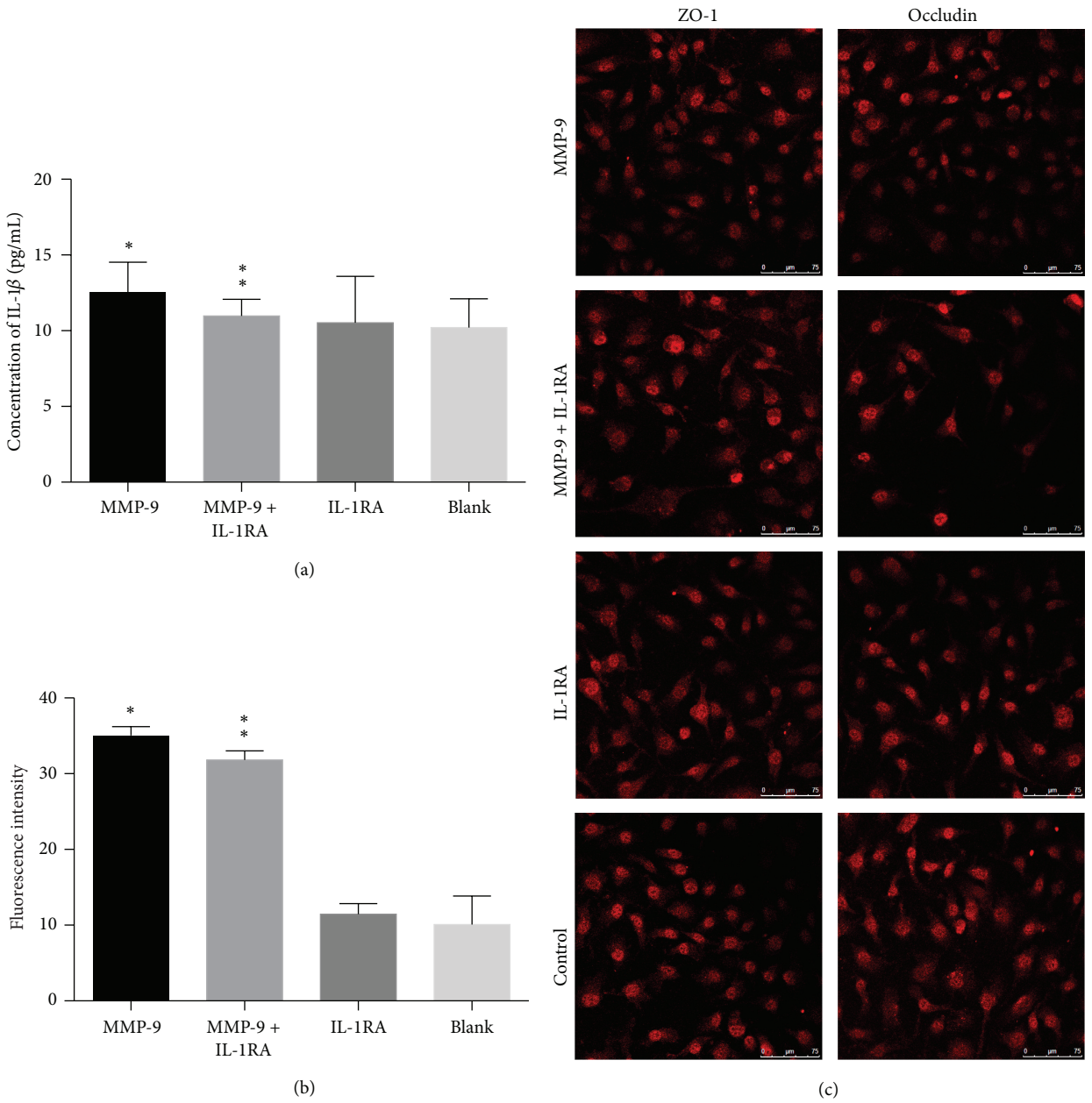

Figure 6: BzATP-induced tight junction disruption and endothelial coculture system hyperpermeability were attenuated by MMP inhibition. (a) The levels of IL-1β were not significantly altered in MMP-9-treated groups versus control groups ($^{*}P > 0.05$). No statistically significant differences were found between IL-1RA + MMP-9 groups and MMP-9 groups in the levels of IL-1β ($^{**}P > 0.05$). (b) Exposure to MMP-9 significantly increased the permeability to FITC-dextran compared with the control group ($^{*}P < 0.05$). However, IL-1RA failed to attenuate MMP-9-induced paracellular hyperpermeability ($^{**}P > 0.05$). (c) Immunofluorescence staining showed that the expression of ZO-1 and occludin in MMP-9 groups was significantly decreased compared with controls, while IL-1RA + MMP-9 groups showed no improvement in the levels of the two tight junction proteins.

altered in MMP-9-treated groups compared with controls. In addition, there were no significant differences in the levels of IL-1β between IL-1RA + MMP-9 and MMP-9 groups ($P > 0.05$, Figure 6(a)).

3.5.2. Hyperpermeability of MMP-9-Induced Endothelial Coculture System Was Not Attenuated by IL-1β Inhibition. Exposure to MMP-9 significantly increased the permeability to FITC-dextran compared with the control group ($P < 0.05$, Figure 6(b)). However, IL-1RA failed to attenuate MMP-9-induced paracellular hyperpermeability ($P < 0.05$, Figure 6(b)).

3.5.3. MMP-9-Induced TJP Disruption Was Not Attenuated by IL-1β Inhibition. Immunofluorescence staining showed that the expression of ZO-1 and occludin in the MMP-9

groups was significantly decreased compared with that of the controls. However, the IL-1RA + MMP-9 groups showed no improvement in the levels of the two tight junction proteins, indicating that IL-1RA treatment failed to reverse the degradation of TJPs (Figure 6(c)).

4. Discussion

Disruption of BBB is a hallmark of brain trauma/stress injury. It is associated with an increase in the permeability of damaged endothelium leading to cerebral edema [4]. The structural integrity of BBB is determined by tight junction proteins (TJPs). In other words, the decreased expression of TJPs in the brain microvessels is strongly correlated with disruption of the BBB [18, 19]. In addition, evidence strongly suggests that P2X7 receptors are activated by extracellular ATP following CNS injury/stress, triggering secondary brain damage [6], and deficits in the structural integrity of the tight junction proteins, leading to BBB dysfunction and brain edema [4, 20]. Therefore, elucidation of the cellular mechanisms of ATP-associated BBB damage may facilitate the development of effective therapeutics to improve patient outcomes after brain injury.

The increasingly important role of P2X7R in the pathophysiology of CNS trauma/stress suggests that targeted therapies hold the key to the treatment of cerebral edema following CNS stress/trauma. Previous reports showed that administration of BBG, an antagonist of P2X7 receptor, improved neurological function and exerted neuroprotective effect in spinal cord and traumatic brain injuries in murine models [21–23]. However, activation of P2X7R-induced disruption of tight junction proteins in human BBB models has not been reported. Therefore, we utilized an *in vitro* coculture BBB model consisting of an immortal human cell line hCMEC/D3 with human astrocytes to investigate the role of ATP/P2X7R signaling in the disruption of tight junction proteins. Our model extends previous work in determining the translational potential of human cells. In the present study, we demonstrated that A438079, a more selective antagonist of P2X7 receptors, attenuated hyperpermeability in a human BBB model as well as disruption of ZO-1 and occludin, which is closely associated with IL-1β and MMP-9 expression.

P2X7R is the receptor mediating ATP-dependent maturation and release of IL-1β. Activation of caspase-1 plays a key role in P2X7R-dependent IL-1β release. ATP/P2X7R signaling leads to the opening of large membrane pores, triggering changes in the intracellular ionic homeostasis to activate the caspase-1 cascade resulting in the transformation of pro-IL-1β to IL-1β [9]. Exposure to Ac-YVAD-CMK, a caspase-1 antagonist, attenuated the maturation of IL-1β induction and inhibited MMP-9 activation and conservation of ZO-1 in mice [24]. Using a human BBB model *in vitro*, we confirmed that the extracellular ATP-induced activation of P2X7R led to the release of IL-1β, which was inhibited by the administration of A438079. Consistent with pharmacological inhibition of P2X7R, a significant reduction in IL-1β expression following experimental brain trauma/stress was observed in the cortex of P2X7 knockout mice, when compared with wild-type mice [22]. In addition, treatment with an IL-1 receptor antagonist followed by BzATP significantly attenuated the disruption of ZO-1 and occludin, indicating that ATP/P2X7R signal-induced degradation of tight junction proteins was strongly associated with IL-1 receptors. Overall, our study suggested that secretion of IL-1β induced by ATP-stimulated P2X7R activation played a crucial role in triggering endothelial hyperpermeability and dysfunction of BBB.

In the present study, we investigated the relationship between IL-1β and MMP-9. IL-1β, one of the proinflammatory cytokines, is an important mediator of brain injuries/stress, and its role in the induction of MMP-9 has been well documented [24–26]. Ranaivo et al. reported that IL-1β enhanced the release of MMP-9 via activation of the ERK pathway [27]. However, Wu and his colleagues argued that IL-1β-induced MMP-9 expression depends on JNK1/2 signaling in astrocytes, involving CaMKII and phosphorylation of c-Jun, which are the upstream and downstream regulators of JNK, respectively [28, 29]. In our study, we found that both IL-1β and MMP-9 were induced after ATP/P2X7R activation. Induction of IL-1β increased the level of MMP-9. However, the levels of IL-1β were not altered in MMP-9-treated groups. Therefore, no obvious interaction exists between MMP-9 and IL-1β following disruption of BBB secondary to brain trauma/stress.

MMPs comprise a number of zinc-dependent endopeptidases that mediate the degradation of extracellular matrix. MMP-9 has a significant role in CNS injury/stress following activation by IL-1β and close association with tight junction protein degradation [30]. ATP-treated glial cultures derived from neonatal C57BL/6 mice showed an increase in MMP-9 activity via activation of the P2X7 receptor [31]. In addition, increased MMP-9 activity promoted the disruption of tight junctions in cerebral endothelial cells, such as occludin and ZO-1, which in turn disrupt the structural integrity and hyperpermeability of BBB [12, 32, 33]. Pharmacological inhibitors of MMP-9 significantly attenuated the disruption of BBB in rats [34]. Similarly, MMP-9 knockout abrogated the increased vascular permeability and restored neurological function [35, 36]. Our study showed that inhibitors of P2X7R and IL-1β prevented the increase in MMP-9 expression and consequently suppressed the degradation of ZO-1 and occludin in human BBB model *in vitro*. Furthermore, inhibition by batimastat decreased the disruption of tight junction proteins, indicating that MMP-9 was essential for ATP-induced hyperpermeability of BBB. These findings strongly supported the hypothesis that MMP-9 was regulated upstream by IL-1β and modulated BBB integrity downstream following CNS trauma/stress, suggesting that MMP-9 may also represent a therapeutic target as well as IL-1β inhibition in the ATP-induced BBB leakage.

Our study has several limitations. First, BBB model *in vitro* does not simulate the *in vivo* conditions, totally. For example, shear stress played a role in BBB physiology *in vivo* [37]. Second, studies suggest that microglia are the main cell type in the brain, which is responsible for IL-1β and IL-18 secretion [38]. Therefore, analysis of the relationship between microglia and other cell types such as astrocytes is critical

to fully understand the mechanism of ATP/P2X7R signaling. Third, BBB disruption is a complex and multistep process involving several interrelated factors. As a result, agents such as P2X7R antagonists that selectively target specific steps in the process are likely to be more effective when deployed in combination with agents that target other processes [39].

5. Conclusions

Our study demonstrated the potential mechanism of ATP/P2X7R signaling that may be targeted to attenuate BBB disruption and brain edema following brain trauma/stress. Concurrently, we tested P2X7R antagonist in a human BBB model, indicating its translational potential. However, a more detailed understanding of ATP/P2X7R pathway is needed. Future studies will focus on elucidating the mechanisms of cytokine-mediated neural plasticity and their implications for the pathophysiology and treatment of brain trauma/stress.

Abbreviations

BzATP: 3′-O-(4-Benzoyl)benzoyl adenosine 5′-triphosphate
BBB: Blood-brain barrier
CNS: Central nervous system
P2X7R: P2X7 receptor
IL-1β: Interleukin-1β
MMP-9: Matrix metalloproteinase-9
TJP: Tight junction protein
ELISA: Enzyme-linked immunosorbent assay
IL-1R: Interleukin-1 receptor
IL-1RA: Interleukin-1 receptor antagonist
TBI: Traumatic brain injury
ASD: Acute stress disorder
PTSD: Post-traumatic stress disorder
HA: Human astrocyte
DMEM: High glucose Dulbecco's Modified Eagle's Medium
FBS: Fetal bovine serum
PMSF: Phenylmethanesulfonyl fluoride
FITC: Fluorescein isothiocyanate.

Competing Interests

The authors declare that they have no competing interests regarding the publication of this paper.

Acknowledgments

This study was funded by the National Natural Science Foundation of China (Grant no. 81271365).

References

[1] R. Bryant, "Post-traumatic stress disorder vs traumatic brain injury," *Dialogues in Clinical Neuroscience*, vol. 13, no. 3, pp. 251–262, 2011.

[2] "The changing landscape of traumatic brain injury research," *Lancet Neurology*, vol. 11, no. 8, p. 651, 2012.

[3] K. N. Corps, T. L. Roth, and D. B. McGavern, "Inflammation and neuroprotection in traumatic brain injury," *JAMA Neurology*, vol. 72, no. 3, pp. 355–362, 2015.

[4] D. Shlosberg, M. Benifla, D. Kaufer, and A. Friedman, "Blood-brain barrier breakdown as a therapeutic target in traumatic brain injury," *Nature Reviews Neurology*, vol. 6, no. 7, pp. 393–403, 2010.

[5] K. W. McConeghy, J. Hatton, L. Hughes, and A. M. Cook, "A review of neuroprotection pharmacology and therapies in patients with acute traumatic brain injury," *CNS Drugs*, vol. 26, no. 7, pp. 613–636, 2012.

[6] B. L. Fiebich, S. Akter, and R. S. Akundi, "The two-hit hypothesis for neuroinflammation: role of exogenous ATP in modulating inflammation in the brain," *Frontiers in Cellular Neuroscience*, vol. 8, article 260, 2014.

[7] G. Burnstock, "Physiopathological roles of P2X receptors in the central nervous system," *Current Medicinal Chemistry*, vol. 22, no. 7, pp. 819–844, 2015.

[8] G. Burnstock, "Purine and pyrimidine receptors," *Cellular and Molecular Life Sciences*, vol. 64, no. 12, pp. 1471–1483, 2007.

[9] D. Ferrari, C. Pizzirani, E. Adinolfi et al., "The P2X7 receptor: a key player in IL-1 processing and release," *Journal of Immunology*, vol. 176, no. 7, pp. 3877–3883, 2006.

[10] T. Takenouchi, S. Sugama, Y. Iwamaru, M. Hashimoto, and H. Kitani, "Modulation of the ATP-lnduced release and processing of IL-1β in microglial cells," *Critical Reviews in Immunology*, vol. 29, no. 4, pp. 335–345, 2009.

[11] B. J. Gu and J. S. Wiley, "Rapid ATP-induced release of matrix metalloproteinase 9 is mediated by the P2X7 receptor," *Blood*, vol. 107, no. 12, pp. 4946–4953, 2006.

[12] K. A. C. Harkness, P. Adamson, J. D. Sussman, G. A. B. Davies-Jones, J. Greenwood, and M. N. Woodroofe, "Dexamethasone regulation of matrix metalloproteinase expression in CNS vascular endothelium," *Brain*, vol. 123, no. 4, pp. 698–709, 2000.

[13] T. Mori, X. Wang, T. Aoki, and E. H. Lo, "Downregulation of matrix metalloproteinase-9 and attenuation of edema via inhibition of ERK mitogen activated protein kinase in traumatic brain injury," *Journal of Neurotrauma*, vol. 19, no. 11, pp. 1411–1419, 2002.

[14] B. B. Weksler, E. A. Subileau, N. Perrière et al., "Blood-brain barrier-specific properties of a human adult brain endothelial cell line," *FASEB Journal*, vol. 19, no. 13, pp. 1872–1874, 2005.

[15] R. K. Sajja, S. Prasad, and L. Cucullo, "Impact of altered glycaemia on blood-brain barrier endothelium: an in vitro study using the hCMEC/D3 cell line," *Fluids and Barriers of the CNS*, vol. 11, no. 1, article 8, 2014.

[16] K. Hatherell, P.-O. Couraud, I. A. Romero, B. Weksler, and G. J. Pilkington, "Development of a three-dimensional, all-human in vitro model of the blood-brain barrier using mono-, co-, and tri-cultivation Transwell models," *Journal of Neuroscience Methods*, vol. 199, no. 2, pp. 223–229, 2011.

[17] G. Sahagun, S. A. Moore, and M. N. Hart, "Permeability of neutral vs. anionic dextrans in cultured brain microvascular endothelium," *American Journal of Physiology—Heart and Circulatory Physiology*, vol. 259, no. 1, part 2, pp. H162–H166, 1990.

[18] P. M. Abdul-Muneer, H. Schuetz, F. Wang et al., "Induction of oxidative and nitrosative damage leads to cerebrovascular inflammation in an animal model of mild traumatic brain injury induced by primary blast," *Free Radical Biology and Medicine*, vol. 60, pp. 282–291, 2013.

[19] X. Chen, Z. Zhao, Y. Chai, L. Luo, R. Jiang, and J. Zhang, "The incidence of critical-illness-related-corticosteroid-insufficiency is associated with severity of traumatic brain injury in adult rats," *Journal of the Neurological Sciences*, vol. 342, no. 1-2, pp. 93–100, 2014.

[20] I. Ng, E. Yap, W. L. Tan, and N. Y. Kong, "Blood-brain barrier disruption following traumatic brain injury: roles of tight junction proteins," *Annals of the Academy of Medicine, Singapore*, vol. 32, no. 5, pp. S63–S66, 2003.

[21] W. Peng, M. L. Cotrina, X. Han et al., "Systemic administration of an antagonist of the ATP-sensitive receptor P2X7 improves recovery after spinal cord injury," *Proceedings of the National Academy of Sciences of the United States of America*, vol. 106, no. 30, pp. 12489–12493, 2009.

[22] D. E. Kimbler, J. Shields, N. Yanasak, J. R. Vender, and K. M. Dhandapani, "Activation of P2X7 promotes cerebral edema and neurological injury after traumatic brain injury in mice," *PLoS ONE*, vol. 7, no. 7, Article ID e41229, 2012.

[23] Y. C. Wang, Y. Cui, J. Z. Cui et al., "Neuroprotective effects of brilliant blue G on the brain following traumatic brain injury in rats," *Molecular Medicine Reports*, vol. 12, no. 2, pp. 2149–2154, 2015.

[24] T. Sozen, R. Tsuchiyama, Y. Hasegawa et al., "Role of interleukin-1β in early brain injury after subarachnoid hemorrhage in mice," *Stroke*, vol. 40, no. 7, pp. 2519–2525, 2009.

[25] G. G. Vecil, P. H. Larsen, S. M. Corley et al., "Interleukin-1 is a key regulator of matrix metalloproteinase-9 expression in human neurons in culture and following mouse brain trauma in vivo," *Journal of Neuroscience Research*, vol. 61, no. 2, pp. 212–224, 2000.

[26] A. R. M. Ruhul Amin, T. Senga, M. L. Oo, A. A. Thant, and M. Hamaguchi, "Secretion of matrix metalloproteinase-9 by the proinflammatory cytokine, IL-1β: s role for the dual signalling pathways, Akt and Erk," *Genes to Cells*, vol. 8, no. 6, pp. 515–523, 2003.

[27] H. R. Ranaivo, S. M. Zunich, N. Choi, J. N. Hodge, and M. S. Wainwright, "Mild stretch-induced injury increases susceptibility to interleukin-1β-induced release of matrix metalloproteinase-9 from astrocytes," *Journal of Neurotrauma*, vol. 28, no. 9, pp. 1757–1766, 2011.

[28] C.-Y. Wu, H.-L. Hsieh, M.-J. Jou, and C.-M. Yang, "Involvement of p42/p44 MAPK, p38 MAPK, JNK and nuclear factor-κB in interleukin-1β-induced matrix metalloproteinase-9 expression in rat brain astrocytes," *Journal of Neurochemistry*, vol. 90, no. 6, pp. 1477–1488, 2004.

[29] C.-Y. Wu, H.-L. Hsieh, C.-C. Sun, and C.-M. Yang, "IL-1β induces MMP-9 expression via a Ca2+-dependent CaMKII/JNK/c-Jun cascade in rat brain astrocytes," *GLIA*, vol. 57, no. 16, pp. 1775–1789, 2009.

[30] P. M. Abdul-Muneer, B. J. Pfister, J. Haorah, and N. Chandra, "Role of matrix metalloproteinases in the pathogenesis of traumatic brain injury," *Molecular Neurobiology*, 2015.

[31] N. Murphy and M. A. Lynch, "Activation of the P2X7 receptor induces migration of glial cells by inducing cathepsin B degradation of tissue inhibitor of metalloproteinase 1," *Journal of Neurochemistry*, vol. 123, no. 5, pp. 761–770, 2012.

[32] F. Chen, N. Ohashi, W. Li, C. Eckman, and J. H. Nguyen, "Disruptions of occludin and claudin-5 in brain endothelial cells in vitro and in brains of mice with acute liver failure," *Hepatology*, vol. 50, no. 6, pp. 1914–1923, 2009.

[33] A. Rubio-Araiz, M. Perez-Hernandez, A. Urrutia et al., "3,4-Methylenedioxymethamphetamine (MDMA, ecstasy) disrupts blood-brain barrier integrity through a mechanism involving $P2X_7$ receptors," *International Journal of Neuropsychopharmacology*, vol. 17, no. 8, pp. 1243–1255, 2014.

[34] V. W. Yong, C. Power, P. Forsyth, and D. R. Edwards, "Metalloproteinases in biology and pathology of the nervous system," *Nature Reviews Neuroscience*, vol. 2, no. 7, pp. 502–511, 2001.

[35] X. Wang, J. Jung, M. Asahi et al., "Effects of matrix metalloproteinase-9 gene knock-out on morphological and motor outcomes after traumatic brain injury," *The Journal of Neuroscience*, vol. 20, no. 18, pp. 7037–7042, 2000.

[36] N. Muradashvili, R. L. Benton, K. E. Saatman, S. C. Tyagi, and D. Lominadze, "Ablation of matrix metalloproteinase-9 gene decreases cerebrovascular permeability and fibrinogen deposition post traumatic brain injury in mice," *Metabolic Brain Disease*, vol. 30, no. 2, pp. 411–426, 2015.

[37] L. Cucullo, M. Hossain, V. Puvenna, N. Marchi, and D. Janigro, "The role of shear stress in blood-brain barrier endothelial physiology," *BMC Neuroscience*, vol. 12, article 40, 2011.

[38] A. Gustin, M. Kirchmeyer, E. Koncina et al., "NLRP3 inflammasome is expressed and functional in mouse brain microglia but not in astrocytes," *PLoS ONE*, vol. 10, no. 6, Article ID e0130624, 2015.

[39] B. P. Walcott, K. T. Kahle, and J. M. Simard, "Novel treatment targets for cerebral edema," *Neurotherapeutics*, vol. 9, no. 1, pp. 65–72, 2012.

Hindawi Publishing Corporation
Neural Plasticity
Volume 2016, Article ID 8058093, 6 pages
http://dx.doi.org/10.1155/2016/8058093

Review Article

Safety Needs Mediate Stressful Events Induced Mental Disorders

Zheng Zheng,[1] Simeng Gu,[1,2] Yu Lei,[1] Shanshan Lu,[1] Wei Wang,[3] Yang Li,[1,4] and Fushun Wang[1]

[1]*School of Psychology, Nanjing University of Chinese Medicine, Nanjing 210023, China*
[2]*School of Psychology, Nanjing Normal University, Nanjing 210023, China*
[3]*Nanjing University of Chinese Medicine, Nanjing, China*
[4]*School of Psychology, Nanjing University of Forest Police, Nanjing 210023, China*

Correspondence should be addressed to Yang Li; 331813615@qq.com and Fushun Wang; 13814541138@163.com

Received 23 April 2016; Revised 9 July 2016; Accepted 3 August 2016

Academic Editor: Malgorzata Kossut

"Safety first," we say these words almost every day, but we all take this for granted for what Maslow proposed in his famous theory of *Hierarchy of Needs*: safety needs come second to physiological needs. Here we propose that safety needs come before physiological needs. Safety needs are personal security, financial security, and health and well-being, which are more fundamental than physiological needs. Safety worrying is the major reason for mental disorders, such as anxiety, phobia, depression, and PTSD. The neural basis for safety is amygdala, LC/NE system, and corticotrophin-releasing hormone system, which can be regarded as a "safety circuitry," whose major behavior function is "fight or flight" and "fear and anger" emotions. This is similar to the Appraisal theory for emotions: fear is due to the primary appraisal, which is related to safety of individual, while anger is due to secondary appraisal, which is related to coping with the unsafe situations. If coping is good, the individual will be happy; if coping failed, the individual will be sad or depressed.

1. Maslow's Hierarchy of Needs Revisit

Maslow's Hierarchy of Needs has been a well-known theory since Abraham Maslow proposed it in 1943 [1] and in his book *Motivation and Personality* in 1954, in which he proposed that human needs can be portrayed in the shape of a pyramid, with the most fundamental levels of needs at the bottom. From bottom to the top are the needs: *physiological needs, safety, belongingness and love, esteem, and self-actualization*. Physiological needs are the physical requirements for the survival of individual and the animal kind, such as food and sex, and safety needs are personal security, financial security, and health and well-being. Maslow proposed that if the physiological needs are relatively satisfied, there then emerges a new set of needs, which may be categorized roughly as the safety needs. The organism may be wholly dominated by them, which may serve as the almost exclusive organizers of behavior, recruiting all the capacities of the organism in their service, and we may then fairly describe the whole organism as a safety-seeking mechanism [1]. But Maslow also found that "practically everything looks less important than safety, even sometimes the physiological needs which being satisfied, are now underestimated. A man may be characterized as living almost for safety alone." [1]. Actually safety needs are more fundamental than physiological needs. Safety needs are personal security, financial security, and health and well-being, which are more fundamental than physiological needs (Figure 1). For example, the deer cannot eat (physiological needs) on the wild prairie when the wolves chase them (safety). Let me take one example from Cosmides and Tooby (2000), who propose that the emotions serve to regulate behavior. He wrote about fear like this: "Imagine walking alone at night and hearing some rustling in the brush. Your energies are aroused to be ready for action, you become acutely aware of sounds that could indicate that you are being stalked, the threshold for detecting movements is lowered, you no longer feel pangs of hunger, attracting a mate is the farthest thing from your mind." [2]. So it is clear that safety needs are more fundamental than physiological needs. Whether physiological needs or safety needs are more

important will affect our opinions about mental disorders, for example, Freud proposed libido (physiological needs) more important.

Safety Needs Can Block Physiological Needs. Safety needs can block physiological needs; the classical example is Miller's Avoidance and Approach experiments (Figure 2) [3]. In 1961, Neal Miller used behavioral measures to assess motivational disposition in rodents (Figure 2). As the animal moves closer to the potential reward (e.g., food), the force exerted to obtain the reward increases. Similarly illustrated is the avoidance: the force the animal exerted to avoid the aversive stimulus (a shock) also increases as the animal comes closer, and furthermore, the slope of the avoidance gradient tended to be steeper than that of approach [3]. Later experiments by Ito found that the organisms tend to be more sensitive to the threatening information and generally process such information faster than the rewarding information [4]. He called this phenomenon negativity bias and attributed it as a protective strategy through evolution, since even a single failure to respond adaptively to a survival threat may preclude passing on genetic information. He found that "as a potential treat looms, the adaptive response of the brain is to amplify these threats and initiate appropriate behavioral responses, such as fleeing, freezing, or attacking." And he found that the negativity bias can be seen across all levels of the neuraxial organization [3]. These data support the notion that safety needs are faster and more fundamental than hedonic needs.

2. Safety Needs—Unexpectancy

Maslow thought adults usually inhibit the reaction for safety needs, so he used infants as an example and found that the child's need for safety is his preference for some kind of undisrupted routine or rhythm. Maslow mentioned, "He seems to want a predictable, orderly world. For instance, injustice, or inconsistency in the parents seems to make a child feel anxious and unsafe. This attitude may be not so much because of the injustices per se or any particular pains involved, but rather because this treatment threatens to make the world look unreliable, or unsafe, or unpredictable." [1]. Maslow also mentioned, "Confronting the average child with new, unfamiliar, strange, unmanageable stimuli or situations will too frequently elicit the danger or terror reactions." Therefore the safety is related to unexpectancy.

This is consistent with the behaviorists, who propose that behavior is a process-form "Stimulus-Reaction", while cognition scientists extend it to "Stimulus-Opinion-Reaction." However, they all depend on a stimulus. Everything around us is stimulus that has the *hedonic value*, which fits into our personal physiological needs. And it also has another feature: happening in an expected way, or unexpected way, which is related to threat and can be called *safety value*. We draw these two features of stressful events in two dimensions: *hedonic value and safety value* (Figure 1). The safety value has nothing to do with the hedonic value, for both the liked things and disliked things can induce unsafety. For example, we worry

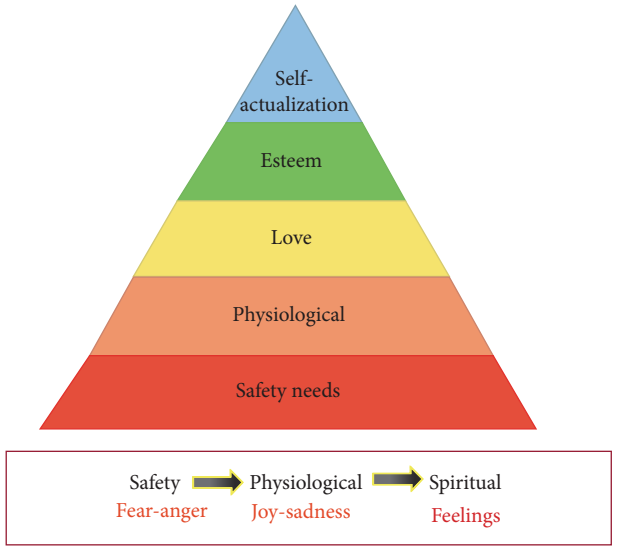

Figure 1: New version for *Hierarchy of Needs*: "*safety-hedonic-esteem-love-self-actualization*". All emotions and feelings depend on whether the stimulus can satisfy the needs of individuals, and the satisfaction of different needs can induce different emotions: safety can induce fear and anger, hedonic needs can induce joy and sadness, and spiritual needs can induce feelings such as love.

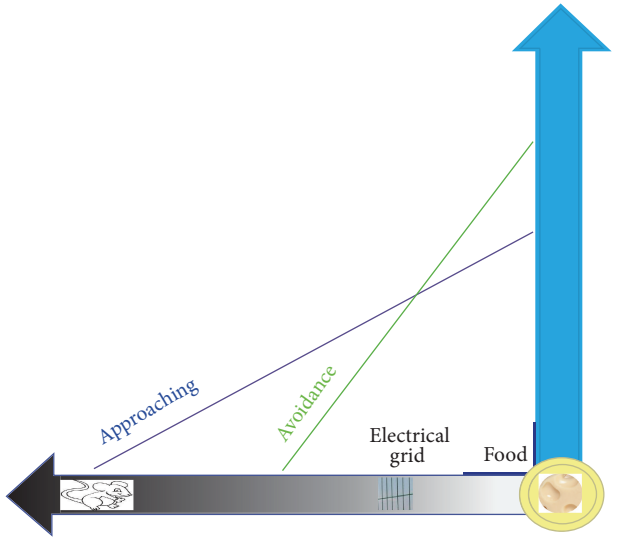

Figure 2: Safety needs can block physiological needs. Approach and avoidance gradients depend on the distance from the goal. Goal includes the food (physiological needs), while the punishments include the foot shock (safety needs). The avoidance slope is steeper and predominates proximally to the goal, whereas the approach gradients are higher at the remote location.

about losing the liked things and also worry about getting the disliked things; and we also will not be angry if we lose the good thing as expected and also get the disliked thing as expected. Even though it is something you liked, if it is unexpected, you still feel afraid and angry. *Therefore the safety is related to unexpectancy*. One feature of the safety need

induced emotion is the rapid detection of potential threats and can initiate appropriate approach/avoidance behaviors.

Prediction Error. The most interesting and influential line of empirical and theoretical work is predication error [5]. The studies were done from electrophysiological recordings of dopamine neurons in awake, behaving monkey in Schultz's lab. The recordings showed that the firing of the dopamine cells only related to "prediction error" [6]. These phased activation does not discriminate different types of rewarding stimuli [6]. And it is quite unexpected that the reward delivery will not elicit dopamine neuron firing, once the animal has learned the stimulus and reward association [6]. Therefore, dopamine neurons are related to expectation about external stimulus rewarding, especially when it is uncertain or prediction error [6, 7].

3. Emotion Flow

The studies of emotions have been expanded exponentially by two prominent researchers: Magda Arnold and Richard Lazarus, who proposed Appraisal theory. Appraisal theory states that emotions result from people's interpretations and explanation of their circumstances. In the structural model of Appraisal theory, Lazarus borrowed the concept of appraisal from Arnold and elaborated the concept as a key factor for emotions: emotional processes depend on the predictability of the stressful events. He distinguishes two basic forms of appraisal, primary and secondary appraisal [8], and he proposed that the primary appraisal and its induced emotions are a faster activating, automatic process, which is similar to the safety need. Indeed, Lazarus distinguishes three types of stressful events: harm, threat, and challenge, which are related to primary appraisal. The secondary appraisal is concerned with coping options, which include blame or credit, coping potential, and future expectations. *It seems that the primary appraisal is related to fear and the secondary is related to anger* (Figure 3). Lazarus mentioned that if a person appraises a situation as motivationally relevant, motivationally incongruent and also holds a person other than himself accountable, the individual would most likely experience anger in response to the situation.

Process model of the Appraisal theory is more accurate to explain the safety needs, for personal safety, which are related to the "unexpected ways of stimulus occurring." The process model proposed two main appraisal processes: perceptual stimuli and associative processing and reasoning. Perceptual stimuli are what the individual picks up from his surroundings, such as sensation of pain or pleasure. Then, the individual performs two main appraisal processes: associative processing, which is memory based, and reasoning, which is a slower and more deliberate process that involves logical thinking about the stimulus.

All stressful events will first induce fear and anger [9]. For example, when you meet a car that quickly passes and stops before you, you will be firstly scared and then blame the car. Let us take another example from Izard's paper [10], *"when Rafe was hit from the back by a wheel chair, the first reaction of him was scared and angry, and showed angry expression and clenched fist. But after he turned back to see Rebecca, a person with hemiplegia whose wheelchair had gone out of control and cause her to crash into Rafe. Rafe's understanding changed his anger to sadness and sympathy."* So when something unexpected occurs, you will first evaluate its threat (fear/anger) and next evaluate its hedonic value (happy/sad) (Figure 3). Similar *emotional flow* happens in our lives all the time: everything in our lives is normally calm as expected; but you will first feel scared (fear) when something unexpected occurs, and then you will blame (anger) the unexpectancy after fear is gone. And afterwards you might feel happy after successfully coping with the stressful events or feel sad if you failed to cope with them. Finally, the stressful events go away, and people calm down. This kind of emotional flow, big or small, long or short, constitutes our everyday emotions. So *fear-anger-happiness-sadness-calm* might constitute the rainbow of emotions or *emotional flow* in our everyday life.

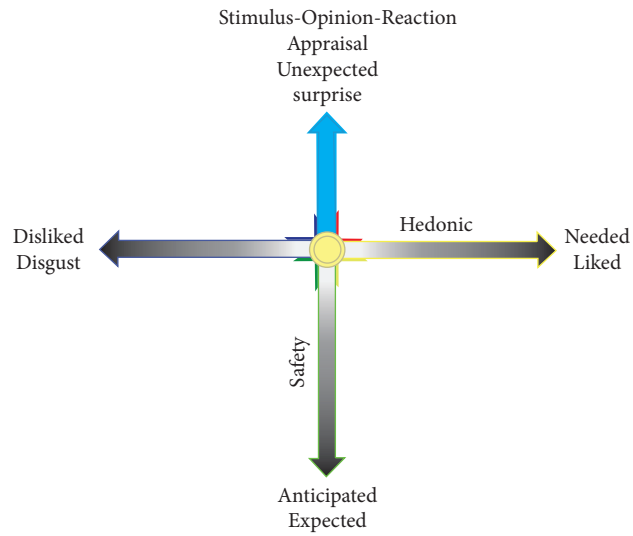

Figure 3: *Stressful events are something that happened unexpectedly.* Every stimulus has the *hedonic value* (horizontal dimension), which fits into our personal needs (pleasant things, needed things, or disliked things or unpleasant things). And it can happen in an expected way, or unexpected ways (vertical dimension), which are called *safety value*.

4. Neural Substrate-Amygdala

The amygdala has been proved to be the neural basis for fear [11], and it is also recognized as the neural basis for stress elicited fear and anxiety [12, 13]. In addition, electrical stimulation of the amygdala promotes autonomous reactions and stress-like behavioral, whereas amygdala ablation induced a marked tameness increase, motivation loss, and fear decrease to aversive stimuli [14, 15]. Amygdala is one of the most important limbic structures that link to fear, which was first suggested by Klüver & Bucy in 1937, who demonstrated that the lesion of the medial temporal lobe resulted in a wide range

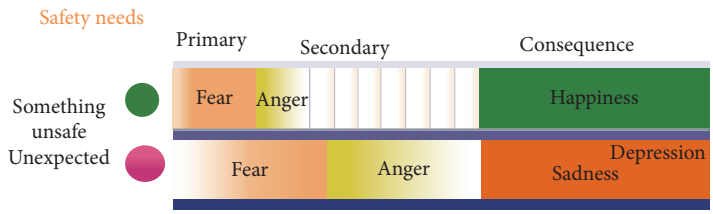

FIGURE 4: *Emotional flow*. Lazarus's primary appraisals are for threads, while secondary appraisals are for coping. Safety needs induce stressful emotions, fear and anger, and stressful behaviors, fight or flight. So fear-anger-happiness-sadness-calm constitutes the *rainbow of emotions or emotional flow* in everyday life. The figure is adopted from our previous publication [30].

of odd behaviors, such as approaching normally to fearful objects [16]. And about 20 years later, Weiskrantz (1956) found that it is the amygdala whose impairment resulted in the odd behaviors, which are called Klüver and Bucy syndrome [15]. These patients with amygdala impaired failed to learn conditioned fear responses. LeDoux puts amygdala as the emotional computer to work out the emotional significance of stimuli [17]. He demonstrated two neural pathways of sensory information from the thalamus to the cortex: (1) A slow-acting *"thalamus-to-cortex circuit,"* whose function is to analyze sensory information in detail, and (2) a fast-acting *"thalamus-amygdala circuit,"* whose major function is to analyze simple stimulus features, which bypass the cortex [18]. These two pathways possibly underlie the two evaluation systems: *the fast one for the fear/anger and the slow one for hedonic*. Other reports, such as findings from Ohman and Soares (1994) also support a fast-acting system for threat detection that involves only minimal cortical processing [19, 20]. In addition, Morris et al. (2001) also reported a patient whose primary visual cortex was impaired and therefore showed no conscious visual perception but showed significant fearful reports [20]. In all, the fast-acting thalamus-amygdala circuit is important for our ancient ancestors to rapidly recognize dangers to help with survival.

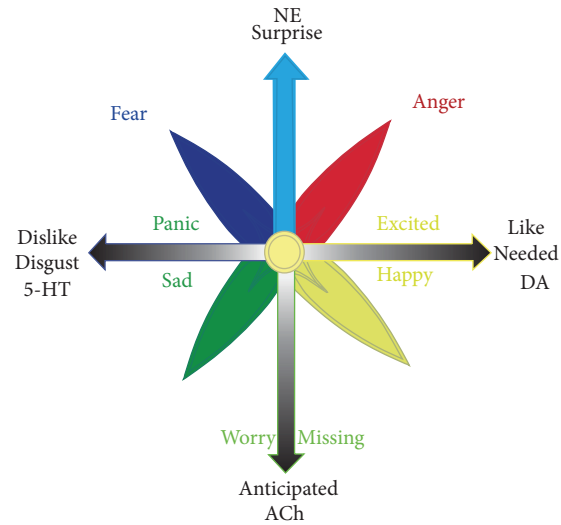

FIGURE 5: *Emotions are due to the hedonic value of the things (physiological needs) and also the way things occur (safety needs)*. The way everything occurs not only induces stressful emotions but also affects the tension of hedonic emotions. The neurotransmitters for these emotions are dopamine (a pleasant marker) and serotonin (unpleasant marker). NE is surprise marker, while Ach is a marker for anticipation. NE is well known for fight (anger) or flight (fear) behaviors.

5. NE-Safety Neuromodulators

It is an evolutionary adaptation for our ancestors to better cope with the unexpected environment with the fast activing thalamus-amygdala circuit. In addition to amygdala, the NE/LC system is important to direct behaviors of the animal to cope with the dangerous environment, and the well-known function of NE/LC system is to induce "fight or flight" behaviors. Take a deer in the wild as an example. When a deer meets a lion, the reaction of the deer is flight (fear), while the reaction of a lion is fight (anger). So the same neurotransmitter NE might undergo two different behaviors. So the emotion fear and anger might also be derived from the same neurotransmitter NE and the same stressful event (Figure 4). NE is released from the locus coeruleus (LC) in the brain to keep the brain alert, which has been described as increasing the "signal to noise" of the sensory inputs [21]. Many reports have implicated LC in alertness, anxiety[22–24]. And LC has been reported to be activated at stressful events: increased LC neuron firings were observed at visual threat [25]. And LC stimulation can induce fearful behaviors [26]. LC sends projections to amygdala [27], which is the most important limbic structure that links to fear [13]. Therefore, amygdala and NE/LC system might constitute the neural structure for safety needs.

Our ancestors navigating rich environments had to face very complicated environments, with many forms of uncertainties [28]. So they evolved an adaptive mechanism to first do a safety check for everything around them. If it would happen in an anticipated way, they will feel calm; instead if something happened surprisingly, they will be scared and angry. Therefore, *fear and anger are due to things happening in an unexpected way* (Figure 4). Of note, the unexpectancy will also increase the tension of hedonic emotions. With the same kind of hedonic stimulus, if it comes in an unexpected way, people will feel excited; instead, people will feel happy. It is the same with sadness or helpless panic (Figure 5).

6. Pathological Conditions

Safety needs can induce diseases, as Maslow mentioned, "One reason for the clearer appearance of the threat or danger reaction in infants, is that they do not inhibit this reaction at all, whereas adults in our society have been taught to inhibit it at all costs. Thus even when adults do feel their safety to be threatened we may not be able to see this on the surface. Infants will react in a total fashion. . .In infants we can also see a much more direct reaction to bodily illnesses of various kinds. . . for instance, vomiting, colic or other sharp pains." [1]. Even the adults can inhibit our reactions, they still can react in some mental disorders. Maslow wrote, "Some neurotic adults in our society are, in many ways, like the unsafe child in their desire for safety, although in the former it takes on a somewhat special appearance. Their reaction is often to unknown, psychological dangers in a world that is perceived to be hostile, overwhelming and threatening." The neurotic individual may be described in a slightly different way with some usefulness as a grown-up person who retains his childish attitude toward the world. This is to say, a neurotic adult may be said to behave as if he were actually afraid of a spanking, or of his mother's disapproval, or of being abandoned by his parents, or having his food taken away from him. It is as if his childish attitude of fear and threat reaction to a dangerous world had gone underground, and untouched by the growing up and learning processes, were now ready to be called out by any stimulus that would make a child feel endangered and threatened [1].

Fear-Phobia. If something happens surprisingly, people will be scared and angry; and if it would happen in an anticipated way, they will feel calm. So for the phobia patients, their problems might be that they cannot successfully accomplish the emotional flow (*fear-anger-happiness-sadness-calm*). The best way to remove fear is anger, these patients are too timid to show anger, so their emotions are checked at emotional flowing from fear to anger. Therefore, anger might be the best treatment for these patients and NE is the neural substrate for them.

Anger-Depression. Depression is characterized by unrelenting sadness accompanied by an inability to derive pleasure from positively hedonic situations. Therefore, depression might be related to the primary appraisal, the worrying about safety instead of physiological satisfaction. Indeed, excessive self-blame and feeling worthless are symptoms of major depression episodes across cultures [29], which is similar to Lazarus's secondary appraisal. So the depressed patients have problems with anger or with coping appraisal or their problem is due to inability to cope with the unsafe stressful situation and showed inward anger. The difference between fear and anger is the direction of the behavior: fear is to throw oneself away from the stimulus and anger is to throw the stimulus away. Depression is the inward anger. Anger is usually fight against the outside stimulus. For these patients, they do not have the ability to throw the outside stimulus due to repeated helplessness, they want to kill themselves.

7. Conclusions

Safety needs are the most fundamental needs for the human kind, which include personal security, financial security, and health and well-being. Safety is the major reason for mental disorders, such as anxiety, phobia, depression, and PTSD. The neural basis for safety is amygdala and LC/NE system, which can be regarded as a "safety circuitry," whose major behavior function is "fight or flight" and "fear and anger" emotions, or conditioned learning for these emotions. Fear and anger are due to the safety needs, while joy and sadness are due to the physiological needs, which should come after safety needs in Maslow's hierarchy of needs. Fear and anger are two sides of one sword, for they will act in different directions: fear is to flight away from the danger and anger is to fight the danger away. They are all due to the stressful events: normally everything is as expected, and life is calm. When something unexpected happens, the individuals first feel scared and then blame the unexpectancy; this is the first safety check. Afterwards the individual will have a hedonic need to see if it fits their personal needs and get the happy or sad emotions. Finally, everything comes to an end, and people return to calmness or miss the lost things and worry for the uncertain bad things. So the emotional rainbow (or emotion flow) *fear-anger-happiness-sadness-missing* constitutes our emotions in everyday life.

Competing Interests

No conflict of interests was declared.

Acknowledgments

The study is also supported by Jiangsu Provincial Natural Science Foundation (no. BK 20151665) (Fushun Wang), Jiangsu Chinese Medicine Foundation (ZD201501), Jiangsu Six Talent Peak (2015-YY-006), Jiangsu Specially Appointed Professorship Foundation, and also the Priority Academic Program Development of Jiangsu Higher Education Institute (PAPD).

References

[1] A. H. Maslow, "A theory of human motivation," *Psychological Review*, vol. 50, no. 4, pp. 370–396, 1943.

[2] L. Cosmides and J. Tooby, *Evolutionary Psychology and the Emotions* , Guilford, New York, NY, USA, 2000.

[3] G. J. Norman, C. J. Norris, J. Gollan et al., "Current emotion research in psychophysiology: the neurobiology of evaluative bivalence," *Emotion Review*, vol. 3, no. 3, pp. 349–359, 2011.

[4] K. Ito, "Ribosome-based protein folding systems are structurally divergent but functionally universal across biological kingdoms," *Molecular Microbiology*, vol. 57, no. 2, pp. 313–317, 2005.

[5] P. Dayan and B. W. Balleine, "Reward, motivation, and reinforcement learning," *Neuron*, vol. 36, no. 2, pp. 285–298, 2002.

[6] W. Schultz, P. Dayan, and P. R. Montague, "A neural substrate of prediction and reward," *Science*, vol. 275, no. 5306, pp. 1593–1599, 1997.

[7] P. Redgrave and K. Gurney, "The short-latency dopamine signal: a role in discovering novel actions?" *Nature Reviews Neuroscience*, vol. 7, no. 12, pp. 967–975, 2006.

[8] Lazarus, *Emotion and Adapation*, Oxford University Press, New York, NY, USA, 1991.

[9] S. Gu, F. Wang, T. Yuan, B. Guo, and H. Huang, "Differentiation of primary emotions through neuromodulators: review of literature," *International Journal of Neurology Research*, vol. 1, no. 2, pp. 43–50, 2015.

[10] C. E. Izard, "Four systems for emotion activation: cognitive and noncognitive processes," *Psychological Review*, vol. 100, no. 1, pp. 68–90, 1993.

[11] L. R. Johnson, M. Hou, E. M. Prager, and J. E. LeDoux, "Regulation of the fear network by mediators of stress: norepinephrine alters the balance between cortical and subcortical afferent excitation of the lateral amygdala," *Frontiers in Behavioral Neuroscience*, vol. 5, article 23, 2011.

[12] P. Vuilleumier, "Cognitive science: staring fear in the face," *Nature*, vol. 433, no. 7021, pp. 22–23, 2005.

[13] J. LeDoux, "Fear and the brain: where have we been, and where are we going?" *Biological Psychiatry*, vol. 44, no. 12, pp. 1229–1238, 1998.

[14] M. Gallagher, B. S. Kapp, R. E. Musty, and P. A. Driscoll, "Memory formation: evidence for a specific neurochemical system in the amygdala," *Science*, vol. 198, no. 4315, pp. 423–425, 1977.

[15] L. Weiskrantz, "Behavioral changes associated with ablation of the amygdaloid complex in monkeys," *Journal of Comparative and Physiological Psychology*, vol. 49, no. 4, pp. 381–391, 1956.

[16] H. Klüver and P. C. Bucy, "Psychic blindness and other symptoms following bilateral temporal lobectomy in Rhesus monkey," *American Journal of Physiology*, vol. 119, pp. 352–353, 1937.

[17] J. Storbeck and G. L. Clore, "On the interdependence of cognition and emotion," *Cognition and Emotion*, vol. 21, no. 6, pp. 1212–1237, 2007.

[18] J. LeDoux, *The Emotional Brain: The Mysterous Underpinnings of Emotional Life*, Simon & Schuster, New York, NY, USA, 1996.

[19] A. Öhman, "The role of the amygdala in human fear: automatic detection of threat," *Psychoneuroendocrinology*, vol. 30, no. 10, pp. 953–958, 2005.

[20] J. S. Morris, B. DeGelder, L. Weiskrantz, and R. J. Dolan, "Differential extrageniculostriate and amygdala responses to presentation of emotional faces in a cortically blind field," *Brain*, vol. 124, no. 6, pp. 1241–1252, 2001.

[21] D. A. Morilak, G. Barrera, D. J. Echevarria et al., "Role of brain norepinephrine in the behavioral response to stress," *Progress in Neuro-Psychopharmacology & Biological Psychiatry*, vol. 29, no. 8, pp. 1214–1224, 2005.

[22] J. D. Bremner, J. H. Krystal, S. M. Southwick, and D. S. Charney, "Noradrenergic mechanisms in stress and anxiety: II. Clinical studies," *Synapse*, vol. 23, no. 1, pp. 39–51, 1996.

[23] J. D. Bremner, J. H. Krystal, S. M. Southwick, and D. S. Charney, "Noradrenergic mechanisms in stress and anxiety: I. Preclinical studies," *Synapse*, vol. 23, no. 1, pp. 28–38, 1996.

[24] K. Itoi, "Ablation of the central noradrenergic neurons for unraveling their roles in stress and anxiety," *Annals of the New York Academy of Sciences*, vol. 1129, pp. 47–54, 2008.

[25] K. Rasmussen, D. A. Morilak, and B. L. Jacobs, "Single unit activity of locus coeruleus neurons in the freely moving cat. I. During naturalistic behaviors and in response to simple and complex stimuli," *Brain Research*, vol. 371, no. 2, pp. 324–334, 1986.

[26] D. E. Redmond Jr., Y. H. Huang, D. R. Snyder, and J. W. Maas, "Behavioral effects of stimulation of the nucleus locus coeruleus in the stump-tailed monkey Macaca arctoides," *Brain Research*, vol. 116, no. 3, pp. 502–510, 1976.

[27] E. Vermetten and J. D. Bremner, "Circuits and systems in stress. I. Preclinical studies," *Depression and Anxiety*, vol. 15, no. 3, pp. 126–147, 2002.

[28] A. J. Yu and P. Dayan, "Uncertainty, neuromodulation, and attention," *Neuron*, vol. 46, no. 4, pp. 681–692, 2005.

[29] R. Zahn, K. E. Lythe, J. A. Gethin et al., "Negative emotions towards others are diminished in remitted major depression," *European Psychiatry*, vol. 30, no. 4, pp. 448–453, 2015.

[30] S. Gu, F. Wang, T. Yuan, B. Guo, and J. H. Huang, "DIfferentiation of primary emotions through neuromodulators: review of literature," *International Journal of Neurology Research*, vol. 1, no. 2, pp. 43–50, 2015.

Hindawi Publishing Corporation
Neural Plasticity
Volume 2016, Article ID 7950781, 10 pages
http://dx.doi.org/10.1155/2016/7950781

Research Article

Shuyu Capsules Relieve Premenstrual Syndrome Depression by Reducing 5-HT_{3A}R and 5-HT_{3B}R Expression in the Rat Brain

Fang Li,[1] Jizhen Feng,[2] Dongmei Gao,[3] Jieqiong Wang,[3] Chunhong Song,[3] Sheng Wei,[3] and Mingqi Qiao[3]

[1]*Fengtai Maternal and Children's Health Hospital of Beijing, Beijing 100069, China*
[2]*Department of Radiology, Shandong Provincial Hospital Affiliated to Shandong University, Jinan 250021, China*
[3]*Key Laboratory for Classical Theory of Traditional Chinese Medicine of Education Ministry, Shandong University of Traditional Chinese Medicine, Jinan 250355, China*

Correspondence should be addressed to Mingqi Qiao; qmingqi@163.com

Received 16 May 2016; Revised 20 July 2016; Accepted 28 July 2016

Academic Editor: Fang Pan

The effects of the Shuyu capsule on 5-HT_{3A}R and 5-HT_{3B}R expression in a rat model of premenstrual syndrome (PMS) depression and on 5-HT_{3A}R and 5-HT_{3B}R expression and hippocampal neuron 5-HT_3 channel current were investigated, to elucidate its mechanism of action against PMS depression. PMS depression model rats were divided into depression and Shuyu- and fluoxetine-treated groups, which were compared to control rats for frontal lobe and hippocampal 5-HT_{3A}R and 5-HT_{3B}R expression and behavior. The depressed model rats displayed symptoms of depression, which were reduced in treated and normal control rats. Frontal lobe and hippocampal 5-HT_{3A}R and 5-HT_{3B}R levels were significantly higher in the model versus the control group and were significantly lower in the Shuyu group. As compared to control rats, the 5-HT_3R channel current in the model group was significantly higher; the 5-HT_3R channel current in hippocampal neurons treated with serum from Shuyu group rats was significantly lower than that in those treated with model group serum. Thus, PMS depression may be related to 5-HT_{3A}R and 5-HT_{3B}R expression and increased 5-HT_3 channel current. Shuyu capsules rectified abnormal 5-HT_{3A}R and 5-HT_{3B}R expression and 5-HT_3 channel current changes in a rat model; this finding may provide insight into treating PMS depression.

1. Introduction

Premenstrual syndrome (PMS), a disease commonly encountered in clinical gynecology, refers to a series of moods, mental and physical symptoms, and signs occurring in the premenstrual period (luteal phase) of reproductive-aged women, including irritability, anxiety, nervousness, breast distention pain, and headache. The abovementioned symptoms automatically mitigate or disappear after menstruation but recur regularly with each menstrual cycle [1, 2]. Epidemiological surveys conducted worldwide have revealed that reproductive-aged women undergo one or more mood and physical PMS-related symptoms [3] that significantly influence their physical and mental health, as well as their quality of life. Moreover, the incidence of PMS has been increasing annually, attracting increased attention from the medical field.

PMS depression is a major type of PMS with features of depression, sullenness, chest distress, sighing, and a depressed mood [4, 5]. It has been reported that monoamine neurotransmitters including 5-hydroxytryptamine 1A receptor, 5-hydroxytryptamine 2A receptor, 5-hydroxytryptamine 2C receptor, and 5-hydroxytryptamine 3 receptor are responsible for premenstrual syndromes [6–11]. Widely distributed in the central nervous system and peripheral nervous system, 5-HT_3R influences the metabolism of neurotransmitters in brain tissues (such as 5-HT, DA, CKK, and GABA) and then influences receptor proteins related to mood, memory, and mental health conditions. To date, five subtypes of the 5-HT_3R, namely, the 5-HT_{3A}R, 5-HT_{3B}R, 5-HT_{3C}R, 5-HT_{3D}R, and 5-HT_{3E}R, have been discovered. Of these, the first two are the major subtypes. In the central nervous system, 5-HT_3 receptor subtypes are involved in the pathological processes of depression [12, 13], anxiety, and withdrawal symptoms, and

5-HT_3R is involved in resistance to depression and anxiety. A previous study has indicated that 5-HT_3R antagonists can enhance the antidepressant effect of 5-HT reuptake inhibitors [14].

Shuyu capsules, a commercially available herbal prescription of traditional Chinese medicine (TCM), is composed of four herbal ingredients: Radix Bupleuri (*Bupleurum chinense* DC.), Radix Paeoniae Alba (*Paeonia lactiflora* Pall.), Rhizoma Cyperi (*Cyperus rotundus* Linn.), and Radix Glycyrrhizae (*Glycyrrhiza uralensis* Fisch.). It has been confirmed that it mitigates the expression of PMS depression symptoms in patients in clinical experiments. Animal experiments have also confirmed that improvements related to such symptoms are concentrated in the relevant cerebral areas. It is often technologically difficult to identify and purify active constituents in TCM prescriptions, and thus they are often not recognized by doctors of western medicine or scientists. We have focused on testing the curative effects of TCM using modern clinical experiments to evaluate the effect of TCM prescriptions [15, 16], with the intent of retaining effective TCM treatments and abandoning ineffective ones. In this respect, a previous study has demonstrated that Shuyu capsules, confirmed to mitigate PMS depression (number 2008L11169), mainly target 5-HT_{3B}R expression levels in areas of the hippocampus and hypothalamus [17, 18]. Nevertheless, the mechanisms by which the Shuyu capsule exerts its functions in these cerebral areas require further explanation.

In the present study, the Shuyu capsule, which comprises a mixture of natural medicinal materials, was used without consideration of the unknown interactions of these compounds [19]. An animal model of PMS depression, created using a chronic restraint-stress method, was given either Shuyu capsules or fluoxetine, and the distribution and protein expression of 5-HT_{3A}R and 5-HT_{3B}R in the prefrontal cortex and hippocampus were determined and compared. Additionally, a drug-containing serum derived from these animals was used as a method of drug delivery in a neuronal culture system, and the expression of 5-HT_3R protein and changes in the 5-HT_3 channel current were investigated to determine the relationship between 5-HT_3R expression and PMS depression at the cellular and molecular levels. In this way, we confirmed the target cerebral areas of the Shuyu capsule in regulating PMS depression and gained insight into its mechanism of action.

2. Materials and Methods

2.1. Laboratory Animals and Ethics Statement. Healthy female SPF Wistar rats weighing 160–180 g were selected. Animals had free access to water and food. The feeding room temperature was 24 ± 1°C and the relative humidity was 50 ± 10%. Animals were provided by the Laboratory Animal Center of Shandong Traditional Chinese Medicine University, license number SCXK (LU) 2011-0003. In the following assays, 72 rats were randomized into 4 groups (n = 18 for behavioral assays; n = 6 for immunohistochemistry; n = 6 for western blotting; n = 6 for serum collection): control group, model group, Shuyu administration group, and fluoxetine administration group. Rats in control group did not give any stimulation while model group were simulated with leg bounded. As to Shuyu capsule and fluoxetine administration groups, medicines were chronically administered to rats when modeling was at the same time.

Laboratory animals were provided care according to "*The Care and Use of Laboratory Animals*" by the Laboratory Animal Center of Shandong University of Traditional Chinese Medicine.

2.2. Chemicals and Drugs. The Shuyu capsule (clinical approval number 2008L11169) used in this experiment was composed of Radix Paeoniae Alba, Radix Bupleuri, Rhizoma Cyperi, and liquorice. Fluoxetine was used as the positive control (Eli Lilly Co., Indianapolis, IN, USA; approval number H20090463). Both Shuyu capsule (0.41 g/Kg/d) and fluoxetine (10 mg/Kg/d) were intragastrically administered to animals for 5 days when experiment needed so.

2.3. Primary Culture of Hippocampal Neurons. The pregnant rats used here were not abovementioned grouped rats and the primary culture steps were as follows. CO_2 was used to anesthetize the rats; their heads were removed rapidly. Alcohol was sprayed on the abdomens of the pregnant rats, the abdomens were split and the embryo was stripped out. Embryo head was removed after stripping and placed into iced phosphate-buffered saline (PBS). The skull was split to expose and open the cerebral cortex. After locating the hippocampus, it was removed and placed into 10 mL of PBS in a centrifugal tube containing ice. Trypsin was added, and the specimens were incubated at 37°C for 20 min; tubes were shaken every 5 min. Cells were collected from the trypsinized samples and washed in DMEM 3 times, and 4 h later, the medium was changed to NBG medium (Neurobasal : B27 : L-Glutamine = 100 : 2 : 1, Gibco/Life Technologies, Carlsbad, CA, USA) for incubation.

2.4. Determination of the Estrous Cycle. All grouped rats were weighed, recorded, and marked with picric acid, and their estrous cycle was determined using the vaginal smear microscopic examination method [20, 21]. On a proestrus vaginal smear, epithelial cell nuclei and a few keratinocytes are present, while on an estrum vaginal smear, anucleate keratinocytes and a few epithelial cells are present. On a postestrus vaginal smear, leukocytes, keratinocytes, and epithelial cell nuclei are found, and on an anestrus vaginal smear, there are large numbers of leukocytes and few epithelial cells and myxocytes.

2.5. Generation of a PMS Depression Rat Model. Rats tend to be active at the acceptance stage (proestrus and estrus), and their estrous behaviors abate or even disappear at the nonacceptance stage (postestrus and anestrus). Rats with regular estrus behaviors and at the nonacceptance stage, and which obtained similar scores in the open-field test and sucrose-preference test, were selected for model building.

The model was generated as previously reported, with some modifications [17], and the specific steps were as

follows. The four legs of the rats were bound crosswise; that is, the front leg and hind leg on the opposite side were bound with sterile gauze (width: 2 cm, and of appropriate length) so as to prevent them from moving freely. The rats were bound in such a way that they were able to move slightly and obtain some food, and the modeling lasted for 5 days. During this process, the same dosage of sterile drinking water was provided to the control group.

2.6. Behavioral Assays. The open-field test [22, 23] was used to measure the locomotor activity of the rats. We employed the XR-Xvideo (including the XR-Xvideo animal behavior video analytical system) for this test. Under dim red light, experimenters held the distal third of the rats' tails and placed them at the center of an open-field test box (size: 50 cm × 50 cm × 40 cm) with black walls and a black floor. The video system recorded behavioral changes during a 5 min period, and the software automatically recorded the general path of their movement. The model test was conducted before experimental animal screening and after model building and drug administration.

Furthermore, the sucrose-preference experiment [24] was used to measure the level of reward response in the rats [25]. Depressive animals showed a general decline in sucrose preference, representing an anhedonia symptom. In the experiment, two bottles of water were provided to the rats for their free selection over a 24 h period. One bottle contained a 1% sucrose aqueous solution, and the other contained pure water. The two bottles were located on opposite sides of the cage. Before the experiment, the rats had free access to water and food. The consumption of tap water and sucrose water was measured by weighing the bottles. The sucrose preference was expressed as the percentage of consumed sucrose water to the total liquid consumed. Sucrose-preference rate = sucrose water consumption (g)/(sucrose water consumed (g) + water consumption (g)) × 100%.

2.7. Immunohistochemistry. According to a stereotaxic atlas of rats, 3 mm of the anterior brain, containing the frontal lobe, and 5 mm of the middle section, containing the hippocampus and hypothalamus, were removed. The removed cerebral tissues were fixed in triformol (Sigma-Aldrich, St. Louis, MO, USA) for 1 week at a temperature of 4°C. Samples were dehydrated in a gradient series of hydrous ethanol and were then treated with xylene to make the samples transparent. Dehydrated samples of cerebral tissues were embedded in paraffin and then sliced by microtome (RM2015; Leica, Wetzlar, Germany) at a thickness of 5 μm. After deparaffinizing and hydration treatments, the sections were again washed with PBS three times, before being incubated with primary antibodies overnight at a temperature of 4°C. The primary antibodies included goat polyclonal antibodies to the 5-HT_{3A} receptor (Abcam, Cambridge, MA, USA; ab51950, 1 : 500) and to the 5-HT_{3B} receptor (Abcam; ab115023, 1 : 50). After washing, the sections were incubated with secondary antibodies (Cy3-labeled donkey anti-goat IgG (H+L); Beyotime, Haimen, China; A0505, 1 : 2000; and Alexa Fluor 488-labeled goat anti-rabbit IgG (H+L); Beyotime, A0423, 1 : 2000) for 2 h. A laser scanning confocal microscope (ZEISS LSM710) was then used to observe the samples [26, 27].

2.8. Western Blot. The primary antibodies used for western blotting included a goat polyclonal to the 5-HT_{3A} receptor (Abcam, ab51950, 1 : 200), a goat polyclonal to the 5-HT_{3B} receptor (Santa Cruz, Dallas, TX, USA; Sc-51198, 1 : 200), and a mouse monoclonal to β-actin (Sigma, A1978, 1 : 1000). The secondary antibodies included rabbit anti-goat IgG-HRP (Abcam, ab6741, 1 : 2000), donkey anti-goat IgG-HRP (Santa Cruz, Sc-2020, 1 : 1000), and goat anti-mouse IgG-HRP (Santa Cruz, Sc-2005, 1 : 2000). Results were monitored by chemiluminescence. A GE Healthcare LAS4000 (Little Chalfont, UK) was used to collect signals, and the built-in IQTL analytic software was adopted for the statistical analysis.

2.9. Serum Collection. About 90 min after last administration of Shuyu capsule/fluoxetine, rats received intraperitoneal injection of 1% pentobarbital sodium (CAS: 57-33-0, Sigma, USA). Then, blood was collected via aorta abdominalis. Blood samples were centrifuged (3000 rpm for 20 min), and the serum was separated and stored at −80°C.

2.10. Whole-Cell Patch Clamp. The voltage clamp mode of the Axon MultiClamp 700B (Molecular Devices, Sunnyvale, CA, USA) was used in this experiment [28]. The clamp voltage was −70 mV, the frequency of the Bessel filter was 2.9 kHz, and the sampling frequency was 20 kHz. The microelectrode was drawn using a microelectrode puller (P97, Sutter, Sacramento, CA, USA) with a resistance of 3–5 MΩ. The microelectrode manipulator (M200, Sutter) of an inverted microscope (IX71, Olympus, Tokyo, Japan) was used to control the electrode entering solutions. When the resistance stabilized, a negative pressure injector was used to break the patch to perform a whole-cell recording mode. Prior to or after breaking the patch, capacitance compensations were made without series-resistance compensation. After setting up the whole-cell mode, cells with series resistance Ra < 20 MΩ were included in the experiment. Phenylbiguanide (PBG; 10 μm) drug administration resulted in quick perfusion of the Y tube beside cells. All experiments were conducted at an indoor temperature of 21 ± 1°C.

2.11. Statistical Analysis. Two-way ANOVA was selected for the open-field test and the sucrose-preference test; GraphPad Prism 5 was used for the one-way ANOVA test. PClamp 10.0 was used for the whole-cell patch clamp recording of the 5-HT_3R current. All data are shown as the mean ± SEM, with the significance level set at $P < 0.05$.

3. Results

3.1. Shuyu Capsules Can Effectively Mitigate Depressive Behavior in a Rat PMS Model. The overall path of movement in an open-field test is mainly used to illustrate animal locomotor activity (Figure 1(a)). Compared with rats in the normal control group, the overall path significance of rats in the

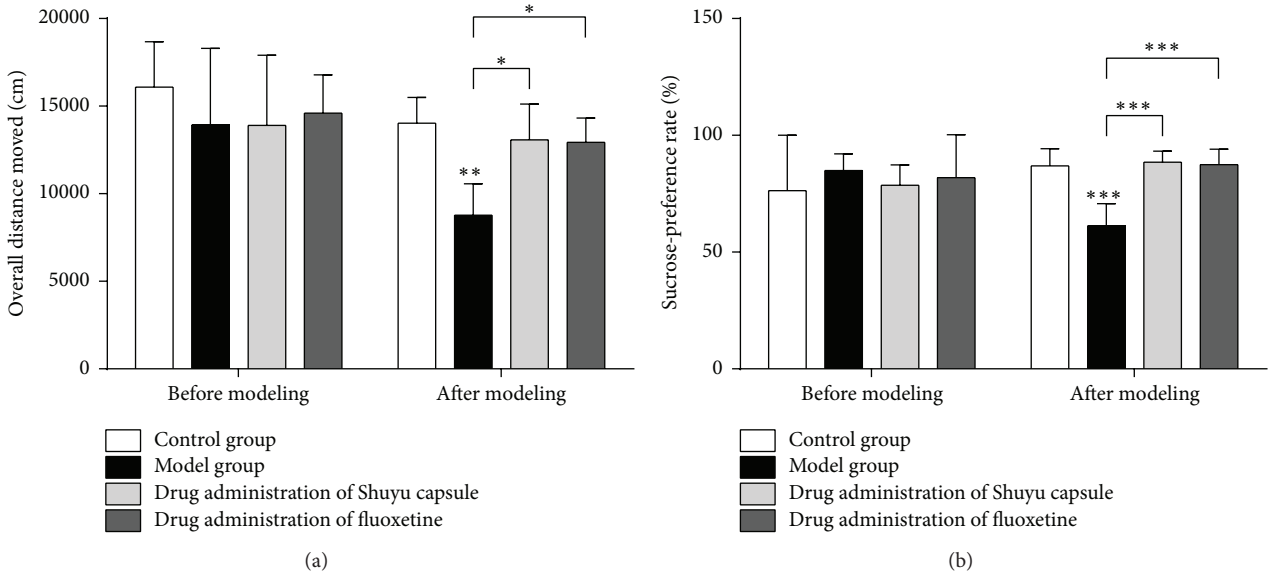

Figure 1: Behavioral assays. (a) Open-field test. (b) Sucrose-preference test. For all assays, testing was performed both before model building and after model building. Moreover, the following groups were analyzed: (1) the control/normal group (white), (2) model group (black), (3) Shuyu capsule group (gray), and (4) positive-control fluoxetine group (charcoal gray). The statistical analysis for the behavior assays was performed by one-way ANOVA ($n = 18$, $^{*}P < 0.05$, $^{**}P < 0.01$, and $^{***}P < 0.001$).

model group was reduced ($P < 0.01$); compared with the model group, the overall path scores of rats given Shuyu capsule and fluoxetine both increased significantly ($P < 0.05$).

The sucrose-preference level of rodents is generally regarded as an expression of the reward response, and depressive animals commonly show a lowered sucrose preference [29]. Compared with the normal group, the sucrose-preference level of the model rats declined significantly ($P < 0.001$), demonstrating the occurrence of typical depressive mood changes in model rats and, hence, demonstrating that the model was successfully constructed (Figure 1(b)). Administration of the Shuyu capsule as well as the positive control (fluoxetine) mitigated the reduction in sucrose intake (Figure 1(b)) in the respective model animal groups ($P < 0.001$); there was no significant difference between the two treated groups.

3.2. Shuyu Capsules Effectively Reduce the Expression of 5-HT_{3A}R and 5-HT_{3B}R in Cerebral Regions in a Rat PMS Model. Western blotting was used to detect the expression of 5-HT_{3A}R and 5-HT_{3B}R in different cerebral regions in the model rats. Regions in the frontal lobes and hippocampi revealed similarly increased expressions of 5-HT_{3A}R in rats (Figures 2(A), 2(a), 2(B), and 2(b)); the expression level of 5-HT_{3A}R in the model rats given the Shuyu capsule was significantly decreased as compared to the model group (Figures 2(A), 2(a), 2(B), and 2(b)). Animals in the positive-control group, which were given fluoxetine, showed a 5-HT_{3A}R expression level that had recovered to a level similar to that of the normal group (Figures 2(A), 2(a), 2(B), and 2(b)). The expression of 5-HT_{3B}R was very similar: the expression of 5-HT_{3B}R was increased in model rats (Figures 2(C), 2(c), 2(D), and 2(d)), while it decreased significantly in rats given the Shuyu capsule (Figures 2(C), 2(c), 2(D), and 2(d)). However, the expression level of 5-HT_{3B}R in the positive-control group given fluoxetine was restored to that of the normal group in the hippocampal area; yet, the expression of 5-HT_{3B}R was not effectively lowered in the frontal region (Figures 2(C), 2(c), 2(D), and 2(d)).

The expression of 5-HT_{3A}R and 5-HT_{3B}R in different cerebral areas showed similar increasing and decreasing trends, which raised the possibility of colocalizing these proteins. Fluorescence immunohistochemistry was used to determine the distributions of these proteins in different cerebral areas and their colocalization. Cells that coexpressed 5-HT_{3A}R and 5-HT_{3B}R in cerebral areas of different groups of rats showed yellow fluorescence (indicated by an arrow in Figure 3), with no apparent difference in the distribution mode. Positive cells were distributed in the frontal lobe area and hypothalamus and were present in the cell membranes of the CA1 and CA3 areas of the hippocampus, with most cells having dot and cone shapes (Figures 3(A–P) and 3(a–p)). The density of cells positive for colocalized 5-HT_{3A}R and 5-HT_{3B}R signals in the different groups paralleled the western blotting results. For example, in the frontal lobe (Figures 3(A–D) and 3(a–d)) and in the hypothalamus (Figures 3(E–H) and 3(e–h)), as well as in the CA1 area of the hippocampus (Figures 3(I–L) and 3(i–l)), the density of 5-HT_{3A}R- and 5-HT_{3B}R-positive cells in the model group far outnumbered that in the normal control group, and the density of 5-HT_{3A}R- and 5-HT_{3B}R-positive cells in rats given the Shuyu capsule was significantly decreased as compared with that in the model group. On the other hand, in the CA3 area of the hippocampus (Figures 3(M–P) and 3(m–p)), there were no

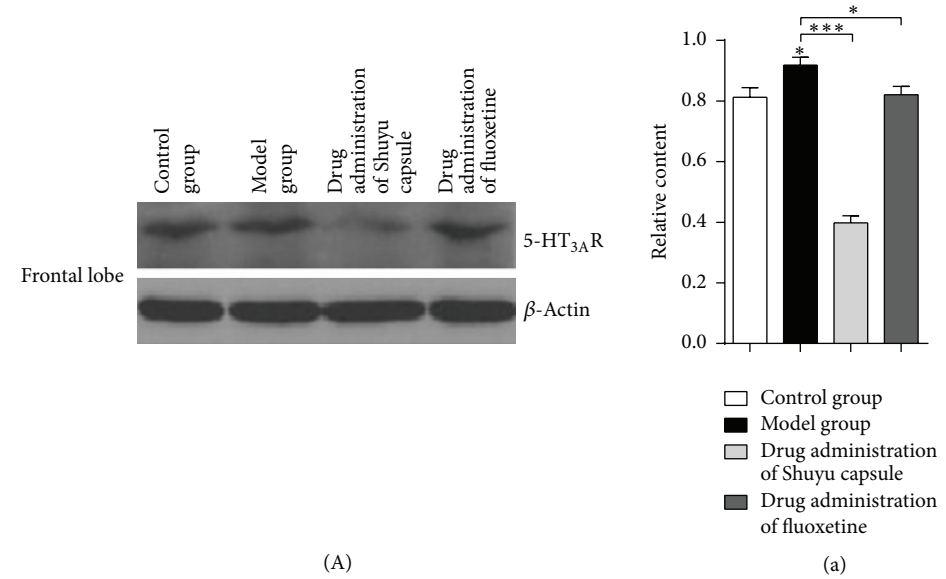

(A) (a)

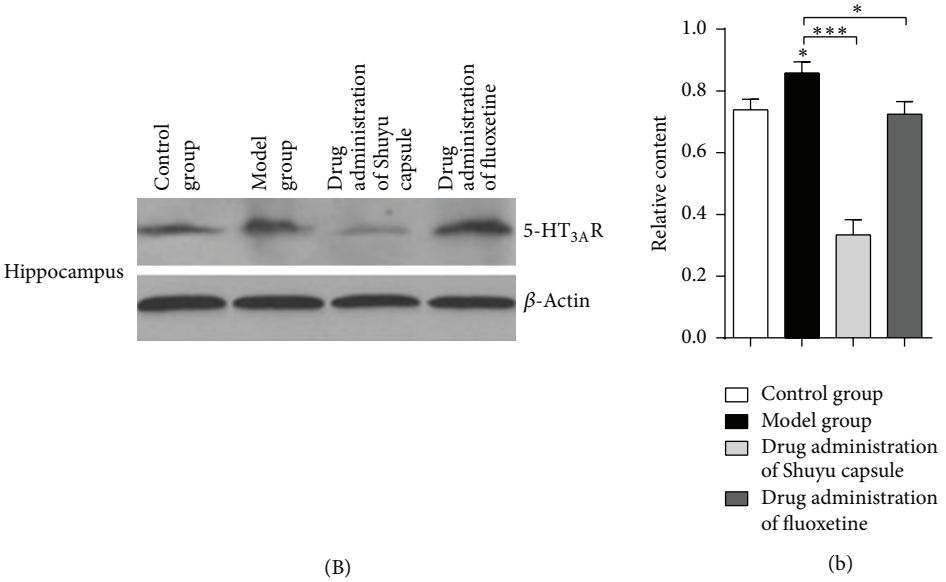

(B) (b)

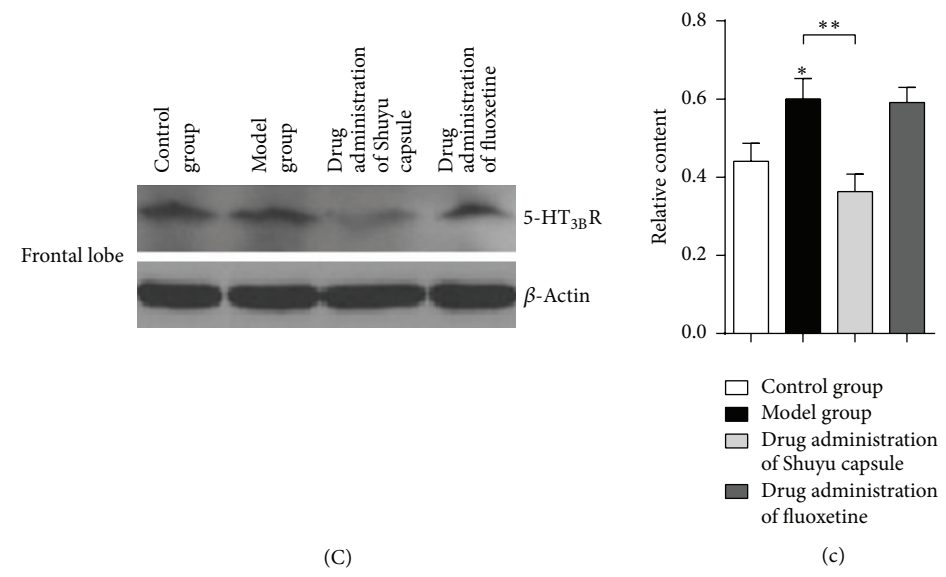

(C) (c)

Figure 2: Continued.

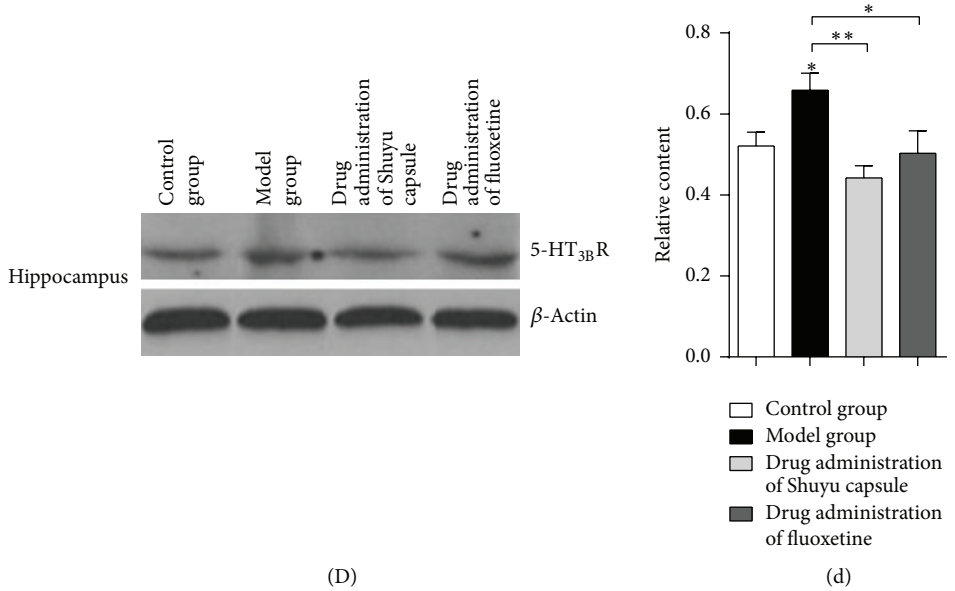

Figure 2: Western blot and analysis of tissue samples. Western blots of frontal lobe samples (A, C) and hippocampus samples (B, D) from each group, including the control/normal group, model group, Shuyu capsule group, and positive-control fluoxetine group. 5-HT_{3A}R antibody was used (A, B) to define 5-HT_{3A}R protein levels among the groups, while 5-HT_{3B}R antibody was used (C, D) to define 5-HT_{3B}R protein levels. A quantitative analysis ($n = 6$) of western blot results (a–d) was performed ($^{*}P < 0.05$, $^{**}P < 0.01$, and $^{***}P < 0.001$).

marked differences in the 5-HT_{3A}R- and 5-HT_{3B}R-positive cell density between the model group and the normal control group, but in rats given the Shuyu capsule, the density of these cells was significantly decreased as compared with the model group.

3.3. Shuyu Capsules Effectively Reduce the Expression of 5-HT_{3A}R and 5-HT_{3B}R in Rat Hippocampal Neurons. We treated primary hippocampal neuron cultures with a drug serum that was extracted from the rats in the different groups, including the normal control group, the model group, the Shuyu capsule administration group, and the fluoxetine administration group. Compared with the normal group, 5-HT_{3A}R protein expression was significantly increased in the hippocampal neurons in the model group ($P < 0.05$). Compared with the model group, 5-HT_{3A}R protein expression in the fluoxetine administration group ($P < 0.01$) and Shuyu capsule administration group ($P < 0.05$) was significantly decreased (Figures 4(A) and 4(a)). Moreover, there were no marked differences in 5-HT_{3A}R protein expression between these two groups.

Furthermore, compared with the normal group ($P < 0.05$), 5-HT_{3B}R protein expression in hippocampal neurons increased, but in the fluoxetine- ($P < 0.001$) and Shuyu capsule-treated groups ($P < 0.01$), 5-HT_{3B}R expression was decreased compared with the model group (Figures 4(B) and 4(b)). There were no marked differences in 5-HT_{3B}R protein expression between these two groups.

3.4. Shuyu Capsule Drug Serum Can Effectively Reduce the Current Density of 5-HT_3 Receptors in Hippocampal Neurons. A drug serum containing the Shuyu capsule effectively reduced 5-HT_3 receptor current density in hippocampal neurons (Figure 5). Compared with the normal group, the 5-HT_3R current density of hippocampal neurons incubated with a serum was increased in the model group ($P < 0.05$). Compared with the model group, the 5-HT_3R current density of hippocampal neurons incubated in the cells treated with Shuyu capsule-containing drug serum was significantly decreased ($P < 0.001$). Similar results were observed in the group given a fluoxetine-containing drug serum ($P < 0.01$).

4. Discussion

We had tested and verified face validity, construct validity, and predictive validity of PMS rat model in our previous studies [30–32]. In this work, we revealed that postmenstrual symptoms occurred in premenstrual phase and disappeared in postmenstrual symptoms in rat model. To be specific, rats showed the symptoms at the nonacceptance period (premenstruum) in estrous cycle and exhibited symptom relief or disappearance at the acceptance period (postmenstrual). Other groups verified PMS or premenstrual dysphoric disorder models with similar strategies and methods [33–35]. In current study, we selected healthy female Wistar rats through the open-field test and vaginal smear screening and created a PMS depression rat model by means of constraint [36] and evaluated these model animals using the open-field test and the sucrose-preference test. The significance of the overall path in model rats as well as their sucrose-preference level decreased, and some core depression symptoms, including listlessness, depression, and indifference, during the PMS period were well modeled. Through macroscopic behavior analysis, it was observed that rats in the model group were

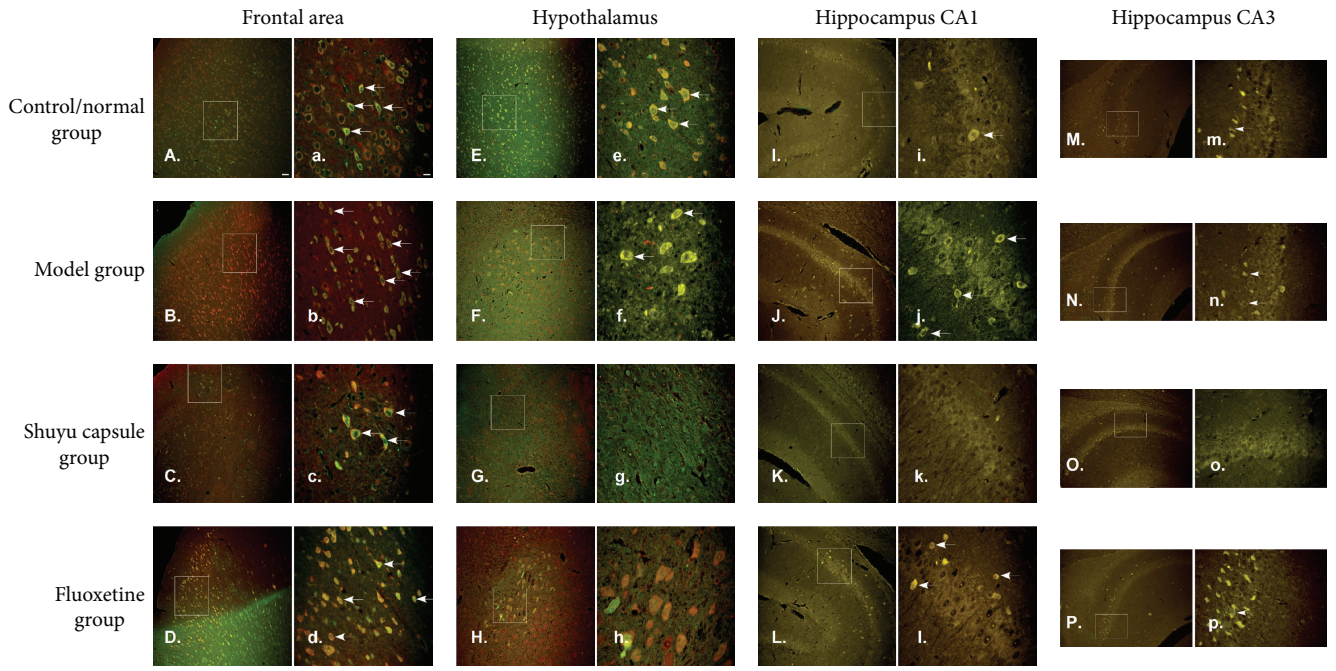

FIGURE 3: 5-HT_{3A}R- and 5-HT_{3B}R-positive cell staining. 5-HT_{3A}R- and 5-HT_{3B}R-positive cells from different cerebral areas were stained, including the frontal lobe (A–D, a–d), hypothalamus (E–H, e–h), hippocampus CA1 (I–L, i–l), and hippocampus CA3 (M–P, m–p). The following samples were stained with both 5-HT_{3A}R and 5-HT_{3B}R antibodies: the control/normal group (A, E, I, M, a, e, I, and m), model group (B, F, J, N, b, f, j, and n), Shuyu capsule group (C, G, K, O, c, g, k, and o), and positive-control fluoxetine group (D, H, L, P, d, h, l, and p). 5-HT_{3A}R- and 5-HT_{3B}R-positive cells were defined by the merged signal (yellow). Scale bar (A–P): 100 μm; scale bar (a–p): 25 μm.

inactive and spiritless, had dull eyes, huddled together for sleep, were insensitive to external stimulation, were slow to respond, and slow to act. Combining the results of the open-field test and the sucrose-preference test, it was judged that model generation was successful.

In our previous study, a total of 73 compounds were identified in the Shuyu capsule [37]. In that study, rats were treated with the Shuyu capsule and their serum was analyzed. Thirteen novel compounds and 49 metabolites were found in rat serum; 14 metabolites were confirmed as novel metabolites of the Shuyu capsule. In the present study, we further investigated how the Shuyu capsule functioned in cerebral regions to begin to elucidate its mechanism of action.

Another study has shown that hormones, including estradiol and progesterone, can partially regulate the functions of the 5-HT receptor, including 5-HT_3R, which is related to anxiety and depression [38]. Both estradiol and progesterone can function as noncompetitive antagonists of 5-HT_3R [39] and reduce the expression of the corresponding mRNA in rats under stressful conditions [40]. The antidepressant and anxiolytic functions of estrogen have been widely recognized, and the underlying mechanism involves modulating the production, activity, and postsynaptic effect of various neurotransmitters, such as 5-HT and GABA, through the estrogen receptors (ERs) [41]. A previous study from our group [37] has shown that a high estrogen level in the hippocampus and increased expression and activity of ERα and ERβ may play an important role in the pathogenesis of PMS depression [42]. The current study demonstrated the antidepressant effect of the Shuyu capsule in a rat model of PMS depression. The western blot results revealed that the Shuyu capsule can significantly reduce 5-HT_{3A}R and 5-HT_{3B}R protein expression in the frontal lobe and hippocampus, similar to the antidepressant and anxiolytic effects of estrogen, which is accompanied by a decrease in the expression of 5-HT_{3A}R and 5-HT_{3B}R.

5-HT_3R forms a nonselective cation channel after being activated, through which sodium, potassium, and calcium ions can pass. The typical antidepressant fluoxetine clearly inhibits the delayed-rectifier potassium current on cerebellar granule neurons, as well as the transient outward potassium current on hippocampal neurons. When used as depression treatment, fluoxetine can also increase cell excitability, by inhibiting the voltage-dependent delayed-rectifier potassium current, hence increasing the antidepressant effect [43, 44]. Some researchers have proposed that a selective 5-HT-reuptake inhibitor, such as fluoxetine, exerts its antidepressant effect by blocking the potassium channel in the 5-HT_3R coupling [45]. The results of this present *in vitro* study showed that the expression of 5-HT_{3A}R and 5-HT_{3B}R proteins in hippocampal neurons incubated with PMS depression model rat sera was significantly increased and that the PMS depression model rat serum activated the 5-HT_3R channel current. This was consistent with the earlier findings that opening of a potassium channel led to the development of depressive symptoms [46–48]. The expression of 5-HT_{3A}R and 5-HT_{3B}R in hippocampal neurons incubated with drug sera from rats in the Shuyu capsule administration group was

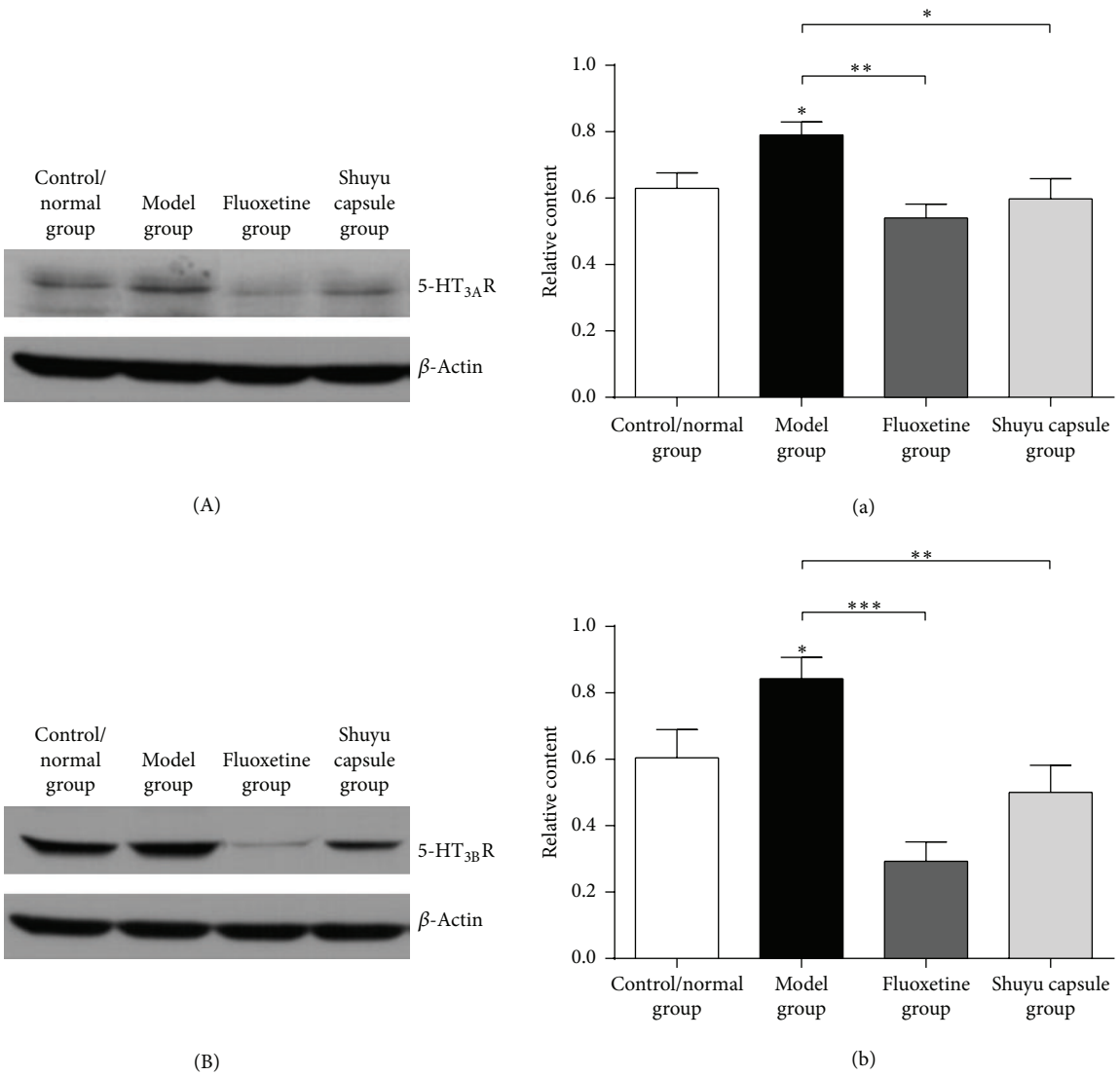

Figure 4: Western blot and primary hippocampal neuron analysis. The following drug serums were extracted and employed to treat primary hippocampal neurons: control/normal group, model group, positive-control fluoxetine group, and Shuyu capsule group. Both antibodies to 5-HT_{3A}R (A) and 5-HT_{3B}R (B) were used to test protein levels in hippocampal neurons among the groups. A quantitative analysis ($n = 6$) of the western blot results (a, b) was performed ($^{*}P < 0.05$, $^{**}P < 0.01$, and $^{***}P < 0.001$).

decreased; moreover, the channel current was also hindered. This is probably because the potassium channel current in the 5-HT_{3A}R and 5-HT_{3B}R coupling was hindered.

Abbreviations

5-HT_3:	5-Hydroxytryptamine 3 receptor
ANOVA:	Analysis of variance
DMSO:	Dimethyl sulfoxide
HRP:	Horseradish peroxidase
NBG medium:	Nutrient broth-glucose medium
PBG:	Phenylbiguanide
PMS:	Premenstrual syndrome
TCM:	Traditional Chinese medicine
PBS:	Phosphate-buffered saline.

Competing Interests

The authors have no conflict of interests to declare.

Authors' Contributions

The manuscript was written through contributions of all authors. All authors have given approval to the final version of the manuscript. All authors discussed the results and approved the manuscript.

Acknowledgments

This work was supported by National Natural Science Foundation of China (Grant no. 81573854).

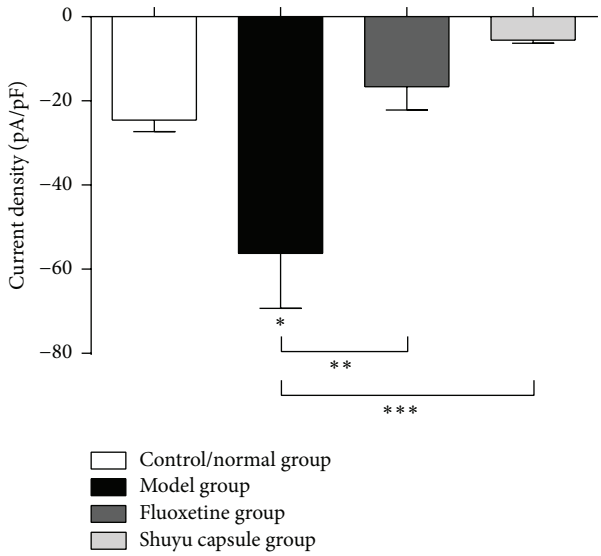

Figure 5: Whole-cell patch clamp analysis of primary hippocampal neurons. In this assay, 5-HT_3R currents were recorded and analyzed for the following groups: the control/normal group (white), model group (black), positive-control fluoxetine group (charcoal gray), and Shuyu capsule group (gray). $n = 6$, $^{*}P < 0.05$, $^{**}P < 0.01$, and $^{***}P < 0.001$.

References

[1] E. W. Freeman, S. M. Halberstadt, K. Rickels, J. M. Legler, H. Lin, and M. D. Sammel, "Core symptoms that discriminate premenstrual syndrome," *Journal of Women's Health*, vol. 20, no. 1, pp. 29–35, 2011.

[2] T. Bäckström, A. Andersson, L. Andreé et al., "Pathogenesis in menstrual cycle-linked CNS disorders," *Annals of the New York Academy of Sciences*, vol. 1007, pp. 42–53, 2003.

[3] T. R. Hylan, K. Sundell, and R. Judge, "The impact of premenstrual symptomatology on functioning and treatment-seeking behavior: experience from the United States, United Kingdom, and France," *Journal of Women's Health and Gender-Based Medicine*, vol. 8, no. 8, pp. 1043–1052, 1999.

[4] G. MacKenzie and J. Maguire, "The role of ovarian hormone-derived neurosteroids on the regulation of $GABA_A$ receptors in affective disorders," *Psychopharmacology*, vol. 231, no. 17, pp. 3333–3342, 2014.

[5] Y. Li, A. L. Pehrson, D. P. Budac, C. Sánchez, and M. Gulinello, "A rodent model of premenstrual dysphoria: progesterone withdrawal induces depression-like behavior that is differentially sensitive to classes of antidepressants," *Behavioural Brain Research*, vol. 234, no. 2, pp. 238–247, 2012.

[6] M. Qiao, Q. Zhao, H. Zhang, H. Wang, L. Xue, and S. Wei, "Isolating with physical restraint low status female monkeys during luteal phase might make an appropriate premenstrual depression syndrome model," *Journal of Affective Disorders*, vol. 102, no. 1–3, pp. 81–91, 2007.

[7] J. Chen, *Impact of Bai Xiangdan Capsules on Hippocampal Gene Expression Profile of Resident Intruder Paradigm-Induced PMDD Liver-Qi Invasion Rat Model*, Shandong University of Traditional Chinese Medicine, 2014.

[8] M. Delgado, A. G. Caicoya, V. Greciano et al., "Anxiolytic-like effect of a serotonergic ligand with high affinity for 5-HT1A, 5-HT2A and 5-HT3 receptors," *European Journal of Pharmacology*, vol. 511, no. 1, pp. 9–19, 2005.

[9] F. Li, Q. M. Xiang, C. H. Song, and M. Q. Qiao, "The study of premenstrual syndromes associated 5-serotonin system," *Medical Recapitulate*, vol. 20, no. 22, pp. 4048–4050, 2014.

[10] K. B. Fink and M. Göthert, "5-HT receptor regulation of neurotransmitter release," *Pharmacological Reviews*, vol. 59, no. 4, pp. 360–417, 2007.

[11] D. Gao, *Studies on the Underlying Mechanism of Liver-qi Sthenic Dispersedness—Analyses on the Differential Expression of Several Important Hormone and Neuraotransmitter Receptor Genes in the Brain Tissue of Premenstrual Symndrome Liver-qi Sthenia Symptom Macaque Model*, Shandong University of Traditional Chinese Medicine, 2006.

[12] R. W. Fuller, "Role of serotonin in therapy of depression and related disorders," *Journal of Clinical Psychiatry*, vol. 52, no. 5, pp. 52–57, 1991.

[13] B. Stoffel-Wagner, "Neurosteroid metabolism in the human brain," *European Journal of Endocrinology*, vol. 145, no. 6, pp. 669–679, 2001.

[14] R. Ramamoorthy, M. Radhakrishnan, and M. Borah, "Antidepressant-like effects of serotonin type-3 antagonist, ondansetron: an investigation in behaviour-based rodent models," *Behavioural Pharmacology*, vol. 19, no. 1, pp. 29–40, 2008.

[15] C. C. Liu, Y. F. Wu, G. M. Feng et al., "Plasma-metabolite-biomarkers for the therapeutic response in depressed patients by the traditional Chinese medicine formula Xiaoyaosan: a ^{1}H NMR-based metabolomics approach," *Journal of Affective Disorders*, vol. 185, pp. 156–163, 2015.

[16] X. He, J. Fang, L. Huang, J. Wang, and X. Huang, "*Sophora flavescens* Ait.: traditional usage, phytochemistry and pharmacology of an important traditional Chinese medicine," *Journal of Ethnopharmacology*, vol. 172, pp. 10–29, 2015.

[17] X. Gao, P. Sun, M. Qiao, S. Wei, L. Xue, and H. Zhang, "Shu-Yu capsule, a Traditional Chinese Medicine formulation, attenuates premenstrual syndrome depression induced by chronic stress constraint," *Molecular Medicine Reports*, vol. 10, no. 6, pp. 2942–2948, 2014.

[18] Q. Tan and H. Y. Zhang, "Effect of Shuyu Capsule on location and expression of 5-hydroxy tryptamine-(3B) receptor in hippocampus and hypothalamus regions in rats with depression emotion," *Chinese Journal of Experimental Traditional Medical Formulae*, vol. 17, pp. 137–140, 2011.

[19] Y. Fang, "Troubleshooting and deconvoluting label-free cell phenotypic assays in drug discovery," *Journal of Pharmacological and Toxicological Methods*, vol. 67, no. 2, pp. 69–81, 2013.

[20] L. M. Jaramillo, I. B. Balcazar, and C. Duran, "Using vaginal wall impedance to determine estrous cycle phase in Lewis rats," *Lab Animal*, vol. 41, no. 5, pp. 122–128, 2012.

[21] A. B. El-Wishy, "The postpartum buffalo. II. Acyclicity and anestrus," *Animal Reproduction Science*, vol. 97, no. 3-4, pp. 216–236, 2007.

[22] M. L. Seibenhener and M. C. Wooten, "Use of the open field maze to measure locomotor and anxiety-like behavior in mice," *Journal of Visualized Experiments*, no. 96, article e52434, 2015.

[23] X. Zhu, T. Li, S. Peng, X. Ma, X. Chen, and X. Zhang, "Maternal deprivation-caused behavioral abnormalities in adult rats relate to a non-methylation-regulated D2 receptor levels in the nucleus accumbens," *Behavioural Brain Research*, vol. 209, no. 2, pp. 281–288, 2010.

[24] Y.-H. Lin, A.-H. Liu, Y. Xu, L. Tie, H.-M. Yu, and X.-J. Li, "Effect of chronic unpredictable mild stress on brain-pancreas relative protein in rat brain and pancreas," *Behavioural Brain Research*, vol. 165, no. 1, pp. 63–71, 2005.

[25] G. Dagyt, I. Crescente, F. Postema et al., "Agomelatine reverses the decrease in hippocampal cell survival induced by chronic mild stress," *Behavioural Brain Research*, vol. 218, no. 1, pp. 121–128, 2011.

[26] C. Wang, T. Feng, Q. Wan, Y. Kong, and L. Yuan, "miR-124 controls *Drosophila* behavior and is required for neural development," *International Journal of Developmental Neuroscience*, vol. 38, pp. 105–112, 2014.

[27] J. Peng, C. Wang, C. Wan et al., "miR-184 is critical for the motility-related PNS development in *Drosophila*," *International Journal of Developmental Neuroscience*, vol. 46, pp. 100–107, 2015.

[28] K. Lin, Y.-Q. Liu, B. Xu et al., "Allocryptopine and benzyltetrahydropalmatine block hERG potassium channels expressed in HEK293 cells," *Acta Pharmacologica Sinica*, vol. 34, no. 6, pp. 847–858, 2013.

[29] A. Ribeiro-Carvalho, C. S. Lima, A. L. Nunes-Freitas, C. C. Filgueiras, A. C. Manhães, and Y. Abreu-Villaça, "Exposure to nicotine and ethanol in adolescent mice: effects on depressive-like behavior during exposure and withdrawal," *Behavioural Brain Research*, vol. 221, no. 1, pp. 282–289, 2011.

[30] Y. Chao, S. Wei, M. Qiao, and J. Wang, "Analysis of Monoamine Neurotransmitter Content in Serum and Different Encephalic Regions of PMS Liver-qi Invasion, Depression rat models," *Journal of Medical Research*, vol. 39, no. 4, pp. 19–22, 2010.

[31] S. Wei and H. Zhang, "Establishment of premenstrual syndrome liver-qi invasion, depression rats model and macro-evaluation," *Laboratory Animal and Comparative Medicine*, vol. 29, no. 3, pp. 142–146, 2009.

[32] H. Zhang, S. Wei, P. Sun, L. Xue, and M. Qiao, *The Content of Sex Hormone and Regulation Hormone in the Peripheral Blood and Different Encephalic Regions of Premens-trual Syndrome Liver-qi Invasion and Liver-qi Depression Model Rats*, World Science & Technology, 2009.

[33] H.-P. Ho, M. Olsson, L. Westberg, J. Melke, and E. Eriksson, "The serotonin reuptake inhibitor fluoxetine reduces sex steroid-related aggression in female rats: an animal model of premenstrual irritability?" *Neuropsychopharmacology*, vol. 24, no. 5, pp. 502–510, 2001.

[34] T. Schneider and P. Popik, "Increased depressive-like traits in an animal model of premenstrual irritability," *Hormones and Behavior*, vol. 51, no. 1, pp. 142–148, 2007.

[35] T. Schneider and P. Popik, "Attenuation of estrous cycle-dependent marble burying in female rats by acute treatment with progesterone and antidepressants," *Psychoneuroendocrinology*, vol. 32, no. 6, pp. 651–659, 2007.

[36] S. Wei, J.-L. Hou, Y.-B. Chao, X.-Y. Du, and S.-B. Zong, "Analysis on content of serum monoamine neurotransmitters in macaques with anger-in-induced premenstrual syndrome and liver-qi depression syndrome," *Journal of Chinese Integrative Medicine*, vol. 10, no. 8, pp. 925–931, 2012.

[37] F. Li, Y. B. Zhang, X. Wei et al., "Metabolic profiling of Shu-Yu capsule in rat serum based on metabolic fingerprinting analysis using HPLC-ESI-MSn," *Molecular Medicine Reports*, vol. 13, no. 5, pp. 4191–4204, 2016.

[38] L. Uphouse, "Female gonadal hormones, serotonin, and sexual receptivity," *Brain Research Reviews*, vol. 33, no. 2-3, pp. 242–257, 2000.

[39] M. Oz, L. Zhang, and C. E. Spivak, "Direct noncompetitive inhibition of 5-HT(3) receptor-mediated responses by forskolin and steroids," *Archives of Biochemistry and Biophysics*, vol. 404, no. 2, pp. 293–301, 2002.

[40] T.-J. Li, B.-P. Yu, W.-G. Dong, H.-S. Luo, L. Xu, and M.-Q. Li, "Ovarian hormone modulates 5-hydroxytryptamine 3 receptors mRNA expression in rat colon with restraint stress-induced bowel dysfunction," *World Journal of Gastroenterology*, vol. 10, no. 18, pp. 2723–2726, 2004.

[41] M. K. Österlund, "Underlying mechanisms mediating the antidepressant effects of estrogens," *Biochimica et Biophysica Acta (BBA)—General Subjects*, vol. 1800, no. 10, pp. 1136–1144, 2010.

[42] U. Halbreich and L. S. Kahn, "Role of estrogen in the aetiology and treatment of mood disorders," *CNS Drugs*, vol. 15, no. 10, pp. 797–817, 2001.

[43] S. Y. Yeung, J. A. Millar, and A. Mathie, "Inhibition of neuronal K_V potassium currents by the antidepressant drug, fluoxetine," *British Journal of Pharmacology*, vol. 128, no. 7, pp. 1609–1615, 1999.

[44] J.-S. Choi, B. H. Choi, H. S. Ahn et al., "Fluoxetine inhibits A-type potassium currents in primary cultured rat hippocampal neurons," *Brain Research*, vol. 1018, no. 2, pp. 201–207, 2004.

[45] L. E. Kennard, J. R. Chumbley, K. M. Ranatunga, S. J. Armstrong, E. L. Veale, and A. Mathie, "Inhibition of the human two-pore domain potassium channel, TREK-1, by fluoxetine and its metabolite norfluoxetine," *British Journal of Pharmacology*, vol. 144, no. 6, pp. 821–829, 2005.

[46] L. N. Zhang, S. W. Su, F. Guo et al., "Serotonin-mediated modulation of Na+/K+ pump current in rat hippocampal CA1 pyramidal neurons," *BMC Neuroscience*, vol. 13, no. 1, article 10, 2012.

[47] L.-L. Zhang, W. Wei, N.-P. Wang et al., "Paeoniflorin suppresses inflammatory mediator production and regulates G protein-coupled signaling in fibroblast—like synoviocytes of collagen induced arthritic rats," *Inflammation Research*, vol. 57, no. 8, pp. 388–395, 2008.

[48] I. Peitz and P. Fromherz, "Electrical interfacing of neurotransmitter receptor and field effect transistor," *The European Physical Journal E*, vol. 30, no. 2, pp. 223–231, 2009.